

https://dspace.org/

Phenotypic and functional characterization of CD56brigh CD16neg natural killer cell subsets within the context of influenza vaccination

Kay, Patti Sheryl

2021

https://hdl.handle.net/10539/33568

Downloaded from a DSpace repository. https://dspace.org/

PHENOTYPIC AND FUNCTIONAL CHARACTERIZATION OF CD56^{bright} CD16^{neg} NATURAL KILLER CELL SUBSETS WITHIN THE CONTEXT OF INFLUENZA VACCINATION

Patti Sheryl Kay

A thesis submitted to the Faculty of Medicine, University of the Witwatersrand, in fulfilment of the requirements for the degree of Doctor of Philosophy

Johannesburg, 2021

DECLARATION

I Patti Sheryl Kay hereby declare that:

a) The research reported in this thesis, except where otherwise indicated is my original work.
b) This thesis has not been submitted for any degree or examination to any other University
c) This thesis does not contain other people's data, pictures, graphs or information, unless specifically stated as being of sourced from other people.
d) This thesis does not contain another person's writing, unless specifically acknowledged as being sourced from other researchers. Where other written sources have been quoted, then:
    i. Their words have been re-written but the general information attributed to them has been referenced;
    ii. Where their exact words have been used, their writing has been placed inside quotation marks and referenced.
e) Where I have reproduced a publication of which I am an author, co-author or editor, I have indicated in detail which part of the publication was written by myself alone and have fully referenced such publications.
f) This thesis does not contain text, graphics or tables copied and pasted from the internet, unless specifically acknowledged, and the source being listed in the thesis and in the References section.

Signed_____ Date_____

ABSTRACT

Natural killer cell (NK) heterogeneity is attributable to the presence of multiple NK cell receptors and co-receptors and whose expression is shaped by genetics and unique antigen exposure during developmental and differentiation pathways. NK cells with bright expression of CD56 but lack CD16 ($CD56^{bright}CD16^{neg}$) are widely distributed throughout various tissues including the lymph nodes which is the site of dendritic cell, NK and T cell interactions and the liver, where they play a role in maintaining liver homeostasis. NK cells can develop an antigen "trained" phenotype which respond differently upon a secondary antigen encounter, and as $CD56^{bright}CD16^{neg}$ NK cells play an important immunoregulatory role during immune responses, understanding antigen mediated alterations of $CD56^{bright}CD16^{neg}$ NK subphenotypes provides insight into those cells that may influence overall immune responses. Furthermore, human $CD56^{bright}CD16^{neg}$ NK cells are believed to undergo further development and maturation giving rise to $CD56^{dim}CD16^{pos}$ NK cells, but this paradigm has been recently challenged. If indeed, $CD56^{dim}$ NK cells arise from $CD56^{bright}CD16^{neg}$ NK cells then an understanding of what constitutes a "normal" antigen response by $CD56^{bright}CD16^{neg}$ NK cells is warranted.

Using an influenza vaccination model, this thesis explored i) $CD56^{bright}CD16^{neg}$ NK subphenotypes which may be associated with a trained immune response, ii) receptors that may be associated with co-regulation (co-stimulation), iii) functional differences between circulating $CD56^{bright}CD16^{neg}$ NK cells with differing migration patterns, as well as iv) developing post-vaccination NK cell responses in comparison to those of CD4 and CD8 T cells. A phenotyping study explored differences in receptor and co-receptor expression patterns between $CD56^{bright}CD16^{neg}$ hepatic and NK cells circulating in the periphery.

A 12 colour flow cytometry panel was developed that simultaneously phenotyped and determined functional ($CD107a^{+}$ and IFNγ) responses of NK and T cells. The panel allowed for the definition of the 4 major NK subsets and co-expression patterns of NKp46, CD27 and CD62L subphenotypes. CD4 and CD8 T cells were phenotyped into central memory (Tcm), effector memory (Tem), effector cells and naive cells. Cytokine responses were determined by intracellular staining for IFNγ and staining for CD107a expression was used to detect degranulation responses. Using an influenza vaccination model, functional and trained immune responses were investigated for 12 healthy volunteers who received a standard 0.5 ml dose of the 2009- Influvac® subunit inactivated influenza vaccine. Venous blood was collected pre-vaccination, 3 days, 6 months and 1 year following vaccination and using the same vaccine preparation with which participants had been vaccinated, influenza antigen responding cells, were determined by comparing *ex vivo* stimulated cells to CD28/CD49d co-

stimulated cells and responses attributable to vaccination were measured by comparing antigen stimulated pre-vaccination cells to post-vaccination cells. As the thesis was focused on the $CD56^{bright}CD16^{neg}$ NK cell subset, all data presented refers to this subset.

Analysis of receptor co-expression patterns revealed that CD27 is predominantly expressed only on $NKp46^{+}$ cells and that NKp46 surface density is greater with CD27 co-expression. $NKp46^{+}$ cells were further defined by CD62L expression as, ($CD62L^{+}$) lymph homing ($lhNKp46^{+}CD27^{+}$ and $lhNKp46^{+}CD27^{-}$) and, ($CD62L^{-}$) peripheral ($pNKp46^{+}CD27^{+}$ and $pNKp46^{+}CD27^{-}$) subphenotypes. Following vaccination, dynamic alterations of subphenotype proportions developed, peaking at 6 months and which by 1 year returned to levels similar to those observed prior to vaccination. Lymph homing NKp46 subphenotype proportions expanded and peripheral NKp46 subphenotype proportions contracted, which suggests that with vaccination, certain $CD56^{bright}CD16^{neg}$ subphenotypes were altered or "trained either through up- or downregulation of co-receptors, or changes in migratory patterns. In addition, the extreme inter-individual diversity in proportions of lymph homing and peripheral $NKp46^{+}$ cells suggested a long term influence on the activating NKp46 receptor, possibly as a consequence of unique antigen exposures.

Co-expression of CD27 functionally delineated $NKp46^{+}$ cells, as $pNKp46^{+}CD27^{+}$ cells were more cytolytic than $pNKp46^{+}CD27^{-}$ cells and both lymph homing subphenotypes (P<0.05). Although a significant loss of $pNKp46^{+}CD27^{-}$ IFNγ producing cells occurred after vaccination (P=0.037 by 6 months), $pNKp46^{+}CD27^{-}$ cells produced more IFNγ than both lymph homing subphenotypes (P<0.05) and $pNKp46^{+}CD27^{+}$ cells, prior to vaccination (P=0.0005) and 1 year post-vaccination (P=0.016). Functional responses could therefore also be delineated by lymph homing properties, as the magnitude of peripheral $NKp46^{+}$ functional ($CD107a^{+}$ and $IFN\gamma^{+}$) responses were greater than those of lymph homing cells.

Monitoring of T cells prior to and following influenza vaccination revealed no changes in CD4 T cell memory proportions, but 3 days following vaccination, both CD8 Tcm and Tem proportions increased whereas naive and effector cells decreased (P<0.05). IFNγ responses remained unchanged following vaccination, for both CD4 and CD8 T cells. However, 6 months after vaccination CD4 T cells degranulated ($CD107a^{+}$) significantly more than pre-vaccination cells (P<0.05), as did CD8 naive and Tem subsets.

$CD56^{bright}$ cells are the predominant NK subset found in the liver and the importance of CD27 in hepatic pathology has been established. To investigate if hepatic perfusate (obtained during liver transplant procedures) provides a suitable source of liver NK cells, hepatic perfusate derived (hpNK) cells from deceased liver donors (n=9) were immunophenotyped and compared to circulating NK cells from healthy age and sex matched donors (n=9). Hepatic NK

cells were enriched for $CD27^+$ cells and CD27 was only expressed on $NKp46^+$ hpNK cells. However, unlike circulating $CD56^{bright}CD16^{neg}$ NK cells, NKp46 surface density remained unchanged and co-expression patterns for $CD27^+CD69^+$ and $CD27^+CD161^+$ subphenotypes differed between hpNK and circulating (P<0.05) NK cells. Immunophenotyping of hpNK cells from an acute liver failure (ALF) patient revealed that, similar to healthy controls, NKp46 expression was unchanged and surface expression of CD27 was confined to $NKp46^+$ cells. However, the percentage $CD56^{bright}CD16^{neg}$ hepatic cells that expressed $CD27^+$ cells was extremely low and few $NKp46^+$ cells expressed CD27. The majority of $NKp46^+$ cells were therefore of a $NKp46^+CD27^-$ subphenotype. Aberrant expression of the T cell memory marker, CD45RO, was found on NK cells from the ALF patient but which was not observed on NK cells from healthy donors.

Overall, given the global emergence of novel respiratory infections, and the subsequent severe impact on human health mediated by “cytokine storms” during infection, it is important to understand what constitutes a ‘normal’ functioning $CD56^{bright}CD16^{neg}$ response. Data from this thesis therefore adds to our understanding of $CD56^{bright}CD16^{neg}$ cNK cells that respond differentially to influenza antigen and which is determined by migratory potential and expression of co-receptors.

PUBLICATIONS AND PRESENTATIONS

PUBLICATIONS FROM THIS THESIS

Kay P, Schramm D and Tiemessen C. A long lived NKp46/CD62L phenotype in $CD56^{bright}CD16^{neg}$ NK cells identified at six months post-influenza vaccination. (In preparation)

Kay P, Schramm D and Tiemessen C. Human $CD56^{bright}CD16^{neg}$ NK subset co-expression of CD27 and NKp46 defines phenotypic and functional responses to *ex vivo* influenza antigen stimulation. (In preparation)

Kay P, Schramm D and Tiemessen C. Differences in CD27 co-expression immunophenotypes between circulating and hepatic perfusate derived $CD56^{br}CD16^{neg}$ NK cells. (In preparation)

PRESENTATIONS FROM THIS THESIS

Kay P and Tiemessen C. Human $CD56^{bright}$ liver/splanchnic-derived NK cells express the CD161 memory associated C-type lectin. Poster presentation: University of the Witwatersrand, Faculty of Health Sciences Research Day. 2014 (Best Poster award)

Kay P and Tiemessen C. Human CD56bright liver/splanchnic derived NK cells show distinct receptor and homing patterns. Poster presentation. ISAC, Fort Lauderdale, USA. 2015

DEDICATION

This thesis is dedicated to the family members of deceased liver donors, who in their darkest moments of grief, having just lost a loved one under sudden and tragic circumstances, gave an organ transplant recipient a new lease on life through their generous gift of agreeing to organ donation. This research project would not have been possible without your consent for collection of hepatic perfusate during the transplant procedure.

I am humbled by your benevolence in your moment of grief.

ACKNOWLEDGEMENTS

I owe my deepest gratitude to the following people and institutions for their contributions in making this study possible:

Firstly, to my supervisor, Prof Caroline Tiemessen who gave me an opportunity at a later stage of my life to fulfil an aspiration of completing a higher degree. Thank you for encouraging me to resume my degree after it was put in abeyance whilst I was treated for and recovering from serious health issues.

To my de facto co-supervisor, Dr Di Schramm, who stepped in when I resumed writing my thesis and whose advice and input was invaluable in keeping me focussed and motivated. I cannot thank you enough.

To my beloved daughters, Siobhan, Carreen and Tennille who accepted their student mother with equanimity and encouraged me along the way.

To my long suffering husband who patiently accepted my ambition to complete this degree. I promise never to mention “natural killer cells” or “immune system” again.

My thanks to the participants who gave consent to participate in the influenza arm of the study and made themselves available for collection of blood for up to a year following vaccination.

My thanks to the organ transplant team at the Donald Gordon Hospital for obtaining informed consent from donors’ families and for collecting hepatic perfusate. Without your participation, parts of this thesis would not have been possible to fulfil.

Finally, my thanks to the Poliomyelitis Research Foundation (PRF), Surgical Research Society of South Africa and the University of Witwatersrand for research and travel funding.

TABLE OF CONTENTS

DECLARATION..... ii
ABSTRACT iii
PUBLICATIONS AND PRESENTATIONS AT MEETINGS vi
DEDICATION…….. vii
ACKNOWLEDGEMENTS..... viii
TABLE OF CONTENTS…..... ix
LIST OF TABLES……..... xvi
LIST OF FIGURES…….... xvii
ABBREVIATIONS..... xxi

CHAPTER 1: INTRODUCTION AND LITERATURE REVIEW

1.1 Introduction…… 1
1.2 Natural killer cells……. 2
1.2.1 NK cell lineage…… 2
1.2.1.1 Transcriptional factor requirements for NK cell lineage divergence…… 3
1.2.2 NK cell developmental pathways……..... 4
1.2.2.1 NK development in bone marrow……. 5
1.2.2.2 NK cell development in the thymus…….. 7
1.2.2.3 NK cell development in secondary lymphoid tissue…….. 7
1.2.3 Trafficking of NK cells…… 8
1.2.4 Anatomical distribution of NK cells in solid organs…….. 9
1**.2.4.1** NK cell development and distribution in the lungs……. 10
1.2.4.2 NK cell development and distribution in the liver …….. 10
1.2.4.3 NK cell development and distribution in the uterus……... 10
1.2.5 Circulating NK cells ……..... 11
1.2.6 NK cell licensing and education…….. 13
1.2.7 NK cell receptor diversity……. 15
1.2.7.1 MHC specific NK cell receptors……. 15
1.2.7.2 Non-MHC specific NK cell receptors…… 16
1.2.7.3 Accessory NK receptors……. 17
1.2.8 NK cells interactions with T, B and dendritic cells……. 19
1.2.9 The role of NK cells in health and disease……. 22
1.2.9.1 NK cells and viral infections……. 23
1.2.9.2 NK cells and transformed cells……..... 24
1.2.9.3 NK cells and maintenance of homeostasis…… 26

1.2.10 NK cells and immune memory…….. 27
1.2.10.1 NK cell recall responses in mouse studies…… 28
1.2.10.2 NK cell recall responses in human studies……... 30
1.3 Influenza…… 31
1.3.1 Influenza A and B virus structure……..…. 32
1.3.2 Viral replication and transmission……... 33
1.3.3 NK cell interactions with influenza…….. 34
1.3.4 Influenza vaccination induced immune responses……..……. 35
1.4 Polychromatic flow cytometry for functional phenotyping of immune cells in health and disease……..……. 37
1.5 Study rationale…….. 38
1.6 Aims and objectives…….. 39

CHAPTER 2: MATERIALS AND METHODS

2.1 Study populations and Sample Collection…….. 40
2.1.1 Influenza vaccine participants……. 40
2.1.2 Healthy donor and control bloods……... 40
2.1.3 Liver transplant perfusate……. 40
2.2 Ethical Clearance……..... 41
2.3 Cell Isolation……. 41
2.3.1 Isolation and cryopreservation of peripheral blood mononuclear cells…..… 41
2.3.2 Hepatic perfusate derived cells…….…….. 42
2.4 Freezing of Plasma Samples……..….. 42
2.5 Thawing and Resting of Cryopreserved Cells……..…….. 42
2.6 *Ex vivo* Cell Stimulations…….…… 43
2.6.1 *Ex vivo* influenza stimulations……..…..... 43
2.6.2 Staphylococcus aureus enterotoxin B stimulations……. 43
2.7 Preparation of stimulated and unstimulated cells for staining……..…..…….. 43
2.8 Staining with fluorochrome conjugated monoclonal antibodies…….…. 44
2.8.1 Staining of cells with amine reactive dye……..……..... 44
2.8.2 Surface staining of cells……... 44
2.8.3 Intracellular cytokine staining of cells (ICS)……..…… 44
2.8.4 CD107a staining for measuring degranulation……..…….. 45
2.8.5 Staining of compensation beads……..…….…… 45

2.9 Statistical Analysis……..……. 45

CHAPTER 3: DEVELOPMENT AND VALIDATION OF A TWELVE COLOUR FLOW CYTOMETRIC PANEL TO STUDY T CELL AND NK PHENOTYPE AND FUNCTION

3.1 Introduction…….. 46

3.2 Materials and Methods……..... 47

3.2.1 Donor sample……..…… 47

3.2.2 Cryopreservation and thawing of samples……..…….. 47

3.2.3 Cell stimulations… ……..... 47

3.2.4 Staining protocols……..…….. 47

3.2.5 Development of polychromatic flow cytometry panels……..…… 48

3.2.5.1 Fluorochromes……..……. 48

3.2.5.2 Fluorescence minus one controls for defining NK subsets……. 48

3.2.5.3 Flow cytometer, instrument settings and compensation settings.. 49

3.2.6 Acquisition of cells and statistical analysis……..……..... 49

3.3 Results…….…….. 49

3.3.1 Development of gating strategies…….…. 49

3.3.1.1 Development of anchor gating strategy…….……..… 49

3.3.1.2 Defining NK subsets using fluorescent minus one gating……..… 50

3.3.1.3 Development of a twelve colour flow cytometry panel……. 51

3.3.2 Validation of flow cytometrically defined NK and T cell phenotypes…… 52

3.3.2.1 Phenotypic validation of the $CD56^{bright}CD16^{neg}$ NK subset…… 52

3.3.2.2 Validation of T cell phenotypes……. 54

3.3.3 Validation of inter-experimental variance…….. 55

3.3.3.1 Inter-experimental variances of NK subsets……..……. 56

3.3.3.2 Inter-experimental variances for NKp46, CD27 and CD62L NK subphenotypes…… 56

3.3.3.3 Validation of $CD56^{bright}CD16^{neg}$ functions…… 57

3.3.3.4 Inter-experimental variances for lymphocyte proportions and T

cell phenotypes…… 58
3.4 Discussion……... 59

CHAPTER 4: FLOW CYTOMETRIC PHENOTYPING OF THE CD56^{bright} CD16^{neg} NK SUBSET

4.1 Introduction……..…….. 63
4.2 Materials and Methods…….……. 64
4.2.1 Study samples……... 64
4.2.2 Sample preparations and staining……..…... 64
4.2.3 Flow cytometry……..... 64
4.2.4 Statistical analysis..... 64
4.3 Results…….…..…….…… 65
4.3.1 CD56^{bright}CD16^{neg} subphenotypes……..…….. 65
4.3.2 Co-expression patterns of CD27 and NKp46…….. 66
4.3.3 Stability of CD27-expressing cells over time……..…. 67
4.3.4 NKp46, CD27 and CD62L Boolean gated phenotypes…….……..… 69
4.3.5 Co-expression of CD27 and CD62L influences NKp46 cell surface density……... 73
4.4 Discussion…..……..… 75

CHAPTER 5: CD56^{bright} CD16^{neg} NK CELL RESPONSES TO 2009- INFLUENZA VACCINATION

5.1 Introduction……..…….. 80
5.2 Materials and Methods……..……. 82
5.2.1 Influenza vaccine participants…….. 82
5.2.2 Cryopreservation and thawing of samples…….. 82
5.2.3 *Ex vivo* flu-stimulations……..... 82
5.2.4 Staining protocols……. 82
5.2.5 Acquisition of cells and data collection……. 83
5.2.6 Statistical analysis..... 83
5.3 Results……. 83
5.3.1 Influenza vaccination induces long lived changes in NKp46 subphenotype proportions …… 83

5.3.1.1 Influenza vaccination changes in lymph homing NKp46CD27^{+} proportions……..… 85

5.3.1.2 Influenza vaccination changes in lymph homing NKp46CD27^{-} proportions ……. 86

5.3.1.3 Influenza vaccination changes in peripheral NKp46CD27^{+} proportions …….. 88

5.3.1.4 Influenza vaccination changes in peripheral NKp46CD27^{-} proportions ……... 89

5.3.2 Lymph homing and peripheral NKp46+ subphenotype degranulation (CD107a) responses……..…….. 91

5.3.2.1 Influence of CD27 co-expression on magnitude of NKp46^{+} degranulating cells……..……..……... 92

5.3.3 Lymph homing and peripheral NKp46+ subphenotype cytokine (IFNγ^{+}) responses…….... 94

5.3.3.1 Influence of CD27 co-expression on magnitude of NKp46^{+} IFNγ producing cells……..……... 95

5.3.4 CD56^{bright}CD16^{neg} NK cells are not polyfunctional……..... 96

5.3.5 Influence of *ex vivo* flu-stimulation on NKp46 cell surface density..... 97

5.4 Discussion……..…… 99

CHAPTER 6: CIRCULATING SOLUBLE FACTORS AND T CELL RESPONSES TO INFLUENZA VACCINATION

6.1 Introduction……..……. 106

6.2 Materials and methods…….…….. 107

6.2.1 Influenza vaccination participants…….…..… 107

6.2.2 Cryopreservation and thawing of samples……..…….…….... 107

6.2.3 Freezing of plasma samples……..… 107

6.2.4 *Ex vivo* flu-stimulations…….….. 107

6.2.5 Staining protocols…….…… 107

6.2.6 Acquisition of cells and statistical analysis…….... 108

6.2.7 Measurement of influenza specific antibodies and proteins (ligands and cytokines) by enzyme linked immunosorbent assay……..… 108

6.2.7.1 Qualitative determination of anti-influenza virus A IgM…… 108

6.2.7.2 Quantitative determination of B-cell activating factor…… 108

6.2.7.3 Quantitative determination of a-proliferation inducing ligand…..... 108

6.2.7.4 Cytometric Bead Array…….. 109

6.3 Results……. 109

6.3.1 IgM levels at baseline and post influenza vaccination…….. 109

6.3.2 Post-vaccination changes in plasma BAFF and APRIL levels……. 110

6.3.3 Influence of vaccination on plasma cytokines…….. 111

6.3.4 CD45RO expression on memory T cell subsets in response to *ex vi*vo influenza antigen stimulation…….…. 113

6.3.5 CD4 and CD8 T cell cytokine (IFNγ) responses to influenza vaccination ……... 115

6.3.6 Evaluation of CD4 and CD8 T cell cytolytic (CD107a) responses to influenza vaccination ……..... 117

6.3.7 Comparison between post-vaccination soluble factors, T cells and $CD56^{bright}CD16^{neg}$ NK cell responses…….…. 120

6.4 Discussion…… 121

CHAPTER 7: PHENOTYPING $CD56^{bright}CD16^{neg}$ HEPATIC NK CELLS

7.1 Introduction…….. 125

7.2 Materials and Methods……... 127

7.2.1 Liver transplant perfusate and isolation of mononuclear cells…….. 127

7.2.2 Thawing and resting of perfusate mononuclear cells…… 127

7.2.3 Immunophenotyping of liver perfusate derived NK cells…… 127

7.2.3.1 Staining protocols……... 127

7.2.3.2 Development of polychromatic flow cytometry panel for perfusate NK cells……..……..... 127

7.2.4 Statistical analysis……..... 128

7.3 Results…….. 128

7.3.1 Evaluation of hepatic perfusate derived and conventional $CD56^{bright}CD16^{neg}$ and $CD56^{bright}CD16^{dim}$ NK subsets……..... 128

7.3.2 Evaluation of $CD56^{bright}CD16^{neg}$ liver derived NK cells for the lymph homing receptor CD62L……... 130

7.3.3 Phenotypic comparisons between cNK and hpNK $CD56^{bright}CD16^{neg}$ and $CD56^{bright}CD16^{dim}$ subsets…….…….. 131

7.3.4 Differences in NKp46, CD27, CD69 and CD161 frequency distributions between $CD56^{bright}CD16^{neg}$ cNK and hpNK subsets …….. 133

7.3.5 Influence of CD27 co-expression on $NKp46^{+}$ conventional and liver perfusate derived NK $CD56^{bright}CD16^{neg}$ subsets……..…….. 138

7.3.6 Acute liver failure case study…… 140

7.4 Discussion……..… 145

CHAPTER 8: DISCUSSION AND CONCLUDING REMARKS

8.1 Discussion……..……..… 151

8.2 Concluding remarks……. 160

REFERENCES……..... 163

APPENDICES

APPENDIX A - Ethics clearance certificate……..... 198

APPENDIX B - Influenza antigen titration……. 199

APPENDIX C - Antibody titrations……..... 200

APPENDIX D – Determining primary fluorescence…… 202

APPENDIX E - List of fluorochromes…… 203

APPENDIX F - Flow cytometer optimization……... 204

APPENDIX G - Flow cytometer system calibration…… 205

APPENDIX H - IgM ELISA……..……..... 208

LIST OF TABLES

CHAPTER 1

Table 1.1: *In vivo* stages of NK cell differentiation in secondary lymphoid tissue… 8

Table 1.2: Human NK receptors and their ligands……. 19

Table 1.3: Major cytokines secreted by innate immune cells……... 20

CHAPTER 3

Table 3.1: Panel description and compensation matrix…… 52

Table 3.2: Frequency of CD27, CD62L and NKp46 expression on NK subsets….. 54

Table 3.3: Phenotyping of CD4 and CD8 T cells characterised by surface expression of CD27, CD62L and CD45RO……. 54

Table 3.4: Coefficient of variation for CD27, CD62L and NKp46 NK cell subphenotypes……. 57

CHAPTER 4

Table 4.1: Proportions CD27, CD62L and NKp46 for the $CD56^{bright}CD16^{neg}$ cell subset…… 65

Table 4.2: Percent CD27 co-expression on $CD56^{bright}CD16^{neg}$ NK cells remains stable over time…… 67

Table 4.3: NKp46, CD62L and CD27 Boolean populations for the $CD56^{bright}CD16^{neg}$ NK subset …… 70

Table 4.4: $NKp46^{+}$ subphenotypes defined by lymph homing properties……. 71

CHAPTER 6

Table 6.1: Post-vaccination IFNγ and CD107a responses for CD4 and CD8 T cells with flu re-challenge…… 120

CHAPTER 7

Table 7.1: Median frequencies and distribution of NKp46, CD27, CD69 and CD161 receptors for $CD56^{bright}CD16^{neg}$ cNK and hpNK subsets…….. 134

LIST OF FIGURES

CHAPTER 1

Figure 1.1: Simplified diagram of NK cell lineage…… 3

Figure 1.2: Putative developmental pathway of innate lymphoid cell restricted lineages……..…… 4

Figure 1.3: Graphic overview of surface proteins marking specific developmental stages of human conventional NK cells…….. 6

Figure 1.4: Multiple sites of NK cell development and proposed trafficking between tissues..... 9

Figure 1.5: Flow cytometry dot plot of mature circulating human NK cells..... 11

Figure 1.6: NK cell activation and target cell recognition..... 14

Figure 1.7: Schematic view of the basic anatomical structure and flow of lymph through a lymph node..... 21

Figure 1.8: Simplified diagram of the splanchnic vasculature..... 26

.

Figure 1.9: Generic illustration of influenza A/B virus..... 32

Figure 1.10: Transmission of 2009- H1N1 influenza virus..... 33

CHAPTER 2

Figure 2.1: Example of a sterile collection device used to collect liver (hepatic) perfusate during organ harvest..... 41

CHAPTER 3

Figure 3.1: Anchor marker panel and anchor gates identifying NK and T cells..... 51

Figure 3.2: Fluorescence minus one (FMO) gating for CD56 and CD16..... 52

Figure 3.3: Representative example of flow cytometry dot plots to validate staining of NK subsets and functional markers 54

Figure 3.4: Representative flow cytometry dot plots to validate staining of CD4 and CD8 T lymphocytes and memory subsets..... 56

Figure 3.5: Inter-experimental variances for $CD56^{bright}$ (A) and $CD56^{dim}$ (B) NK subsets..... 57

Figure 3.6: Inter-experimental variances for CD27, CD62L or NKp46 expression on NK subsets..... 58

Figure 3.7: Validation of inter-experimental variances of functional responses for the $CD56^{bright}CD16^{neg}$ NK subset..... 59

Figure 3.8: Inter-experimental variances for T lymphocytes..... 60

CHAPTER 4

Figure 4.1: Percent expression of CD27, CD62L and NKp46 cells for the $CD56^{bright}CD16^{neg}$ subset 65

Figure 4.2: CD27 and NKp46 co-expression patterns for the $CD56^{bright}CD16^{neg}$ subset..... 66

Figure 4.3: CD27 proportions remain stable over time..... 68

Figure 4.4: Gating strategy to define $NKp46^{+}$ subphenotypes 68

Figure 4.5: CD27 proportions remain stable over a year for lymph homing and peripheral subphenotypes 69

Figure 4.6: $CD56^{bright}CD16^{neg}$ Boolean co-expression patterns for CD62L, CD27 and NKp46 surface receptors..... 70

Figure 4.7: Wide inter-individual variances of $NKp46^{+}$ subphenotypes..... 72

Figure 4.8: CD27 co-expression on NKp46+ cells is associated with higher NKp46 surface density..... 73

Figure 4.9: Dynamic influence of CD27 and CD62L on NKp46 cell surface density.. 74

CHAPTER 5

Figure 5.1: Boolean gated $CD56^{bright}CD16^{neg}$ lymph homing and peripheral $NKp46^{+}$ subphenotypes..... 84

Figure 5.2: The effect of influenza vaccination on the distribution of $lhNKp46CD27^{+}$ responding cells..... 85

Figure 5.3: Illustration summarizing $lhNKp46CD27^{+}$ subphenotype distributions before and after influenza vaccination……. 86

Figure 5.4: The effect of influenza vaccination on the distribution of $lhNKp46CD27^{-}$ cells..... 87

Figure 5.5: Illustration summarizing $lhNKp46CD27^{-}$ subphenotype distributions before and 6 months after influenza vaccination……. 87

Figure 5.6: The effect of influenza vaccination on the distribution of $pNKp46CD27^{+}$ responding cells..... 88

Figure 5.7: Illustration summarizing $pNKp46CD27^{+}$ subphenotype distributions before and 6 months after influenza vaccination……..... 89

Figure 5.8: The effect of influenza vaccination on the distribution of $pNKp46CD27^{-}$ responding cells..... 90

Figure 5.9: Illustration summarizing pNKp46CD27^{-} subphenotype distributions before and 6 months after influenza vaccination…….. 90

Figure 5.10: Lymph homing and peripheral NKp46 subphenotype CD107a^{+} flu-stimulation..... 91

Figure 5.11: Effect of CD27 co-expression on magnitude of pNKp46^{+} degranulating responses to flu-stimulation..... 93

Figure 5.12: Differences in the magnitude of degranulating (CD107a^{+}) cells between lymph homing and peripheral NKp46^{+} subphenotypes..... 93

Figure 5.13 Lymph homing and peripheral NKp46 subphenotype cytokine (IFNγ^{+}) responses to *ex vivo* flu-stimulation……..……... 94

Figure 5.14: Influence of CD27 co-expression on magnitude of pNKp46^{+} cytokine (IFNγ) responses..... 95

Figure 5.15: Differences in the magnitude of IFNγ producing cells between lymph homing and peripheral NKp46^{+} subphenotypes..... 96

Figure 5.16: CD107a and IFNγ co-expression on CD56^{bright}CD16^{neg} NK cells..... 97

Figure 5.17: Effect of *ex vivo* flu-stimulation on NKp46 cell surface density..... 98

CHAPTER 6

Figure 6.1: Circulating plasma IgM levels following influenza vaccination……..... 110

Figure 6.2: Circulating plasma BAFF levels following influenza vaccination..... 111

Figure 6.3: Effect of influenza vaccination on secreted cytokines..... 112

Figure 6.4: Effect of vaccination on expression of CD45RO on memory CD4 T cell subsets..... 113

Figure 6.5: Effect of vaccination on expression of CD45RO on memory CD8 T cell subsets..... 114

Figure 6.6: CD4 IFNγ responses to vaccination and *ex vivo* flu-stimulation..... 115

Figure 6.7: CD8 IFNγ responses to vaccination and *ex vivo* flu-stimulation..... 116

Figure 6.8: CD4 degranulation (CD107a+) responses to vaccination and ex vivo flu- stimulation..... 117

Figure 6.9: CD8 degranulation (CD107a+) responses to vaccination and *ex vivo* flu- stimulation..... 118

Figure 6.10: Differences in CD107a expression between central and effector memory subsets for CD4 and CD8 T cells..... 119

Figure 6.11: Key findings at 3 days and 6 months post-vaccination following intramuscular influenza vaccination..... 121

CHAPTER 7

Figure 7.1: Differences in CD3- lymphocyte proportions between PBMCs and hepatic perfusate..... 129

Figure 7.2: Differences in $CD56^{bright}$ subset proportions between circulating and hepatic-derived NK cells..... 130

Figure 7.3: Differences in frequency distribution of CD62L proportions between circulating and hepatic $CD56^{bright}CD16^{neg}$ subsets..... 131

Figure 7.4: Differences in frequency distribution of CD27, CD161, CD69 and NKp46 between $CD56^{bright}CD16^{neg}$ and $CD56^{bright}CD16^{dim}$ cNK and hpNK subsets..... 132

Figure 7.5: Phenotypic comparisons between cNK and hpNK$CD56^{bright}CD16^{neg}$ subsets..... 134

Figure 7.6: NKp46 co-expression on $CD27^{+}CD56^{bright}CD16^{neg}$ cNK and hpNK cells..... 135

Figure 7.7: Representative dot plot of CD69 and CD161 co-expression on $CD27^{+}$ circulating and hepatic $CD56^{bright}CD16^{neg}$ NK cells..... 136

Figure 7.8: Differences between circulating and liver $CD56^{bright}CD16^{neg}$ Boolean calculated CD27, CD69, CD161 NK subphenotypes..... 137

Figure 7.9: Influence of CD27 co-expression on NKp46 cell surface density for $CD56^{bright}CD16^{neg}$ circulating and hepatic NK subsets..... 139

Figure 7.10: Influence of CD27 co-expression on CD161 and CD69 cell surface density for $CD56^{bright}CD16^{neg}$ circulating and hepatic NK subsets..... 140

Figure 7.11: Differences in receptor expression between healthy liver and acute liver failure $CD56^{bright}CD16^{neg}$ cells..... 141

Figure 7.12: Boolean gated CD27, CD69, CD161 subphenotypes of acute liver failure and healthy liver $CD56^{bright}CD16^{neg}$ NK cells..... 142

Figure 7.13: CD45RO surface expression on healthy and acute liver failure CD4 and CD8 T cells..... 143

Figure 7.14: Differences in CD27 and CD45RO receptor expression for healthy liver and acute liver failure CD4 and CD8 T cells..... 144

CHAPTER 8

Figure 8.1: Graph depicting dynamic changes of $CD56^{bright}CD16^{neg}$ subphenotype proportions following influenza vaccination..... 155

Figure 8.2: Schematic outline of proposed trafficking of $CD56^{bright}CD16^{neg}$ lymph homing and peripheral NKp46 cells following vaccination..... 157

ABBREVIATIONS

Ag	antigen
ALF	acute liver failure
AML	acute myeloid leukemia
APC	allophycocyanin
APC Cy7	allophycocyanin cyanine 7
APC H7	allophycocyanin hilite 7
APRIL	a proliferation-inducing ligand
ASF	area scaling factor
BAFF	B-cell activating factor
BV	brilliant violet
°C	degree Celsius
Ca^{2+}	calcium
CD	cluster of differentiation
CHILP	common helper-like ILC progenitor
CHS	contact hypersensitivity response
CILP	common ILC-restricted progenitor
CLP	common lymphoid progenitor
CMV	cytomegalovirus
cNK	circulating NK cell
CO_2	carbon dioxide
CTL	cytotoxic T lymphocyte
CV	coefficient of variation
DC	dendritic cell
EBV	Epstein-Barr virus
ECD	R Phycoerythrin-Texas Red®
EDTA	ethylenediaminetetraacetic acid
FITC	fluorescein isothiocyanate
FMO	fluorescent minus one
FSC-A	forward scatter area
FSC-H	forward scatter height
g	g-force
HA	influenza haemagglutinin

HBV	hepatitis B virus
HCV	hepatitis C virus
HEVs	high endothelial venules
HIV	human immunodeficiency virus
HLA	human leukocyte antigen
HMPV	human metapneumonia
HSC	haematopoietic stem cell
HSCT	haploidentical stem cell transplant
HTK	histidine-tryptophan-ketoglutarate
hpNK	hepatic perfusate derived NK cell
hrs	hours
ICS	intracellular cytokine staining
ID2	inhibitor of DNA binding 2
i.e.	that is
IFNα	interferon-alpha
IFNβ	interferon-beta
IFNγ	interferon-gamma
Ig	immunoglobulin
IL	interleukin
IL-7R	interleukin-7 receptor
IL-15RA	interleukin-15 receptor, alpha unit
ILC	innate lymphoid cells
ILT	immunoglobulin-like transcript
ITAM	immunoreceptor tyrosine-based activating motif
ITIM	immunoreceptor tyrosine-based inhibitory motifs
KIRs	killer immunoglobulin-like receptors
L	litres
LAIV	live attenuated influenza vaccines
LFA	lymphocyte function associated antigen 1
lhNKp46CD27^{+}	lymph homing NKp46^{+}CD27^{+}
lhNKp46CD27^{-}	lymph homing NKp46^{+}CD27^{-}
LIL	liver infiltrating lymphocytes
LIR	leucocyte immunoglobulin-like receptor
LMPP	lymphoid-primed multipotential progenitor

LN	lymph node
M1	matrix 1
M2	matrix 2
MCMV	murine cytomegalovirus
MFI	mean fluorescent intensity
Mg^{2+}	magnesium
MIC	MHC-class-Ⅰ-polypeptide-related
µg	microgram
µl	microlitre
ml	millilitre
mins	minutes
MVA	modified vaccinia virus Ankara
NA	neuraminidase
NCR	natural cytotoxicity receptors
neg	negative
NK	natural killer cells
NKDIs	NK developmental intermediates
NKP	NK cell precursors
nm	nanometre
Pac blue	Pacific blue
PBMCs	peripheral blood mononuclear cells
PBS	phosphate buffered saline
PE Cy	phycoerythrin cyanine
PE	phycoerythrin
$pNKp46CD27^{+}$	peripheral $NKp46^{+}CD27^{+}$
$pNKp46CD27^{-}$	peripheral $NKp46^{+}CD27^{-}$
PMTs	photomultiplier tubes
pos	positive
pre	pre-vaccination
QA	quality assurance
QDot®	quantum dot®
RAG	recombinant-activating gene
RNA	ribonucleic acid
RNP	ribonucleoprotein

ROR	retinoic acid orphan receptor
rpm	revolutions per minute
SANBS	South African National Blood Services
SD	standard deviation
SEB	*Staphylococcus aureus* enterotoxin B
sIgM	secreted immunoglobulin M
SIP1	sphingosine-1-phosphate
SIPR-1	sphingosine-1-phosophate receptor 1
SLOs	secondary lymphoid organs
S:N	signal to noise
SSC-A	side scatter area
T cell	T lymphocyte cell
Tcm	central memory T cell
Tem	effector memory T cell
TGF-β	transforming growth factor β
T_H1	T helper 1
T_H17	T helper 17
TIV	trivalent inactivated vaccines
TNFα	tumor necrosis factor alpha
Tpm	peripheral memory T cell
TRAIL	tumour-necrosis-factor-related-apoptosis-inducing ligand
ULBP	cytomegalovirus UL16-binding protein
uNK	uterine NK cells
V	volts
VACV	vaccinia virus
viz.	namely

CHAPTER 1:
Introduction and literature review

1.1 Introduction

Maintaining a constant state of homeostasis is critical for the survival of living organisms. However, living organisms are exposed to infection causing pathogens such as fungi, bacteria, viruses and parasites, as well as foreign substances such as chemicals and harmful inorganic material. Furthermore, aberrations in cellular control mechanisms can lead to the development of malignancies. All multicellular organisms have an innate immune system (Beutler, 2004), whereas jawed vertebrates have both innate and adaptive immune systems (Cooper and Alder, 2006) which provide protection against this assault.

Cells of the adaptive immune system recognize and respond to foreign antigen in a specific manner, adapt to previously unseen molecules, discriminate between self and non-self and mount a rapid memory or recall response to a previously encountered antigen which depends upon somatic diversification of antigen-receptor genes. In contrast, elements of the innate immune system are inherited traits and in place before infection or injury occurs. Cells of the innate immune system are able to distinguish "self" from "non-self" through constitutive expression of generic receptors that recognize unique products of microbial metabolic pathways not found on eukaryotic cells (Janeway and Medzhitov, 2002).

In humans, protection against infection and malignancies is provided by co-ordinated interactions between the innate and adaptive immune systems. Natural killer (NK) cells belong to the innate immune system and are critical in the early defense against viral infections and transformed cells. NK cells circulating through the blood comprise of mainly of $CD56^{dim}$ NK cells, but a minor subset defined as $CD56^{bright}CD16^{neg}$ NK cells express various homing molecules that mediate their migration to various solid organs and lymph nodes (LNs). $CD56^{bright}CD16^{neg}$ NK cells are considered immunoregulatory (Cooper et al., 2001b) and differ from $CD56^{dim}$ NK cells in their cytotoxic capacity, proliferative response to IL-2, NK receptor repertoire and expression of adhesion molecules (Cooper et al., 2001a). Human studies on $CD56^{bright}$ NK cells are limited, as mice do not express CD56 and until recently, human studies of NK cells have largely focused on the predominant $CD56^{dim}$ subset. Recent evidence has revealed that NK cells can display elements of a "memory-like" or "trained" response to antigen and the understanding of how the $CD56^{bright}CD16^{neg}$ NK cell subset contributes to immune responses is evolving. Using a human influenza vaccination model this study focuses on how $CD56^{bright}CD16^{neg}$ NK cell subphenotypes differ immunophenotypically and functionally in response to influenza antigen. The suitability of hepatic perfusate as a source of liver-derived NK cells for phenotypic characterization is also explored. The influenza vaccination and NK

cell perfusate models were therefore utilized to gain further insights into understanding the role of the understudied $CD56^{bright}CD16^{neg}$ NK cell subset.

1.2 Natural killer cells

Morphologically, natural killer (NK) cells are large granular lymphocytes which make up approximately 5% - 20% of circulating lymphocytes (Robertson and Ritz, 1990). NK cells are a member of a group of diverse immune cells with overlapping developmental and phenotypic characteristics designated as innate lymphoid cells (ILC). ILCs are defined by their lymphoid morphology, an absence of myeloid phenotypic markers and an absence of recombination-activating gene (RAG) dependant rearranged receptors (Spits and Cupedo, 2012). A system based on T helper lymphocyte (T_H) cell nomenclature categorises ILCs into 3 groups: Group 1 ILCs, are defined by their ability to produce interferon (IFN)-γ but not T_H2 and T_H17 cell associated cytokines; Group 2 ILCs produce T_H2 associated cytokines in response to interleukin (IL) IL-25 stimulation and Group 3 ILCs produce T_H17 associated cytokines IL17-A and IL-22 (Spits et al., 2013). Originally considered as a group 1 ILC, circulating conventional (cNK) cells have more recently been classified as a group on their own (Diefenbach et al., 2014) and are phenotypically described as $CD3^-CD14^-CD19^-$ lymphocytes that express CD56 (NKH-1) (Lanier et al., 1989a; Nagler et al., 1989; Ritz et al., 1988) and CD16 (Lanier et al., 1983; Perussia et al., 1983).

1.2.1 NK cell lineage

In an adult human, there are approximately 2 billion NK cells circulating at any given time (Blum and Pabst, 2007) and as they are considered relatively short lived, require constant replenishment to maintain a state of immunological homeostasis. Human conventional NK (cNK) cells originate from bone marrow derived self-renewing lineage negative cluster of differentiation (CD) $CD34^+$ haematopoietic stem cells (HSCs) (Spits et al., 1995), which give rise to all red blood cells and leucocytes. NK cell precursors arise from a common oligopotent lymphoid progenitor (CLP) sharing a developmental origin with T lymphocyte cells (T) cells, bursa of Fabricius (B) cells and ILCs (Freud and Caligiuri, 2006; Kondo et al., 2010; Sanchez et al., 1994) before commitment to a NK lineage (Male et al., 2014). A simplified diagram of circulating NK cell lineage is depicted in **Figure 1.1.**

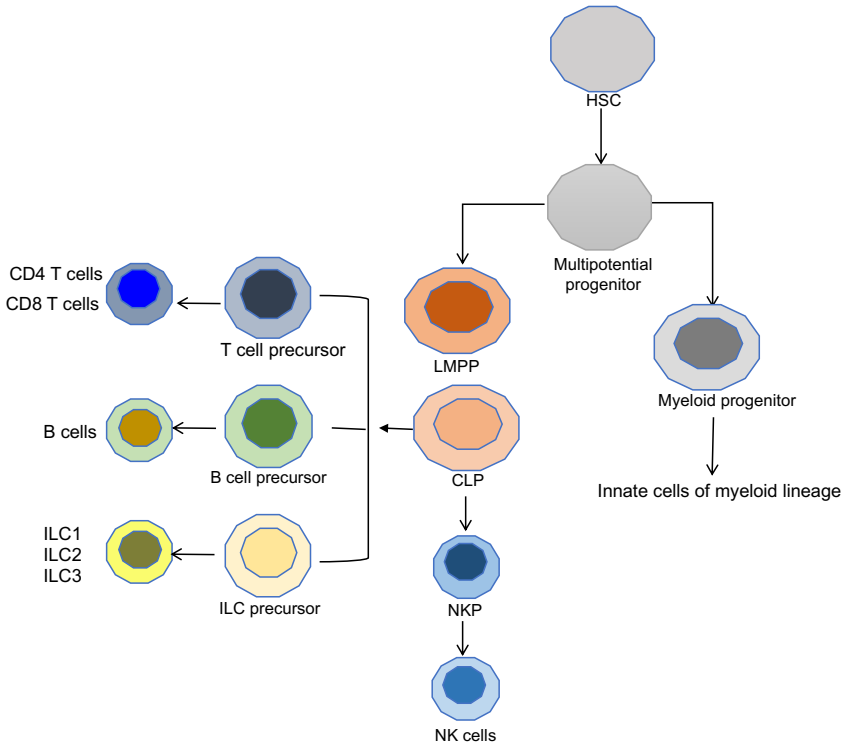


Figure 1.1: Simplified diagram of NK cell lineage. A self-renewing lineage negative haematopoietic stem cell (HSC) gives rise to a multipotential progenitor which can develop into a myeloid progenitor or a lymphoid-primed multipotential progenitor (LMPP). A common lymphoid progenitor (CLP) commits to precursor T cell, B cell, ILC1, 2 or 3 and NK lineages.

1.2.1.1 Transcriptional factor requirements for NK cell lineage divergence

The proposed nomenclature of the 3 ILC groups and cNK cells does not depend on the signature cytokines associated with each group but rather the influence of transcription factors for lineage divergence. The transcriptional factor, GATA3 is required for ILC development and is expressed on all ILCs (Klein Wolterink et al., 2013; Serafini et al., 2014; Zhong et al., 2016). cNK cell development requires the transcriptional repressor inhibitor of DNA binding 2 (ID2) (Yokota et al., 1999) as do all currently identified ILCs regardless of which group they fall into. The requirements for further development for each ILC group differ, with group 2 and 3 ILCs requiring retinoic acid orphan receptor (ROR) RORγt (Cella et al., 2009) and group 1, T–bet (the T_H1 cell-associated transcription factor encoded by *Tbx21*) whereas NK cells also require cooperation between eomesodermin and T-bet to regulate function and development (Gordon et al., 2012). The leucine zipper transcription factor, E4BP4, is suggested as a NK lineage specific factor as mice deficient in this factor have a severe loss of mature NK cells unlike T and B cells which are maintained in normal numbers (Di Santo, 2009; Gascoyne et al., 2009; Kamizono et al., 2009).

Despite considerable advances in understanding and identifying ILC progenitors, delineating their development in relation to each other is still ongoing and currently ILC1, ILC2 and ILC3 cells are considered as "helper like" cells whereas cNK cells are "killer like". Using an ID2 reporter mouse model (Rawlins et al., 2009), it was shown that upon transfer into alymphoid mice, a $Lin^{-}Id2^{+}IL\text{-}7R\alpha^{+}\ \alpha4\beta7^{+}Flt3^{-}CD25^{-}$ progenitor can generate all ILC lineages but not cNK cells, suggesting the presence of a restricted common helper-like ILC progenitor (CHILP) and that cNK cells may branch off earlier from a putative common ILC-restricted progenitor (CILP) (**Figure 1.2**).

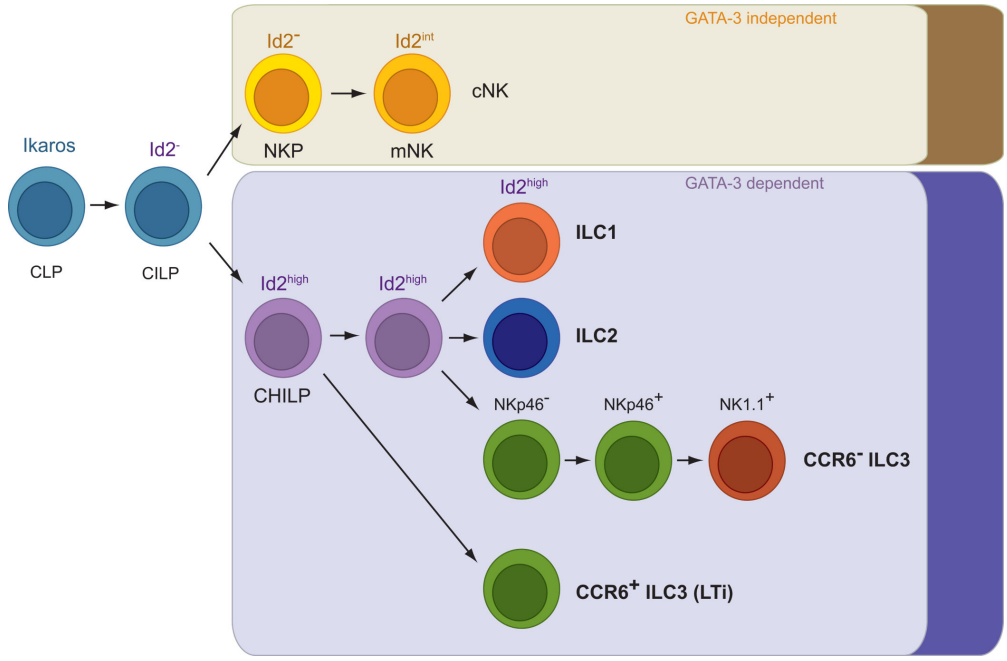


Figure 1.2: Putative developmental pathway of innate lymphoid cell restricted lineages. After branching from the common lymphoid progenitor (CLP), it is proposed that a ILC-restricted progenitor (CILP) may exist that gives rise to cNK cells and a restricted helper-like ILC progenitor (CHILP) which in turn gives rise ILC1, ILC2 and ILC3 restricted lineages. Reproduced from (Diefenbach et al., 2014).

1.2.2 NK cell developmental pathways

A complete NK cell developmental pathway remains to be clearly defined (Eissens et al., 2012; Freud and Caligiuri, 2006) and our current understanding is primarily based on murine studies and *in vitro* systems (Colucci et al., 2003; Yokoyama et al., 2004). The spleen filters blood and harbours many immune cells and has therefore been a major source of information for the study of cNK cells, but subsequent studies have now shown multiple extramedullary sites for further development of NK cells from a $CD34^{+}$ HSC including cord blood (Eissens et al., 2012; Renoux et al., 2015), spleen (Eissens et al., 2012), liver (Eissens et al., 2012; Moroso et al., 2010), tonsils (Freud et al., 2006; Renoux et al., 2015), peripheral lymph nodes (Freud et al.,

2005; Freud et al., 2006), inguinal lymph nodes (Eissens et al., 2012) and uterus (Sojka et al., 2014a). Although NK cells are widely distributed through the human body and may vary in phenotype and numbers compared to cNK cells, the core transcriptional identities that differentiate between $CD56^{bright}CD16^{neg}$ and $CD56^{dim}CD16^{pos}$ NK subsets are maintained (Dogra et al., 2020).

In vivo stages of mouse NK development have been described (Kim et al., 2002), but extrapolating these data as a representative of orthologous human NK developmental intermediates (NKDIs) remains a challenge, as mouse NK cells do not express CD56, but are rather defined by the expression of NK1.1 (killer-cell lectin-like subfamily B) and DX5 (an integrin α_2 chain). Despite this limitation, advances in our understanding of human NK cell developmental pathways have been made through investigating the acquisition and loss of receptors on the NK cell surface, which although not necessarily unique to NK cells, are expressed at critical stages of development driven by underlying molecular mechanisms. Furthermore, developmental pathways of $CD56^{bright}$ and $CD56^{dim}$ NK cells remain controversial with early evidence indicating that $CD56^{dim}$ NK cells are derived from $CD56^{bright}$ cells (Lanier et al., 1986) whereas recent studies suggest the contrary (Wu et al., 2014).

1.2.2.1 NK development in bone marrow

Bone marrow derived $CD34^+$ HSC cells can be induced to develop into $CD56^+$ NK cells (Miller et al., 1994; Miller et al., 1992), therefore it is accepted that NK cells arise from a $CD34^+$ HSC (Yu et al., 2013) and although all stages of NK development have been identified in bone marrow (Eissens et al., 2012; Renoux et al., 2015), *in vivo* NK developmental pathways and sites of development are still not well defined (Di Santo, 2006) and developmental relationships between NK subsets is not clear (Scoville et al., 2017). Cytokines do however, play a critical role in the development of cNK cells (Abel et al., 2018). IL-15 promotes the differentiation of cytolytic NK cells from a $CD34^+$ HSC (Mrozek et al., 1996) and is a critical step in early development and differentiation of mouse NK cells (Williams et al., 1997). Signalling of IL-15 is mediated via the IL-2 receptor β chain (CD122) and NK cell deficiencies are found in mice lacking either CD122 or IL-15 (Kennedy et al., 2000).

Multiple markers have been used to define intermediate stages of human NK cell development (Abel et al., 2018; Eissens et al., 2012; Freud and Caligiuri, 2006) and in the absence of NK cell specific markers it is extremely difficult to determine a lineage-specific developmental pathway. Various molecular mechanisms drive the development of human NK cells from a

$CD34^+$ HSC (Freud et al., 2006; Vosshenrich et al., 2005), with priming by dendritic cells (Lucas et al., 2007) and licensing by major histocompatibility genes class-I (MHC-I) (Kim et al., 2005) playing a crucial role in the final stages of NK cell development into fully functional mature cells. Despite the complexity of defining human NK cell intermediates, it is generally accepted that differentiation occurs through discrete stages of maturation (Colucci et al., 2003; Freud and Caligiuri, 2006; Freud et al., 2006).

Overall, each stage of NK cell development is characterized by the acquisition and/or loss of receptors with progenitor cells ultimately becoming restricted in lineage choice to develop into a fully functional uni-lineage cell, although many surface receptors expressed by NK cells are found on other immune cells, acquisition of these receptors is stage specific during NK development. There is currently no consensus on definitive phenotypes of NK progenitor cells, although an NK-lineage restricted $Lin^-CD34^+CD38^+CD123^-CD45RA^+CD7^+CD10^+CD127^-$ progenitor cell has been described (Renoux et al., 2015), which was found to be present in both foetal and adult tissues, implying that this NK cell precursor is conserved throughout ontogeny. The loss of CD34 expression is believed to mark the transition of NK cell precursors from stage 2 into stage 3 (Freud et al., 2006) which is also the earliest stage in which NK cell progenitors start expressing receptors (CD161) used to define immature NK cells (Loza et al., 2002). There is, however, reasonable consensus of the necessary role of CD122 expression in pre-NK development, the acquisition of CD161 by immature NK cells and the acquisition of CD56, CD16, natural cytotoxicity receptors (NCRs) and killer immunoglobulin-like receptors (KIRs) in the final stages of NK development which are summarized in **Figure 1.3**.

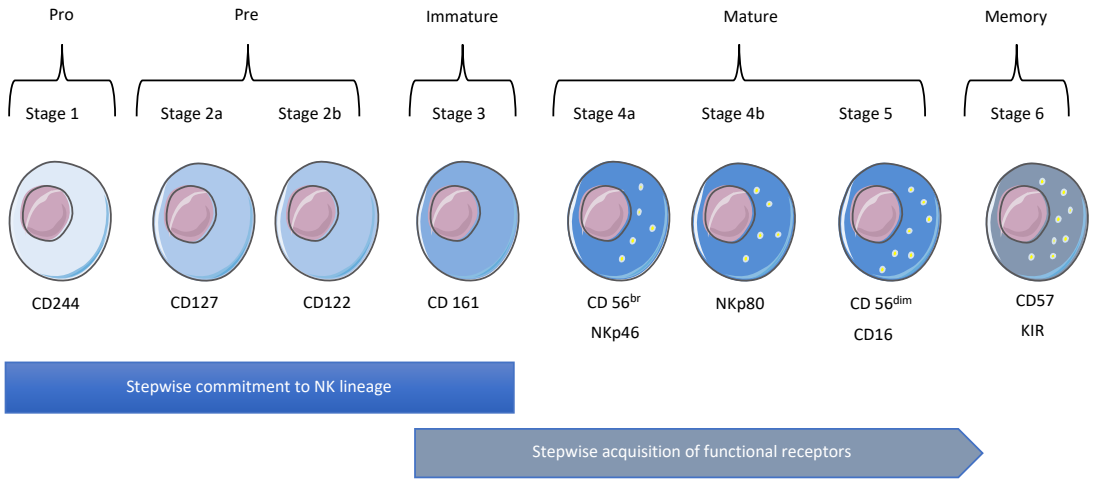


Figure 1.3: Graphic overview of surface proteins marking specific developmental stages of human conventional NK cells. Stepwise development of fully functional mature NK cells (stages 4, 5 and 6) from a bi-potential lymphoid progenitor (stage 1 pro-NK cell). Lineage restriction starts at stage 2 with IL-15 responsive CD122 expression. Acquisition of receptors

from stage 3 (immature NK) include, the natural cytotoxicity receptors, lectin family receptors and KIRs (members of the immunoglobulin superfamily).

Although stage 4 represents mature NK cells due to the acquisition of surface antigens that confer functional properties, it is considered that the final stages of mature NK cell development (stage 5) are characterized by acquisition of CD16 and KIRs) (Freud and Caligiuri, 2006). This is based on evidence from *in vitro* (Miller and McCullar, 2001) and *in vivo* (Vitale et al., 2004a) studies which indicate that KIR acquisition is cumulative and occurs late in NK cell maturation. However, multiple flow cytometric studies continuously reveal evolving complexity of NK cell phenotypes and functions and it is now proposed that a further stage (stage 6) be included to represent NK cells that display memory like properties (Scoville et al., 2017; Yu et al., 2013).

1.2.2.2 NK cell development in the thymus

A T cell/NK bipotential progenitor cell is found in human foetal thymus tissue (Sanchez et al., 1994) and is distinct from cNK cells. In murine models, CLPs that migrate to the thymus can commit to becoming an NK/T cell progenitor by developing into CD4-CD8- precursors (Douagi et al., 2002; Ikawa et al., 1999; Michie et al., 2000) from which a small number commit to the NK lineage (Vargas et al., 2011). Similar to cNK cells, thymic NK cells require IL-15 for development, however require the thymus where they arise from early precursors (Ribeiro et al., 2010; Vargas et al., 2011; Vosshenrich et al., 2006) as well as the GATA-3 transcription factor for further development (Vosshenrich et al., 2006) as the absence of GATA-3 results in the lack of thymic NK cells (Garcia-Peydro et al., 2006; Smyth and Nutt, 2006).

1.2.2.3 NK cell development in secondary lymphoid tissue

Identifying IL-15 responsive human NK intermediates analogous to murine models is difficult as detection by flow cytometry of CD122 expression on freshly isolated $CD34^+$ HSCs is below the detection limit (Freud et al., 2005; Shibuya et al., 1993; Yu et al., 1998). By using flow cytometry to detect sequential loss and upregulation of CD34, CD117 and CD94 expression as a surrogate for CD122 (Freud et al., 2006) was able to show the differentiation of NK cells into 4 discrete stages within secondary lymphoid tissue (SLT) (**Table 1.1**).

Table 1.1: *In vivo* stages of NK cell differentiation in secondary lymphoid tissue. Flow cytometric analysis of CD34, CD117 and CD94 surface expression allows for 4 NK cell developmental stages. Adapted from (Freud and Caligiuri, 2006).

	Stage 1	Stage 2	Stage 3	Stage 4
CD34	+	+	-	-
CD117	-	+	+	+/-
CD94	-	-	-	+

Thereby, stages 1 and 2, which include $CD34^{+}$ cells, representing the earliest stages in the development of human NK cells are present in human lymph nodes (LN) and tonsils providing evidence that lymph nodes are a site for developing a $CD16^{neg}CD56^{bright}CD34^{low}$ NK cell phenotype in humans. Furthermore, LN $CD56^{bright}CD16^{neg}$ NK cells are transcriptionally distinct compared to NK cells resident in other tissues (Dogra et al., 2020) and exhibit key transcriptional features similar to that of tissue resident memory T cells (Kumar et al., 2017; Mackay et al., 2016; Masopust and Soerens, 2019).

1.2.3 Trafficking of NK cells

The presence of immature NK cells in peripheral blood which, upon stimulation with IL-1 and IL-12, develop into mature NK cells (Bennett et al., 1996) indicates that NK precursors traffic from the bone marrow to extramedullary sites via the peripheral circulation. Currently there is no overall consensus as to how various human NKDIs should be defined (Yu et al., 2013), but NK cells can develop in multiple sites outside the bone marrow and these cells require different transcriptional signals, display different phenotypes and exhibit different functional capacities. Extramedullary sites which must have a tolerogenic environment due to high antigen exposure (liver) and the presence of human leucocyte antigen (HLA) mismatched tissue (developing foetus in the uterus) are enriched for $CD56^{bright}$ NK cells and both LN and lung $CD56^{bright}CD16^{neg}$ cells are transcriptionally distinct to that of bone marrow and other sites (Dogra et al., 2020), suggesting a unique role for this NK subset within these tissues.

The repertoire of chemokine receptors differs between $CD56^{dim}$ and $CD56^{bright}$ NK cells (Campbell et al., 2001) and the expression of homing and chemotactic receptors on NK cells help facilitate homing and egress from tissues in response to chemokines expressed on organ-specific cell types. This would affect the homing of specific NK cells to these organs under certain pathological and physiological conditions, but whether NK cells remain *in situ* or traffic under steady state conditions is unknown. There is evidence that trafficking of NK cells under steady state conditions occurs as adoptive transfer experiments in mice have shown that

splenic NK cells home to the liver, bone marrow and spleen of recipient mice (Cooper et al., 2002; Prlic et al., 2003; Ranson et al., 2003) and further adoptive transfer experiments into syngeneic non-irradiated recipient mice confirmed that within 24 hours, the percentage of transferred NK cells was similar to that of recipient NK cells in the lung, liver, LN and bone marrow (Gregoire et al., 2007).

Although it can be argued that multiple sites of NK cell development partially explains NK diversity, the significance of multiple sites for NK cell development and the presence of phenotypically distinct tissue resident NK subsets still remains unclear. However, as precursor and mature NK cells are present in multiple tissues, it is proposed that NK cells may move between tissues during different stages of maturation (**Figure 1.4**).

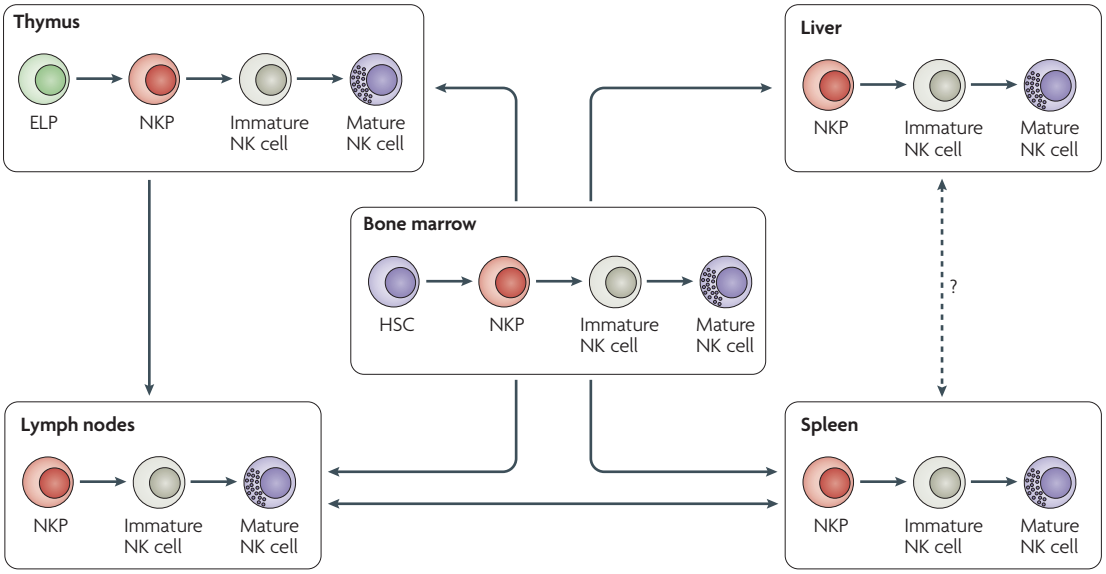


Figure 1.4: Multiple sites of NK cell development and proposed trafficking between tissues. NK cells develop from an early lymphoid precursor (ELP) in the thymus or a haematopoietic stem cell (HSC) in the bone marrow. Committed NK cell precursors (NKP) are present in all sites which develop into immature NK cells which under the influence of various signals develop into mature NK cells. NKPs, immature and mature NK cells may recirculate between tissues. Reproduced from (Huntington et al., 2007)

1.2.4. Anatomical distribution of NK cells in solid organs

The presence of NK cells in multiple organs outside of primary and secondary lymphoid tissues implies that NK cells may undergo differential developmental pathways that could help elucidate the origins of phenotypically diverse NK cells and their functions. The role of these cells in control of disease, transformation and as modulators of immune responses therefore requires further characterisation with many questions still remaining to be answered.

1.2.4.1 NK cell development and distribution in the lungs

NK cells present in human lungs have a similar phenotype to cNK cells (Carrega et al., 2008) and comprise mainly a differentiated $CD56^{dim}CD16^{pos}$ NK cells which are hyporesponsive to stimulation (Marquardt et al., 2017). These cells, however, express a higher frequency of killer cell immunoglobulin-like receptors (KIR) compared to other tissue NK cells even during development of the human foetus (Ivarsson et al., 2013) (Ivarsson et al., 2013). As found in cNK, a minority proportion of NK cells are $CD56^{bright}CD16^{neg}$, but in the lungs, they mainly express the tissue residency marker CD69 (Marquardt et al., 2017) and of these, a substantial proportion display a transcriptional signature that indicates tissue residency (Marquardt et al., 2019). In contrast, the terminally differentiated ($CD57^{+}$) $CD56^{dim}CD16^{pos}$ subset shares a transcriptional profile with that of cNK cells (Dogra et al., 2020).

1.2.4.2 NK cell development and distribution in the liver

Various studies have shown that liver-infiltrating lymphocytes (LILs) are phenotypically different from lymphocytes circulating in the peripheral blood and that these LILs also exhibit different cytotoxic and antigen specificities (Doherty et al., 1999). Immature NK cells are found in the liver of peri-natal mice suggesting that the liver may be a site for NK development. In mice, these immature liver NK cells have a $CD11b^{low}CD49b^{-}Ly49^{-}$ phenotype (Takeda et al., 2005) and express the tumour-necrosis-factor-related-apoptosis-inducing ligand (TRAIL) which similar to human cord blood immature NK cells (Zamai et al., 1998), can kill their targets *in vitro* and *in vivo* in a TRAIL-dependant manner (Takeda et al., 2005).

In humans, a $T\text{-}bet^{+}Eomes^{-}CD49a^{+}$ NK subset present in the liver is not found in peripheral blood or hepatic afferent and efferent venous blood (Marquardt et al., 2015). These $CD49^{+}$ NK cells are of a $CD56^{bright}$ phenotype, have undergone clonal expansion and degranulate poorly but express high levels of inflammatory cytokines, however, this phenotype was only present at a low frequency (average of 2.3%) and was identified only in 12 of 29 livers examined in the study. More recently, though, a $CXCR6^{+}$ or $CD49e^{-}$ NK phenotype that is rarely found in the periphery, has been identified in human liver (Aw Yeang et al., 2017; Harmon et al., 2016; Stegmann et al., 2016) that lacks T-bet expression but highly expresses Eomes (Aw Yeang et al., 2017; Cuff et al., 2016; Harmon et al., 2016; Stegmann et al., 2016).

1.2.4.3 NK cell development and distribution in the uterus

In mice, the number of NK cells present in the uterus increase significantly during pregnancy and comprise up to 70% of lymphocytes in the endometrium (Sojka et al., 2018a; Sojka et al., 2018b) playing an important role in the formation of the foetal-maternal interface as well as

vascular remodelling of the placenta (Sojka et al., 2019). Phenotypically, uterine NK (uNK) cells are $CD56^{bright}$ and express CD94 and NKG2A but lack expression of CD16 (Eriksson et al., 2004). Similar to cNK cells though, uNK cells also require IL-15 for development (Ashkar et al., 2003), express perforin, granzyme and produce IFNγ (Ashkar et al., 2000; Parr et al., 1990), but appear normal in Tbet – deficient mice (Tayade et al., 2005) and are transcriptionally distinct from cNK cells having different microRNA profiles (Ni et al., 2015). Understanding the role and development of NK cells in the uterus has however proven to be difficult, as the virgin uterus comprises mainly of tissue resident NK cells whereas as during pregnancy, there is a recruitment of cNK cells to the uterine environment (Doisne et al., 2015; Sojka et al., 2018a; Sojka et al., 2019) adding to the extreme heterogeneity of uterine NK populations and much needs to be understood in this developing field of immunology.

1.2.5 Circulating NK cells

Early precursor NK cells are not present in the peripheral blood (Eissens et al., 2012) and most (90-95%) of peripheral blood (circulating) human NK cells express the low affinity CD16 FcγRIII IgG receptor with dim co-expression of CD56, whereas a minority (5-10%) of cNK cells express CD56 brightly and are CD16 positive or negative. Expression of the FcγRIII IgG receptor on $CD16^{bright}$ NK cells mediates antibody dependant cell cytotoxicity (ADCC) interactions, whereas $CD56^{bright}$ NK cells express both the high affinity IL-2Rαβγ and intermediate affinity IL-2Rβγ receptors and are therefore responsive to IL-2 signals producing abundant IFNγ. $CD56^{bright}$ NK cells are therefore considered immunoregulatory and play an important role in mediating immune responses through interactions with various cells. Based on the surface density of CD56 and CD16 human NK cells are therefore defined into 4 subsets, namely: $CD56^{bright}CD16^{neg}$; $CD56^{bright}$ $CD16^{pos}$; $CD56^{dim}CD16^{neg}$ and $CD56^{dim}CD16^{bright}$; (Cooper et al., 2001a) (**Figure 1.5**), with different functional characteristics.

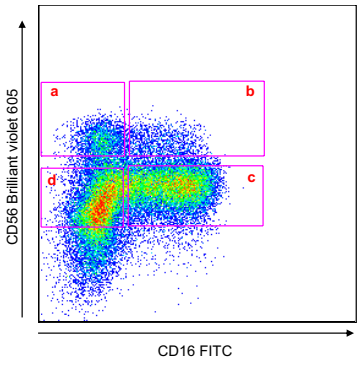


Figure 1.5: Flow cytometry dot plot of mature circulating human NK cells. NK cells are defined as $CD3^{-}CD14^{-}CD19^{-}$ lymphocytes with mature human NK cells phenotypes based on surface expression of CD56 and CD16. a) $CD56^{bright}CD16^{neg}$. b) $CD56^{bright}$ $CD16^{pos}$. c) $CD56^{dim}$ $CD16^{neg}$ and d): $CD56^{dim}$ $CD16^{bright}$.

CHAPTER 1:
Introduction and literature review

The circulation of NK cells found in the periphery is still not clearly understood, but 2 main NK subsets common to both human and mouse peripheral blood and spleen (referred to as NK1 and NK2) have been defined (Crinier et al., 2018). These are present in peripheral blood and the spleen, suggesting that splenic NK subsets are derived from peripheral blood as it circulates through the body. Furthermore, $CD56^{bright}$ NK cells are present in seroma fluid (which represents an accumulation of afferent lymph following surgery) (Carrega et al., 2014; Montalto et al., 2010), providing evidence that $CD56^{bright}$ NK cells may exit peripheral tissues and recirculate to secondary lymphoid organs (SLOs) through lymphatic vessels and therefore high endothelial venules (HEVs) may not necessarily be the only portal of entry utilised by NK cells into LNs. Upon leaving SLOs via the efferent lymphatic vessels, lymph re-enters the circulation via the subclavian vein and $CD56^{bright}CD16^{neg}$ NK cells recirculate via the peripheral blood to the SLOs (Carrega et al., 2014; Montalto et al., 2010) via the periphery. Migration of NK subsets to tissues is mediated by differential expression of specific chemokines (Carrega et al., 2014) and consistent with their expression of lymph homing (CD62L) receptors, $CD56^{bright}$ NK cells are abundant in the lymph nodes.

It is currently accepted that $CD56^{dim}$ NK cells represent a more mature phenotype whereas $CD56^{bright}$ NK cells are a functional but less mature phenotype (Freud et al., 2005; Poli et al., 2009) and that development therefore represents a linear-differentiation model. Differences in the telomere length of $CD56^{dim}$ and $CD56^{bright}$ cells support this hypothesis (Romagnani et al., 2007), as circulating and lymph node $CD56^{bright}$ NK cells have longer telomeres than $CD56^{dim}$ cNK cells. Furthermore, $CD56^{bright}$ NK cells, unlike $CD56^{dim}$ cells, express the receptor for stem cell factor (CD117) as well as homing receptors for SLOs and the alpha chain of IL-7R (Cooper et al., 2001a; Cooper et al., 2001b; Hanna et al., 2004). This hypothesis is also supported by evidence in partial mini-chromosome maintenance 4 deficiency during which $CD56^{bright}$ NK cells fail to proliferate in response to IL-2 or Il-15 and there is a selective loss of $CD56^{dim}$ NK cells (Gineau et al., 2012). Finally, it is further proposed that the differentiation from a $CD56^{bright}$ phenotype to a KIR^{+} and $CD16^{+}$ $CD56^{dim}$ phenotype occurs because of immune activation in peripheral lymph nodes, as nonreactive LN display few NK cells that express KIR or CD16 unlike reactive LNs (Romagnani et al., 2007).

However, as $CD56^{dim}CD16^{bright}$ NK cells can upregulate CD56 and lose CD16 during activation, the hypothesis that $CD56^{dim}$ and $CD56^{bright}$ NK cells undergo separate developmental pathways has not been excluded (Campbell et al., 2001). This is supported by the observation that patients with GATA 2 mutations lose $CD56^{bright}$ NK cells but still have $CD56^{dim}$ NK cells (Mace et al., 2013). This suggests separate developmental pathways,

although these $CD56^{dim}$ NK cells are functionally impaired and reduced in number, indicating some requirement for $CD56^{bright}$ cells. Clonal tracking during haematopoiesis in rhesus macaques also suggests that $CD56^{bright}$ NK and $CD56^{dim}$ NK cells arise separately from each other and that one subset cannot arise from the other (Wu et al., 2014).

The controversy around mature $CD56^{bright}$ and $CD56^{dim}$ human NK cell development therefore remains to be resolved. However, independent of which developmental pathway proves to be correct, alterations in $CD56^{bright}$ NK cells would perturb immunoregulatory mechanisms mediated by $CD56^{bright}$ NK cells and if it is a precursor cell to $CD56^{dim}$ cells, then $CD56^{dim}$ cell cytolytic activity is likely to be disturbed. Therefore, research studies into the basic biology of $CD56^{bright}$ NK cells warrant further investigation.

1.2.6 NK cell licensing and education

During development, NK cells undergo an education process before achieving functional maturity and self-tolerance (Anfossi et al., 2006; Kim et al., 2005). Normal healthy cells express abundant MHC-I molecules that can be downregulated on stressed cells or virus infected and transformed cells. Early studies indicated that NK cells lysed infected or transformed cells with downregulated major histocompatibility complex (MHC) proteins, giving rise to the “missing self” hypothesis (Ljunggren and Karre, 1990) i.e. NK cells recognized infected cells or transformed cells in the absence of certain “self” molecules and provided immune surveillance by eliminating cells with aberrant MHC expression (Bix et al., 1991). The molecular mechanism was identified by (Karlhofer et al., 1992) in IL-2 stimulated $Ly\text{-}49^{+}$NK cells from C57BL/6 mice when it was revealed that the inhibitory Ly-49 receptor specifically recognized MHC class I antigens and prevented lysis of target cells. A similar role was next identified in humans where the control of NK functional activity was shown through engagement of inhibitory KIR receptors with MHC-I molecules (Colonna and Samaridis, 1995; Wagtmann et al., 1995). Thereby NK cells become educated through ligation of KIRs with their cognate MHC ligand expressed on autologous cells.

However, this hypothesis remained incomplete as several studies reported self-tolerance by NK cells to MHC deficient cells (Fernandez et al., 2005; Kim et al., 2005). NK cells that lack expression of inhibitory receptors are not autoreactive but are hyporesponsive to MHC-I deficient cells (Anfossi et al., 2006; Fernandez et al., 2005) and are deemed to be “unlicensed” (Kim et al., 2005) i.e. despite engagement of their activating receptors to a target cell, NK cells remain non-responsive. Thereby, NK cells are required to be "licensed” following an education

process (Kim et al., 2005) and only NK cells that have engaged their inhibitory receptors with self MHC-I molecules during development become fully functionally competent mature NK cells, whereas those that do not bind MHC-I molecules during development remain uneducated with a diminished response to missing-self (Anfossi et al., 2006).

Every mature NK cell balances its activation threshold depending on the strength of inhibitory signals received during development to adapt to the host's MHC phenotype (Brodin et al., 2009a). The combined engagement of inhibitory, activating and adhesion receptors allows NK cells to sense their target (Raulet and Vance, 2006) and integration of these signals will determine the outcome (**Figure 1.6**).

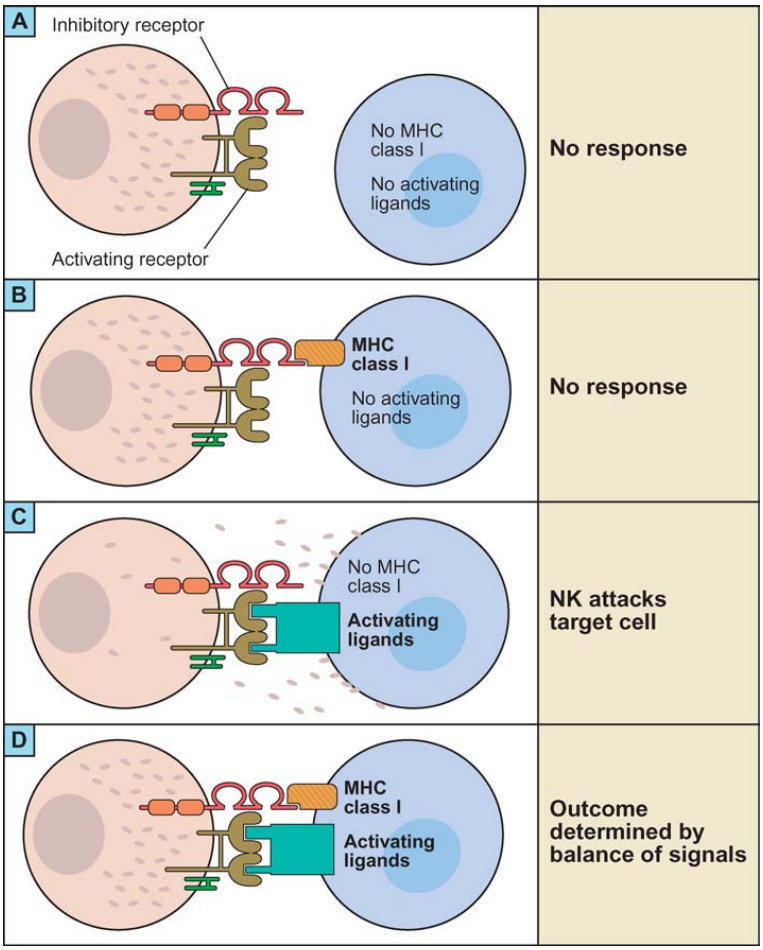


Figure 1.6: NK cell activation and target cell recognition. (A) NK cells expressing inhibitory receptors which have not engaged their cognate MHC-I molecule remain hyporesponsive. (B) Engagement of inhibitory NK receptors to MHC-I molecules in the absence of activating ligands results in no response (C) NK cells degranulate in response to target cells lacking MHC-I expression but expressing activating ligands (D) Engagement of inhibitory NK receptors to MHC-I molecules as well as engagement of NK activating receptor to a ligand expressed on a target cell is determined by a balance of signals. Taken from (Lanier, 2005).

1.2.7 NK cell receptor diversity

NK diversity is generated via two mechanisms: KIR genes (Parham, 2005) and expression of various non-genetically encoded surface receptors influenced by NK cell education (Bjorkstrom et al., 2010; Juelke et al., 2010; Yu et al., 2010), epigenetics (Cichocki et al., 2013) and viral encounters (Beziat et al., 2012; Bjorkstrom et al., 2011; Foley et al., 2012; Petitdemange et al., 2011). With this combination of genetic and epigenetic factors across individuals, more than100,000 NK phenotypes have been identified and an individual can have as many as 6,000 to 30,000 NK phenotypes (Horowitz et al., 2013) with each NK cell expressing a unique pattern of MHC-specific and MHC nonspecific receptors. These receptors include inhibitory, activating, cytokine and chemokine receptors, adhesion molecules and co-receptors/accessory molecules and jointly play a critical role in mediating different NK function.

1.2.7.1 MHC specific NK cell receptors

Vertebrates express major histocompatibility genes (MHC) and their products. Two major sets of MHC genes are MHC-I and MHC -II and under healthy conditions nucleated human cells express MHC-I encoded HLA-A, -B, -C, -G which act as inhibitory ligands for specific NK cell receptors (Lanier, 2008; Long, 1999; Moretta et al., 1997). The KIRs (Colonna and Samaridis, 1995) belong to the immunoglobulin superfamily and are the second most polymorphic genes in humans after human leucocyte antigen (HLA) genes (Parham, 2005) and overall, KIRS are expressed on $CD56^{dim}$ NK cells (Bjorkstrom et al., 2010) but not on $CD56^{bright}$ NK cells (Pende et al., 2019).

Inhibitory interactions between KIRs and MHC-I are mediated by signalling through immunoreceptor tyrosine-based inhibitory motifs (ITIM) (Moretta and Moretta, 1997) whereas activating KIRs associate with a signalling adapter molecule DAP12 which contains an immunoreceptor tyrosine-based activating motif (ITAM). Killer immunoglobulin-like receptors specific for HLA-A (Dohring et al., 1996; Pende et al., 1996), HLA-B (Litwin et al., 1994; Vitale et al., 1996), HLA-C (Colonna and Samaridis, 1995; Wagtmann et al., 1995) and HLA-G (Cantoni et al., 1998; Rajagopalan and Long, 1999) have been identified. Therefore each NK cell has its own unique repertoire of receptors (Santourlidis et al., 2002) but will express at least one inhibitory receptor (Middleton et al., 2002) thus educating signal strength varies between NK cells (Brodin and Hoglund, 2008).

The non-classical HLA-E class-I molecule is recognised by NKG2 C-type lectin family receptors (Houchins et al., 1991) which form heterodimers with CD94 (Lazetic et al., 1996).

HLA-E can signal through either the inhibitory NKG2A receptor or the NKG2C activating receptor, but the inhibitory receptor is dominant. Thus HLA-E^+ target cells are killed only by $NKG2C^+$/$NKG2A^-$ NK cells (Bottino et al., 2000; Moretta et al., 2000; Moretta et al., 2001). The leucocyte immunoglobulin-like receptor (LIR) /immunoglobulin-like transcript (ILT) family is an additional class of HLA- specific receptors and the inhibitory receptor, LIR1 (now commonly known as LILRB1) and ILT2 can broadly recognise HLA class-I (Borges et al., 1997; Colonna et al., 1997; Cosman et al., 1997) whereas LILR2 and ILT4 are thought to recognise HLA-F (Lepin et al., 2000).

1.2.7.2 Non-MHC specific NK cell receptors

The NCRs, NKp30 (Pende et al., 1999) NKp44 (Vitale et al., 1998) and NKp46 (Sivori et al., 1997) are members of the immunoglobulin superfamily, but share no homology with each other (Pende et al., 1999; Pessino et al., 1998; Vitale et al., 1998). NKp30 and NKp46 is constitutively expressed on NK cells (Sivori et al., 1997) whereas NKp44 is expressed on activated NK cells (Vitale et al., 1998). Cooperation between NCRs and the level of NCR expression on an NK cell, mediates NK cell cytotoxicity of certain tumour cell lines (Pende et al., 1999; Pessino et al., 1998; Vitale et al., 1998) and despite the recognition and killing of tumour cells as a result of downregulation of MHC molecules, NCRs are not-MHC specific receptors.

The ligands for NKp46 are unknown, but NKp46 directly recognises influenza haemagglutinin (HA) (Mandelboim et al., 2001) as well as Sendai virus (Arnon et al., 2001) and Newcastle disease virus (Jarahian et al., 2009) haemagglutinin-neuraminidase. Although the NCRs are widely distributed across NK subsets, NKp30 and NKp46 are expressed more brightly on $CD56^{bright}$ NK cells which may suggest an additional requirement for a higher surface density of these receptors in effecting functional responses (Alter and Altfeld, 2009). NKp46 contributes to humoral immune responses in a murine cytomegalovirus (MCMV) model in which a deficiency of NKp46 impacted NK maturation and function as well as preventing migration to the lymph nodes in MCMV infected mice. This resulted in impaired generation of protective murine MCMV antibodies due to limited follicular CD4 T cells (Miletic et al., 2017) indicating that NKp46 deficiency has a compounding effect on immune cell interactions.

In contrast to NCRs, the activating C-type lectin NKG2D, recognises stress-inducible MHC-I proteins and not pathogen-encoded protein (Raulet, 2003). Binding to its endogenous ligands cytomegalovirus UL16-binding protein (ULBP), MHC-class-I-polypeptide-related (MIC) sequence A and B (MICA) and (MICB), mediates lysis of target cells (Cerwenka and Lanier,

2001; Raulet, 2003, 2004) and triggers NK cells to stop migrating and activate the cytoskeletal reorganisation important for developing the immunological synapse (Bryceson et al., 2006a; Culley et al., 2009; Orange, 2008). An additional activating receptor expressed on most peripheral or circulating NK cells is CD16, which is responsible for ADCC reactions and is a low-affinity Fc receptor for immunoglobulin (Ig) IgG (Ravetch and Bolland, 2001). CD16 associates with FcεRIγ (Hibbs et al., 1989) and/or CD3ζ (Lanier et al., 1989b).

1.2.7.3 Accessory NK cell receptors

As discussed above, NK cell receptors therefore employ different molecular means of recognising of HLA class-I downregulation during viral infections, tumour transformation or cells undergoing stress. Once the inhibitory signal is removed, NK cells become activated and the balance of signals between activating and inhibitory receptors determines whether an NK cell is activated to lyse a target cell however, this does require a distinct pattern of co-ordinated responses between receptors (Bryceson et al., 2006a) to protect healthy cells from NK mediated lysis. Indeed, NK cells express a various additional receptors, which are not directly involved in NK cell development or immune surveillance.

Some of these receptors contribute to regulating NK cell activity along with the main triggering receptors, an example being 2B4, which can act as a co-receptor or enhance the effects of CD16, NKG2D and the NKp46 and NKp30 NCRs (Assarsson et al., 2005; Bryceson et al., 2009; Kubin et al., 1999; Nakajima et al., 1999; Sivori et al., 2000), but often the functional significance of additional receptors expressed on human NK cells is not yet fully understood. For example CD27, was originally identified as a T cell differentiation antigen (van Lier et al., 1987) and is associated with memory responses in T cell biology, as its expression is regulated by antigen-specific stimulation of T cells (De Jong et al., 1992). In humans, CD27 surface expression differs between NK cell subsets being mainly expressed on $CD56^{bright}CD16^{neg}$ NK cells (Vossen et al., 2008) and although in mice, CD27 differentiates NK cells into functionally different phenotypes (Hayakawa and Smyth, 2006) its functional expression on human NK cells remains largely unknown. There is some evidence that the same applies to human NK cells (Silva et al., 2008), but few published studies have addressed this topic.

During surveillance, NK cells are required to migrate to sites of injury, infection or transformation and NK cells are actively recruited to these sites (Holmberg et al., 1981; McIntyre and Welsh, 1986; Natuk and Welsh, 1987) and within the *in vitro* setting, NK cells transmigrate across endothelial cells at a faster rate than T cells (Bender et al., 1987; Bianchi

et al., 1993; Pinola et al., 1994). Emigration of immune cells from the peripheral blood involves a multistep adhesion cascade (Butcher and Picker, 1996; Springer, 1995) and NK cells express various homing molecules which help mediate this process. Lymphocyte function-associated antigen (LFA-1) (although found on both $CD56^{dim}$ and $CD56^{bright}$ subsets), is constitutively expressed at higher levels on $CD56^{dim}$ NK cells whereas $CD56^{bright}CD16^{neg}$ NK cells in particular, are enriched for the lymph-homing molecule, CD62L, which is expressed at a higher density on $CD56^{bright}$ NK cells compared to all other peripheral leucocytes (Frey et al., 1998). CD62L expression represents a non-activated ILC (Bar-Ephraim et al., 2019) and can recirculate from blood through the LNs, similar to naïve T cells. Indeed, $CD56^{bright}$ NK cells comprise the primary NK subset within SLO (Fehniger et al., 2003), as CD62L mediates the extravasation of immune cells to LNs, by binding to high endothelial venules (HEVs) which facilitates slow rolling of immune cells (Frey et al., 1998).

Overall therefore, NK cells express a variety of receptors that are differentially expressed between $CD56^{bright}$ and $CD56^{dim}$ NK cells and thereby define the overall characteristics of each NK subset. However, it still remains to be clarified what factors are predominant in determining inherent susceptibility or protection from infection (Rouse and Sehrawat, 2010). A more comprehensive list of NK receptors and co-receptors showing phenotypic comparisons between $CD56^{bright}$ and $CD56^{dim}$ NK cells is summarised in **Table 1.2.**

Table 1.2: Human NK receptors and their ligands.

Molecule	Ligand	CD56^{bright}	CD56^{dim}
HLA-specific receptors			
Inhibitory			
KIR2DL1 (CD158a)	HLA-Cw2, 4, 5, 6	−	Subsets
KIR2DL2/3 (CD158b)	HLA-C1, few HLA-B[b]	−	Subsets
(CD158d)[a]	HLA-G	−	Subsets
KIR2DL5 (CD158f)	?	−	Subsets
KIR3DL1 (CD158e1)	HLA-A-Bw4, HLA-B-Bw4	−	Subsets
KIR3DL2 (CD158k)	HLA-A*03 and *11	−	Subsets
ILT2/LIR-1 (CD85J)	Different MHC- I alleles	.	Subsets
LAG-3 (CD223)	MHC- II	Activated NK cells	
Activating			
KIR2DS1 (CD158h)	HLA-C2	−	Subsets
KIR2DS2/3 (CD158j)	?	−	Subsets
KIR2DL4 (CD158d)[a]	HLA-G	−	Subsets
KIR2DS4 (CD158i)	HLA-A*11 and some HLA-C	−	Subsets
KIR2DS5 (CD158f)	?	_	Subsets
KIR3DS1 (CD158e1)	HLA-Bw4, HLA-F	−	Subsets
Non-HLA-specific receptors			
Natural cytotoxicity receptors			
Activating			
NKp30 (CD337)	BAT-3, HSPG, B7-H6	++	+
NKp44 (CD336)	Viral HA, HSPG, 21spe-MLL5 - Nidogen-1	Activated NK cells	Activated NK cells
NKp46 (CD335)	CFP (properdin), viral HA and HN, PfEMP1	++	+
NKp80	AICL	All PB NK cells	All PB NK cells
KLRG1	Cadherins		
CD2 receptor family			
2B4 (CD244)	CD48	All PB NK cells	All PB NK cells
C-type lectin			
Inhibitory			
NKG2A /KLRD1 (CD159a/CD94)	HLA-E (H), Qa-1[b] (M)	+	Subsets
Activating			
NKG2C, E	HLA-E (H); Qa-1[b] (M)	−	Subsets
NKG2D (CD314)	MIC-A/B (H), ULPBS, RAE-1, MULT-1, H60 (M),	All PB NK cells	All PB NK cells
Antibody dependent cell mediated cytotoxicity			
Activating			
FcγRIII (CD16)	IgG	-/+	+/++
Co-receptors			
DNAM-1 (CD226)	LFA-1, Nectin-2 (CD112), PVR (CD155)	All PB NK cells	All PB NK cells
Homing receptors			
L-Selectin (CD62L)	GLyCAM-1, MadCAM-1	++	Subsets

Taken and adapted from (Sivori et al., 2019).

1.2.8 NK cells interactions with T, B, and dendritic cells

Communication between innate and adaptive arms of the immune system is key to providing an effective immunological defence for vertebrates (Bird, 2017; Rieckmann et al., 2017) and this involves cell-cell interactions as well as signals received through soluble factors such as cytokines.

Cytokines secreted by innate cells can act in an autocrine, paracrine or endocrine manner and actions of cytokines can have immunosuppressive effects on the immune system or promote inflammation. Their role in immune regulation is critical and it is believed that dysregulation of their production plays an integral role in the development of autoimmunity (O'Shea et al., 2002) or what is referred to as a "cytokine storm" (Tisoncik et al., 2012). Importantly, cytokines recruit further innate and adaptive immune cells into an area of inflammation and act as a critical link between the two systems thereby orchestrating the overall immune response. **Table 1.3** lists the major cytokines secreted by cells of the innate immune system.

Table 1.3: Major cytokines secreted by innate immune cells.

Cytokine	Function
TNFα*	Mediates acute inflammation Synthesis of acute phase proteins by liver
IL-1β*#	Mediates acute inflammation
IL-2*#	Early mediator of innate response to intracellular pathogens.
Type 1 interferons (IFNα and IFNβ)	Modulate immune system Provide early defense against virus infected cells
IL-6*	Stimulates liver to produce acute phase proteins
IL-10	Regulates innate and cell-mediated immunity
IL-12#	Promotes T_H1 differentiation Promotes production of IFNγ by NK and T cells
IL-15#	Stimulates NK cell proliferation
IL-18#	Stimulates NK cell to produce IFNγ
TGF-β	Inhibits macrophages Inhibits T and B cell proliferation
IFNγ#	Activates macrophages Promotes B cell isotype switching Promotes T_H1 differentiation Increases expression of MHC class-I and II Increases antigen processing and presentation to T cells

*Cytokines implicated as prime drivers of a "cytokine storm" (Tisoncik et al., 2012).
Cytokines important in NK cell biology. Taken from (Fehniger et al., 2003).

Once antigen is bound to B cell receptors, CD4 T helper co-stimulation is required for activation of B cells to proliferate and differentiate into either memory or antibody-secreting effector cells (Crotty, 2015). Although not a prerequisite for CD8 priming (Epstein et al., 1995), *in vitro* evidence suggests that interactions occur between B cells and CD8 T cells, so B cells are therefore potentially involved in CD8 T cell priming (Barnaba et al., 1990; Ke and Kapp, 1996; Yefenof et al., 1990), which requires the presence of CD4 T helper cells (Castigli et al., 2005) and this intricate network of immune cell interactions is under the influence of cytokines secreted by multiple immune cells, including B,T and NK cells.

$CD56^{bright}CD16^{neg}$ cells are considered the primary source of NK derived cytokines (Cooper et al., 2001a) and as they are abundant in the LNs they can participate in interactions with other arms of the immune system and provide a link between the adaptive and innate immune systems (Fehniger et al., 2003). Secondary lymphoid organs are a complex structure of specialized lymphoid tissue comprising an outer capsule of connective tissue and an inner cortex designed to trap foreign antigen present in the lymph fluid (**Figure 1.7**).

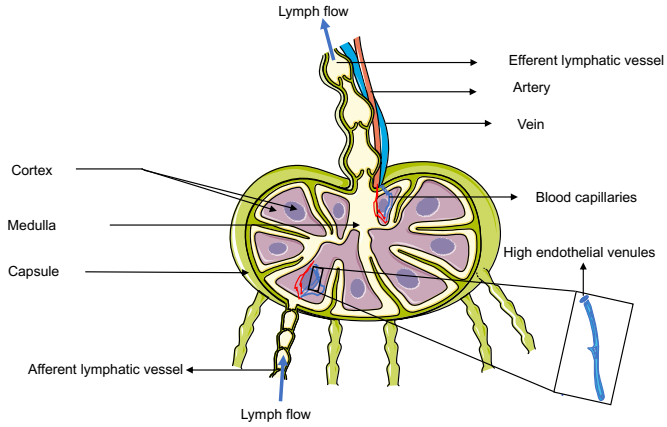


Figure 1.7: Schematic view of the basic anatomical structure and flow of lymph through a lymph node. Lymphatic fluid enters the cortex through the afferent lymphatic vessel and exits via the efferent lymphatic vessel. Adapted from Smart.servier.com Creative Commons Attribution 3.0 Unported License

The inner cortex is further divided into two functional inner and outer regions surrounding a medulla, through which circulating lymphatic fluid enters through the afferent lymphatic vessel and exits through the efferent lymphatic vessel. Naïve B and T cells and antigen presenting dendritic cells (DCs) are clustered in the cortex where, upon encounter with foreign antigen, B and T cells become activated and mature lymphocytes initiate adaptive immune responses and it is within this environment that $CD56^{bright}$ NK cells influence adaptive immune responses through interactions with DCs and secretion of cytokines such as IFNγ (Bajenoff et al., 2006; Martin-Fontecha et al., 2004).

Although $CD56^{bright}$ NK cells do not secrete IL-2, they constitutively express the high affinity IL-2Rαβγ and intermediate affinity IL-2Rβγ receptors and respond to low picomolar concentrations of IL-2 (Caligiuri et al., 1993; Caligiuri et al., 1990). A dynamic interaction exists between $CD56^{bright}$ NK cells and T cells in LNs, where endogenous T cell derived IL-2 activates $CD56^{bright}$ NK cells to produce IFNγ (Fehniger et al., 2003), which may in turn influence

antigen- specific immune responses. Following pathogen uptake e.g. viruses, DCs migrate to LNs where they co-localize with NK cells in the T cell area and promote $CD56^{bright}CD16^{neg}$ activation and IFNγ production through IL-12 and proliferation through IL-15 (Ferlazzo et al., 2004). These interactions are critical as early activation of NK cells is essential for rapid containment of viral infections before the development of adaptive immune responses. Furthermore, using a mouse study, (Martin-Fontecha et al., 2004) showed that NK cells could be recruited to LNs through injection with mature DCs and with certain adjuvants and that this correlated with the induction of a T_H1 response.

Taken together these studies indicate the clear and necessary role that NK cells play in helping modulate elements of the adaptive immune system in the development of memory responses. Therefore, it is important to understand which NK phenotypes are involved in driving the activation of virus-specific elements of the humoral system and crosstalk between various arms of the immune that can be aimed at improving current vaccination strategies.

1.2.9 The role of NK cells in health and disease

Although CD56 has historically been used to describe human NK cells (Nagler et al., 1989), the role of CD56 in human NK cell biology is still not known, but healthy individuals rarely harbor a $CD56^{neg}$ NK phenotype, unlike patients suffering from various pathological conditions where loss of CD56 on NK cells has been observed in chronic viral conditions such as human immunodeficiency virus (HIV) (Mavilio et al., 2005), cytomegalovirus (CMV) (Della Chiesa et al., 2012), hepatitis C virus (HCV) (Gonzalez et al., 2009) and hantavirus (Bjorkstrom et al., 2011). In addition to chronic viral infections, a greater magnitude of $CD56^{neg}$ NK cells has been identified in patients following haematopoietic stem cell transplants from cord blood (Lu et al., 2008) and as immune function declines in the elderly, a decrease in $CD56^{bright}$ NK cells occurs (Camous et al., 2012). Therefore, the expression of CD56 is critical for the normal functioning of NK cells, yet multiple other NK receptors are also involved in NK responses to viral or transformed cells as well as the maintenance of a tolerant environment in solid organs such as the liver and uterus.

As the phenotype of NK cells is proving to be more heterogeneous than previously believed, it has become increasingly clear that this heterogeneity is linked to functional differences. The complexity of NK cells therefore provides for a division of labour driven by phenotypically distinct NK populations which play multiple roles in the immune system by either eliminating target cells upon activation or by production of cytokines and chemokines which activate dendritic cells.

1.2.9.1 NK cells and viral infections

The heterogeneity of NK cell receptors is required for the performance of multiple functions. Killer immunoglobulin-like receptors are key receptors controlling the development and education of NK cells (Rajalingam, 2012) and KIR allelic variants are associated with differential outcomes in mother-to-child HIV transmission (Hong et al., 2013), but the presence of activating receptors on the NK cell surface plays a crucial role in counterbalancing the effects of inhibitory HLA-specific NK receptors, when cytolytic activity against transformed and virus infected cells is required (Lanier, 2005; Moretta et al., 2001). Viruses have developed multiple means of evading the cytotoxic T lymphocyte (CTL) response (Horst et al., 2011) including downregulation of MHC-I. This makes the cell more susceptible to NK lysis, so the role of NK cells is critical for surveillance of virus-infected cells (Jost and Altfeld, 2013). Yet, viruses have also evolved an evasion mechanism, which includes virus encoded class-I decoy molecules that interfere with the KIR system (Lisnic et al., 2010). Human CMV encodes multiple proteins that modulate NK cell recognition of CMV infected cells (Fielding et al., 2014; Wilkinson et al., 2008) and expresses a homolog of MHC-I that binds LILRB1 preventing activation of NK cells (Beck and Barrell, 1988; Farrell et al., 1997). Dependent upon the amino sequence of the viral binding site, *in vitro*-expanded LILRB1^{+} NK cells have different abilities to control viral dissemination of human CMV compared to LILRB1^{-} NK cells, whereas expression of NKG2C has no impact on long-term control of human CMV by NK cells (Chen et al., 2016). Cytomegalovirus (CMV) infected cells upregulate HLA-E expression (Tomasec et al., 2000) as a means to evade detection by NKG2A^{+} NK cells but during CMV infection (both acute and chronic) there is an expansion of NKG2C^{+}/NKG2A^{-} NK cells (Guma et al., 2004; Lopez-Verges et al., 2011; Sun et al., 2009) which allows for the elimination of CMV-infected cells.

These studies indicate the extent of NK immune pressure on viruses and in turn, the plasticity of NK cells in being able to mount counter measures. The NCRs are key activating receptors mediating NK cell cytotoxicity against numerous of viruses with the phenotype of responding NK cells playing a major role in the recognition of virus-infected cells. Although the cellular ligands for the NCRs have not been identified, human metapneumovirus (HMPV) infected cells express an unidentified ligand for NKp46, as NKp46 deficient mice are more susceptible to HMPV (Diab et al., 2017). NKp46 and NKp44 directly interact with sialic acid residues on HA expressed by Sendai and influenza viruses, however NKp30 is unable to mediate such interactions (Arnon et al., 2001), although it can interact with the pp65 antigen of human CMV (Arnon et al., 2005). The importance of NCR-mediated protection against viral infections is indicated in patients living with HIV who have diminished expression of NCRs (De Maria et al.,

2003; Mavilio et al., 2003) and patients with low NK cytotoxic activity are more prone to viral infections including herpes complex virus (HSV) (Biron et al., 1989; Ching and Lopez, 1979), Epstein – Barr virus (EBV) (Joncas et al., 1989; Merino et al., 1986) and CMV (Quinnan et al., 1982). The critical role specifically of NKp46 in control of viral infections is widely documented including studies on influenza (discussed in detail in section 1.2.3), HCV (Golden-Mason et al., 2012), HIV (Frias et al., 2015; Wong et al., 2010) and CMV (Magri et al., 2011).

Accessory molecules can either be altered or remain unaltered during viral infections. The co-activating receptors 2B4 and CD161, remain unaltered in viremic patients with HIV (Kottilil et al., 2004; Mavilio et al., 2003; Moretta et al., 2001; Parato et al., 2002) and even though the role of CD27 expression on human NK cells is not fully understood, *in vivo* studies show that $CD27^{pos}CD56^{bright}$ NK cells may be involved in the clearance of HCV in HIV positive patients (Eisenhardt et al., 2014) and patients co-infected with HIV and HCV have a reduced frequency of $CD56^{bright}$ co-expressing CD27 (Kaczmarek et al., 2017). Therefore, much still remains to be elucidated about the role of accessory molecules in NK cell-mediated clearance of viral infections, but must provide co-stimulation signals to resting NK cells to become fully activated during discrete activation steps (Bryceson et al., 2006b).

Furthermore, viruses can alter the same NK receptor in different ways, for example, NKG2D expression is suppressed during human herpes virus-6 infection (Schmiedel et al., 2016) but is not perturbed in viremic patients with HIV (Kottilil et al., 2004) highlighting the importance of NK cell heterogeneity in receptor expression in controlling multiple viruses that employ differing immune evasion tactics. Indeed heterogeneity of NK cell receptor expression is dictated by genetics and epigenetic factors that are influenced by unique viral encounters (Horowitz et al., 2013), which probably provides a survival fitness to certain individuals.

1.2.9.2 NK cells and transformed cells

Similar to virus-infected cells, downregulation of MHC-I can occur during tumorigenesis (Bubenik, 2003) providing a means of CTL evasion by tumour cells and patients suffering from classical NK deficiency are more prone to various malignancies (Spinner et al., 2014) pointing to the importance of NK cells in providing protection against such events. Evidence to support this was found in a longitudinal study of 3,500 people over a 10-year period, where higher *ex vivo* cytolytic activity of NK cells correlated with reduced cancer risk (Imai et al., 2000).

The role of NCRs has also been investigated and patients being affected by acute myeloid leukemia (AML) have a low density of NKp30, NKp46 and NKp44 surface expression on their

NK cells (Costello et al., 2002), although the mechanism for this downregulation is unclear. Surface density correlates with the ability of NKp46^{+} cells to kill target tumour cells (Sivori et al., 1999) and NKp44 cooperates with NKp46 in cytolytic activity against certain tumour target cells (Vitale et al., 1998). Although two tumour ligands, BAT 3 and B7-H6, have been identified for the NKp30 receptor (Brandt et al., 2009; Pogge von Strandmann et al., 2007), tumour ligands for NKp44 and NKp46 are not known. There are little data on human studies, but the functional importance of CD27 surface expression has been shown in murine studies of solid tumours where CD27^{pos} NK cells are the predominant tumour infiltrating phenotype in a fibrosarcoma model (Hayakawa et al., 2011) and CD27^{pos}CD11b^{neg} organ-specific NK cells protect against melanoma metastases to the liver (Ballas et al., 2013).

NK cell activity has been utilised to improve patient outcomes within the haploidentical stem cell transplant (HSCT) setting. Donor-derived “alloreactive” NK cells specific for self-HLA alleles, allows for the elimination of patient cells missing that particular allele and improving the 5-year survival outcome in AML (Ruggeri et al., 2002). There is an additional role for LILRB1 within the context of cellular transformation. LILRB1^{+} NK cells are expanded in advanced breast and prostate cancer patients (Mamessier et al., 2011; Pasero et al., 2016; Roberti et al., 2015) and blocking of LILRB1^{+} has been shown to enhance the anti-tumour activity of NK cells in multiple myeloma, leukemia, lymphoma and other solid tumours both in an *in vitro* and *in vivo* setting (Chen et al., 2020) suggesting that blocking of LILRB1 represents a novel strategy for immunotherapy in various cancers. It is hypothesized that the expansion of NKG2C^{+}/NKG2A^{-} NK cells mediates the improved outcome in AML (Cichocki et al., 2016; Elmaagacli et al., 2011; Green et al., 2013) and chronic myelogenous leukemia (Takenaka et al., 2015) patients following post-transplant reactivation of CMV.

Interestingly, lactobacilli in the gut mediate laminar propria resident NK cell activity against cancer cells, through induction of TRAIL (Horinaka et al., 2010), indicating that NK cells can recognise and act against tumour cells and do not require downregulated MHC. Overall, therefore, given the critical importance of NK cell surveillance and protection against tumour development and the propensity for CD56^{bright} residency in certain solid organs, a deeper understanding of CD56^{bright} subphenotypes and differences in function associated with these subphenotypes would inform the development of future immunotherapies.

1.2.9.3 NK cells and maintenance of homeostasis

NK cells display functions other than protection against viruses and tumour transformation, which includes vascular remodelling of tissue in cancer (Bruno et al., 2013) and the uterus during early pregnancy (Robson et al., 2012). In addition, trophoblast cells lack MHC expression, yet the uterus remains tolerant to the developing embryo. The uterus is unique, in that the resident NK cells are of a "super bright" CD56 phenotype that surround the conceptus and display little cytotoxicity (Moffett and Colucci, 2014) but rather, activation of these cells promotes better implantation of trophoblasts (Hiby et al., 2008; Xiong et al., 2013).

The liver is highly vascularized, receiving approximately 25% of its blood from the hepatic artery and 75% via the portal vein, which drains from the splanchnic circulation and includes a large amount of foreign antigen from the gastrointestinal tract. This dual blood supply delivers more than 2000 litres (L) of blood into the liver daily where it diffuses into the hepatic capillary system and sinusoids, ultimately exiting liver parenchyma via the hepatic vein. (**Figure 1.8**).

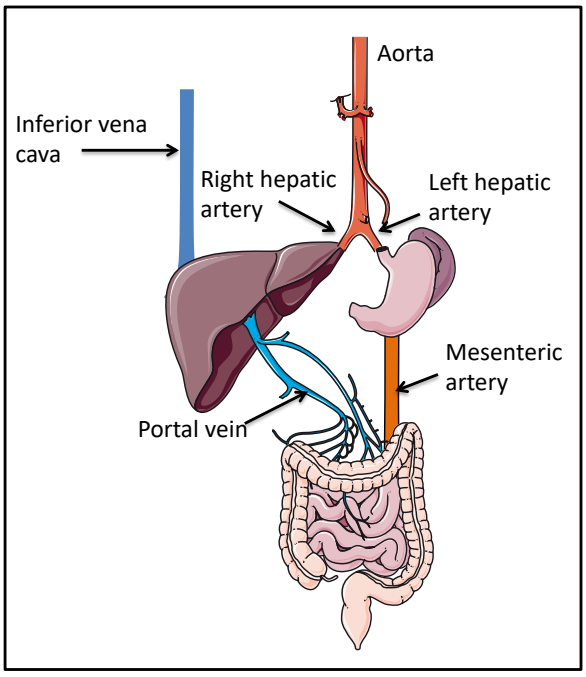


Figure 1.8: Simplified diagram of the splanchnic vasculature. Adapted from Smart.servier.com
Creative Commons Attribution 3.0 Unported License

Unlike the uterus which provides a sterile environment, hepatic NK cells residing or circulating through in the liver are required to maintain tolerance to the vast amount of antigen to which they are exposed, while still responding to pathogens. $CD56^{bright}$ NK cells are abundant in the liver environment, so it can be assumed that they play an important role in these diverse

immune requirements. Although the developmental relationship between $CD56^{bright}$ and $CD56^{dim}$ NK cells remains to be resolved (Scoville et al., 2017), the diverse NK cell repertoire that is found in human liver was recently shown using 29-colour flow cytometry and cluster analysis of high-dimensional data (Filipovic et al., 2019). This offers an interesting insight into liver NK cell biology as Strauss Albee (Strauss-Albee et al., 2015) found that immune experience drove NK diversity at the cost of cytotoxicity. Therefore, it can be postulated that the extreme heterogeneity of liver NK phenotypes and subphenotypes is driven by multiple encounters with antigen and maintains homeostasis of the liver as a consequence of this. Indeed, unlike kidney transplants, recipients of a liver transplant are less likely to reject the organ (Ramos et al., 1995) and liver recipients of other solid organ transplants are less likely to reject these organs if co-transplanted with a liver allograft (Rasmussen et al., 1995).

Yet, despite this tolerance, NK cells play a critical role in preventing liver fibrosis through recognition of HCV-infected cells. Killing of stellate cells in HCV-infection is mediated by $NKG2D^{+}$ (Glassner et al., 2012) and $NKp46^{+}$ NK cells (Kramer et al., 2012) which accumulate in the liver of HCV patients. However in their absence, liver fibrosis is enhanced (Melhem et al., 2006; Radaeva et al., 2006) which suggest that not only do certain NK phenotypes play an antiviral role in hepatitis infection but also serve as regulatory cells essential for the remodelling of fibrotic tissue.

The liver is therefore an important immunological organ which requires a balance between immune tolerance and protection (Crispe, 2009; Hudspeth et al., 2013) and as its microenvironment constantly changes, it is instrumental in regulating systemic homeostasis (Ben-Moshe and Itzkovitz, 2019) warranting further studies in the role of NK cells within this hepatic environment.

1.2.10 NK cells and immune memory

Investigations into the phenotype of memory or recall immune responses within the context of vaccination and natural infection have historically been confined to cells of the adaptive immune system, as conventional immunological dogma has dictated that memory or recall responses cannot be elicited by cells of the innate immune system.

Invertebrates do not possess an adaptive immune system analogous to that of vertebrates, yet there is evidence of specificity and long-lasting immune responses across a range of invertebrates. *Drosophila melanogaster* develops a resistance to *Streptococcus pneumoniae* when injected with a sublethal dose and rechallenged, unlike unprimed fruitflies which

succumb to the infection (Pham et al., 2007). Similarly, red flour beetles, *Triboleum castaneum*, also show evidence of immune specificity. Following priming with heat-killed *Escherichia coli*, they are more likely to survive a subsequent exposure to *E.coli*, than exposure to a heterologous bacterium (Roth et al., 2009). Even more primitive organisms such as tunicates possess recall responses despite the lack of recombination activating genes (Kurtz, 2005; Little and Kraaijeveld, 2004; Schmid-Hempel, 2005).

These studies therefore, provide proof of principle that immune memory can exist outside of the adaptive immune system. Notably the distinction between innate and adaptive immunity is becoming less clear-cut than was previously understood. It is of interest to note that although incomplete and at a low frequency, V(D)J recombination has been observed in NK cells (Borghesi et al., 2004; Igarashi et al., 2002; Kouro et al., 2002; Pilbeam et al., 2008; Yokota et al., 2003). Indeed, NK cells exhibit 'memory-like" responses; ILCs display similar properties as T cells and are classified into groups 1, 2 and 3 based on these properties (Vivier et al., 2018); innate CD8 T cells have been described in mice that are able to differentiate into memory cells independent of foreign antigen (Arlettaz et al., 2004a; Barbarin et al., 2017; Jameson et al., 2015; Van Kaer, 2015) and $CD8^+$ T cells with NK-like properties include CD56 expression as well as other NK receptors such as KIRs have been described (Arlettaz et al., 2004a; Arlettaz et al., 2004b; Bjorkstrom et al., 2012; Warren et al., 2006). These data clearly indicate overlapping properties of immune cells exhibited by different arms of the immune system that are challenging the prevailing paradigms on immune function.

1.2.10.1 NK cell recall responses in mouse studies

Gathering evidence of immune memory in NK cells was first shown in mice, when specific and non-specific NK responses to mouse cytomegalovirus (MCMV) were shown (Dokun et al., 2001). Murine NK cells express the activating receptor, Ly49H, which confers resistance to MCMV infection in mice. The authors showed that during early MCMV infection, IFNγ production was independent of Ly49H expression, whereas with later infection, $LY49H^+$ NK cells selectively proliferated but these cells remained unresponsive to vaccinia virus (VACV) infection. This early study probably represents what is now termed a "trained" immune response. The emerging concept of trained immunity is eloquently defined by Netea et al., (Netea et al., 2020) as: "the long-term functional reprogramming of innate immune cells, which is evoked by exogenous or endogenous insults and which leads to an altered response towards a second challenge after the return to a non-activated state. The secondary response to the subsequent non-specific stimulus can be altered in such a way that the cells respond

more or less strongly than to the primary response, conferring context-adjusted and time-adjusted responses".

Antigen-specific contact hypersensitivity reactions (CHS) to haptens in Rag-/- mice (O'Leary et al., 2006) have been demonstrated using 2,4-dinitrofluorobenzene and oxalone. Not only were these reactions specifically elicited in mice that had been previously sensitized, but this hapten-specific response was transferred to mice after adoptive transfer of liver-derived NK cells from sensitized mice. It was also found that the specificity resided in LyC49-I+ NK cells of which the functional analogue in humans is the KIR receptor. A further significant finding from the same group found that NK cells developed specific memory to HIV, influenza and vesicular stomatitis virus vaccine antigen (Paust et al., 2010), but not to structurally diverse viral antigens. In this study, the group showed clearly that NK cell recall responses in mouse models were specific for challenge antigens and that no NK cell memory responses were elicited when mice were challenged with an antigen to which they had not been previously sensitized. Furthermore, antigen-specific contact hypersensitivity in B and T cell deficient mice was mediated by hepatic NK cells that expressed CXCR6, but not by naïve or splenic NK cells. The importance of hepatic NK cells in these responses was emphasized in a later study (Zhang et al., 2016) which showed that NK cell-mediated CHS responses are impaired in mice that have reduced numbers of liver resident NK cells.

NK cells activated non-specifically by inflammatory cytokines can acquire characteristics of immune memory, including self-renewal and extended lifespan as well as the ability to mount a secondary response. Cytokine activated NK cells that are transferred into mice are phenotypically similar to the recipient's naive NK cells and do not constitutively produce IFNγ. These cells though have an extended life and upon re-stimulation they produce significantly more IFNγ, but not granzyme B and kill targets in a manner similar to that of naive cells (Cooper et al., 2009). It is therefore suggested that unlike neutrophils with high turnover, the ability of innate cells with a low turnover, such as macrophages and NK cells is more likely to be trained (Netea et al., 2020).

The results of the above studies present compelling data to provide proof of concept that NK cells have memory or recall like properties in mice. But the mechanisms driving these responses need to be clarified and understood before a comprehensive model of memory or recall can be developed.

1.2.10.2 NK cell recall responses in human studies

Our understanding of NK cell memory responses has relied heavily on murine models, but observations from various human studies has inferred that NK memory may also apply. In a human mother-to-child HIV transmission study, NK responses to Env and Reg peptide pools was associated with reduced transmission (Tiemessen et al., 2009) and a further study on the same cohort of women revealed that HIV peptide specific NK responses were associated with lower viral load, higher CD4 counts and higher magnitude CD4 T cell responses (Tiemessen et al., 2010). It is of interest to note that that women with $CD3^{neg}$ (NK) responses also had a higher magnitude of CD4 T cell responses. Whether this is a result of genetic influences or interactions between NK cells and the adaptive immune system remains to be investigated, but the NK phenotype responding to Env and Reg peptides needs to be further characterized.

Cytomegalovirus is species-specific, having adapted within its own mammalian host. Functional Ly49 genes do not exist in humans but $NKG2C^+$ NK cells expand within an *in vitro* setting (Guma et al., 2004). Similar to what has been shown in murine $Ly49H^+$ responses during MCMV, $NKG2C^+$ NK cells exist as low precursor levels in CMV naive individuals and human CMV-seropositive individuals have a higher frequency of CD94/NKG2C cells compared to seronegative individuals (Guma et al., 2004; Guma et al., 2006). NK cells play an essential role in immune responses to CMV in humans, as individuals with NK cell deficiencies experience life-threatening consequences when infected with CMV or other herpesviruses (Biron et al., 1989; Etzioni et al., 2005; Orange, 2006). CMV infection shapes the receptor repertoire of NK cells (Guma et al., 2004) and $NKG2C^+$ cells expand in CMV-exposed humans during acute infections with Chikungunya (Petitdemange et al., 2011) or Hanta virus (Bjorkstrom et al., 2011), as well as during HIV infection (Thomas et al., 2012). Furthermore, $CD57^+$ $NKG2C^+$ cells expand during acute CMV infection (Lopez-Verges et al., 2011) and this feature is long-lived and transferrable, since following allo-human stem cell transplant, $NKG2C^+$ NK cells from seropositive CMV donors expand in response to recipient CMV antigen, unlike $NKG2C^+$ NK cells from CMV-seronegative donors (Foley et al., 2012).

Of interest, NK memory-like responses have also been described for extracellular organisms as well, using a malaria infection model. Human volunteers were experimentally infected with *Plasmodium falciparum* (McCall et al., 2010) and venous blood was drawn from volunteers pre- and post-infection. Specific recall NK responses were observed following *ex vivo* stimulation with *P. falciparum* infected erythrocytes, which was partially dependant on the presence of endogenous IL-2 and completely reliant on the presence of memory $CD3^+$ T cells.

Finally, tumour infiltrating $CD56^{bright}CD16^{neg}$ NK cells that show specificity for tumour cells has been identified (Frankel et al., 2010). An autologous tumour line and tumour infiltrating lymphocytes were expanded from a regressing pancreatic adenocarcinoma following immunomodulatory treatment with an anti-CTLA-4 antibody (Ipilimumab). Analysis of the lymphocytes revealed that the majority of NK cells were of a $CD56^{bright}CD16^{neg}$ phenotype and the individual NK phenotypes were sorted. Autologous infiltrating lymphocytes and sorted $CD56^{bright}CD16^{neg}$ cells were reactive to tumours whereas $CD3^{+}$ cells were not. Furthermore the $CD56^{bright}CD16^{neg}$ cells showed specificity for the autologous pancreatic tumour cell line and to a prostate cancer cell line, but not to 5 other pancreatic cell lines or either to colon, ovarian, glioma, breast, lung or melanoma cancer cell lines.

It has therefore been shown in *ex vivo* human and *in vivo* mouse model studies that NK cells can respond in a trained or memory-like manner to antigenic stimulation with elements similar to that of T cell memory or recall responses and suggests interactions between NK cells and memory T cells via soluble factors or through cell to cell interactions. The phenotype of NK cells responding in this manner in humans remains to be characterized as it is suggested that stage 6 NK cells ($CD56^{dim}$, KIR^{+} and $CD57^{+}$), which is the final stage in NK development, represents the generation of “adaptive” NK cells (Abel et al., 2018). However, as discussed above, $CD56^{bright}$ NK cells are implicated in trained responses, are abundant in various solid organs and have longer telomeres and therefore, if longevity is important for developing trained immunity it cannot be ruled out that $CD56^{bright}$ NK cells may have a role to play in NK cell memory responses. It is also plausible that the reason $CD56^{bright}$ NK cells are abundant in LNs and certain solid tissues, is that these are the locations where they become trained through receptor interactions with unique environmental stimuli and antigens, generates the extreme heterogeneity observed in NK cells as these receptors are up- or downregulated. Being responsive to proliferation signals received through the IL2-R they produce an “effector memory” type cell that is able to respond to the same stimulation signals in a memory-like manner.

1.3 Influenza

Influenza viruses are single stranded negative sense ribonucleic acid (RNA) viruses (Pons, 1971) belonging to the Orthomyxoviridae family of which three genera (Influenza A, B and C) infect humans. They share a common genetic ancestor but have diverged genetically and re-assortment between genera has not been reported, although genetic re-assortment is reported within each genus.

1.3.1 Influenza A and B virus structure

Influenza viruses are round or spherical in shape with a matrix 1 (M1) protein enclosing an internal core encasing a nuclear export protein, ribonucleoprotein and RNA- dependant RNA polymerase. The outer lipid layer is studded with HA and neuraminidase (NA) proteins with matrix 2 (M2) ion channels traversing the lipid layer (**Figure 1.9**).

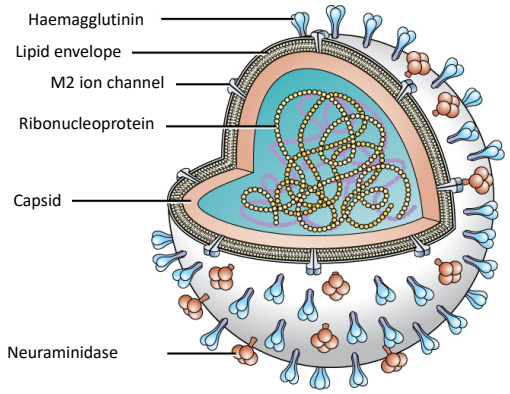


Figure 1.9: Generic illustration of influenza A/B virus. Creative commons image available for download with Windows 365.

The internal M1 and ribonucleoprotein (RNP) type-specific proteins determine the genera and show cross reactivity, whereas the external HA and NA antigens are subtype and strain-specific antigens.

The influenza A and B virus genomes comprise of eight negative-sense, single -stranded RNA segments coding for ten essential proteins as well as strain dependant accessory proteins. However, due to the segmented nature of the genome, antigenic shift can occur, during which influenza A acquires HA and NA segments from another subtype and if re-assortment occurs between human and animal viruses, the encoded novel antigenic protein is foreign to the human immune system. Pandemic influenza arises when the novel virus spreads amongst immunologically naïve humans (Ahmed et al., 2007) which can lead to unprecedented morbidity and mortality as recorded during the 1918 outbreak of H1N1 “Spanish Flu” (Kash et al., 2006; Pappas et al., 2008; Tumpey et al., 2005).

Similarly, a new swine origin influenza A (H1N1) virus resulting from multiple re-assortment events in both humans and swine emerged in the USA and Mexico, in early 2009. The re-assorted H1N1 virus (comprising swine, avian and human segments) was transmitted from swine to humans (Garten et al., 2009; Smith et al., 2009) and as human viruses can “spill back” to swine, this likely represents a single gene pool (Ma et al., 2008) (**Figure 1.10**).

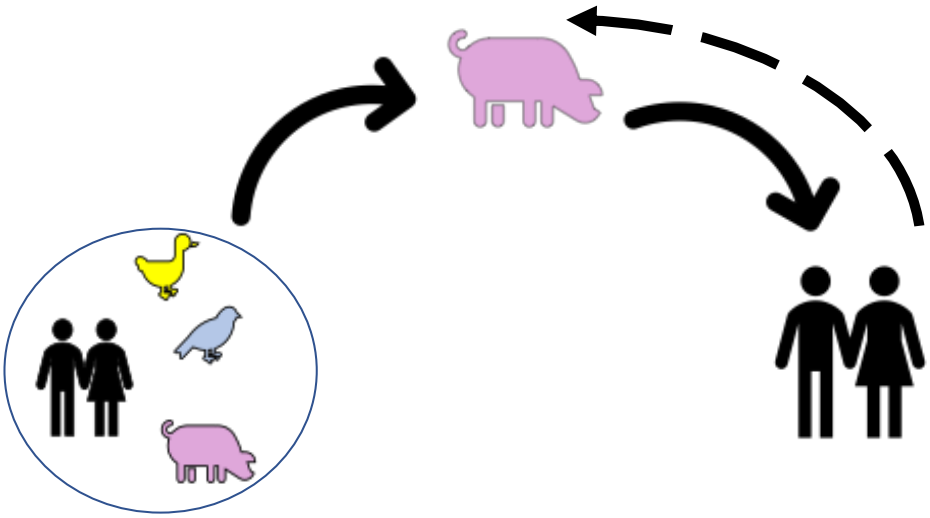


Figure 1.10: Transmission of 2009- H1N1 influenza virus. A re-assorted influenza virus comprising swine, avian and human gene segments was transmitted to swine and then to humans (depicted by solid arrows). Human viruses are thought to potentially "spill back" to swine (dotted arrow).

In contrast to antigenic shift, "antigenic drift" can occur as a result of host immune pressure and to allow for the same host to be re-infected, mutations in antigenic epitopes resulting from polymerase substitutions are selected (Bedford et al., 2014). Antigenic drift is evident in circulating seasonal influenza viruses and, when this occurs, the reformulation of annual influenza vaccine preparations is required.

1.3.2 Viral replication and transmission

Influenza A and B are more common causing more severe disease than C, although influenza C can cause respiratory infections in young children (Matsuzaki et al., 2006). Virus movement from cell to cell is limited by cell type and mucous layers, however sialic acid cleavage by NA enhances viral movement (Cohen et al., 2013) influences viral transmission and invasion of ciliated epithelium of human airways (Matrosovich et al., 2004).

In humans the virus recognizes α2,6 N-acetylneuraminic (sialic acid) (Gambaryan et al., 1997; Matrosovich et al., 2000) situated on the host's cell surface (Gamblin and Skehel, 2010; Hamilton et al., 2012; Weis et al., 1988) and binding to α2,6 sialic residues triggers endocytosis of the virion. The virus is trafficked to the endosome, where the lower pH mediates a conformational change in HA and opening of the M2 ion channel facilitates release of the packaged viral RNP, enabling transfer of the virion to the cytoplasm (reviewed in (Dou et al., 2018)). Using the host's machinery and transport pathways viral RNPs gain entry to the

nucleus where transcription and replication occur. Following export from the nucleus into the cytoplasm, the virus uses the host's translation machinery for protein synthesis and the newly assembled virus is released from the host cell in a manner dependant on its viral NA.

1.3.3 NK cell interactions with influenza

In early influenza infection, various cytokines known to stimulate NK cells are produced including type 1 interferons and IFNγ (Weiss et al., 2010), IL-12 (Monteiro et al., 1998), IL-18 (Liu et al., 2004) and IL-15 (Fawaz et al., 1999) reflecting that NK cells are exposed to stimulatory signals in these early stages of infection. In human studies a marked reduction in NK cell numbers has been shown in severe or lethal H1N1 influenza infection (Denney et al., 2010; Fox et al., 2012) and the early control of influenza infection is also indicated in mouse studies showing the critical and necessary role that NK cells play in clearing influenza virus infection (Gazit et al., 2006). Protection against influenza infection is mediated by NKp46 via interactions with sialic acid residues which leads to the increased killing of influenza-infected cells (Mandelboim et al., 2001). The recognition of NKp46 by influenza HA largely relies on a conserved sugar-carrying residue (threonine 225) and importantly, this recognition is conserved among different influenza strains (Arnon et al., 2004). The virus has however developed an evasion strategy to counteract NKp46 recognition and uses its NA protein to cleave sialic acid residues from NKp46, thereby preventing recognition of viral HA and reducing the elimination of infected cells (Bar-On et al., 2013).

Interactions between NK and T cells during influenza infection have been demonstrated with both arms of the immune system influencing each other. The influence of influenza-A specific IL-2 produced by T cells was shown by (He et al., 2004) in an *ex vivo* setting. Purified NK cells were unable to produce IFNγ and required the presence of T cells, but if anti- IL-2 antibody was added to the stimulation mix even in the presence of T cells, IFNγ responses by NK cells were reduced. The authors concluded therefore, that IL-2 produced by influenza-A specific T cells was required for IFNγ responses by NK cells. On the other hand, in a murine model, the generation of CD8 CTL responses to influenza was shown to require the presence of NK cells (Kos and Engleman, 1996) as during the early stages of infection, NK cells were not only an abundant source of IFNγ (Brandstadter and Yang, 2011) but perforin also helped prime CTL responses (Ge et al., 2012). The significance of NK priming of CTL responses during influenza infection has recently been shown by Liu, *et al*., 2018b. Influenza virus can directly infect NK cells (Guo et al., 2009; Manicassamy et al., 2010; Mao et al., 2009), and NK cells infected with high dose (LD_{50}) virus have impaired NK cell IFNγ and cytolytic activity (Liu et al., 2018b), which is accompanied by reduced virus-specific CTL responses. Although low dose (LD_{25})

influenza infection also infected NK cells, functional activity was maintained and adoptive transfer of splenic NK cells harvested from mice infected with low doses of virus, reversed the weakened virus-specific CTL response. Importantly, the weakened CTL response could not be reversed when splenic NK cells were adoptively transferred from healthy uninfected donors, implying that NK cells had retained a specific "memory" or trained response to viral infection.

Impaired primary CD4 and CD8 T cell memory responses to influenza virus has also been shown in CD27-/- mice which is accompanied by reduced virus-specific CD8 T cell memory responses, indicating that CD27 co-stimulation is required for long term generation of T cell memory (Hendriks et al., 2000). Furthermore, CD27 plays a critical role in the accumulation of influenza virus-specific T cells in the lung (site of infection) and the lung draining lymph nodes by stimulating survival of activated T cells (Hendriks et al., 2003), but persistent co-stimulatory signals mediated by CD27-CD70 interactions can lead to exhaustion of the T cell pool (Tesselaar et al., 2003).

Much remains to be understood about the immune responses to influenza antigen in the lung. Lungs contain NK cell phenotypes similar to those found in the periphery, including a similar proportion of $CD56^{bright}CD16^{-}$ NK cells (reviewed in Hervier et al., 2019 (Hervier et al., 2019)) which play an important role in control of influenza infection (Cooper et al., 2018), yet, due to excess degranulation, are also implicated in lung damage (Scharenberg et al., 2019). Lung $CD103^{+}$ DCs however, remain uninfected and carry influenza protein to draining LN and cross present antigen to CD8 T cells and induce influenza virus-specific responses. This is however, dependent on the expression of a type 1 IFN receptor present on $CD103^{+}$ DCs (Helft et al., 2012).

1.3.4 Influenza vaccination induced immune responses

Vaccine efficacy is measured either by using a haemaglutination inhibition test or by determining virus neutralizing antibody titres since antibody development is the key protective immune response to intramuscularly administered influenza vaccination in healthy individuals. The efficacy however, of annual influenza vaccines is limited by viral evolution as the prime immune response to seasonal influenza vaccination is a B cell mediated antibody response to HA and this varies between strains. As antibody responses are specific, they therefore do not provide cross reactive protection to other strains, hence the requirement for annual adjustments to vaccine formulations if antigenic drift occurs.

Both quadrivalent and trivalent inactivated vaccines (TIV) as well as live attenuated influenza vaccines (LAIV) are available formulations for immunization against influenza, but there is controversial evidence as to which vaccine offers better protection against influenza infection (Ambrose et al., 2011; Eick et al., 2009; Wang et al., 2009). Vaccination against seasonal influenza has decreased efficacy in older adults with an effectiveness ranging between 17% and 53% (Bernstein et al., 1999; Goodwin et al., 2006; Jefferson et al., 2005) and vaccination prevents culture confirmed illness in only 30%-40% of cases (Gross et al., 1995; Nicholson et al., 2003). Antibody responses to influenza vaccination are also reduced in patients that are immune compromised making it advisable not to administer LAIV to immunocompromised individuals (Joshi et al., 2009). The impaired antibody response to influenza vaccination in HIV-infected patients is attributable to deficiencies in their innate immunity (Pallikkuth et al., 2011a), yet patients with rheumatoid arthritis that have been treated with rituximab (which targets CD20 expressed on B cells), maintain a cellular response similar to that of healthy controls (Arad et al., 2011) but have an impaired humoral response following influenza vaccination. Therefore, despite the interactions between various arms of the immune system (section 1.1.8) that are required for optimal immune responses, robust cellular responses can be maintained under certain conditions.

Cells of the innate immune system recognize conserved pathogen-associated molecular patterns (PAMPs) on foreign antigen and modulate adaptive immune responses, so therefore offer the potential to be included in either the development of a universal vaccine able to offer protection across viral strains, or help improve current vaccine efficacy to better protect vulnerable populations. Lymph node dendritic cells play a key role in driving the activation of virus-specific T cells and formation of B cell memory (Gonzalez et al., 2010; Woodruff et al., 2014) and following influenza vaccination in mice, there is a rapid increase in NK cell mediated IFNγ production in the draining lymph nodes, which with IL-6, regulates B cell responses to influenza (Farsakoglu et al., 2019). Therefore, interactions between adaptive and innate immune systems are necessary to mount a vaccine mediated protective response to influenza virus. Heterologous immunity can develop after encounters with a pathogen, which subsequently confers a response to an unrelated pathogen (Clark, 2001; Selin et al., 1998; Welsh and Selin, 2002) so the development of a universal vaccine is therefore attractive, particularly within the context of heterologous immunity. Given the complexity of immune interactions, not only in direct cell-cell interactions, but also the influence of soluble and anatomical location, much still remains to be elucidated and investigations into the basic biology of these interactions are not only required but essential.

1.4 Polychromatic flow cytometry for functional phenotyping of immune cells in health and disease

Many questions around the immune system still remain unanswered, but with the development of the first flow cytometer by the Herzenberg group (Hulett et al., 1969) the ability to immunophenotype and assign functionality to cells at a single cell level has revolutionised our understanding and knowledge of the human immune system. Based on the premise that through binding of a fluoroscein labelled monoclonal antibody to a receptor of interest, antibody secreting B cells were identified and isolated (Hulett et al., 1969) and differences in cytotoxic capabilities of T lymphocytes based on bright or dim expression of Thy 1.2 were shown (Cantor et al., 1975). This proved to be a powerful means of characterizing immune cell. The inclusion of multiple fluorophore conjugated monoclonal antibodies allowed for binding of specific epitopes of interest at a single cell level in one experiment and changes in immune cells during the course of disease could be characterized driving the need for further advances in polychromatic flow cytometry (> 5 colours) (Roederer et al., 1997).

Major advances in polychromatic flow cytometry were driven by HIV studies which included phenotyping T memory cells (Mosmann and Coffman, 1989; Mosmann et al., 1997; Picker et al., 1995; Thomas and Lefrancois, 1988), characterisation of immune dysfunction (Hengel and Nicholson, 2001), monitoring of disease progression (Schnittman et al., 1990), (Roederer et al., 1995) (Margolick et al., 1995) (Delobel et al., 2005) and an understanding of the immune cells driving immune reconstitution inflammatory syndrome in patients starting anti-retroviral treatment (Wilson and Sereti, 2013).

The application of polychromatic flow cytometry in these diverse studies has highlighted the various scientific questions addressed in HIV immunology which could be applied to the study of other immune cells and in the context of other infections. However, it was realised that human immune cells circulating in the periphery comprised hundreds of different cell (De Rosa and Roederer, 2001), each with different functional capacities and in varying degrees of activation and memory development, which required the identification of multiple markers at a single cell level. This drove the need for even further developments in flow cytometry, both in instrumentation, fluorochromes, reagents and data analysis programs and since then, polychromatic flow cytometry has become a tool widely used in the field of immunophenotyping cells in basic and translational research. This does bring with it however, technical challenges (Perfetto et al., 2006a) because of the precision required for accurate measurements of multiple fluorochromes with spectral overlap. Therefore, to ensure optimum

instrument performance and reproducibility of results, constant instrument monitoring and strict adherence to a daily quality assurance (QA) program is required (discussed in greater detail in chapter 4, section 4.1) as interlaboratory variances on the same sample set and batches of reagents can be wide (Maecker et al., 2005).

The recent development of mass cytometry or cytometry by time-of-flight (CyTOF) has also allowed for detection of up to 40 cellular markers, without the complications of spectral overlap. This technology was recently used to measure 32 different parameters on peripheral NK cells from unrelated individuals and monozygotic twins, revealing for the first time, the extremely broad diversity of NK cells at a phenotypic level (Horowitz et al., 2013). These data when combined with genetic analysis, revealed that variations in activating receptor expression is a consequence of prior antigen exposure unique to each individual, whereas inhibitory receptor expression is largely determined by genetics. The authors calculated that within their cohort of 5 sets of twins and 12 unrelated individuals, there were approximately 124,651 unique NK cell phenotypes. Despite this diversity, a limiting factor would be that the study focussed on NK phenotypic markers and activating and inhibitory receptors, rather than on accessory molecules and co-receptors which help facilitate cytolytic function or production of cytokines in mature activated NK cells. Notwithstanding the valuable information this technology provides, it is still not widely available to laboratories because of cost and expertise constraints and many laboratories rely on conventional laser-based instruments. Conventional polychromatic flow cytometry is therefore still an important technological resource for the study of diverse NK cell phenotypes and the monitoring of NK functional responses to antigens.

Studies are emerging which highlight that the conventional classification of NK cells into $CD56^{bright}$ and $CD56^{dim}$ subsets is insufficient to explain different functions in subset-associated phenotypes. The significant plasticity of the NK cell within and amongst individuals and the ongoing advancements in instrumentation and availability of specific monoclonal antibodies against different epitopes relating to phenotypic and functional parameters will not only strengthen our insights into the dynamic role of NK cells in immune responses, but may also contribute to determining what factors define or drive the NK functional phenotype.

1.5 Study rationale

Increasingly evidence is emerging that NK cells not only respond innately but can become "trained" following an initial encounter with antigen or with vaccination and respond to a second encounter with the same antigen in a "memory-like" manner. $CD56^{bright}CD16^{neg}$ NK cells play an important immunoregulatory role but are still a relatively under researched NK subset than

the predominant $CD56^{dim}CD16^{pos}$ subset circulating in the periphery. Currently, humans are facing the challenge of emerging viruses novel to the adaptive immune system, hence the importance of innate cells providing immune protection during the development of adaptive responses. NK cells are rapid responders and are at the forefront of eliminating virally infected cells, but in certain instances are implicated in the development of tissue injury during the process of killing virally infected cells. Yet conversely, hepatic NK cells remain tolerant within the antigen laden environment of the liver and are important in maintaining liver homeostasis. The activation of NK cells requires co-operation between accessory molecules or co-receptors with NK activating receptors and a deeper understanding of immunoregulatory $CD56^{bright}CD16^{neg}$ NK subphenotypes are required, so as to provide a basis to understand various mechanisms underpinning immunologically induced pathology or tolerance, as well as protection against disease through natural infection or immunisation.

1.6 Aims and objectives

As the $CD56^{bright}CD16^{neg}$ NK subset is considered immunoregulatory and is the most abundant NK subset present in the lymph node and hepatic environment, the overall objective of this study was to use an influenza vaccination model to monitor post-vaccination functions and phenotypes so as to identify vaccination imprinted alterations in $CD56^{bright}CD16^{neg}$ NK subphenotypes that may traffic from the periphery to the lungs or lymph nodes. An NK cell perfusate model was utilized in addition, to gain further insights into understanding the role of the understudied $CD56^{bright}CD16^{neg}$ NK cell subset.

The specific objectives were:

1. To develop and optimize a multi-colour flow cytometry panel of known memory markers for CD8 T cells, in addition to other potential candidate markers, in order to simultaneously characterise NK subsets and CD4 and CD8 T cell phenotypes and functions.
2. To describe unique $CD56^{bright}CD16^{neg}$ NK subphenotypes that may be altered through innate immune stimulation or acquisition of a “memory” or “trained” response using an influenza vaccination model.
3. To determine alterations in $CD56^{bright}CD16^{neg}$ NK subphenotypes prior to, and following, influenza vaccination, and to compare these to the development of CD4 and CD8 T cell responses.
4. To describe phenotypes of hepatic NK cells and compare to matched peripheral blood NK cells, from individuals with healthy or diseased livers, using liver perfusate as a source of hepatic NK cells.

CHAPTER 2:
Materials and Methods

2.1 Study Populations and Sample Collection

2.1.1 Influenza vaccine participants

Twelve healthy (HIV^- ve) participants (2 males [Caucasian] and 10 females [1 Black African, 1 Coloured and 8 Caucasian]) with a median age of 36.5 years; (range: age 28 – 57 years), were vaccinated with a standard 0.5 ml dose of Influvac® subunit inactivated (no adjuvant) influenza vaccine (Solvay Pharmaceuticals), containing 15 µg each haemaglutinin and neuraminidase antigen of strains A/California/7/2009(H1N1)-like virus; A/Perth/16/2009(H3N2)-like virus and B/Brisbane/60/2008 virus). Fifteen to 18 millilitres (ml) venous blood was collected in ethylenediaminetetraacetic acid (EDTA) tubes from participants at pre-vaccination, 3 days post-vaccination, and 6 months post-vaccination time points and for 5 participants, blood was collected 1 year post-vaccination. Samples were processed within 4 hours (hrs) of collection. Pre-vaccination blood was collected from all participants during the first week of April, prior to the advent of the influenza season. Two participants had a history of regular annual influenza vaccinations and 4 participants had been vaccinated the preceding year. At the time of sample collection no participant reported clinical symptoms suggestive of active influenza infection.

2.1.2 Healthy donor and control bloods

A normal, healthy donor buffy coat (250 ml; leukocyte-enriched whole blood from an HIV-1 and hepatitis B virus (HBV) negative donor) was obtained from the South African National Blood Services (SANBS) and processed within 3 hrs. Aliquots of peripheral blood mononuclear cells (PBMCs) isolated from the donor blood were used for flow cytometry panel development (Chapter 3) and served as a control to ensure reproducibility of data across experiments over time.

Venous blood (15 – 18 ml) was collected in EDTA tubes from healthy controls (4 males aged 27 – 57 years and 5 females aged 30 – 54 years) and processed within 4 hrs of collection. These bloods served as peripheral blood controls for phenotypic characterization of hepatic NK cells (Chapter 7).

2.1.3 Liver transplant perfusate

The *ex vivo* liver (hepatic) perfusate that is usually discarded as waste after transplantation of a liver was collected from 9 deceased liver donors (6 males aged 17 – 51 and 3 females aged 38 – 52) and an acute liver failure (ALF) patient (female aged 46). Routinely with liver transplantation, the aorta is clamped and the liver flushed *in situ* via the portal vein and hepatic artery with up to 2 litres (L) cold histidine-tryptophan-ketoglutarate (HTK) preservation buffer.

After resection the liver is perfused with a further 1 to 2 L cold HTK and if required reduced in size or “split” during the “back table” preparation. The perfusate generated at this stage was collected in sterile containers (**Figure 2.1**) and processed within 8 hrs of collection.

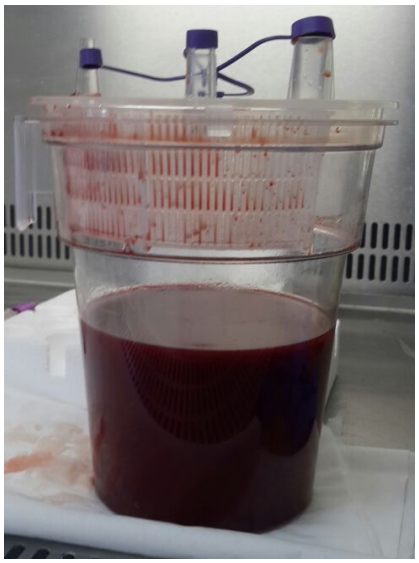


Figure 2.1: Example of a sterile collection device used to collect liver (hepatic) perfusate during organ harvest. Following clamping of the aorta, cold histidine-tryptophan-ketoglutarate (HTK) buffer is perfused through the liver via the portal vein and hepatic artery until perfusate runs clear.

2.2 Ethical clearance

Ethics approval was obtained from the Human Research Ethics Committee of the University of Witwatersrand, ethical clearance certificate M2011137 (**Appendix A**). Written informed consent was obtained from vaccinees at the time of enrolment in the influenza study and participants acting as controls for hepatic phenotyping comparisons. Transplant co-ordinators of the Donald Gordon Transplant unit obtained written consent from relatives of deceased organ donors for the collection of hepatic perfusate at the time of organ donation. Permission was obtained from the Chief Executive Officers for collection of hepatic perfusate at Life Hospitals, Mediclinic and Netcare private hospitals.

2.3 Cell Isolation

2.3.1 Isolation and cryopreservation of peripheral blood mononuclear cells

Peripheral blood mononuclear cells (PBMCs) from influenza vaccinated and control participants for hepatic NK cell comparisons, were isolated from whole blood by Ficoll-Paque^{TM} Plus (GE-Healthcare Bio-Sciences AB, Sweden) density gradient centrifugation. Briefly, 10 ml of whole blood was carefully layered onto 20 ml Ficoll-Paque ^{TM} Plus (room temperature) and centrifuged in a Sigma 4K15 centrifuge for 30 minutes (mins) at 800 x g-force (g) with the brake off. The top plasma layer was removed, transferred to a 15 ml falcon

tube (Becton Dickinson, New Jersey, USA) and further processed as described in section 2.4. The PBMC layer was removed and transferred to a 50 ml falcon tube (Becton Dickinson, New Jersey, USA) and washed twice with calcium and magnesium (Ca^{2+} and Mg^{2+}) free phosphate buffered saline (PBS; Highveld Biological; final volume 50 ml) by centrifugation at 300 X g for 10 mins (brake on). Cell pellets were resuspended in 5 to 10 ml PBS and cell viability determined using an improved Neubauer haemocytometer after dilution at a ratio of 1:1 with 0.4% trypan blue (Merck-Sigma, United Kingdom). The mononuclear cells were washed one last time and the cell pellets resuspended in a cryoprotectant containing 90% heat inactivated fetal bovine serum (FBS) (Gibco Life Technologies, USA) and 10% dimethyl sulfoxide (DMSO) (Sigma-Aldrich, UK) at a cell concentration of 5 X 10^6 cells per ml. Aliquots (1 ml) were pipetted into 2 ml cryovials and placed in a Mr Frosty™ freezing container at -80°C. Frozen cells were transferred to liquid nitrogen tanks for long term storage of cells until required.

2.3.2 Hepatic perfusate derived cells

Hepatic perfusate was dispensed into 50 ml falcon tubes and centrifuged at 400 X g for 10 mins. The supernatant was discarded and cells were layered onto Ficoll-Paque ™ Plus at a 1:1 ratio and cells isolated by density gradient centrifugation and stored as described above in section 2.3.1.

2.4 Freezing of plasma samples

Plasma removed during the Ficoll-Paque™ Plus density gradient centrifugation step described above in section 2.3.1, was spun at 2 600 revolutions per minute (rpm), for 15 mins at room temperature in a Sigma 4K15 centrifuge and finally aliqoted into 2 ml cryovials and stored at -80 °C until required.

2.5 Thawing and resting of cryopreserved Cells

Cryovials containing 1 ml aliquots of cells were removed from liquid nitrogen and thawed in a 37°C water bath until a pea-sized pellet of ice remained. Cryovials were wiped with 70% ethanol to maintain aseptic conditions and cells resuspended in 1 ml pre-warmed R10 (RPMI 1640 medium (Gibco Life Technologies, USA) supplemented with 10% heat-inactivated FBS (Gibco Life Technologies, USA) and 1% penicillin/streptomycin/glutamine (Gibco™)). Cells were transferred to 15 ml Falcon tubes (Becton Dickinson, New Jersey, USA) containing 8 ml pre-warmed R10 and benzonase® (50 U/ml) (Merck Millipore, Germany) (R10/benzonase). Cells were centrifuged at 300 X g at room temperature for 10 mins. The wash step was repeated in R10 to ensure all traces of DMSO were removed and viable cell numbers quantified as described in section 2.3.1, to ensure a viability of at least 80%. Cells were finally

resuspended in R10 at a concentration of 2 X 10^6 cells/ml. Cells used for phenotyping were rested overnight in an incubator (37°C and 5% CO_2) while those for the influenza vaccine arm of the study were rested for 6 – 7 hrs.

2.6 *Ex vivo* Cell Stimulations

2.6.1 *Ex vivo* influenza stimulations

To control for inter-assay variation, pre- and post-vaccination time points for each participant were performed in the same experiment. Thawed and rested cells were checked for viability with trypan blue staining, centrifuged at 300 x g and resuspended in R10 medium in polypropylene flow cytometry tubes to give a final concentration of 2 x 10^6 cells per ml. *Ex vivo* influenza stimulations (abbreviated to flu-stimulations), using pre-titrated (**Appendix B**) Influvac (Solvay Pharma) preparation with which participants had been vaccinated, were performed at a concentration of 0.5 µg/ml. PBMC's were incubated in a 37°C humidified incubator with 5% CO_2 for 12 - 13 hrs. The co-stimulatory antibodies CD49d and CD28 (BD Pharmingen™) were included for optimal detection of T cell responses to antigen stimulation at a final concentration of 1 µg/ml and protein transport inhibitors Brefeldin A (10 µg/ml; Sigma-Aldrich, St-Louis, USA) and GolgiStop (0.7 µl/ml; BD Biosciences, California, USA) were added and cells were incubated for a further 6 hrs in a 37°C humidified incubator with 5% CO_2. Control (co-stimulated) cells were prepared in the same manner but with the exclusion of flu antigen and were included for each time-point

2.6.2 *Staphylococcus aureus* enterotoxin B stimulations

Staphylococcus aureus enterotoxin B (SEB; Sigma Aldrich, USA) was used for stimulation of PBMCs for IFNγ (cytokine secretion) and CD107a (cell degranulation antibody titrations. Briefly, PBMC rested overnight were checked for viability and centrifuged at 300 x g for 10 mins and resuspended in R10 medium at a concentration of 2 x 10^6 cells per ml. SEB was added to give a final concentration of 1 µg/ml and in the presence of the co-stimulatory antibodies and protein transport inhibitors the PBMC incubated in a 37°C humidified incubator with 5% CO_2 for 6 hrs.

2.7 Preparation of stimulated and unstimulated cells for staining

Cells were resuspended in 4 ml PBS (Ca^{2+} and Mg^{2+} free, Highveld Biological) and centrifuged twice at 400 X g for 4 mins. After discarding the supernatant the cell pellets were resuspended in PBS to give a concentration of 2 x 10^6 cells/ml and 1 ml aliquots dispensed into 4 ml polystyrene flow cytometry tubes (BD Biosciences). Following centrifugation at 400 x g for 4

mins, the supernatant was discarded and tubes blotted on clean paper towelling to allow for a concentrated pellet of cells.

2.8 Staining with fluorochrome conjugated monoclonal antibodies

To ensure consistent staining in each experiment, pre-titrated (**Appendix C**) fluorochrome conjugated monoclonal antibodies were combined into a master mix, before 100 µl aliquots were dispensed into tubes containing 2 x 10^6 cell pellets.

2.8.1 Staining of cells with amine reactive dye

Amine LIVE/DEAD® discriminator (Invitrogen, Molecular Probes) was prepared according to the manufacturer's instructions and a 1 µl aliquot added to prepared cell pellets (section 2.7) and the suspension mixed and incubated in the dark at room temperature for 10 mins before commencement of surface staining.

2.8.2 Surface staining of cells

Following staining with amine dye (section 2.8.1), aliquots of 100 µl pre-titrated fluorochrome conjugated monoclonal antibodies were added to 2 x 10^6 prepared cell pellets and incubated in the dark at room temperature for 20 mins. Cells were washed by adding 2.5 ml 1% wash buffer (PBS supplemented with 1% FBS) and centrifuged at 400 x g for 4 min. For cells only requiring surface staining, the supernatant was discarded and cells resuspended in 300 µl 1% paraformaldehyde (Thermo Scientific) and kept at 4^{o}C in the dark until acquired (within 24 hrs of staining) on a BD LSRFortessa (BD Biosciences, La Jolla, CA, USA). For cells requiring intracellular cytokine staining (ICS) (section 2.8.3), the supernatant was discarded following the centrifugation step and tubes gently blotted to leave a cell pellet.

2.8.3 Intracellular cytokine staining of cells (ICS)

Prepared (and surface stained) cells were permeabilized and fixed by adding 250 µl BD Cytofix/Cytoperm™ and incubated in the dark for 15 mins at room temperature. 2.5 ml 1X BD Perm/Wash buffer™ was added and cells were centrifuged at 400 x g for 4 min. To remove all traces of permeabilisation solution the supernatant was discarded, wash cycle repeated, supernatant discarded and tubes blotted on paper towel. Aliquots of 100 µl pre-titrated fluorochrome conjugated monoclonal antibodies were added and cells were incubated for 45 mins at 4^{o}C in the dark. Cells were washed twice by adding 2 ml 1X BD Perm/Wash buffer™ and centrifuging at 400 x g for 4 mins and resuspended in 300 µl 1% paraformaldehyde. Cells were kept at 4^{o}C in the dark and acquired within 24 hrs of staining on a BD LSRFortessa (Becton-Dickinson, La Jolla, CA, USA).

2.8.4 CD107a staining for measuring degranulation

Staining for measurement of degranulation was performed by adding pre-titrated CD107a Pacific blue (Bio-Legend, San Diego, USA) in the same step as described for the addition of co-stimulatory antibodies in sections 2.6.1 and 2.6.2.

2.8.5 Staining of compensation beads

Single stained, anti-mouse Ig, κ polystyrene microparticle beads (BD™ CompBeads) and BD™ CompBeads negative control beads (BD Biosciences) were used for compensation purposes. Single stained compensation beads were prepared by adding 1 drop of compensation beads to 100 µl PBS. Pre-titrated antibody was added and tubes incubated in the dark at room temperature for 20 min. Two ml of PBS was added to each tube and centrifuged for 10 mins at 200 x g. The supernatant was discarded and beads resuspended in 300 µl 1% paraformaldehyde and kept in the dark at 4^{o}C for no longer than 24 hrs until acquired. The same protocol was followed for negative beads but without the addition of fluorochrome-conjugated antibody.

2.9 Statistical Analysis

Flow cytometric data (including Boolean gated data) were analysed using FlowJo^{TM} software for Mac (version 9.9.4), Ashland. Means, medians, ranges, coefficient of variation (CV), and statistical comparisons (nonparametric Wilcoxon and Mann-Whitney U tests) were performed using Prism 5 (GraphPad software). Statistical significance was defined as a *P* value of <0.05.

CHAPTER 3
Development and Validation of a Twelve Colour Flow Cytometric Panel to Study T cell and NK Phenotype and Function

3.1 Introduction

NK cells are large granular lymphocytes that do not express CD3, CD14 or CD19, and are phenotypically characterised by expression of CD56 (Robertson and Ritz, 1990). Differential co-expression of CD56 and CD16 delineates NK cells into 4 subsets (Cooper et al., 2001a) with expression of multiple surface receptors determining phenotypic heterogeneity of NK cells. NK cell function is tightly regulated by the integration of signals from multiple activating and inhibitory receptors, which include natural cytotoxicity receptors (NCR) (Pende et al., 1999; Sivori et al., 1997; Vitale et al., 1998), C-type lectin-like receptors and the CD158 family of killer immunoglobulin-like receptors (KIRs) (Colonna and Samaridis, 1995). IFNγ is considered the prototypical cytokine and is secreted upon receiving secondary signals from IL-2, IL-12, or the IL-15/IL-15RA complex (Caligiuri, 2008) and NK cells are critical in providing protection from viral infections (Biron et al., 1989) and the lysing of transformed cells (Kiessling et al., 1975) through the release of perforin and granzyme cytolytic enzymes. Because they play an important role in health and disease, phenotypic characterization of NK cells not only provides us with a better understanding of the diversity of NK cells, but also allows us to realize their impact on physiologic and pathophysiologic processes. Such knowledge can be harnessed for therapeutic applications in various disease conditions.

Flow cytometry is a powerful analytical tool that has enabled the characterization and functional analysis of cells within heterogenic cell populations. Advances in flow cytometry have increased the possibility for more complex polychromatic panels (Bigos et al., 1999; Roederer et al., 1997), facilitating a deeper understanding of the distribution and interaction of different immune cell types (Tung et al., 2007) thus providing valuable insights into immunological disorders or diseases. Although polychromatic flow cytometry can detect multiple epitopes at a single cell level and greatly improve our understanding of the nuances of the human immune system (Perfetto et al., 2004), it has also introduced a complexity of technical challenges as there are no standardized protocols for flow cytometric phenotyping and assessment of cell function. Factors impacting the quality of polychromatic flow cytometry data include:

a) choice of fluorochromes - not all fluorochromes work well together in a panel for reasons unknown, or are suitable as a marker for the receptor under investigation (Lamoreaux et al., 2006),
b) inclusion or exclusion of a live/dead cell discriminator to eliminate undesirable measurement errors (Perfetto et al., 2006b),

c) lack of standardisation of assays to allow for reproducibility and consistency of results (Lamoreaux et al., 2006; Maecker et al., 2005),
d) placement of flow cytometry gates (Maecker et al., 2005) and different gating strategies defining NK phenotypes and functions with subsequent interpretation of data,
e) inadequate instrument monitoring and validation (Perfetto et al., 2006a),
f) spectral overlap resulting in complications with compensation (Roederer, 2001).

Key to this study was the development of a polychromatic flow cytometry panel. In this chapter, the design and validation of a 12 colour flow cytometry panel is described that simultaneously phenotypes and determines functional responses of T cells and NK cells, allowing the definition of the 4 major NK subsets, NK subphenotypes and T cell memory compartments.

3.2 Materials and Methods

3.2.1 Donor sample.

A normal donor buffy coat (Chapter 2, section 2.1.3) was used to develop and validate the 12 colour flow cytometry panel and served as a control to provide data for inter-experiment variation.

3.2.2 Cryopreservation and thawing of samples

PMCs were isolated from the donor sample and aliquots cryopreserved as described in Chapter 2, section 2.3.1 and thawed and rested as described in Chapter 2, section 2.5.

3.2.3 Cell stimulations

Ex vivo flu- stimulations (Chapter 2, section 2.6.1) were performed for validation of T cell and NK cell subsets and SEB stimulations (Chapter 2, section 2.6.2) for detection of IFNγ and CD107a antibody titrations.

3.2.4 Staining protocols

Cells were prepared for staining as described in Chapter 2, section 2.7. Cells were then stained to eliminate dead cells (Chapter 2, section 2.8.1), stained for expression of surface receptors (Chapter 2, section 2.8.2) and stained intracellularly (Chapter 2, section 2.8.3) for detection of IFNγ and CD3 (which can be downregulated upon antigen stimulation). Detection of CD107a for degranulation was performed as described in Chapter 2, section 2.8.4. and compensation beads prepared as outlined in Chapter 2, section 2.8.5.

3.2.5 Development of polychromatic flow cytometry panels

3.2.5.1 Fluorochromes

A standard LSRFortessa (Becton-Dickinson, La Jolla, CA, USA) fitted with a 488 nm blue laser, 405 nm violet laser, 640 nm red laser and 355 nm ultra-violet laser was used in this study. The choice of fluorochromes was therefore determined by the filter configuration, laser types and the availability of fluorochrome conjugates. Wherever possible bright fluorochromes were chosen for dim markers and fluorochromes providing good separation of populations were preferentially chosen. For critical markers such as those discriminating between NK subsets, the amount of contaminating spillover from other channels was taken into consideration such that there was maximum detection sensitivity and minimal spreading error (Perfetto et al., 2004) (**Appendix D: determination of primary fluorescence**).

To ensure the best separation between positive and negative populations (Lamoreaux et al., 2006), titrations were firstly performed on fluorochrome conjugated antibodies (**Appendix C: antibody titrations**) for the following fluorochrome conjugated monoclonal antibodies used in the flow cytometry panels (**summarised in Appendix E**): anti-CD14 allophycocyanin cyanine 7 (APC Cy7) or allophycocyanin hilite 7(APC H7), anti-CD19 APC Cy7 or anti-CD19 APC H7, anti-IFNγ (Alexa fluor 700), anti-CD62L allophycocyanin (APC), anti-NKp46 phycoerythrin (PE) obtained from BD Pharmingen; anti-CD8 quantum dot 705 (QDot® 705) or anti-CD8 brilliant violet 705 (BV 705) anti-CD4 phycoerythrin cyanine 5.5 (PE Cy 5.5), anti- CD56 brilliant violet 605 (BV 605), anti-CD3 phycoerythrin cyanine 7 (PE Cy7), anti-CD16 fluoroscein isothiocyanate (FITC), anti-CD27 phycoerythrin cyanine 5 (PE Cy5), anti-CD107a Pacific blue (Pac Blue), and anti-CD45RO R Phycoerythrin-Texas Red® (ECD) obtained from Beckman Coulter.

3.2.5.2 Fluorescence minus one controls for defining NK subsets

Cell markers that may be expressed as a continuum from dim to bright such as CD56 and CD16 do not present as discrete negative and positive populations and the complexity is compounded where markers are co-expressed, making it difficult to determine correct placement of gates. Fluorescent minus one (FMO) experiments were performed for CD56 and CD16 expression to determine NK subsets by staining unstimulated PBMCs with a full panel with the exclusion of CD56 for the CD56 FMO and CD16 for the CD16 FMO. A fully stained panel was included for each FMO as a control.

3.2.5.3 Flow cytometer, instrument settings and compensation settings

Before commencement of the study, system optimisation as described by Perfetto *et al*., 2006 (**Appendix F**) was undertaken to assess instrument performance and a modified quality assurance (QA) protocol (Perfetto et al., 2006b) performed which included system calibration and system standardisation (**Appendix G**). To ensure the correct allocation of fluorochromes to each parameter and that primary fluorescence was maintained, single stained and unstained polystyrene BD CompBeads™ (**Appendix G**) were used to generate compensation matrices before acquisition of each experiment and spectral overlap calculated electronically using FlowJo™ software for Mac (version 9.9.4).

3.2.6 Acquisition of cells and statistical analysis

Between 750,000 and 1 X 10^6 cells were acquired for all experimental data at a flow rate of no more than 7,000 events per second and 10,000 compensation beads at a flow rate of no more than 300 events per second. Data were collected using BD FACSDiva™ software (version 6) and imported into FlowJo™ software for Mac (version 9.9.4), Ashland for development of gating strategies and data analysis. Proportions of gated cells were calculated as a percent (%) of the parent population using FlowJo™ Software for Mac (version 9.9.4), Ashland and Prism (version 5) software was used to calculate the CV of gated cells from experiments run over time.

3.3 Results

3.3.1 Development of gating strategies

3.3.1.1 Development of anchor gating strategy

Band-pass and long-pass filters allow for photons of a specific wave-length to be detected by photomultiplier tubes (PMTs), but with the addition of each fluorochrome to polychromatic flow cytometry panels, spectral overlap cannot be avoided and some fluorochromes do not necessarily work well in combinations with others (Lamoreaux et al., 2006). A 6 colour "anchor marker panel" was developed first comprising of CD3 PE-Cy7, CD4 PE-Cy5.5, CD8 Qdot 705, CD56 BV605, CD16 FITC with CD14 and CD19 APC-Cy7 and a far red live/dead discriminator combined into a single "dump" channel. Singlets were selected by plotting forward scatter height (FSC-H) against forward scatter area (FSC-A) (**Figure 3.1A**) and lymphocytes selected (**Figure 3.1B**) based on side scatter area (SSC-A) and FSC-A parameters. Monocytes ($CD14^+$), B cells ($CD19^+$) and dead cells were excluded in a dump channel. Live $CD3^+$ and $CD3^-$ cells defined T cells (CD4 and CD8) and $CD56^{pos/neg}CD16^{pos/neg}$ NK cells (**Figure 3.1C**), respectively. Discrimination of $CD3^-$ NK cells based on CD16 and CD56 expression (**Figure**

3.1D), required FMO gating (discussed in section 3.3.1.2), whereas CD4 and CD8 T cells were clearly separated (**Figure 3.1E**).

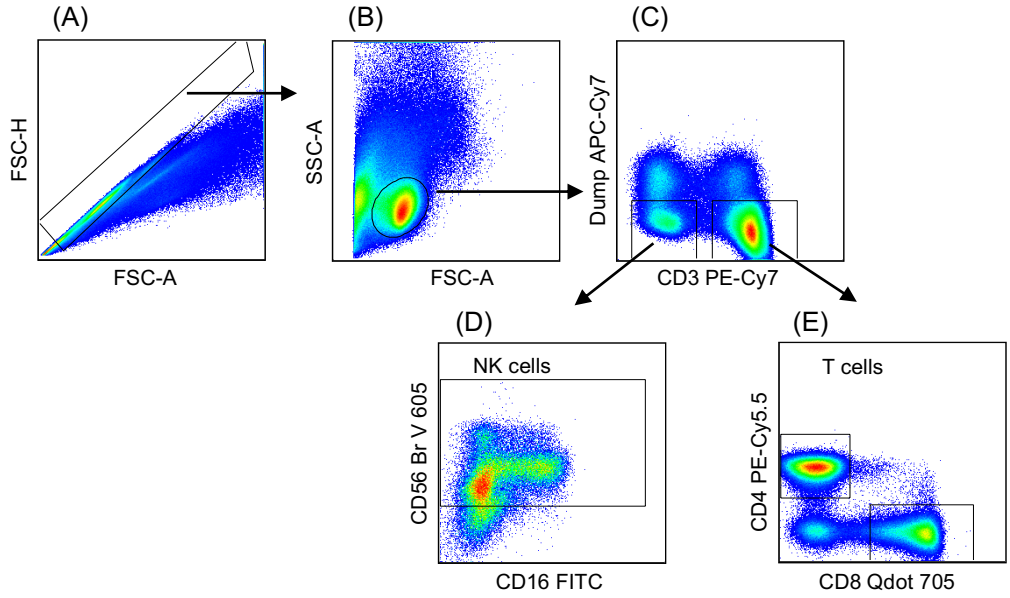


Figure 3.1: Anchor marker panel and anchor gates identifying NK and T cells. Doublets were excluded with forward scatter area (FSC-A) and forward scatter height (FSC-H) gates (A) and lymphocytes selected on granularity, side scatter area (SSC-A) and size (FSC-A) (B). B cells, monocytes and dead cells were excluded in a dump channel and $CD3^{+}$ and $CD3^{-}$ cells (C) gated to identify NK cells (D) and CD4 and CD8 T cells (E).

Once the anchor marker gating strategy was developed and placement of gates verified, the gates remained constant for all experiments and were not changed or moved.

3.3.1.2 Defining NK subsets using fluorescent minus one gating

As CD56 is expressed as a continuum from very dim to bright, FMO gating was applied to $CD3^{-}$ NK cells (**Figure 3.2**) to differentiate between $CD56^{bright}$ and $CD56^{dim}$ cells and distinguish gating for CD16 co-expression. FMO gating allowed for correct placement of gates for CD56 (**Figure 3.2A**) and CD16 (**Figure 3.2B**), differentiating NK cells into 4 subsets viz. $CD56^{bright}CD16^{neg}$, $CD56^{bright}CD16^{dim}$, $CD56^{dim}CD16^{bright}$ and $CD56^{dim}CD16^{neg}$ (**Figure 3.2C** a,b,c,d, respectively) which conforms with the 4 NK subsets described by Cooper *et al*., (2001). Importantly, FMO gating allowed for the correct placement of gates to exclude $CD56^{neg}CD16^{neg}$ cells (e) not treated as NK cells.

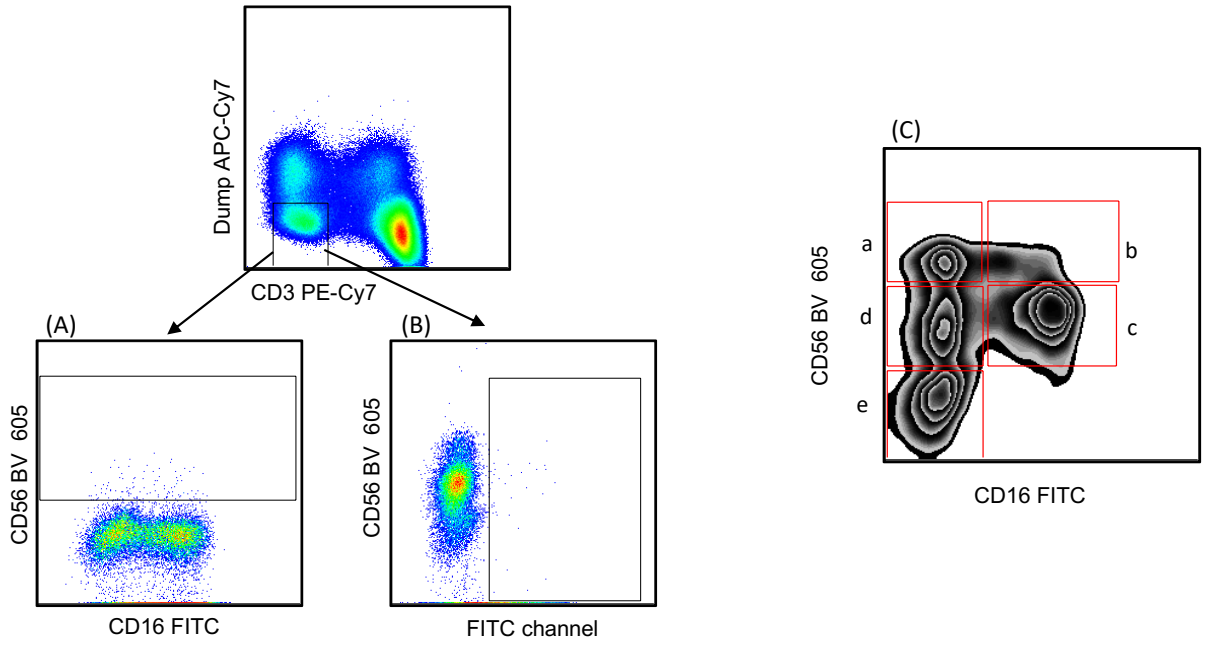


Figure 3.2: Fluorescence minus one (FMO) gating for CD56 and CD16. Three aliquots of thawed and rested PBMCs were stained and acquired on an LSRFortessa set up for a full panel. One panel excluded staining for CD56 (the CD56 FMO) (A) the second excluded staining for CD16 (the CD16 FMO) (B). A full panel that included both CD56 and CD16 (C) was used as a control for the FMO's and for correct placement of gates. Four NK subsets were identified: (a) $CD56^{bright}CD16^{neg}$; (b) $CD56^{bright}CD16^{pos}$; (c) $CD56^{dim}CD16^{pos}$ and (d) $CD56^{dim}CD16^{neg}$. The $CD56^{neg}CD16^{neg}$ gate (e) was determined by fluorescence minus one and excluded from NK analysis. Abbreviations: neg = negative; pos = positive.

3.3.1.3 Development of a twelve colour flow cytometry panel

Once fluorochromes were successfully combined into an anchor marker panel, secondary markers were included. The use of many fluorochromes in a single panel results in multiple spectral overlaps (Roederer, 2001) which cannot always be successfully compensated. FITC was preferentially chosen for anti-CD16 and BV605 for anti-CD56 due to the minimal spillover between these 2 channels. Evaluation of the compensation matrix confirmed that the multiple fluorochromes were successfully compensated and spillover between anti-CD16 FITC and anti-CD56 BV605 was minimal (**Table 3.1**) with primary fluorescence (**Appendix D**) achieved for each fluorochrome used in the panel.

Table 3.1: Panel description and compensation matrix.

Panel Description												
12 colours	**IFNγ**	**CD62L**	**CD14/19/ far red amine**	**CD16**	**CD107a**	**NKp46**	**CD27**	**CD3**	**CD45RO**	**CD4**	**CD56**	**CD8**
NK cells	IFNγ	CD62L	*(-ve)	CD16	CD107a	NKp46	CD27	*(-ve)	-	-	CD56	-
T cells	IFNγ	CD62L		-	CD107a	-	CD27	CD3	CD45RO	CD4	-	CD8
Compensation Matrix												
	AlFluor 700	**APC**	**APC-Cy7**	**FITC**	**Pac Blue**	**PE**	**PE-Cy5**	**PE-Cy7**	**ECD**	**PE-Cy5.5**	**Qdot 605**	**Qdot 705**
AlFluor 700		1.475	42.51	0.36888	0	0.2125	0.1558	0.6805	0.1134	0.9512	0.05784	12.3
APC	58.71		26.57	0	0	0	2.607	0.1709	0	0.525	0.06991	10.34
APC-Cy7	7.891	3.354		0	0	0	0.1439	1.019	0	0	0	0.5347
FITC	0	0	0		0	22.38	1.705	0.1441	9.164	0.5656	1.212	0.138
PacBlue	0	0	0	0		0	0	0	0	0	0.472	0
PE	0	0	0	0.8875	0		9.407	0.6359	43.49	3.669	11.46	1.413
PE-Cy5	35.73	55.62	17.36	0.08242	0	1.05		8.672	0.6036	36.97	0.1242	14.51
PE-Cy7	1.322	0	23.97	0.2594	0	2.37	0.8119		1.206	0.204	0.2407	0.2973
ECD	0.08691	0.1162	0	0.2583	0	11.75	31.92	3.007		14.87	17.66	5.158
PE-Cy5.5	17.68	2.874	11.77	0.4391	0	33.63	16.78	31.01	14.36		3.629	36.8
BV 605	0	0	0	0	12.44	0.3105	1.225	0.1217	2.797	0.4089		22.61
BV705	15.51	0.3313	8.405	0	23.4	0	0.09388	1.715	0	2.511	0.1644	

*(-ve): gated population for exclusion
Single stained, anti-mouse Ig, κ polystyrene microparticle beads (BD™ CompBeads) were used to determine the compensation matrix

3.3.2 Validation of flow cytometrically defined NK and T cell phenotypes

3.3.2.1 Validation of the $CD56^{bright}CD16^{neg}$ NK cell subset

The main objective of this study was to analyse $CD56^{bright}CD16^{neg}$ NK responses to 2009-influenza vaccine in relation to T cell memory responses. Therefore, a basic phenotyping analysis was done on CD28/CD49d co-stimulated and flu-antigen stimulated cells to ensure that the 12 colour flow cytometry panel could clearly delineate the $CD56^{bright}CD16^{neg}$ NK subset into phenotypes and provide IFNγ and CD107a functional data with the stimulation protocol and reagents used in the study. The 12 colour panel was able to distinguish 4 NK subsets defined by expression of CD16 and CD56 (**Figures 3.3A and B**) and NK subphenotypes (**Figures 3.3 (A1) and 3.3 (B1)**) based on the expression of NKp46, an important natural cytotoxicity receptor for NK cell recognition of viral haemagglutinin (Mandelboim et al., 2001), the lymph homing marker CD62L (Frey et al., 1998) and CD27 shown to functionally delineate NK cells in humans (Vossen et al., 2008) and mice (Hayakawa and Smyth, 2006). Cytokine (IFNγ) and CD107a (degranulation) effector molecules were also distinguishable (**Figures 3.3 (A2) and 3.3 (B2)**).

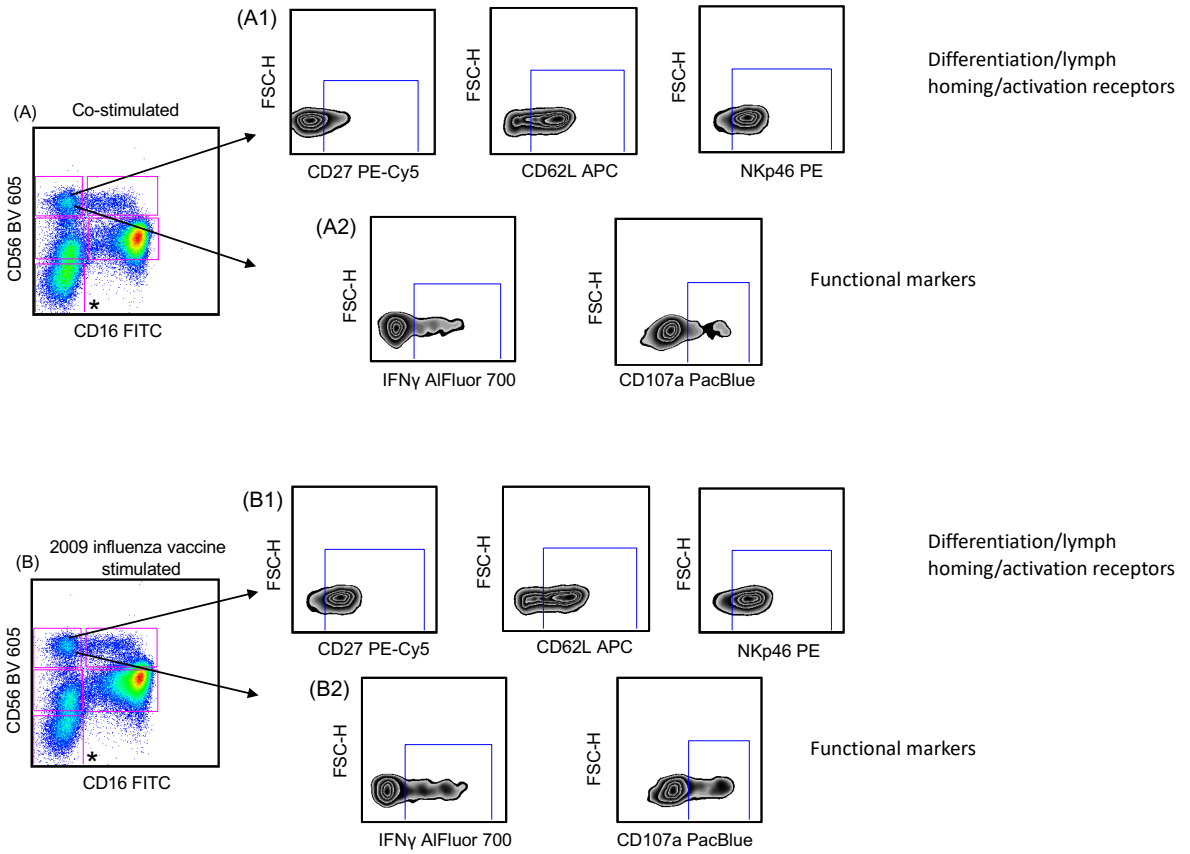


Figure 3.3: Representative example of flow cytometry dot plots to validate staining of NK subsets and functional markers. PBMCs were prepared and stained under the same stimulation conditions and staining protocols as test samples. Top panel: Co-stimulated (control) (A) and flu- stimulated (B) $CD56^{bright}D16^{neg}$ NK cells were gated for (B1) CD27, CD62L and NKp46 expression (as indicated) to identify differentiation/lymph homing/activation receptors and (B2) IFNγ and CD107a (as indicated) functional responses. *$CD56^{neg}CD16^{neg}$ population was determined by FMO gating and excluded from NK data analysis. Abbreviations: neg = negative; FMO = fluorescence minus one.

Peripheral NK cells and their subsets are heterogenous in expression of cell surface molecules which is reflected in the diversity of their functions. Compared to $CD56^{dim}$ NK cells, $CD56^{bright}$ NK cells are enriched for CD62L (Frey et al., 1998) and CD27 (Vossen et al., 2008) but NKp46 is expressed on all major NK subsets. To ensure that the fluorochrome conjugated monoclonal antibodies chosen to label CD27, CD62L and NKp46 would not only provide adequate staining (**Figures 3.3 A1 and B1**) in the same mix with the other conjugates under the experimental conditions used in this study, but also agree with expression frequencies reported in the literature, the NK subsets were further phenotyped based on their frequency of expression of CD27, CD62L and NKp46 (**Table 3.2**).

Table 3.2: Frequency of CD27, CD62L and NKp46 expression on NK subsets

	CD27	CD62L	NKp46
$CD56^{bright}CD16^{neg}$	48.46	55.13	86.80
$CD56^{bright}CD16^{dim}$	55.98	65.65	98.96
$CD56^{dim}CD16^{bright}$	31.08	18.45	90.04
$CD56^{dim}CD16^{neg}$	26.28	4.95	38.30

Data are presented as the mean of 5 experiments for CD27 and NKp46 and 4 experiments for CD62L.

The phenotyping data indicated that both $CD56^{bright}$ subsets were enriched for CD62L and CD27 compared to $CD56^{dim}$ subsets and NKp46 was expressed ubiquitously across 3 major NK subsets. The unconventional $CD56^{dim}CD16^{neg}$ subset is not well characterised, but expression of the activating receptor, NKp46, agreed with a recent study (Roberto et al., 2018) which reported low expression levels of NKp46. The 12 colour flow panel confirmed that, compared to $CD56^{dim}$ NK subsets, $CD56^{bright}CD16^{neg}$ NK cells are enriched for CD27 and CD62L and that NKp46 is expressed on the vast majority of cells defined as NK cells. This is consistent with what is reported in the literature (Frey et al., 1998; Silva et al., 2008).

3.3.2.2 Validation of T cell phenotypes

The development of memory T cell cells is influenced by the site of infection and tissue type in which infection has occurred (Woodland and Kohlmeier, 2009). T cell memory phenotypes are therefore heterogeneous, but it is generally accepted that CD27 is expressed on naïve and a subset of memory T cells (De Jong et al., 1992). During T cell activation and memory development, various surface receptors are differentially regulated including expression of CD45RO (Akbar et al., 1988) and CD62L (Sallusto et al., 1999). For the current study, T cell phenotypes were broadly characterised as indicated in **Table 3.3**.

Table 3.3: Phenotyping of CD4 and CD8 T cells characterised by surface expression of CD27, CD62L and CD45RO.

	CD27	CD62L	CD45RO
Naive	+	+	-
Central memory	+	+	+
Effector memory	-	-	+
Effector	-	-	-

CD4 and CD8 T cells were gated off live CD3+ cells and were clearly separated on flow cytometry dot plots (**Figures 3.4A and 3.4B**) with little discernible difference between co-stimulated and flu- stimulated cells. CD4 and CD8 T cells were then quadrant gated for CD62L and CD27 surface expression (**Figure 3.4C and 3.4D**) and each quadrant gated for CD45RO positive and negative populations. A representative example of gated CD45RO populations is shown (**Figures 3.4E** and **3.4F**). All populations and subsets were clearly distinguishable although it was noted that CD45RO expression was downregulated with flu-stimulation (percent CD45RO expression is indicated in **Figures 3.4E and 3.4F**). Despite the downregulation of CD45RO on stimulated cells, a naïve phenotype and 3 populations broadly representative of T cell memory phenotypes **(Table 3.3)** were clearly distinguishable.

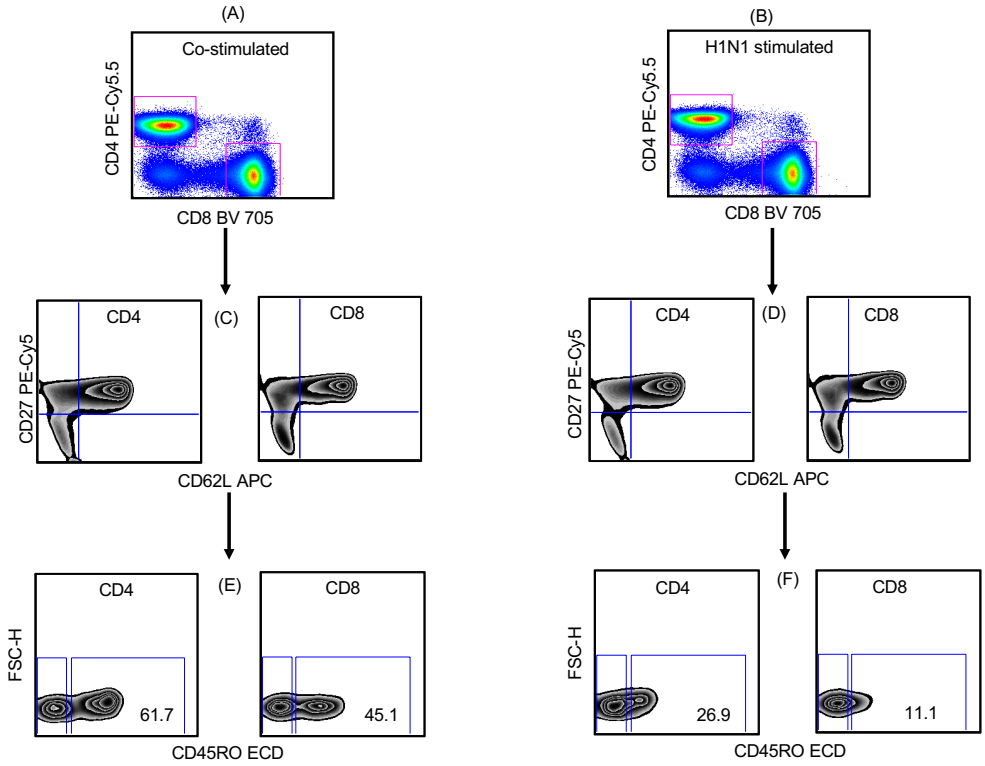


Figure 3.4: Representative flow cytometry dot plots to validate staining of CD4 and CD8 T lymphocytes and memory subsets. Using the same experimental conditions described in Section 2.7 and 2.9, CD4 T lymphocytes, stained with PE-Cy5.5 and CD8 T lymphocytes, stained with BV705 could be clearly delineated in co-stimulated (A) and flu-stimulated (B) cells. CD4 and CD8 populations were quadrant gated for CD27 and CD62L surface expression (C) and (D) and each quadrant then gated for CD45RO expression (E) and (F). Numbers in CD45RO$^+$ gates indicate percent CD45RO of parent population.

3.3.3 Validation of inter-experimental variance

To determine the degree of inter-experimental variances, flow data from 5 experiments (conducted over a period of months) using blood bank donor co-stimulated cells was analysed. In the absence of any standardized guidelines, the coefficient of variation (CV), mean and

standard deviation (SD) (calculated using Prism 5, GraphPad Software) of key parameters were plotted to ascertain variances of experimental data between experiments.

3.3.3.1 Inter-experimental variances of NK subsets

Inter-experimental variances for the $CD56^{bright}$ NK subsets was first determined. There was little variation between experiments measuring $CD56^{bright}CD16^{neg}$ NK cells (CV 5.11%) and this variation was marginally greater when $CD56^{bright}CD16^{dim}$ NK cell populations were assessed (CV 7.73%) (**Figure 3.5A**). Inter-experimental variances were greater for the predominant $CD56^{dim}CD16^{bright}$ NK subsets (CV 9.08%) (**Figure 3.5B**) and particularly so for the "unconventional" $CD56^{dim}CD16^{neg}$ subset which had a CV of 14.8%.

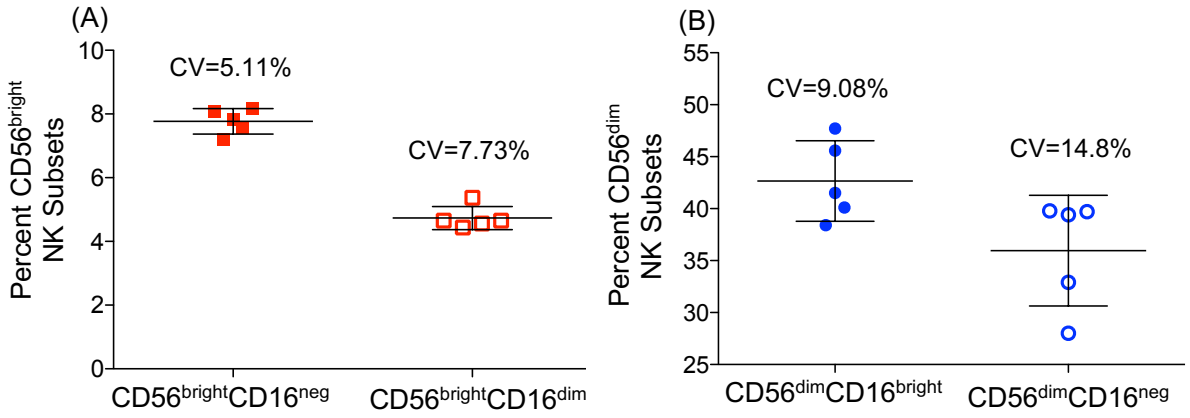


Figure 3.5: Inter-experimental variances for $CD56^{bright}$ (A) and $CD56^{dim}$ (B) NK subsets. Variances between experiments were determined using co-stimulated PBMCs from a blood bank donor. Error bars represent one standard deviation (1SD) from the mean (confidence interval of 95%) of 5 experiments. CVs, means and standard deviations were calculated using Prism (Version 5.0; GraphPad Software).

3.3.3.2 Inter-experimental variances for NKp46, CD27 and CD62L NK subphenotypes

As observed for the NK subsets the variances between experiments for the CD27, CD62L and NKp46 NK subphenotypes for both $CD56^{bright}$ compartments was low compared to that for the $CD56^{dim}$ subsets (**Figure 3.6**). CVs were the largest for CD62L (8.66% and 15.62% for $CD56^{bright}CD16^{neg}$ and $CD56^{bright}CD16^{dim}$, respectively), possibly because the mean could only be calculated from 4 experiments. Critically, inter-experimental CVs and SD were good for the $CD56^{bright}CD16^{neg}$ subset and CVs were less than 10% for any sub-phenotype. CVs for the NK subphenotypes are summarised in **Table 3.4**.

Table 3.4: Coefficient of variation for CD27, CD62L and NKp46 NK subphenotypes.

	CD27	CD62L	NKp46
$CD56^{bright}CD16^{neg}$	3.54	8.66	3.84
$CD56^{bright}CD16^{dim}$	7.07	15.62	0.64
$CD56^{dim}CD16^{bright}$	11.61	25.01	7.06
$CD56^{dim}CD16^{neg}$	9.29	15.76	22.49

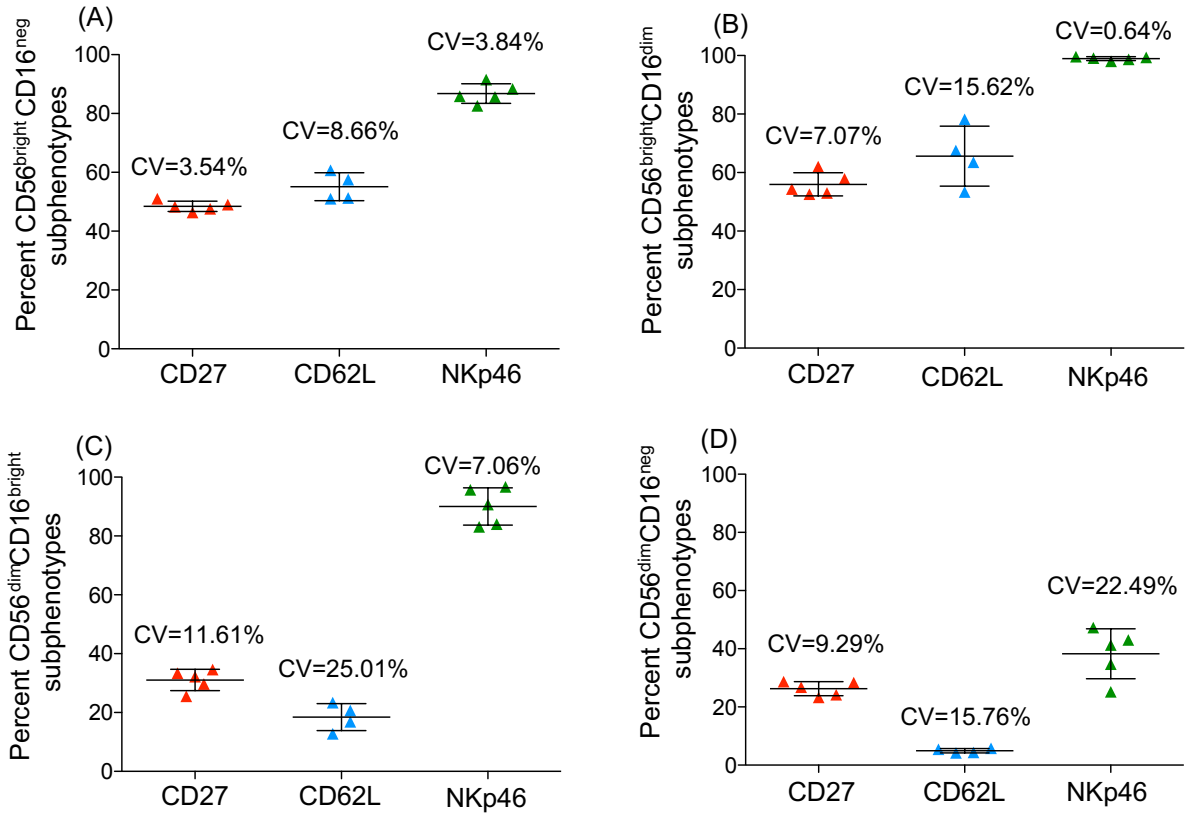


Figure 3.6: Inter-experimental variances for CD27, CD62L or NKp46 expression on NK subsets. Inter-experimental variances for CD27, CD62L or NKp46 expression for $CD56^{bright}CD16^{neg}$ (A), $CD56^{bright}CD16^{dim}$ (B), $CD56^{dim}CD16^{bright}$ (C) and $CD56^{dim}CD16^{neg}$ (D) NK subsets was determined using co-stimulated PBMCs from a blood bank donor. Error bars represent 1SD from the mean (confidence interval of 95%) of 5 experiments for CD27 and NKp46 and 4 experiments for CD62L. CVs, means and standard deviations were calculated using Prism (Version 5.0; GraphPad Software).

3.3.3.3 Validation of $CD56^{bright}CD16^{neg}$ functions

Inter-experimental variances for functional responses were limited to the $CD56^{bright}CD16^{neg}$ NK subset, which is the main focus of the current study. Reproducibility of degranulation and cytokine functional results was more challenging as slight variations in stimulation and degranulation assays between experiments adds to the complexity of inherent variations in

polychromatic flow cytometry data analysis. To determine the magnitude of functional responses, IFNγ and CD107a frequencies of co-stimulated cells were subtracted from 2009-influenza vaccine stimulated cells to adjust for background responses. CVs for IFNγ and CD107a (**Figure 3.7**) were higher than those for the NK phenotypes and subphenotypes, however, since all time-points for each individual in this study were run simultaneously in the same experiment, any inter-experimental variances would be reflected in each time-point, thus any observed trends would remain valid.

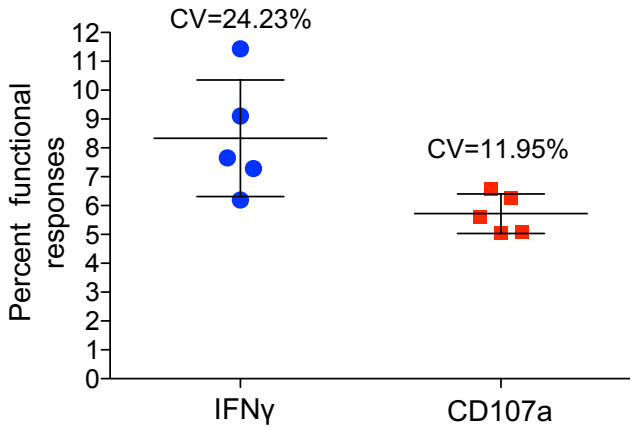


Figure 3.7: Validation of inter-experimental variances of functional responses for the $CD56^{bright}CD16^{neg}$ NK subset. IFNγ and degranulation (CD107a) responses were determined by subtracting co-stimulated (background) proportions from stimulated proportions. Error bars represent 1SD from the mean (confidence interval of 95%) of 5 experiments. CVs, means and standard deviations were calculated using Prism (Version 5.0; GraphPad Software).

3.3.3.4 Inter-experimental variances for lymphocyte proportions and T cell phenotypes

Inter-experimental variances for $CD3^+$ and $CD3^-$ lymphocytes as well as those for CD4 and CD8 T lymphocytes are presented in **Figures 3.8A** and **3.8B**. CVs for $CD3^+$ (2.9%) and $CD3^-$ (6.5%) lymphocytes were low, as were those for CD4 and CD8 T cell subsets (4.33% and 7.38%, respectively) and naïve CD4 T and CD 8 T cells with CVs of 6.04% and 7.41% respectively. Whereas CD8 effector cells showed a small variance (6.23%) compared to CD4 effector cells (11.71%), both CM and EM CD8 phenotypes showed a greater level of dispersion around the mean with CVs of 25.45% and 18.77%, respectively compared to the CD4 CM and EM phenotypes (8.9% and 3.65%, respectively) (**Figures 3.8C and 3.8D**). (CD62L staining was poor for one experiment, so participant data from the experiment was excluded from final analysis).

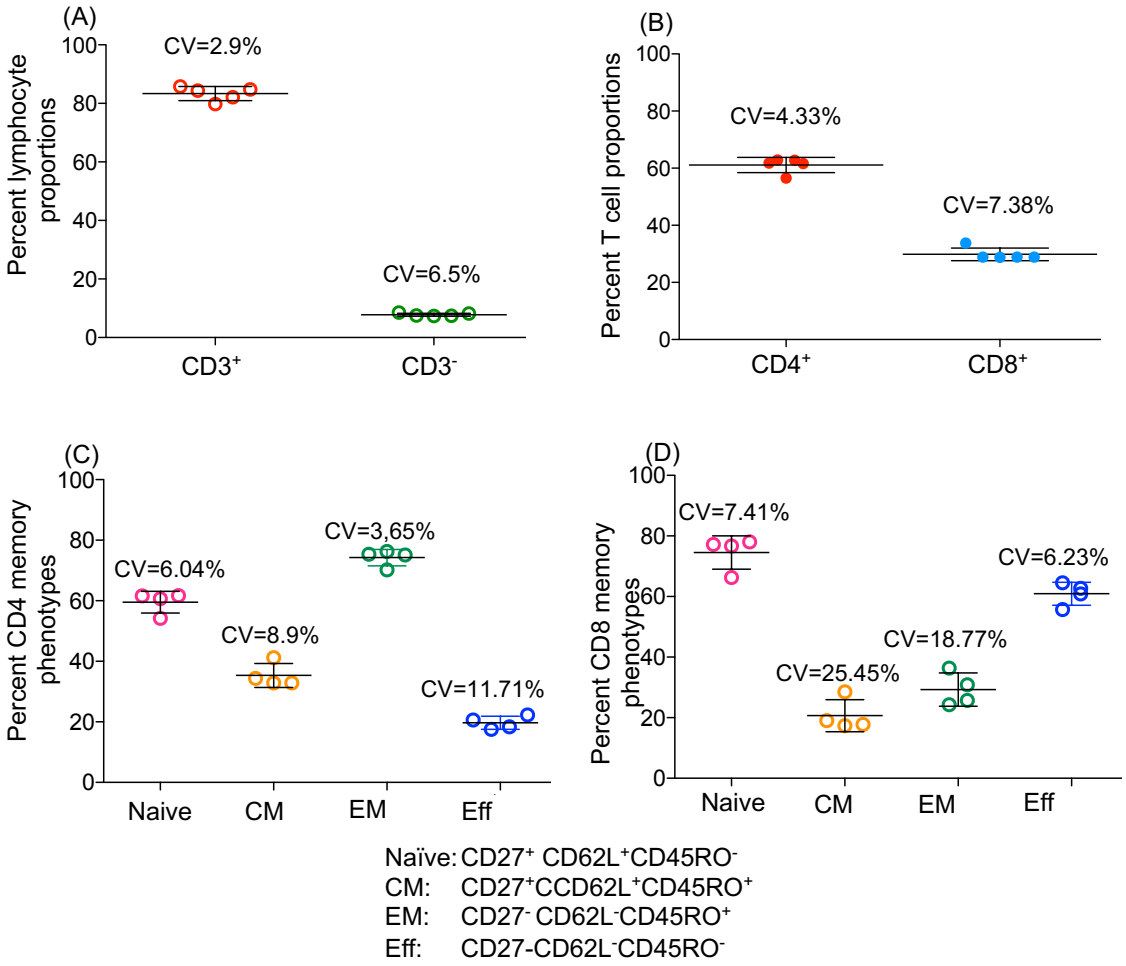


Figure 3.8: Inter-experimental variances for T lymphocytes. The degree of variation between 5 experimental data sets using co-stimulated control cells is presented for $CD3^-$ and $CD3^+$ cells (A), T cells ($CD4^+$ and $CD8^+$) (B) CD4 (C) and CD8 memory phenotypes (D). Error bars represent 1SD from the mean (confidence interval of 95%) of 5 experiments. CVs, means and standard deviations were calculated using Prism (Version 5.0; GraphPad Software). Abbreviations: CM=Central memory; EM = Effector memory; Eff = Effector cells. Note: only 4 repeats were available for memory phenotypes due to poor staining of CD62L for a single experiment.

3.4 Discussion

A key component to this study was the development of a 12 colour flow cytometry panel capable of studying human NK cell phenotype and function. Multiple steps and control measures were employed to ensure that cellular characteristics and functional responses could be detected and measured and that results generated were both valid and consistent across experiments.

Polychromatic flow cytometry provides valuable insights into the dynamics of immune responses however there are multiple technical challenges inherent to flow cytometry as

demonstrated by a study where flow cytometry data generated from different laboratories that were using the same protocol, lyophilised reagents and pooled cryopreserved PBMCs showed a coefficient of variance of up to 55% for T cell responses (Maecker et al., 2005). Critically, these researchers did not include a protocol for flow cytometer instrument monitoring and quality control which could have accounted for the inter-laboratory differences reported.

The detection of specific fluorescent emissions by flow cytometers relies on optical filters, lasers, laser alignment and precision of fluorescence measurements as detected by PMTs. If one or more of these parameters are compromised, data generated from that experiment would also be compromised. For this study a strict QA program, as developed by Perfetto, Ambrozak, et al. (2006), was therefore implemented. Once instrument performance was optimised, calibration of the system was performed to determine an acceptable voltage range and a maximum allowable CV for each detector. Daily fluorescence measurements were monitored using validation beads (standardisation) and recorded on a chart. Before each experiment validation beads were run to ensure that all fluorescent parameters fell within the pre-determined voltage range and that CVs were equal to, or less, than the allowable maximum for that PMT.

The filter configuration, number of lasers and commercial availability of fluorochromes are inherent limitations for developing of any polychromatic flow cytometry panel. For the purposes of the functional arm of the current study, the $CD56^{bright}CD^{neg}$ NK subset had to be clearly identifiable on a flow cytometry dot plot. Since surface expression of CD56 ranges from dim to bright and can be difficult to separate on a flow cytometry plot, CD56 conjugated to a brilliant™ violet (BV605) polymer dye was used. This allowed not only for better resolution of populations not clearly identifiable from adjacent populations but also allowed for separation of NK cells with surface expression of CD16. Furthermore, spectral overlap from other channels into the BV605 channel was significantly reduced and with the use of FMO controls consistent gating could be applied thus allowing for the separating cells negative for CD56 from those cells that express CD56 very dimly. Since amine reactive dyes react with amine groups and stably remain within the cytoplasm after entering cells through damaged membranes, the inclusion of the amine live/dead discriminator (Invitrogen) helped remove measurement errors resulting from the non-specific binding of antibody conjugates to dead cells (Perfetto et al., 2006b). As technical challenges increase with each additional fluorochrome in a flow panel, CD14 (monocytes) and CD19 (B-cells) antigens, not expressed by the target cell populations, were both labelled with APC-Cy7. This fluorochrome has the

same spectral properties as that of the far red live/dead cell discriminator used in the panel to allow for creating an exclusion or "dump" channel.

Analysis indicated that CD4 and CD8 T cell subsets and memory phenotypes were valid but downregulation of CD45RO was observed with flu-stimulation. A published study using CMV and HIV peptides to stimulate PBMCs (Chattopadhyay et al., 2009) and ECD to stain CD45RO T cell memory phenotypes shows images with clearly visible CD45RO stained cells, suggesting that the CD45RO downregulation observed in the current study is specific to the 2009- influenza vaccine antigen. CD45 contains α-2.6 sialic acid residues (Sato et al., 1993) and binding of haemagglutinin is mediated via interactions with α-2.6 sialic acid residues and it cannot be excluded that the downregulation of CD45RO surface expression was a consequence of receptor engagement similar to that observed upon NKp46 engagement with H1N1 antigen (Jost et al., 2011).

For the influenza vaccination arm of the study, pre- and post-vaccination PBMCs from participants were collected over a period of a year and to prevent any inter-experimental variation, all time-points for an individual were run simultaneously in a single experiment using a single flow cytometer. By putting these various measures in place, viz. daily instrument QA, choice of fluorochromes for critical markers, the elimination of unwanted and dead cells in the same channel and strict adherence to stimulation and staining protocols, technical and experimental challenges were reduced and the validity of data ensured. PBMCs prepared, aliquoted and cryopreserved from a single blood bank donor served as controls and were included with each experimental run to monitor inter-experimental variances by calculating the CV using Prism (Version 5.0; GraphPad Software). The same gates were applied to all participant samples run in the same experiment for $CD3^{+}$, $CD3^{-}$, CD45RO, CD27, CD62L, NKp46, IFNγ and CD107a, but as CD56 and CD16 expression were heterogeneous between participants, pre-vaccination co-stimulated cells were used to gate these receptors at an individual level and then applied to all samples for that particular participant.

It is well recognized that variability exists in flow data and because it is difficult to state that distributions are significantly different with a greater spread of data, the spread was quantitated using both SD and CV. Importantly, the CV for the $CD56^{bright}CD16^{neg}$ phenotype was low (5.11%) indicating little inter-experimental variance. Variance for CD27, CD62L and NKp46 subphenotypes was also consistent across experiments with CVs of 3.54%, 8.66% and 3.84%, respectively. Subphenotype variance for the $CD56^{dim}$ subsets however was

higher, particularly for CD62L expression on the $CD56^{dim}CD16^{bright}$ subset which had a CV of 25.01% and NKp46 expression on the $CD56^{dim}CD16^{neg}$ "unconventional" subset which had a CV of 22.49%. These CVs were not deemed to be of concern as neither subphenotype is widely expressed on these NK subsets and could be attributable to measurement error due to small cell numbers.

Although $CD56^{bright}CD16^{neg}$ subset functional responses for IFNγ (CV=24.23%) and CD107a (CV=11.95%) showed a greater variance than that of the phenotype and subphenotypes it was noted that when a stimulated sample generated a greater magnitude of response, the co-stimulated sample (background) was also higher thus, the overall magnitude reflected the same trend and was not due to inconsistencies in experimental protocol or instrument reliability. As all time-points for each participant was run in a single experiment this trend would be reflected across all time-points and results would therefore be valid, regardless of magnitude of responses. Importantly, the 12 colour flow cytometry panel described in this chapter identified 4 NK phenotypes $CD56^{bright}CD16^{neg}$, $CD56^{bright}CD16^{dim}$, $CD56^{dim}CD16^{bright}$ and $CD56^{dim}CD16^{neg}$ with the proportions of the $CD56^{bright}CD16^{neg}$ NK subset expressing CD27, CD62L and NKp46 being similar to what is reported in the literature.

In summary, a 12 colour polychromatic flow cytometry panel able to phenotype and functionally describe NK cells was developed. Strict monitoring, control of instrument performance and inter-experimental variances validated the integrity of the flow cytometry data. Furthermore, the integrity of stimulation and staining protocols was confirmed as functional responses followed similar trends over time. Importantly, the 12 colour polychromatic flow cytometry panel characterized NK subset and subphenotypes that are consistent with reports in the literature. Furthermore, at a functional level it was shown that NK cells degranulate and produce IFNγ in response to *ex vivo* 2009-influenza vaccine derived antigen.

CHAPTER 4:
Flow cytometric phenotyping of the CD56^{bright} CD16^{neg} NK subset

4.1 Introduction

NK cell heterogeneity between individuals is determined by genetics and environmental influences (Horowitz et al., 2013). It is hypothesized that NK receptor diversity is an evolutionary conserved means of generating NK adaptive responses in a RAG-independent manner across vertebrates (Paust et al., 2017). Organ-specific chemokines affect the distribution of tissue resident NK cells, which are thought to recirculate to SLOs via lymphatic vessels (Carrega et al., 2014). CD56^{bright}CD16^{neg} NK cells circulating in the peripheral blood are enriched for CD62L surface expression, a lymph-homing adhesion molecule, which mediates the trafficking of cells to the SLOs (Frey et al., 1998), yet not all CD56^{bright}CD16^{neg} NK cells express CD62L. Peripheral CD56^{bright}CD16^{neg} NK cells therefore comprise cell subsets (to be referred to as subphenotypes) able to traffic to secondary lymphoid organs (SLO)s (CD62L^{+}) and CD62L^{-} cells whose recirculation and trafficking patterns are unknown.

In mice, CD27 delineates NK cells into two subsets, with CD27^{+} cells interacting with dendritic cells (DCs) and an enhanced capacity to migrate to the lymph nodes (Hayakawa and Smyth, 2006). Adaptive RAG-independent contact hypersensitivity (CHS) responses in mice are mediated by specific CD27^{-} liver resident NK subsets (O'Leary et al., 2006), but require an initial sensitization step and as CHS responses are blocked in L-selectin genetically deficient mice, this suggests that sensitization of NK cells possibly occurs in the lymph nodes (Diacovo et al., 1998). A member of the TNF-R superfamily (Camerini et al., 1991), CD27 is expressed on human B, T and NK lymphocytes and although the role of CD27 expression on human NK cells is not fully understood, differences in receptor expression and cytotoxic responses between human CD27^{high} and CD27^{low} NK cells have been shown, suggesting that CD27 can be used as a marker to differentiate functionally different NK subsets in humans (Silva et al., 2008).

NK cells use multiple means of generating recall responses, which include antigen-specific, cytokine induced or memory-like responses (reviewed in (Paust et al., 2017)). Regardless of which mechanism is involved in generating a memory NK cell response, antigen recognition is required. NKp46 directly recognises influenza HA (Arnon et al., 2004) and is ubiquitously expressed on resting and activated NK cells and is therefore present on NK cells in the lymph nodes where interactions with influenza antigen occur. Although it is known that CD56^{bright} NK cells are enriched for CD27 and CD62L, little is known about co-expression patterns of NKp46 with CD27 and CD62L in healthy individuals.

CHAPTER 4:
Flow cytometric phenotyping of the CD56^{bright} CD16^{neg} NK subset

Polychromatic flow cytometry generates complex interwoven data making data reduction challenging and subsequent data analysis and interpretation difficult. The primary aim of this chapter therefore, was to investigate phenotypic differences between peripheral CD56^{bright}CD16^{neg} NK cells able to migrate to the lymph nodes via high endothelial venules (HEV)s (CD62L^{+}) and those likely to remain within the periphery (CD62L^{-}), so as to provide a framework on which to base a functional analysis strategy to investigate NK subphenotypes which may be implicated in memory responses to 2009- influenza vaccination.

4.2 Materials and Methods

4.2.1 Study samples

Co-stimulated (control) pre-vaccination PBMC samples from twelve 2009- influenza vaccinated participants (section 2.1.1) were used for phenotyping analysis and to develop a framework for Boolean analysis.

4.2.2 Sample preparation and staining

PBMCs were isolated from whole blood and aliquots cryopreserved as described in section 2.3.1 and thawed and rested as described in section 2.5. Cells were co-stimulated as described in section 2.6.1. Cells were prepared for staining (section 2.7) and then stained to eliminate dead cells (section 2.8.1) and surface stained (section 2.8.2). Antigen stimulated T cells are stained intracellularly for detection of cytoplasmic CD3. Although control cells were not antigen stimulated, CD3 was stained intracellularly (section 2.8.3), to ensure conformity in staining methods between co-stimulated (control) and antigen stimulated samples.

4.2.3 Flow cytometry

Compensation beads were stained as described in section 2.8.5 and data acquired as described in section 3.2.6

4.2.4 Statistical analysis

Proportions of gated cells were calculated as a percent (%) of the parent population using FlowJo^{TM} Software for Mac (version 9.9.4), Ashland and Prism (version 5) software was used to calculate the CV, mean, median, and range (minimum to maximum).

A Boolean gating strategy was applied to selected cells and proportions calculated using the Boolean function of FlowJo^{TM} Software for Mac (version 9.9.4), Ashland. The nonparametric Wilcoxin signed rank test was applied to determine differences between matched samples using Prism (version 5). P<0.05 was considered significant.

4.3 Results

4.3.1 CD56^{bright}CD16^{neg} subphenotypes

CD56^{bright} NK cells are generally thought to be immature precursors to CD56^{dim} cells (Freud and Caligiuri, 2006) and are described as immunoregulatory (Cooper et al., 2001b) with distinct functional capacity enabled by multiple NK receptors. To understand variations in expression of surface receptors in a cohort of healthy individuals, NKp46, CD62L and CD27 surface receptors were examined using co-stimulated cells (which served as controls for influenza vaccine experiments) from the pre-vaccination time-point. NKp46, CD62L and CD27 variances and proportions were determined on gated CD56^{bright}CD16^{neg} cells and medians, ranges and CVs were calculated (**Table 4.1** and **Figure 4.1**).

Table 4.1: Proportions CD27, CD62L and NKp46 for the CD56^{bright}CD16^{neg} subset

Marker	Mean (%)	Median (%)	Range (%)
CD27	27.62	27.55	12.6 - 47.7
CD62L	58.92	59.45	32.2 - 84
NKp46	86.48	87.75	59.4 - 95.2

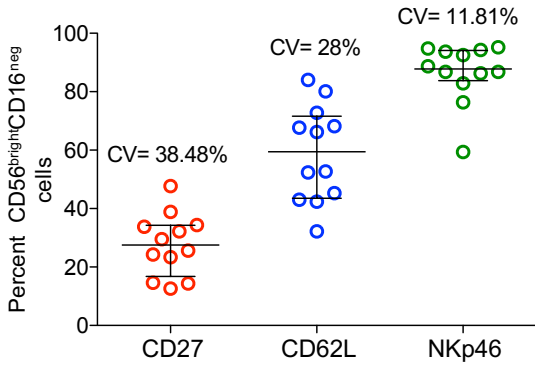


Figure 4.1: Percent expression of CD27, CD62L and NKp46 cells for the CD56^{bright}CD16^{neg} subset. Co-stimulated cells from the pre-vaccination time-point were used to investigate proportions (%) and variances between twelve unvaccinated individuals. Error bars represent medians with interquartile ranges. CVs were calculated using Prism Version 5.0 (GraphPad Software).

NKp46 was expressed on the majority of CD56^{bright}CD16^{neg} cells (median 87.75%; range 59.4% - 95.2%) which agrees with other studies (Horowitz et al., 2013; Silva et al., 2008) and proportions were the least varied between individuals (CV=11.81%), which is not unexpected, given the critical role of NKp46 as a major NK cell activating receptor, whereas CD27 proportions were the lowest (median 27.55%; range 12.6% - 47.7%) with the largest inter-individual variances (CV=38.48%) for the three receptors under investigation. Similar to CD27, variances between individuals were wide (CV=28%) but a larger proportion of

CD56^{bright}CD16^{neg} expressed CD62L (median 59.45%; range 32.2% - 84%) indicating that in some individuals a large proportion (up to 84%) of CD56^{bright}CD16^{neg} NK cells could migrate out of the periphery to SLOs. Unlike the inherent requirement of NKp46 in NK cell immune surveillance, the large inter-individual variances for CD27 and CD62L receptors suggests that immune function or status could be influencing cell surface expression of these two receptors.

4.3.2 Co-expression patterns of CD27 and NKp46

CD27$^+$ NK cells produce a greater magnitude of IFNγ and TNFα inflammatory cytokines compared to CD27$^-$ NK cells (Fu et al., 2011; Silva et al., 2008) therefore similar to mouse NK cells, CD27 can be used as a marker to functionally differentiate NK subsets in humans (Silva et al., 2008). NKp46 does not function independently in enabling NK cell cytokine secretion or in mediating cytotoxicity and requires a synergistic interaction between activating receptors on resting NK cells (Bryceson et al., 2006b) and so co-expression patterns of NKp46$^+$ and CD27$^+$ cells (**Figure 4.2**) were therefore assessed. Currently there are no published data on co-expression patterns of these receptors for the CD56^{bright}CD16^{neg} NK subset.

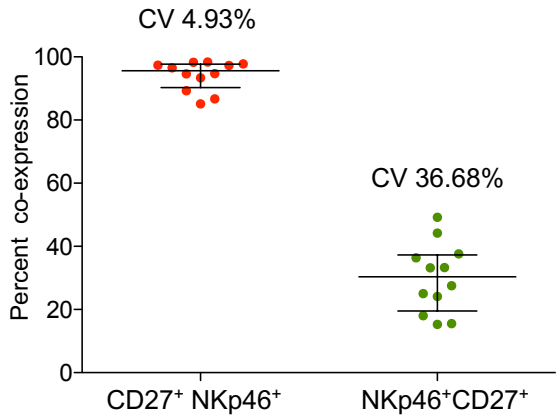


Figure 4.2: CD27 and NKp46 co-expression patterns for the CD56^{bright}CD16^{neg} subset. Co-stimulated cells from the pre-vaccination time-point were used to investigate variances between individuals and the proportion of CD27$^+$ cells that co-express NKp46 and the proportion of NKp46$^+$ cells that co-express CD27. Error bars represent medians with interquartile ranges. CVs were calculated using Prism Version 5.0 (GraphPad Software).

Strikingly, the proportion of CD27$^+$ cells that co-expressed NKp46 was extremely high (median 95.6% with a range of 85.1% - 98.4%), with a very low coefficient of variation between individuals (CV = 4.93%), therefore the large majority of CD27$^+$ cells were of a CD27$^+$NKp46$^+$ phenotype for all participants regardless of variations in overall CD27 proportions. In contrast, the median proportion of gated NKp46 cells with surface expression of CD27 was 30.4%, with wide variances between individuals (15.3% - 49.2%; CV=36.68%) reflecting that the observed CD56^{bright}CD16^{neg} variations in CD27$^+$ proportions are attributable to the proportion of NKp46$^+$ cells that co-express CD27.

4.3.3 Stability of CD27-expressing cells over time

NK cells are considered to be short lived with a turnover time of approximately two weeks for mature human NK cells in the blood (Zhang et al., 2007). CD27-expressing cells for the CD56^{bright}CD16^{neg} subset were extremely varied between individuals, raising the question about whether this represented cells in flux, or a stable population for each individual influenced by unique antigen encounter. To explore this question, co-stimulated CD56^{bright}CD16^{neg} cells from pre- and post-vaccination time-points were gated for CD27 surface expression to understand if CD27 proportions remained stable or fluctuated over time (data summarised in **Table 4.2**).

The pre-vaccination time-point was considered to represent the baseline and comparisons were made between this time-point and post-vaccination time-points. Despite wide inter-individual differences, the proportion of NKp46^{+} cells with surface expression of CD27 remained remarkably stable for each individual over time, indicating long term stable expression of CD27 for each individual (P>0.05) (**Figure 4.3**).

Table 4.2: Percent CD27 co-expression on CD56^{bright}CD16^{neg} cells remains stable over time

	*CD56^{bright}CD16^{neg}			
	Pre-vaccination	**Post-vaccination**		
Subjects		**3 days**	**6 months**	**1 year**
1	32.2	34.5	28.3	28.9
2	24.3	25.6	24.4	28.8
3	14.4	18.6	18.4	16.9
4	23.4	24.6	22.3	27.5
5	47.7	50.2	49.5	49.2
6	25.6	24.7	23.4	24
7	12.6	8.11	14.1	8.78
8	33.8	38.1	28.4	
9	29.5	32.3	27.4	
10	38.9	39.4	41	
11	34.4	34.8	30.3	
12	14.6	14.7	13.9	
MEAN	**27.6**	**28.8**	**26.8**	**26.3**
MEDIAN	**27.55**	**28.95**	**25.9**	**27.5**

* Numbers in the table represent the percent of CD56^{bright}CD16^{neg} NK cells with surface expression of CD27.

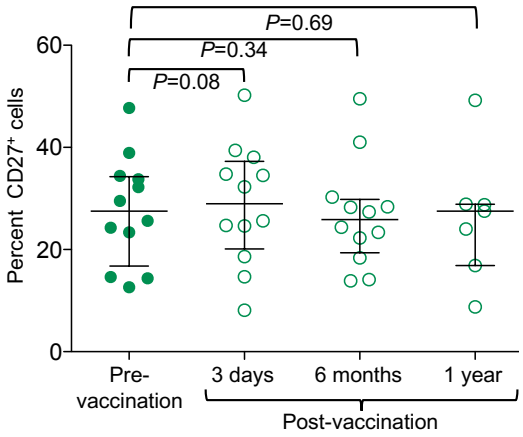


Figure 4.3: CD27 proportions remain stable over time. Co-stimulated CD56^{bright}CD16^{neg} NK cells were gated for CD27 surface expression and comparisons made between pre- and post-vaccination time-points to observe changes for up to a year following vaccination. *P*-values were obtained using the Wilcoxon signed rank t-test and values <0.05 considered significant.

Despite the observation that CD27 populations remaining stable over time at a "bulk" NKp46 subset level, this does not preclude changes that may occur at a subphenotype level. Cells that express CD62L are able to migrate to the lymph nodes. To explore CD27 proportions at a subphenotype level, co-stimulated NKp46^{+} cells were gated for CD62L^{+} and CD62L^{-} cells (representing lymph homing (lh) and peripheral (p) NKp46^{+} cells) and each of these populations gated further for CD27^{+} and CD27^{-} subphenotypes. By using this gating strategy 4 subphenotypes were defined as: lhNKp46^{+}CD27^{+}, lhNKp46^{+}CD27^{-}, pNKp46^{+}CD27^{+} and pNKp46^{+}CD27^{-}. (**Figure 4.4**).

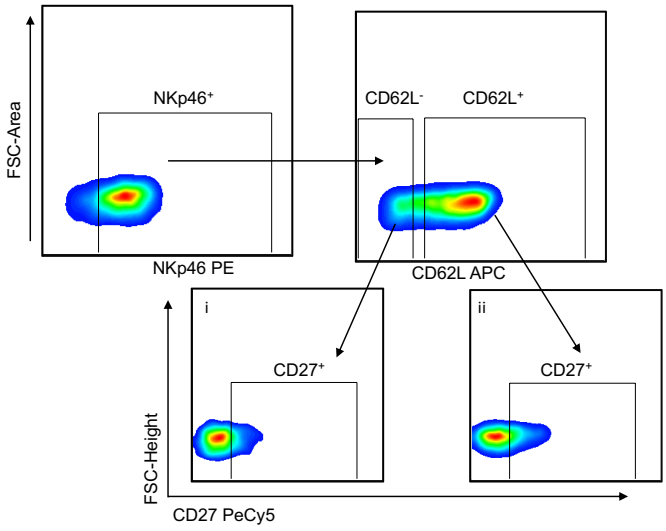


Figure 4.4: Gating strategy to define NKp46^{+} subphenotypes. To determine CD27 proportions at a subphenotype level, NKp46^{+} cells (A) were gated for CD62L^{+} (lymph homing) and CD62L^{-} (peripheral) subphenotypes (B). CD27^{+} cells likely to remain in the periphery (NKp46^{+}CD62L^{-} CD27^{+} subphenotype) are represented in dot plot (C) and the NKp46^{+}CD62L^{+}CD27^{+} subphenotype most likely to migrate to lymph nodes are represented in dot plot (D).

With the exception of a single individual who had a sharp drop in pNKp46CD27^{+} cells from 21.8% at the pre-vaccination time-point to 7.5% three days post-vaccination (but which by one year recovered to 9.18%), the frequency of CD27 cells remained stable for both subphenotypes (**Figures 4.5A** and **4.5B**) indicating that no subtle shifts of CD27 cell surface expression had taken place over a period of one year (*P*>0.05).

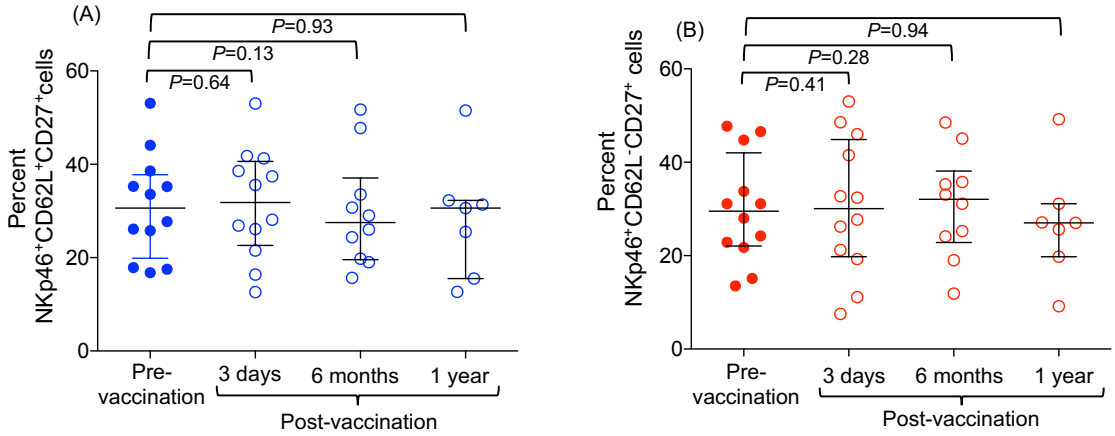


Figure 4.5: CD27 proportions remain stable over a year for lymph homing and peripheral subphenotypes. To observe changes in NKp46^{+}CD27^{+} proportions, co-stimulated cells from pre- and post-vaccination time-points were compared for the lymph-homing NKp46 subphenotype (A) and for the peripheral NKp46 subphenotype (B). *P*- values were obtained using Wilcoxon signed rank test and *P* values <0.05 were considered significant. * Only ten CD62L^{+} samples were available six months post-vaccination.

4.3.4 NKp46, CD27 and CD62L Boolean gated phenotypes

Boolean gating algorithms which when applied to individually gated populations create a combination of positive and negative subsets in all possible combinations. CD62L, was expressed on a greater frequency of cells than CD27, with a wide co-efficient of variation indicated that the number of CD56^{bright}CD16^{neg} NK cells able to migrate to the lymph nodes differs between individuals. Thus, a Boolean algorithm (FlowJo data analysis software) was applied to CD62L, CD27 and NKp46 to explore combination frequencies of these three surface receptors within the CD56^{bright}CD16^{neg} NK subset (**Figure 4.6**) and to determine which of these combinations predominate.

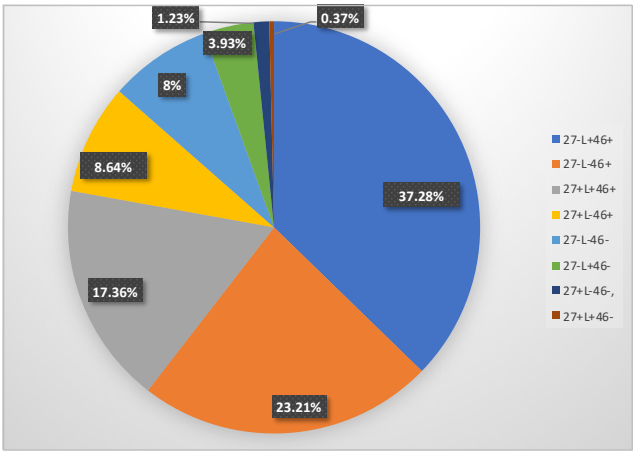


Figure 4.6: CD56^{bright}CD16^{neg} Boolean co-expression patterns for CD62L, CD27 and NKp46 surface receptors. Using cells from the pre-vaccination time-point, a Boolean gating strategy was applied to CD62L^{+}, CD27^{+} and NKp46^{+} cells expressed on the CD56^{bright}CD16^{neg} NK subset and relative proportions of Boolean combinations calculated using FlowJo software (Treestar Inc.) The numbers in black boxes represent the percent mean proportion for each combination of receptors. Abbreviations: 27=CD27; L=CD62L and 46=NKp46.

Interpreting data sets generated by polychromatic flow cytometry is complex due to the multidimensional nature of the data (Roederer et al., 2011) and manually trying to interpret subtle data set combinations is difficult, but with the current study, at a superficial level, certain phenotypic trends were observed. The predominant subphenotype co-expressed NKp46 and CD62L (37.28%) but not CD27 and the 2nd most predominant subphenotype only expressed NKp46 (23.21%). Co-expression of all 3 receptors under investigation made up 17.36% whereas 8.64% of cells co-expressed NKp46 and CD27 but not CD62L. Only 8% of Boolean gated CD56^{bright}CD16^{neg} cells were negative for all 3 subphenotypes under investigation and a total of 13.51% cells (4 subphenotypes) did not express NKp46, whereas 86.49% (4 subphenotypes) expressed NKp46. Boolean combinations are summarised in **Table 4.3** in order of most to least prevalent Boolean population.

Table 4.3: NKp46, CD62L and CD27 Boolean populations for the CD56^{bright}CD16^{neg} NK subset

Phenotype	Mean (%)	S.D
NKp46^{+}CD62L^{+} CD27^{-}	37.28	10.4
NKp46^{+}CD62L^{-}CD27^{-}	23.21	14.35
NKp46^{+}CD62L^{+}CD27^{+}	17.36	7.74
NKp46^{+}CD62L^{-}CD27^{+}	8.64	5.71
NKp46^{-}CD62L^{-}CD27^{-}	8.00	6.88
NKp46^{-}CD62L^{+}CD27^{-}	3.93	3.5
NKp46^{-}CD62L^{-}CD27^{+}	1.23	0.99
NKp46^{-}CD62L^{+}CD27^{+}	0.37	0.53

S.D=Standard deviation

Importantly, these data indicate that in the absence of NKp46 expression, few cells express the other co-receptors under investigation in the current study, suggesting that expression of CD27 and CD62L, either singly or co-expressed, is tightly regulated and predominantly occurs on NKp46^{+} cells, which may either be lymph homing or peripheral. Based on NKp46, CD62L and CD27 expression, CD56^{bright}CD16^{neg} cells can therefore be categorised into 4 subphenotypes providing a framework to investigate differences between multiple subphenotypes. The NKp46^{+} subphenotypes, which were defined on the basis of lymph homing properties, are summarised in **Table 4.4**.

Table 4.4: NKp46^{+} subphenotypes defined by lymph homing properties

Phenotype	Description	Abbreviation
NKp46^{+}CD62L^{+}CD27^{+}	Lymph homing NKp46^{+}CD27^{+}	lhNKp46CD27^{+}
NKp46^{+}CD62L^{+}CD27^{-}	Lymph homing NKp46^{+}CD27^{-}	lhNKp46CD27^{-}
NKp46^{+}CD62L^{-}CD27^{+}	Peripheral NKp46^{+}CD27^{+}	pNKp46CD27^{+}
NKp46^{+}CD62L^{-}CD27^{-}	Peripheral NKp46^{+}CD27^{-}	pNKp46CD27^{-}

Of the NKp46^{+} subphenotypes, a total of 54.64% were lymph homing (CD62L^{+}) which comprised 37.28% CD27^{-} cells and 17.36% CD27^{+} cells, indicating that most NKp46 lymph homing cells (lhNKp46^{+}CD62L^{+}) did not express CD27. CD27 and CD62L were minimally expressed in the absence of NKp46 (1.23% and 3.93%, respectively) with the proportion of CD56^{bright}CD16^{neg} NK subset that co-expressed CD62L and CD27 as a double population (mean=0.37%; range=0%-1.8%) being extremely low.

NK cells are heterogenous and as only 59.4% of the CD56^{bright}CD16^{neg} NK subset expressed NKp46 in some individuals (section 4.2.1, **Table 4.1**), it could be postulated that CD27 and CD62L would be present on a higher proportion of CD56^{bright}CD16^{neg} cells that do not express NKp46. However, only one individual had 1.8% of CD56^{bright}CD16^{neg} cells that co-expressed CD27 and CD62L in the absence of NKp46, whereas all other individuals had less than 1% and even 0% in some instances. These data offer an interesting “snapshot” of human CD56^{bright}CD16^{neg} NK subset heterogeneity which is based on the analysis of only 3 cell surface receptors. As indicated in section 4.2.1, **Table 4.1,** surface expression for CD62L and CD27 receptors varied widely between individuals, yet in the instance of CD27, remained remarkably stable over time for each individual, suggesting an environmental influence, which is governed by unique immune exposures. Indeed, each individual’s profile revealed a wide diversity in the proportional distribution of subphenotypes. The inter-individual diversity in NKp46^{+} subphenotype profiles is reflected in **Figure 4.7** where the data for each study participant are presented.

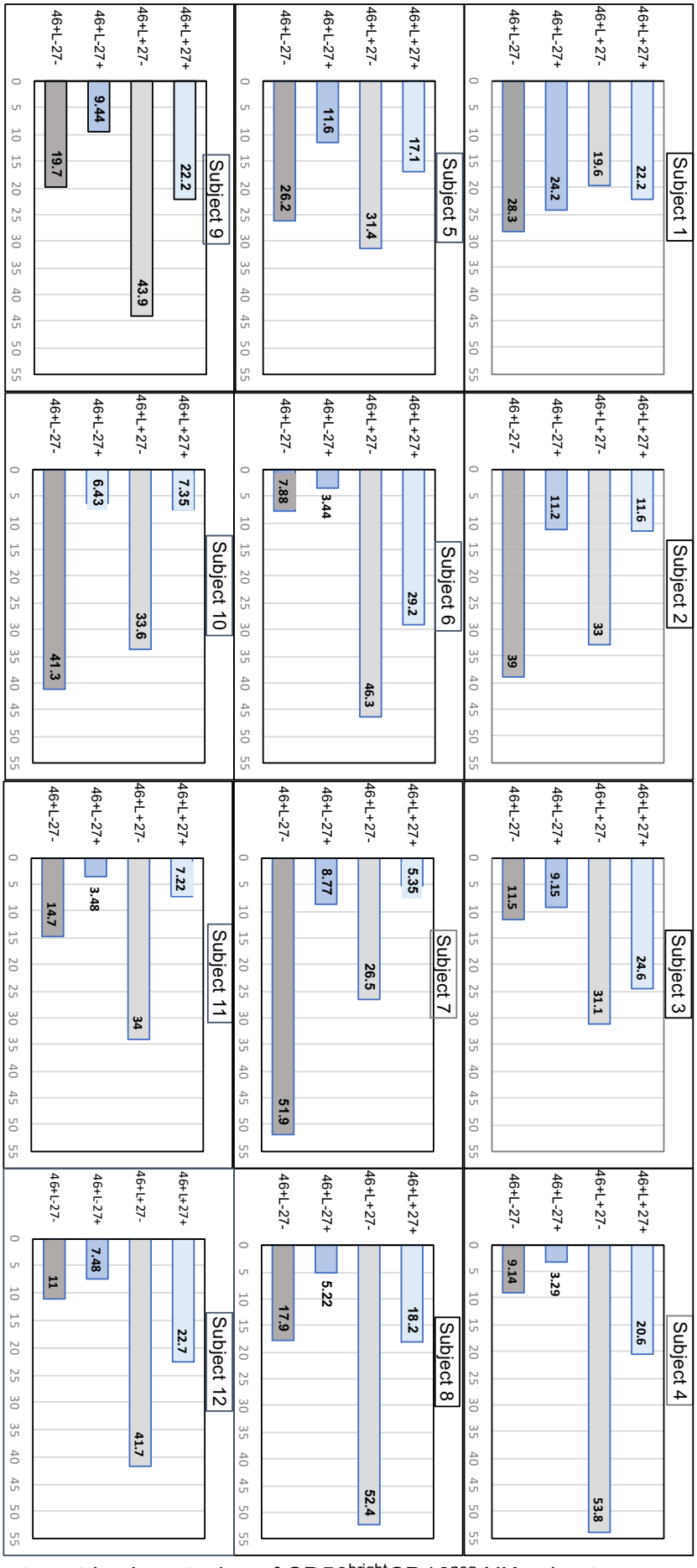


Figure 4.7: Wide inter-individual variances of NKp46^{+} subphenotypes. Wide inter-individual variances in CD27 and CD62L frequencies, influence overall proportions of NKp46^{+} Boolean subphenotypes. To determine subphenotype frequencies, CD56^{bright}CD16^{neg} cells were Boolean gated for CD62L, CD27 and NKp46 surface expression and relative proportions of Boolean combinations calculated using using FlowJo software (Treestar Inc.). Eight Boolean populations were generated but only data from the 4 NKp46^{+} subphenotypes are presented. Bar charts were generated in Excel (Windows 365) and the numbers in charts represent mean (%) proportion of the total of 8 Boolean subphenotypes.

In summary, Boolean statistics revealed that:

A) NKp46, delineates the CD56^{bright}CD16^{neg} subset into subphenotypes, with differing lymph homing capacities but overall, a larger majority of NKp46 cells have the capacity to migrate to the lymph nodes whereas a smaller proportion remain in the periphery.

B) CD62L and CD27 surface expression is tightly regulated as it is only found on NKp46^{+} cells (whether lymph homing or peripheral).

C) CD27 and CD62L proportions vary widely between individuals (possibly a consequence of unique antigen exposures) which is reflected in both lymph homing and peripheral NKp46 subphenotypes.

4.3.5 Co-expression of CD27 and CD62L dynamically influences NKp46 cell surface density.

Findings indicated that CD27 surface expression is only found on NKp46^{+} cells and although there are limited data on the NKp46^{+}CD27^{+} suphenotype, (Vossen et al., 2008) showed that cell surface expression of NKp46 is increased with CD27 co-expression. NKp46 cell surface density is variable and influences the physiological triggering of NK cells against autologous, allogeneic and xenogeneic target cells is determined by NKp46 cell surface density (Sivori et al., 1999). To investigate if NKp46 cell surface density is greater with CD27 co-expression, cells from the pre-vaccination time-point were gated for NKp46^{+}CD27^{+} and NKp46^{+}CD27^{+} subphenotypes (**Figure 4.8A**) and cell surface density measured using median fluorescent intensity (MFI) statistics (FlowJo v.9.9.4 TreeStar Inc.).

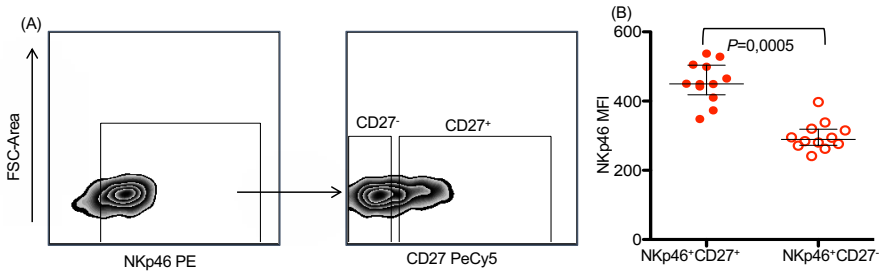


Figure 4.8: CD27 co-expression on NKp46^{+} cells is associated with higher NKp46 surface density. The median fluorescent intensity (MFI) from pre-vaccination co-stimulated cells were used to compare NKp46 subphenotypes by gating NKp46^{+} cells for CD27^{+} and CD27^{-} cells (A) to delineate NKp46 cells into NKp46^{+}CD27^{+} and NKp46^{+}CD27^{-} subphenotypes for MFI analysis (B). *P*-values were determined using the Wilcoxon signed rank t-test and values <0.05 considered significant. Median values and interquartile ranges are presented with the error bars.

Without exception for any study participant, the NKp46 MFI of the NKp46^{+}CD27^{+} subphenotype was significantly greater in magnitude than that for the NKp46^{+}CD27^{-} subphenotype (*P*=0.0005) (**Figure 4.9B**) agrees with the Vossen study. This suggests that CD27 may mediate increased cell surface density of NKp46 which could therefore play a role as one of the receptors involved in the triggering of NKp46 activation by lowering the activation threshold.

To determine whether co-expression of CD27 is associated NKp46 surface density for both lymph homing and peripheral NKp46 cells NKp46^{+} Boolean subphenotypes were analysed next. The results were ubiquitously similar for all participants and NKp46 surface density increased with CD27 co-expression, for both lymph homing (*P*=0.005) and peripheral (*P*=0.005) NKp46 cells (**Figure 4.9A**).

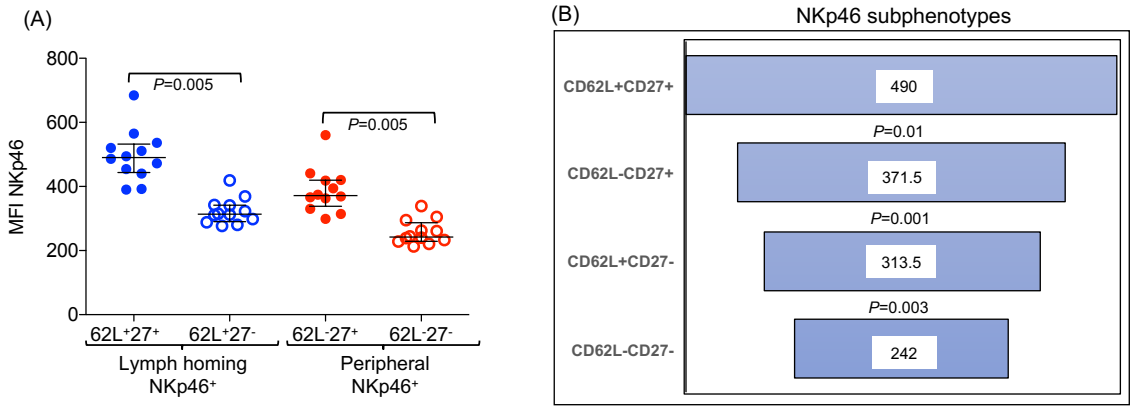


Figure 4.9: Dynamic influence of CD27 and CD62L on NKp46cell surface density. To determine NKp46 cell surface density, the median fluorescent intensity (MFI) from pre-vaccination co-stimulated cells were used for comparisons between NKp46 subphenotypes. Co-expression of CD27 is associated with increased NKp46 cell surface density for both lymph homing (CD62L^{+}) and peripheral NKp46 (CD62L^{-}) subphenotypes (A). Medians and interquartile ranges are represented with the error bars. NKp46 surface density is greater with CD27 co-expression which is independent of lymph homing ability (B). NKp46 MFI values are shown in the bars of the funnel chart. The funnel chart was generated in Excel (Windows 365) and P-values shown calculated using the Wilcoxon signed rank test. *P*-values of <0.05 were considered significant.

Therefore, when NKp46^{+} cells were analysed within the context of CD27 co-expression (**Figure 4.9B**), NKp46 surface density was greater with CD27 co-expression which was independent of lymph homing ability and there was a significant decrease in NKp46 MFI between each subphenotype, with highest NKp46 surface density observed for the NKp46^{+}CD62L^{+}CD27^{+} subset and lowest for NKp46^{+}CD62L^{-}CD27^{-} cells.

An influence of CD62L was noted however as lhNKp46CD27^{-} cells had a higher NKp46 MFI than pNKp46CD27^{-} cells (*P*=0.003) and NKp46 MFI for lhNKp46CD27^{+} cells was higher than that of pNKp46CD27^{+} cells (*P*=0.01) (**Figure 4.9B**). These data therefore indicate an additional requirement for a higher density of NKp46 surface expression for cells migrating to the lymph nodes and that this increase in surface density takes place before migration to the lymph nodes. Given the role of NK cells in viral infections and cell surface density requirements for the triggering of NKp46 in response to target cells, these data provide novel insights into surface receptors that may influence increasing NKp46 cell surface density, particularly within the context of NK immune cells able to migrate to the lymph nodes.

4.4 Discussion

In this immunophenotyping study, two surface receptors (CD27 and CD62L) were investigated to understand their co-expression patterns with NKp46. By applying a Boolean gating strategy to CD27, CD62L and NKp46 cells from the pre-vaccination time-point, a simplified framework was devised to investigate phenotypic and functional differences between subphenotypes able to migrate to the LNs via HEVs and those likely to remain in the periphery. Boolean gates delineated NKp46, CD62L and CD27 into eight different subphenotypes, of which four expressed NKp46. Based on lymph homing properties and co-expression of CD27 NKp46^{+} subphenotypes could be defined as NKp46^{+}CD62L^{+}CD27^{+} (lhNKp46 cells with CD27 co-expression), NKp46^{+}CD62L^{+}CD27^{-} (lhNKp46 cells without CD27 co-expression), NKp46^{+}CD62L^{-}CD27^{+} (pNKp46 cells with CD27 co-expression) and NKp46^{+}CD62L^{+-}CD27^{-} (pNKp46 cells without CD27 co-expression).

NKp46, CD62L and CD27 frequencies were firstly examined to understand differences in expression levels of these receptors and to provide baseline proportions and ranges for the individuals recruited into the study. NKp46 was expressed on the majority of cells (87.75%), but in some individuals was as low as 59.4% yet comprised up to 95.2% of NK cells for others. Frequencies of NKp46-expressing NK cells are decreased in the elderly (Almeida-Oliveira et al., 2011). Sample numbers in the current study did not allow for a correlation between age and frequencies of NKp46^{+} NK cells. However except for two individuals, NKp46 was expressed on more than 90% of CD56^{bright}CD16^{neg} cells for all other participants. In contrast to NKp46 with a CV of 11.81%, frequencies for CD62L and CD27 (CV=28% and 38.48%, respectively) varied widely between individuals but the immunological significance is unknown as few studies have investigated normative ranges for NK receptors in healthy individuals (Angelo et al., 2015). Taken together, the three receptors under investigation (albeit with

widely differing frequencies) were all detected on CD56^{bright} cells which are considered to be a more immature NK cell type (Freud and Caligiuri, 2006).

NK cell development from iNK to mNK cells (discussed in Chapter 1) is a multistep process that is still to be fully elucidated, but development of NK cells from a pluripotent progenitor cell to a lineage committed, fully functional, mature cell, occurs in an ordered fashion as defined by surface expression of receptors characterising each discrete stage (Freud and Caligiuri, 2006). During human NK cell maturation, NKp46 and CD56^{bright} cells are expressed by stage 4 and are considered less mature than CD56^{dim} NK cells, with the final stages of development being the CD56^{dim} cytolytic stage 5, followed by a CD57^{+} memory stage 6 (Abel et al., 2018). CD11b^{-}CD27^{-} human NK cells represent a mature phenotype corresponding to the CD56^{dim} NK subset (Fu et al., 2011) and CD62L and CD27 follow similar decreasing trends in surface expression during development from a CD94^{high}CD56^{bright} phenotype to the more mature CD94^{low}CD56^{dim} phenotype (Yu et al., 2010). Based on the assumptions of the above studies, Boolean gated NKp46 cells comprised of subphenotypes considered to be at differing stages of maturation with lhNp46CD27^{+} the least mature and pNKp46CD27^{-} the most mature, which interestingly displayed the largest range amongst individuals, suggesting the influence of differing immune experiences in the development of mature NK cell phenotypes. Recently however, the dogma of a linear progression of NK cells from immature CD56^{bright} to mature CD56^{dim} cells has been questioned (Berrien-Elliott et al., 2015; Mace et al., 2013; Maciejewski-Duval et al., 2016; Michel et al., 2016; Wu et al., 2014). CD62L as a marker of NK cell immaturity (Juelke et al., 2010) is also controversial as it associates with a more mature NK phenotype in mice (Peng et al., 2013b).

Full functional capability of maturing NK cells only occurs following a “licensing” process during which self-tolerance is acquired and functional activation of mature peripheral NK cells is determined by a threshold, or “rheostat” adapted to the host’s MHC phenotype (Brodin et al., 2009a). In the current study it was shown that both CD62L and CD27 are almost exclusively expressed on NKp46^{+} cells. In particular, the NKp46^{-}CD62L^{+}CD27^{+} subphenotype was barely detectable, with a mean of 0.37% and a range of 0% to 1.8%. NK cells with full cytolytic potential are considered to be educated NK cells with a wide range of surface receptors able to regulate NK cell responses to antigen. Taken that both CD27 and CD62L receptors were only expressed only on NKp46^{+} cells and CD56^{bright}CD16^{neg} NK cells can undergo further development and maturation as well as a licensing process, the phenotyping data presented in this chapter suggests that expression of CD27 and CD62L receptors is specifically acquired during the maturation and developmental stages of NKp46^{+} NK cells and are therefore either

a requirement for this process or their surface expression is a consequence of NKp46 education.

Only three receptors were included in the Boolean gating strategy and as NKp46 was expressed at high frequency with less inter-individual variance (thereby limiting the diversity score), gated NKp46, CD62L and CD27 subphenotypes were surprisingly diverse amongst participants. The extreme variances in both CD27 and CD62L frequencies were clearly reflected in all combinations of NKp46^{+} subphenotypes, indicating that NKp46 immunophenotype diversity for the CD56^{bright}CD16^{neg} subset is attributable to variances in CD27 and CD62L expression. NKp46 directly recognises influenza HA and variations could be explained within the context of an individual's unique exposure to viral antigens and NKp46 interactions with these ligands. Indeed, the extreme heterogeneity of healthy human NK cells is due to genetic and epigenetic factors and surface expression of activating receptors is determined by environment with NK cell responses to transformed cells and pathogens mediated by adaptable expression of activating and co-stimulatory molecules (Horowitz et al., 2013). As the observed diversity of CD27 and CD62L could be a consequence of antigen encounters unique to each individual, the heterogeneity of expression of these surface receptors on NKp46 subphenotypes could be a reflection of epigenetic influences on developing and maturing NKp46^{+}CD56^{bright} NK cells, with the impact on individual immune responses to future antigen encounters, remaining to be explored.

The data, however, revealed that CD27 expression on NKp46^{+} cells remains remarkably stable over time, whether co-expressed with the CD62L lymph homing molecule or likely to remain within the peripheral circulation. Whether these two subphenotypes represent CD27^{+} cells recirculating between the periphery and lymph nodes or two separate subphenotypes that are replenished to maintain a stable population, remains to be elucidated. These data are novel but only represent a time frame of a year for a cohort of healthy individuals and it is not known if the proportions of CD27^{+} cells increase or decline over a period of years. Further studies that investigate NKp46 CD27^{+} cells are warranted to better understand the basic biology of this receptor, given its role in various pathological disorders in humans (Ballas et al., 2013; Hayakawa et al., 2011; Kaczmarek et al., 2017).

Various murine and human studies also provide evidence that CD27 and CD62L may be critical for NKp46 function. Murine models indicate that CD62L NK cells are important for the accumulation of mature hepatic NK cells in response to adenovirus infection (Peng et al., 2013b) and the recruitment of NK cells in the control of B16 melanoma LN metastases (Chen

et al., 2005). Data from human NK cells are not as well described, but CD27 defines a functionally different NK subset (Vossen et al., 2008) and CD62L is instrumental in the trafficking of CD56^{bright} NK cells to SLOs (Frey et al., 1998) where NK cells are involved in antigen presentation. Furthermore, a role for CD27 and CD62L has also been shown in human viral infections with a reduction in CD27 and CD62L NK cells in patients chronically co-infected with HIV and HCV (Kaczmarek et al., 2017), yet HIV positive patients with a higher frequency of CD27 NK cells can clear acute HCV infection (Eisenhardt et al., 2014). Interactions of virally infected and transformed cells would require activation of NK cells through an activation receptor, but NK cells are heterogeneous with a repertoire of multiple receptors for tight regulation of NK function and activation. The aforementioned murine and human studies indicated a requirement for both CD27 and CD62L in NK responses to transformed and virus infected cells yet neither is an activating receptor. Human CD56^{bright}CD16^{neg} NK cells are enriched for CD27 and CD62L cells and as shown in the current study, are not expressed in the absence of NKp46, it can therefore be deduced that the data presented in the aforementioned studies are a reflection of CD27 and CD62L mediated changes in virus/NKp46 interactions.

NKp46 cell surface density is important for triggering of NK cell activation (Sivori et al., 1999) forming micro-clusters at the immune synapse thereby lowering the threshold for NK cell activation (Hadad et al., 2015). In mice, CD27^{hi} NK cells have a lower activation threshold (Hayakawa and Smyth, 2006) and functionally, CD27^{+} NK cells produce more IFNγ than CD27^{-} NK cells (Fu et al., 2011). In the current study, without exception for any participant, NKp46 cell surface density was increased for both lymph homing and peripheral cells with CD27 co-expression. NK cells are recruited to the LNs where they provide IFNγ for T cell priming (Martin-Fontecha et al., 2004) and interestingly, surface density of NKp46 was greater on lhNKp46CD27^{-} cells compared to pNKp46CD27^{-} cells, indicating an influence of CD62L on NKp46 surface density which is independent of CD27 surface expression. This suggests an additional requirement for increased NKp46 cell surface expression within the lymph nodes as overall, NKp46 cell surface density on lhNKp46 CD27^{+} cells is greatest and cell surface density on pNKp46CD27^{-} cells the least, creating a hierarchical pattern of NKp46 surface density. These novel data suggest a coordinated influence of CD27 and CD62L on NKp46 cell surface density based on lymph homing capacity and surface expression of CD27. Whether this is a consequence of a sequential gain or loss in receptors on NKp46 cells, or if this reflects an education process rather than stages in cell maturation remains to be elucidated. Yet CD27 proportions remained constant for both CD27^{+} subphenotypes for at least a year, which is extremely interesting within the context of wide variances between individuals, as this

suggests that each individual maintains a stable pool of CD27^{+} NK cells that may mediate NK function through increasing NKp46 cell surface density and thereby lowering the activation threshold for NKp46 cells.

Microenvironment plays a crucial role in the differentiation and development of NK cells (Fu et al., 2014). Peripheral LNs are critical for induction of memory responses and following vaccination, mature CD27^{high} cells are the predominant NK phenotype recruited to the lymph nodes in an IFNγ dependent manner (Watt et al., 2008) whilst in humans, CD56^{bright}CD16^{neg} cells are the predominant NK subset within the lymph nodes where they act as a link between adaptive and innate arms of the immune system (Fehniger et al., 2003). In the current study, NKp46^{+} cells comprised both CD27^{+} (lower activation threshold) and CD27^{-} (higher activation threshold) subphenotypes, with differing migratory capacities mediated by CD62L expression so could either represent heterogeneous NKp46 phenotypes undergoing separate developmental pathways or a continuum of a single developmental pathway requiring circulation through the lymph nodes and periphery with concomitant loss of CD27. However, the possibility exists that both CD27^{+} and CD27^{-} subphenotypes could be involved in NK cell recall responses if they are able to migrate to lymph nodes, the site of antigen presentation and interactions between NK cells and dendritic cells (Bajenoff et al., 2006; Ferlazzo et al., 2004; Gonzalez et al., 2010; Moretta, 2002) and where CD56^{bright}CD16^{neg} cells are responsible for cell proliferation (Vitale et al., 2004b).

In conclusion, CD62L and CD27 phenotyping revealed valuable data not previously or widely described in the literature for the CD56^{bright}CD16^{neg} NK subset. Importantly it was shown, not only that CD27 and CD62L surface expression is confined to NKp46^{+} cells, but that these receptors also associate with an increase in NKp46 surface density. Based on these characteristics and by applying Boolean statistics to the CD56^{bright}CD16^{neg} subset, NKp46^{+} cells are delineated into lymph homing and peripheral blood subphenotypes, thereby providing a framework within which to analyse phenotypic and functional responses to influenza vaccination and *ex vivo* flu-stimulation.

CHAPTER 5:
$CD56^{bright}$ $CD16^{neg}$ NK cell responses to influenza vaccination

5.1 Introduction

Influenza infection remains a major public health concern and several studies indicate the critical role of NK cells in the early control and protection against influenza infection (Achdout et al., 2003; Du et al., 2010; Gazit et al., 2006). Inactivated influenza trivalent vaccination has been shown to induce NK cell activity (Long et al., 2008; Schapiro et al., 1990), but human studies investigating NK phenotypes implicated in influenza vaccination responses are limited (He et al., 2006; Jegaskanda et al., 2013; Jost et al., 2011; Kay et al., 2014; Long et al., 2008; Schapiro et al., 1990).

NK cells are highly cytolytic and can mediate killing of target cells via a granule dependent pathway which does not require de novo synthesis of proteins (Peters et al., 1991). Lung damage caused by rapid destruction of the respiratory epithelium (Taubenberger and Morens, 2006) is believed to have been a significant cause of death during the 1918-1919 H1N1 influenza pandemic, which in certain individuals, may have been due to increased host immune response (Kash et al., 2006) caused by excess NK cell degranulation (Scharenberg et al., 2019). NKp46 is critical for the lysis of influenza-infected cells (Arnon et al., 2004; Mandelboim et al., 2001), but the activation of NK cells is tightly regulated and co-receptors such as 2B4 are thought to mediate the effects of NKp46 (Bryceson et al., 2006a, b; Chuang et al., 2000; Sivori et al., 2000). CD27 plays a critical role in the accumulation of influenza virus specific T cells in the lung (site of infection) and the lung draining LNs by stimulating the survival of activated T cells (Hendriks et al., 2003) indicating a role for this receptor in T cell immune responses to influenza. Differences in receptor expression and cytotoxic responses between human $CD27^{+}$ and $CD27^{-}$ NK cells have been shown. $CD27^{+}$ NK cells produce a greater magnitude of IFNγ and TNFα inflammatory cytokines compared to $CD27^{-}$ NK cells (Fu et al., 2011; Silva et al., 2008) suggesting that CD27 can be used as a marker to differentiate functionally different NK subsets in humans (Silva et al., 2008). Furthermore, *in vivo* studies show that $CD27^{+}CD56^{bright}$ NK cells may be involved in the clearance of hepatitis C in HIV-infected patients (Eisenhardt et al., 2014) and HIV/HCV co-infected patients have reduced frequencies of $CD56^{bright}$ NK cells co-expressing CD27 (Kaczmarek et al., 2017).

Peripheral LNs are critical for the induction of memory responses against antigen that is introduced via the skin and in L-selectin (CD62L) deficient mice the development of antigen specific T cells is impaired (Catalina et al., 1996) . Lymph nodes are believed to be the site of sensitization of NK cells responsible for RAG independent CHS responses, as blocking of CD62L ablates CHS responses in sensitized mice (Catalina et al., 1996; Catalina et al., 1999;

Diacovo et al., 1998) and although the role of CD27 in human NK cell recall responses is not clear, specific CD27^{-} liver resident NK subsets have been implicated in RAG-independent CHS responses in mice (O'Leary et al., 2006). Intramuscularly administered vaccines drain into regional LNs (Gretz et al., 1997), arriving at specific antigen collection sites within minutes of vaccination (Woodruff et al., 2014). Following influenza vaccination, NK cells are recruited to the LNs, accumulating in the interfollicular area (Farsakoglu et al., 2019) where they are involved in complex cross-talk with DC's (Cooper et al., 2004; Farsakoglu et al., 2019; Ferlazzo and Morandi, 2014; Ferlazzo et al., 2004; Fernandez et al., 1999; Zitvogel, 2002). CD56^{bright} NK cells are enriched for CD62L expression, which mediates entry to LNs by binding with high efficiency to HEVs (Frey et al., 1998). Upon arrival in the LNs, CD56^{bright} NK cells are able to proliferate and produce abundant IFNγ (Vitale et al., 2004b) which in turn, influences adaptive immune responses (Bajenoff et al., 2006; Martin-Fontecha et al., 2004; Scharton and Scott, 1993).

As T and B cells can undergo somatic rearrangement which allows for specific recognition of a previously encountered antigen, classical memory immune responses are confined to cells of the adaptive immune system. These memory cells are epigenetically and phenotypically distinct from their naïve counterparts, are long-lived and able to mount a rapid and more robust secondary response. NK cells cannot undergo somatic rearrangement and are therefore unable to mount "classical" memory responses. However, evidence of NK memory-like or recall responses is continually emerging, which includes antigen-specific, cytokine induced or memory-like responses ((Cooper et al., 2009; Newhook et al., 2017; O'Leary et al., 2006; Sun et al., 2009) and reviewed in (Paust et al., 2017)). "Memory" NK cells are able to self-renew, undergo immense expansion and contraction, are long-lived and can mount a secondary response to specific antigens (Cooper et al., 2009; Dokun et al., 2001; O'Leary et al., 2006; Sun et al., 2009). Recently, changes of responding NK phenotypes to modified vaccinia virus Ankara (MVA) vaccination have been shown that leads to long term "imprinting" of NK cells, such that, cells responding to a second boost are functionally and phenotypically different from those responding to a priming event (Palgen et al., 2019).

Mounting evidence indicates that NK cells are able to develop virus-induced memory responses and studies, although limited, have also shown that vaccination induces phenotypic and functional NK cell changes both in humans (Costanzo et al., 2018; Jost et al., 2011; Palgen et al., 2019) and macaques (Vargas-Inchaustegui et al., 2016).

Virus-induced (antigen-specific) NK recall responses have been described in mice. Murine NK

cells express the Ly49H receptor which directly recognises the m157 protein of MCMV and following the adoptive transfer of Ly49H^{+} cells into mice lacking this receptor a secondary expansion occurs that is antigen-specific, as MCMV lacking the m157 protein do not induce Ly49H NK proliferation (Sun et al., 2009). Similar to murine Ly49H NK cell recognition of the viral m157 protein, NKp46 directly recognises the influenza haemagglutinin and mediates killing of infected cells (Mandelboim et al., 2001) providing a body of evidence on which to model a NK recall response that is based on viral antigen-induced proliferation through specific receptor/ligand interactions.

Earlier analysis (**Table 4.3** in Chapter 4, section 4.2.4) revealed that CD27 and CD62L are almost exclusively expressed on NKp46 cells and that CD27, in particular, could act as a co-receptor for NKp46, as CD27 co-expression associated with a higher NKp46 surface density and despite wide variances between individuals, surface expression within individuals remained remarkably stable over time. Therefore, the main aim of this chapter was to explore functional and phenotypic differences between lymph homing and peripheral NKp46^{+} subphenotypes of CD56^{bright}CD16^{neg} NK cells responding to influenza vaccination and monitor post-vaccination "imprinting" of NK cells which may be suggestive of long term "memory-like" or recall responses.

5.2. Materials and Methods

5.2.1. Influenza vaccine participants

Venous blood was collected from twelve vaccinated participants (described in Chapter 2, section 2.1.1).

5.2.2 Cryopreservation and thawing of samples

Aliquots of stored PBMC from participants (Chapter 2, section 2.3.1) were thawed and rested as required (Chapter 2, section 2.5).

5.2.3 *Ex vivo* flu-stimulations

Ex vivo flu-stimulations were carried out as described in Chapter 2, section 2.6.1 on pre- and post- vaccination samples.

5.2.4 Staining protocols

Cells were prepared for staining as described in Chapter 2, section 2.7. Briefly, cells were stained to eliminate dead cells (Chapter 2, section 2.8.1) as well as for the expression of surface receptors (Chapter 2, section 2.8.2) in addition to being stained intracellularly (Chapter

2, section 2.8.3) for detection of IFNγ and CD3 (which can be downregulated upon antigen stimulation). Degranulation was detected by staining for CD107a (Chapter 2, section 2.8.4). Single staining of compensation beads was performed as describe in Chapter 2, section 2.8.5.

5.2.5 Acquisition of cells and data collection

Stained cells for flow cytometry analysis were acquired and data collected as described in Chapter 2, section 3.2.6.

5.2.6 Statistical analysis

The proportion of gated cells were calculated as a percent (%) of the parent population using FlowJo^{TM} Software for Mac (version 9.9.4), Ashland and Prism (version 5) software to calculate medians and interquartile ranges. The nonparametric Wilcoxin signed rank test was applied to determine differences between matched samples using Prism (version 5). $P<0.05$ was considered significant.

5.3 Results

5.3.1 Influenza vaccination induces long lived changes in NKp46 subphenotype proportions

Twelve healthy subjects were vaccinated with the trivalent inactivated influenza vaccine (2009) and the dynamics of NK cell responses over time was investigated upon re-stimulation of PBMCs with the vaccine antigen. Pie charts were generated of the percentage of the Boolean CD56^{bright}CD16^{neg} subphenotypes for the controls and in response to flu re-stimulation, and examined at the following timepoints - pre-vaccination, and 3 days, 6 months and 1 year post-vaccination (**Figure 5.1**).

Expansions and contractions occurred over time in the lymph-homing (lh)NKp46CD27^{-} subphenotype and in both peripheral subphenotypes (pNKp46CD27^{+} and pNKp46CD27^{-}) in the control cultures. In response to flu-stimulation however, the proportion of both lymph homing subphenotypes increased whereas both peripheral subphenotypes decreased post-vaccination. Expansions and contractions were prevalent only for NKp46^{+} cells that co-expressed CD27 and/or CD62L for both controls and flu-stimulated cells as the small proportion of NKp46^{-}CD62L^{-}CD27^{-} CD56^{bright}CD16^{neg} cells remained unchanged at all timepoints compared to pre-vaccination frequencies for controls and flu-stimulated cells ($P>0.05$). Similarly, NKp46^{-} cells that co-expressed either CD27 or CD62L or both CD27 and CD62L (combined into a single set) remained unchanged at all post-vaccination timepoints when compared to pre-vaccination ($P>0.05$).

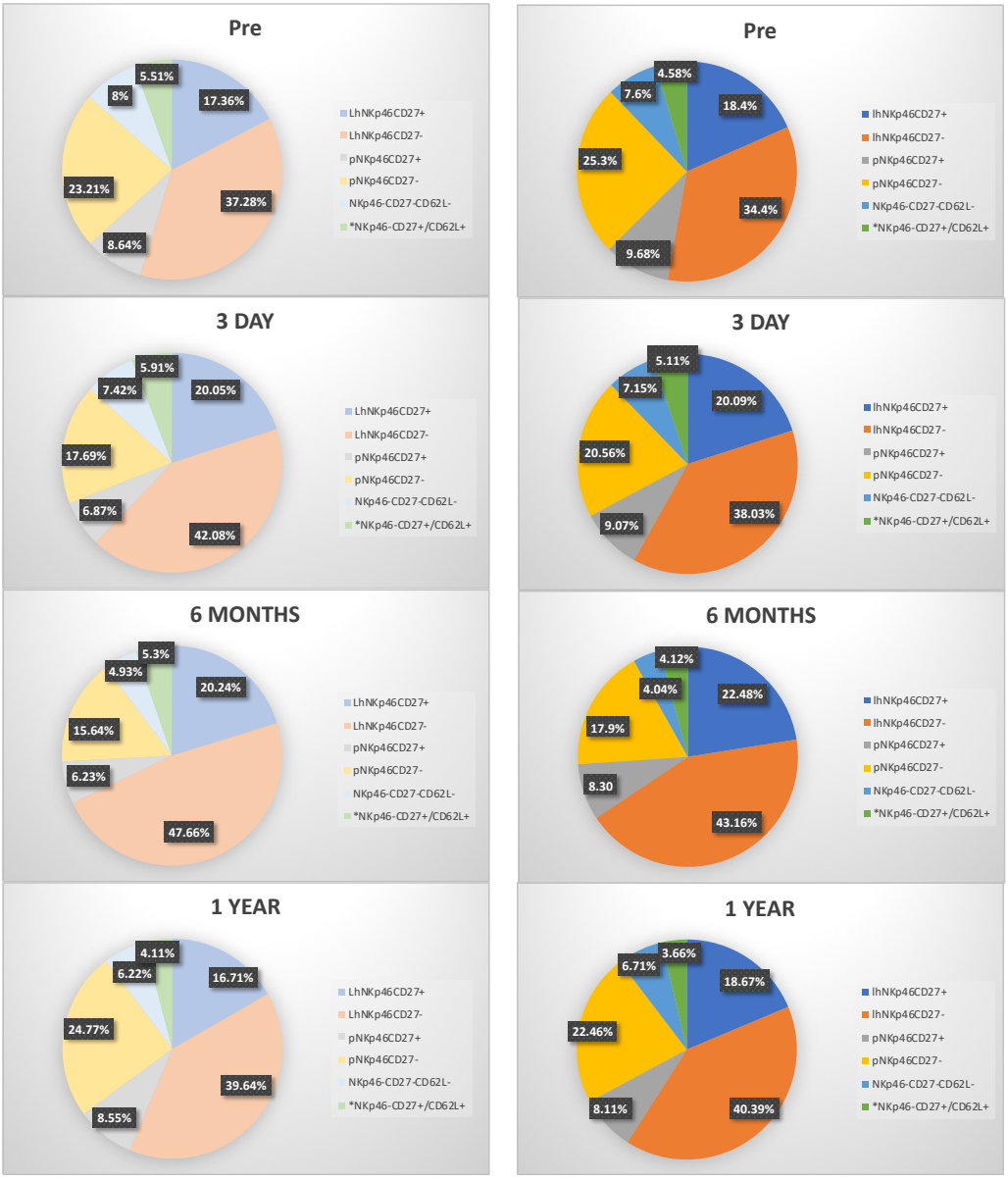


Figure 5.1: Boolean gated CD56^{bright}CD16^{neg} lymph homing and peripheral NKp46^{+} subphenotypes. CD56^{bright}CD16^{neg} cells positive for surface expression of NKp46, CD62L and CD27 were gated and the subphenotype combinations and relative proportions determined by applying a Boolean gated algorithm (FlowJo^{TM} software for Mac version 9.9.4, Ashland.) for controls (left panel) and flu-stimulated (right panel) CD56^{bright}CD16^{neg} cells.
*NKp46^{-}CD27^{+}/CD62L^{+} = CD56^{bright}CD16^{neg} cells that do not express NKp46, but express CD62L, or CD27, or both. Data from these 3 subphenotypes were combined into a single set for graphical display purposes due to small population sizes of individual sets.

Since complex differences were apparent in the dynamic response over time of the 4 NKp46^{+} subphenotypes in both control and flu-stimulated cells (Figure 5.1), the individual NKp46^{+} subphenotype longitudinal responses between control and flu-stimulated cultures were

compared to gain insights into subphenotype expansions and contractions attributable to *in vivo* influenza vaccination.

5.3.1.1 Influenza vaccination changes in lymph homing NKp46CD27^{+} proportions

lhNKp46CD27^{+} responses did not differ significantly (P=0.91) between controls and flu-stimulated cells before vaccination however significantly more (P=0.049) lhNKp46CD27^{+} cells responded to flu re-stimulation 6 months post-vaccination and this was maintained up to 1 year (P=0.047) (**Figure 5.2**).

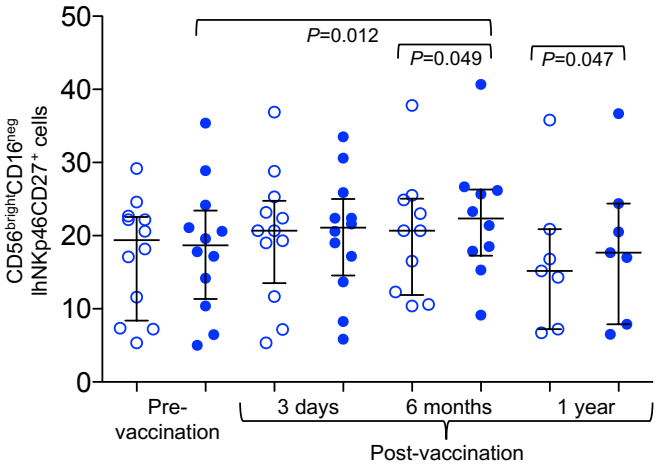


Figure 5.2: The effect of influenza vaccination on the distribution of lhNKp46CD27^{+} cells. Proportions of lhNKp46CD27^{+} cells were compared between control (no flu) and flu-stimulated PBMCs prior to vaccination (pre-) and at 3 days, 6 months and 1 year post-vaccination. Paired comparisons were performed using Wilcoxon signed rank test and P-values of <0.05 were considered significant. Error bars represent medians with interquartile ranges. Open symbols represent controls (no flu) and closed symbols represent flu-stimulated cells.

The significant increase in lhNKp46CD27^{+} proportions 6 months after vaccination (P=0.012), suggested not only an increased magnitude of vaccine-responsive cells, but also the presence of a pool of long lived cells. This was not observed in co-stimulated cells (P=0.64, 3 days and P=0.23, 6 months post-vaccination). These data highlight the antigen-specific nature and the longevity of the influenza vaccine response, and support the concept of long-lived functional reprogramming of NK cells as a consequence of influenza vaccination. The relative dynamics between lhNKp46CD27^{+} pre- and 6 months post-vaccination co-stimulated (controls) and flu-stimulated cells, are graphically depicted in **Figure 5.3**.

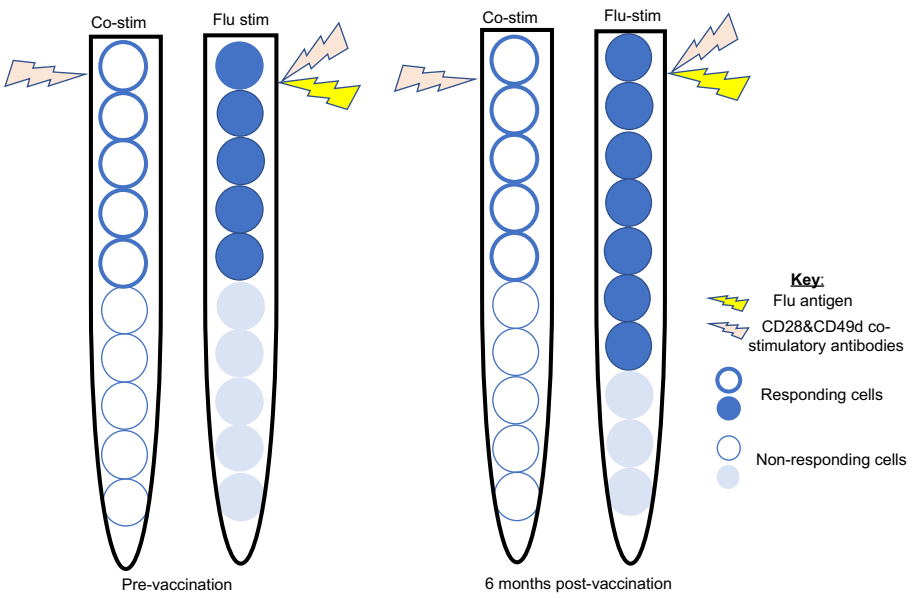


Figure 5.3: Illustration summarizing lhNKp46CD27^{+} subphenotype distributions before and 6 months after influenza vaccination. Prior to vaccination, there was no change in cells responding to responding to flu compared to co-stimulated controls. At 6 months post-vaccination, co-stimulated cells remained at pre-vaccination levels, whereas the proportion of lhNKp46CD27^{+} cells responding to flu re-challenge was greater than pre-vaccination levels.

These unique results indicate potentially an important role for lhNKp46CD27^{+} cells and therefore the CD56^{bright}CD16^{neg} subset in a trained memory or NK recall response. Furthermore, this minor NK subset may not necessarily be a less mature subset but rather a distinct NK subphenotype that can undergo an education process mediated by encounters with a specific antigen and that vaccination induces long term phenotypic "training" of this CD56^{bright}CD16^{neg} NK subset.

5.3.1.2 Influenza vaccination changes in lymph homing NKp46CD27^{-} proportions

As for lhNKp46CD27^{+} cells there were no marked differences lhNKp46CD27^{-} cells before vaccination between control and flu-stimulated cells (P=0.15). Interestingly following vaccination, this subphenotype increased over 6 months, but to a greater extent in the controls compared to flu-stimulated cultures (P=0.021 and P=0.027 at 3 days and 6 months, respectively) (**Figure 5.4**). These findings suggest an expansion of lhNKp46CD27^{-} cells responsive to co-stimulation by CD28 and/or CD49d antibodies (as is given as a cocktail of both antibodies), but an inhibition of this response in the presence of flu as a stimulus (as cells are costimulated with CD28 andCD49d antibodies together with the flu preparation).

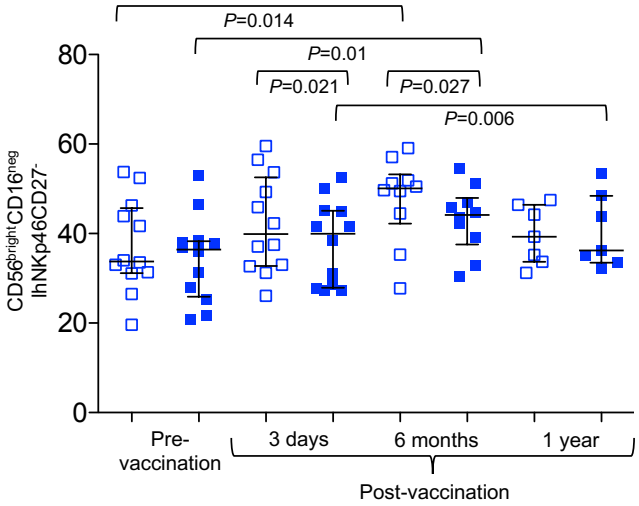


Figure 5.4 The effect of influenza vaccination on the distribution of IhNKp46CD27$^-$ responding cells. Proportions of IhNKp46CD27$^-$ cells were compared between control (no flu) and flu-stimulated PBMCs prior to vaccination (pre-) and at 3 days, 6 months and 1 year post-vaccination. Paired comparisons were performed using Wilcoxon signed rank test and *P*-values of <0.05 were considered significant. Error bars represent medians with interquartile ranges. Open symbols represent controls (no flu) and closed symbols represent flu-stimulated cells.

The relative dynamics of IhNKp46CD27$^-$ cells pre- and 6 months post-vaccination for flu-stimulated and control cells, are graphically depicted in **Figure 5.5**.

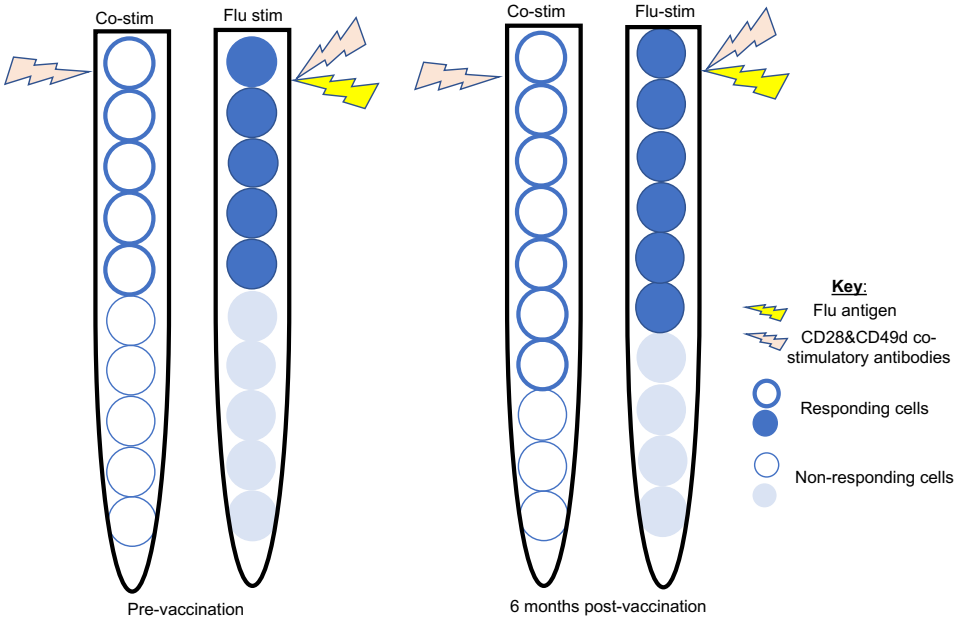


Figure 5.5: Illustration summarizing IhNKp46CD27$^-$ subphenotype distributions before and 6 months after influenza vaccination. Prior to vaccination there was no change in cells responding to flu compared to co-stimulated controls. At 6 months post-vaccination this subphenotype increased but co-stimulated control cells increased to a greater extent compared to flu-stimulated cells.

5.3.1.3 Influenza vaccination changes in peripheral NKp46CD27^{+} proportions

Prior to vaccination proportions of pNKp46CD27^{+} cells did not differ significantly between control and flu-stimulated cultures, although the latter appear elevated. The apparent outlier at the pre-vaccination timepoint, was the same individual whose CD27 proportions made up 47.7% of CD56^{bright}CD16^{neg} NK cells (**Table 4.1**). However, a greater proportion of cells responded to flu-stimulation compared to controls at 3 days post-vaccination (*P*=0.0005) and this difference was maintained up to 6 months (*P*=0.02) (**Figure 5.6**). Compared to the pre-vaccination timepoint the proportions of pNKp46CD27^{+} cells were significantly decreased in both controls and flu-stimulated cultures by 6 months, (*P*=0.02 and *P*=0.03, respectively) compared to pre-vaccination (graphically depicted in **Figure 5.7**).

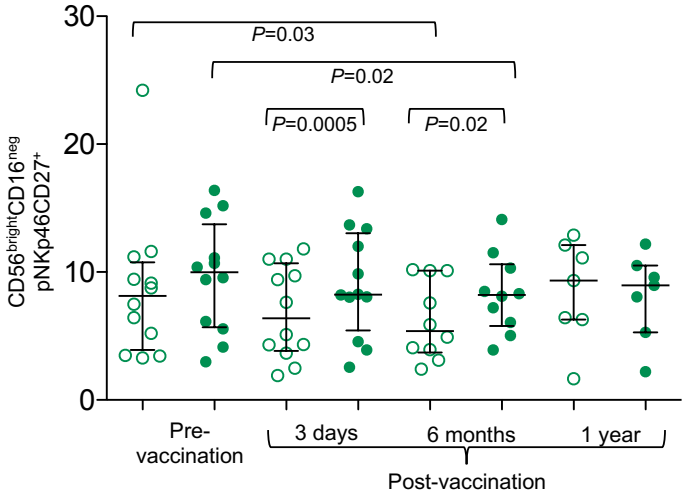


Figure 5.6: The effect of influenza vaccination on the distribution of pNKp46CD27^{+} responding cells. Proportions of pNKp46CD27^{+} cells were compared between control (no flu) and flu-stimulated PBMCs prior to vaccination (pre-) and at 3 days, 6 months and 1 year post-vaccination. Paired comparisons were performed using Wilcoxon signed rank test and *P*-values of <0.05 were considered significant. Error bars represent medians with interquartile ranges. Open symbols represent controls (no flu) and closed symbols represent flu- stimulated cells.

Therefore, unlike the lhNKp46CD27^{+} cells which increased in proportion by 6 months post-vaccination in response flu (but with no change in co-stimulated proportions), pNKp46CD27^{+} cells decreased in co-stimulated and flu-stimulated cultures, indicating either a reduced response by NKp46^{+} cells or changes in co-expression of CD62L and/or CD27 post-vaccination. The relative dynamics of lhNKp46CD27^{-} cells pre- and 6 months post-vaccination for flu-stimulated and control cells, are graphically depicted in **Figure 5.7**.

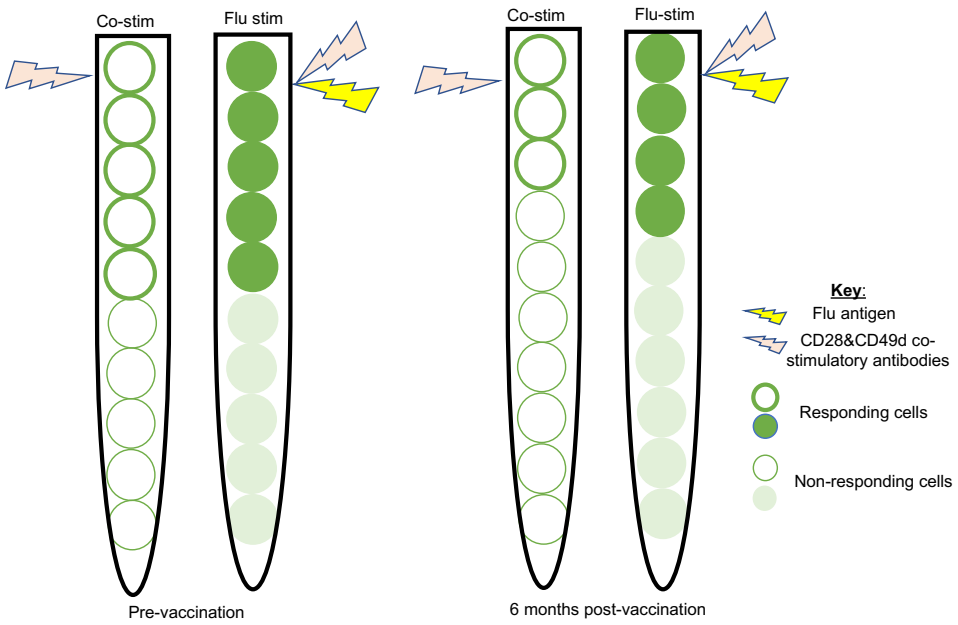


Figure 5.7: Illustration summarizing pNKp46CD27^{+} subphenotype distributions before and 6 months after influenza vaccination. Prior to vaccination there was no change in cells responding to flu compared to co-stimulated controls. At 6 months post-vaccination, At 6 months post-vaccination this subphenotype decreased but co-stimulated control cells to a greater extent than flu-stimulated cells.

5.3.1.4 Influenza vaccination changes in peripheral NKp46CD27^{-} proportions

Examination of pNKp46CD27^{-} cell proportions revealed that these reflected those of pNKp46CD27^{+} cells and although 2009- influenza vaccine antigen stimulated cells did not significantly increase in comparison to co-stimulated cells by 3 days post-vaccination they did show an increased trend which by 6 months was significant (*P*=0.049) (**Figure 5.8**). Similar to pNKp46CD27^{+} cells, by 6 months post-vaccination, a significantly lower proportion of pNKp46CD27^{-} cells, were able to respond to either flu-stimulation or CD28/CD49d co-stimulation (*P*=0.014 and *P*=0.03, respectively) (graphically depicted in **Figure 5.9**).

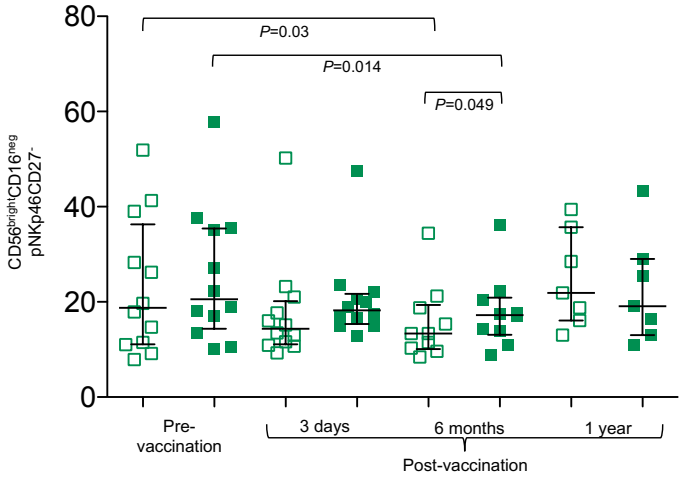


Figure 5.8: The effect of influenza vaccination on the distribution of pNKp46CD27^{-} responding cells. Proportions of pNKp46CD27^{-} cells were compared between control (no flu) and flu-stimulated PBMCs prior to vaccination (pre-) and at 3 days, 6 months and 1 year post-vaccination. Paired comparisons were performed using Wilcoxon signed rank test and *P*-values of <0.05 were considered significant. Error bars represent medians with interquartile ranges. Open symbols represent controls (no flu) and closed symbols represent flu-stimulated cells.

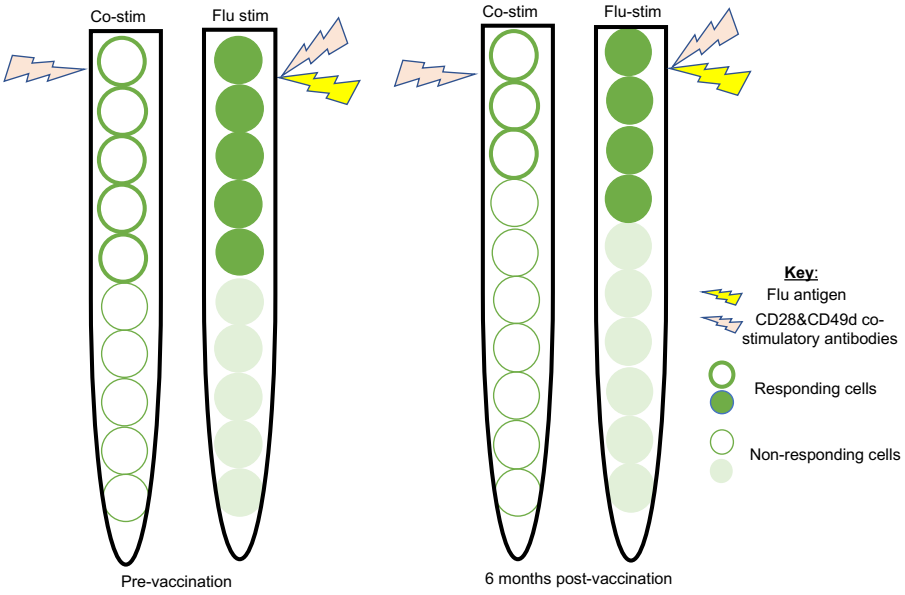


Figure 5.9: Illustration summarizing pNKp46CD27^{-} subphenotype distributions before and 6 months after influenza vaccination. Prior to vaccination there was no change in cells responding to flu compared to co-stimulated controls. At 6 months post-vaccination this subphenotype decreased but co-stimulated control cells to a greater extent than flu-stimulated cells.

Overall, these data demonstrate that the peripheral and lymph homing NKp46 subphenotypes (pNKp46CD27^{+}, pNKp46CD27^{-}, lhNKp46CD27^{+} and lhNKp46CD27^{-}) show no changes in proportion prior to vaccination with flu-stimulation, but following vaccination, peripheral and

lymph homing NK proportions differed. Peripheral subphenotypes responded with similar dynamics (**Figures 5.7 and 5.9**) and indicated that they were independent of CD27 co-expression, whereas, lymph homing NKp46 cells (**Figures 5.3 and 5.5**) responded with different dynamics according to CD27 expression.

5.3.2. Lymph homing and peripheral NKp46^{+} subphenotype degranulation (CD107a) responses

Since recognition and elimination of influenza infected cells is mediated by direct binding of NKp46 α-2,6 sialic acid residues to influenza HA protein (Arnon et al., 2004) and by activating lysis of virus infected cells (Mandelboim et al., 2001), longitudinal vaccine-induced degranulation (CD107a) responses were next investigated (**Figure 5.10**). CD107a expression was significantly increased in flu-stimulated lh- and pNKp46CD27^{+} cells as well as lh- and pNKp46CD27^{-} cells prior to vaccination and for all post-vaccination timepoints (except P>0.05 in lhNKp46CD27^{-} cells at 1 year post-vaccination) compared to co-stimulated cells (**Figures 5.10A, B, C and D**).

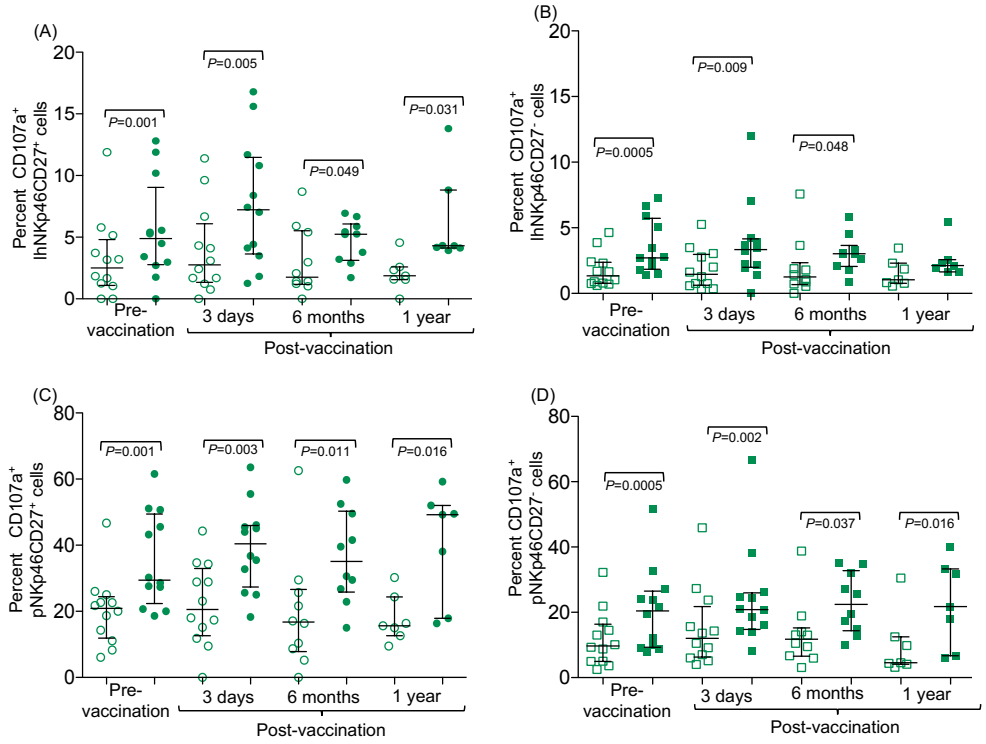


Figure 5.10: Lymph-homing and peripheral NKp46 subphenotype CD107a^{+} degranulation responses to flu-stimulation. Comparisons are shown between co-stimulated cells (open symbols) and flu-stimulated cells (solid symbols) and for lhNKp46CD27^{+} (A), lhNKp46CD27^{-} (B), pNKp46CD27^{+} (C) and pNKp46CD27^{-}(D) subphenotypes. Error bars indicate medians with interquartile ranges. Paired comparisons were performed using Wilcoxon signed rank and *P*-values of <0.05 were considered significant. Error bars represent medians with interquartile ranges.

These findings suggest that degranulation occurs de novo as a direct consequence of *in vitro* flu-stimulation, and displayed broad variability in response between different individuals. Given that the flu stimulus was a very potent inducer of degranulation, any subtle differences in cytolytic capability following influenza vaccination may not be evident. Vaccine primed degranulation may also have occurred very early following vaccination (before 3 days) as there was a trend to a greater degranulation response for CD27$^+$ cells, particularly for the lhNKp46$^+$CD27$^+$ subphenotype (*P*=0.052), yet, if this is indeed the case, then these responses are short lived.

5.3.2.1 Influence of CD27 co-expression on magnitude of NKp46$^+$ degranulating cells

Cell surface expression of CD27 influences NK cell function (Fu et al., 2011; Vossen et al., 2008) and CD56^{bright} or CD27$^+$ NK cells are considered to define an NK regulatory subset which target cells that express inflammatory molecules (Fu et al., 2014). To understand if CD27 preferentially influenced the cytolytic function of NKp46 subphenotypes differences in degranulation responses to flu-stimulation between CD27$^+$ and CD27$^-$ NKp46 subphenotypes were directly compared by correcting for background responses (determined by subtracting co-stimulated CD107a responses from flu-stimulated responses). Comparing lymph homing subphenotypes, while CD27$^+$ cells were significantly more cytolytic than CD27$^-$ cells only at 1 year post-vaccination (p=0.016), a pattern of increased CD107a expression on CD27$^+$ cells relative to CD27$^-$ cells was evident (**Figure 5.11A**). These results would need to be verified with larger sample numbers, however the consistent pattern across all timepoints of higher CD107a expression on CD27+ versus CD27- cells suggests that CD27 co-expression is very likely associated with enhanced cytolytic capability. A role for CD27 was very convincingly evident for the peripheral subphenotypes which are prevalent at much higher frequencies than lymph homing subsets. Peripheral NKp46CD27$^+$ cells were significantly more cytolytic than pNKp46CD27$^-$ cells prior to influenza vaccination (*P*=0.016) and at 3 days (*P*=0.003), 6 months (*P*=0.027) and 1 year (*P*=0.016) post-vaccination (**Figure 5.11B**).

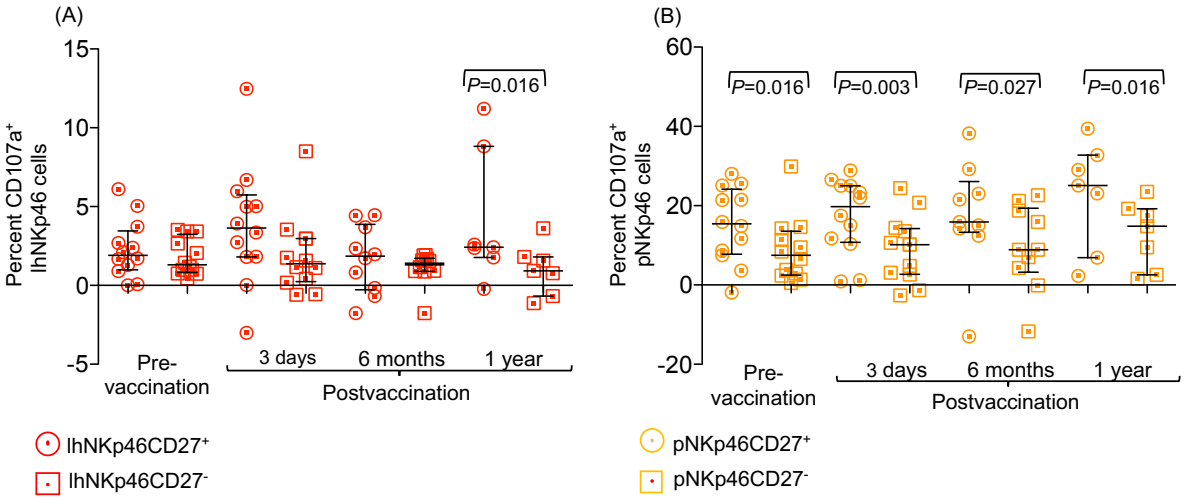


Figure 5.11: Effect of CD27 co-expression on magnitude of pNKp46^{+} degranulating responses to flu-stimulation. To determine if CD27 co-expression on NKp46^{+} subphenotypes influences magnitude of responding degranulating cells, comparisons were made between NKp46CD27^{+} and NKp46CD27^{-} subphenotypes after adjusting for background responses (determined by subtracting co-stimulated frequencies from flu-stimulated frequencies). Paired comparisons were performed using Wilcoxon signed rank test and *P*-values of <0.05 were considered significant. Error bars represent medians with interquartile ranges.

Taken together, these findings provide novel insights into cytolytic capability of lymph homing NKp46^{+} cells able to migrate to SLO's and NKp46^{+} cells within the peripheral circulation and reveals a role for CD27 co-expression in peripheral NKp46 mediated cytolytic responses with the pNKp46CD27^{+} subphenotype proving to be the most cytolytic (Figure **5.12**).

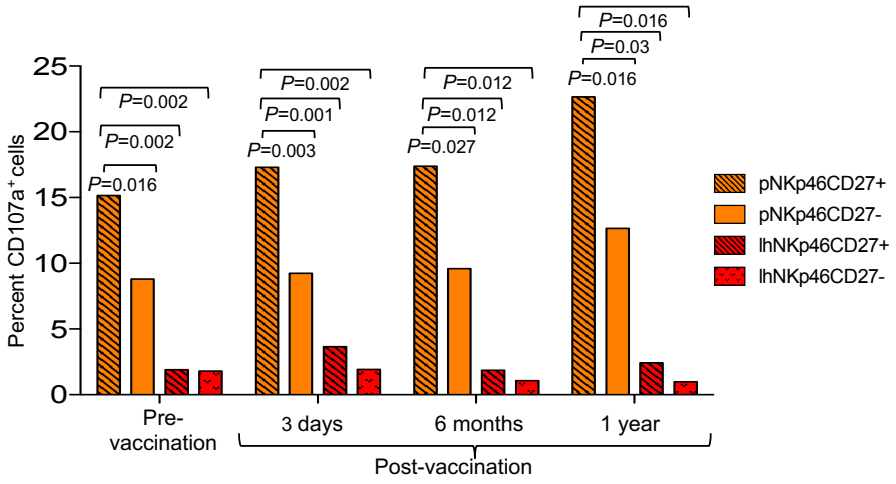


Figure 5.12: Differences in the magnitude of degranulating (CD107a^{+}) cells between lymph homing and peripheral NKp46^{+} subphenotypes. Medians were calculated following corrections for background CD107a responses and *P*-values represent comparisons between pNKp46CD27^{+} cells and pNKp46CD27^{-}, lhNKp46CD27^{+} and lhNKp46CD27^{-} subphenotypes. Paired comparisons were performed using Wilcoxon signed rank test and *P*-values of <0.05 were considered significant.

5.3.3. Lymph homing and peripheral NKp46^{+} subphenotype cytokine (IFNγ^{+}) responses

NK cells provide an early source of IFNγ in the lungs contributing to both innate and adaptive antiviral responses, as shown for vaccinia virus infection (Abboud et al., 2016) and are essential for Th1 polarization of naïve CD4 T cells within the LN (Martin-Fontecha et al., 2004). The capacity of NKp46 subphenotypes to produce IFNγ in response to influenza vaccination was next analysed. (**Figure 5.13**).

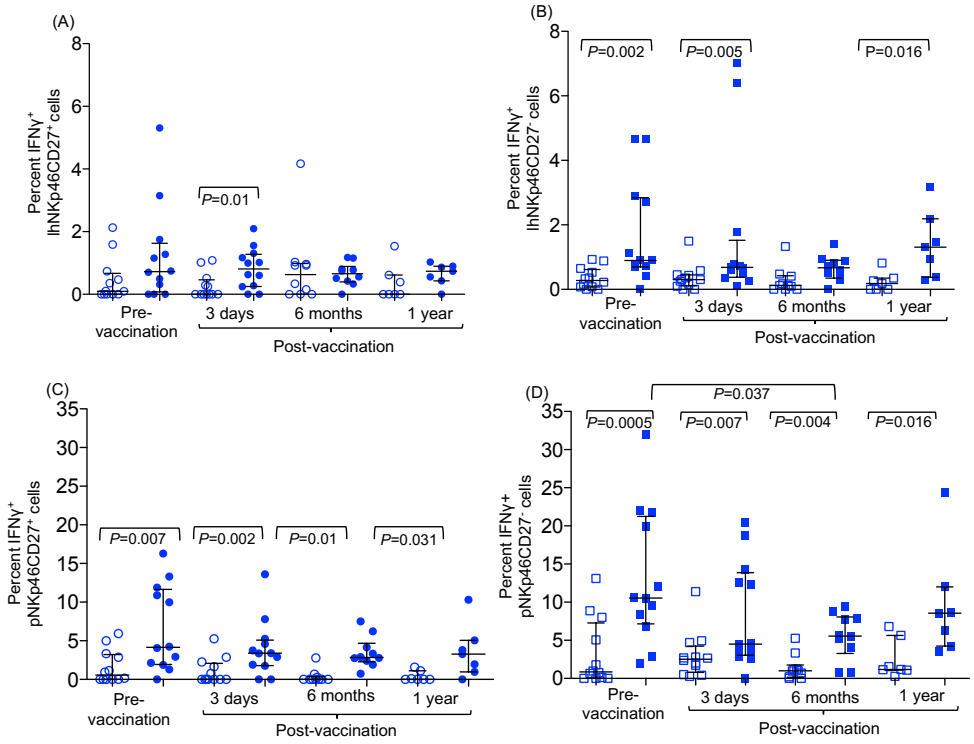


Figure 5.13: Lymph homing and peripheral NKp46 subphenotype cytokine (IFNγ^{+}) responses to *ex vivo* flu-stimulation. Comparisons are shown between co-stimulated cells (open symbols) and flu-stimulated cells (solid symbols) for lhNKp46CD27^{+} (A), lhNKp46CD27^{-} (B), pNKp46CD27^{+} (C) and pNKp46CD27^{-} (D) subphenotypes. Error bars indicate medians with interquartile ranges. Paired comparisons were performed using Wilcoxon signed rank test and *P*-values of <0.05 were considered significant. Error bars represent medians with interquartile ranges.

Flu-stimulated lhNKp46CD27^{+} cells produced more IFNγ than co-stimulated cells (*P*=0.01) at 3 days post-vaccination (**Figure 5.13A**). On the other hand, flu-stimulated lhNKp46CD27^{-} cells responded with a greater frequency than in co-stimulated cells, at pre-vaccination, and at 3 days and 1 year post-vaccination (*P*=0.002; *P*=0.005; *P*=0.016, respectively) (**Figure 5.13B**).

In contrast to lymph homing NKp46 subphenotypes, frequencies of both IFNγ-producing peripheral NKp46 subphenotypes were significantly increased in response to *ex vivo* flu-

stimulation compared with co-stimulated cells for all timepoints, (P<0.05) (**Figures 5.13C and D**). *In vivo* vaccination influenced post-vaccination responses as the frequency of IFNγ^{+} responding cells for both pNKp46CD27^{+} and pNKp46CD27^{-} subphenotypes decreased post-vaccination. This was particularly noticeable for the pNKp46CD27^{-} subphenotype, as the frequency of cells responding to flu-stimulation with intracellular IFNγ production, started decreasing within 3 days after vaccination, which by 6 months was significant (P=0.037) (**Figure 5.12D**). Murine models have shown that the phenotype of murine lung NK cells comprises approximately 70% CD27^{-} cells and that NK cells are rapidly recruited to the lungs from other sites following influenza infection (Wang et al., 2012), therefore it could be postulated that the reduction in pNKp46CD27^{-} IFNγ^{+} cells may be a consequence of antigen responding IFNγ^{+} cells being recruited to the lungs following vaccination.

5.3.3.1. Influence of CD27 co-expression on magnitude of NKp46^{+} IFNγ producing cells

NK cells are able to rapidly secrete IFNγ upon cell activation (De Maria and Moretta, 2011) and differences between lymph homing and peripheral NKp46 IFNγ responses according to CD27 co-expression were next assessed. After adjusting for background IFNγ responses, the frequency of lhNKp46CD27^{-} cells responding to flu-stimulation was greater than the frequency of lhNKp46CD27^{+} cells at 6 months (P=0.006) and at 1 year (P=0.03) (**Figure 5.14A**), whereas before vaccination, pNKp46CD27^{-} cells produced more IFNγ than pNKp46CD27^{+} cells (P=0.0005). The frequency of IFNγ-expressing pNKp46CD27^{-}cells declined within 3 days of vaccination and differences were lost, but recovered by 1 year (P=0.016) (**Figure 5.14B**).

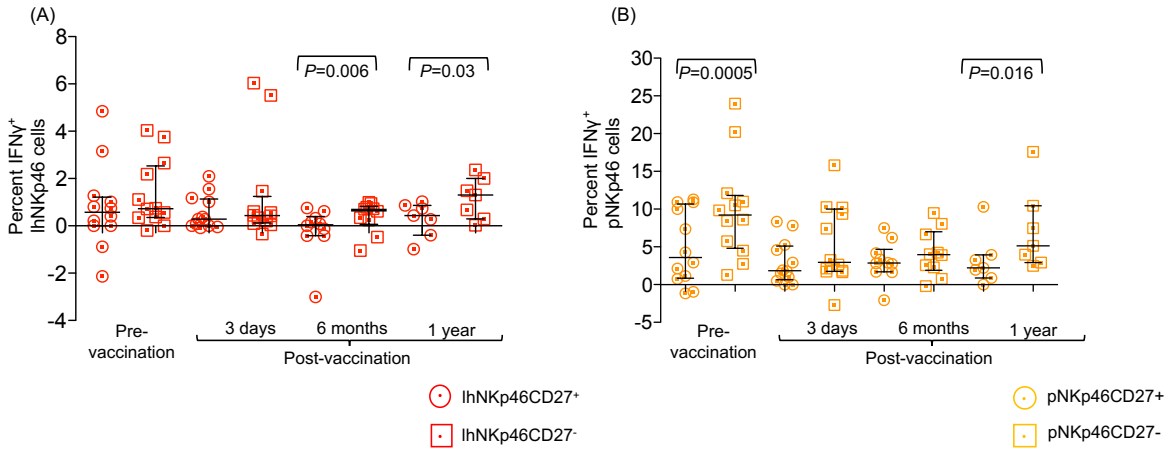


Figure 5.14: Influence of CD27 co-expression on magnitude of pNKp46^{+} cytokine (IFNγ) responses. Comparisons were made between NKp46CD27^{+} and NKp46CD27^{-} subphenotypes after adjusting for background responses (determined by subtracting co-stimulated from flu-stimulated IFNγ^{+} cell frequencies). Paired comparisons were performed using Wilcoxon signed rank test and P-values of <0.05 were considered significant. Error bars represent medians with interquartile ranges.

Similar to degranulating cells, peripheral NKp46 IFNγ responses were greater in magnitude than those of lymph homing cells but in contrast to CD107a^{+} degranulating cells, the magnitude of IFNγ response was greater for CD27^{-} cells and pNKp46CD27^{-} cells were the most abundant producers of intracellular IFNγ (**Figure 5.15**).

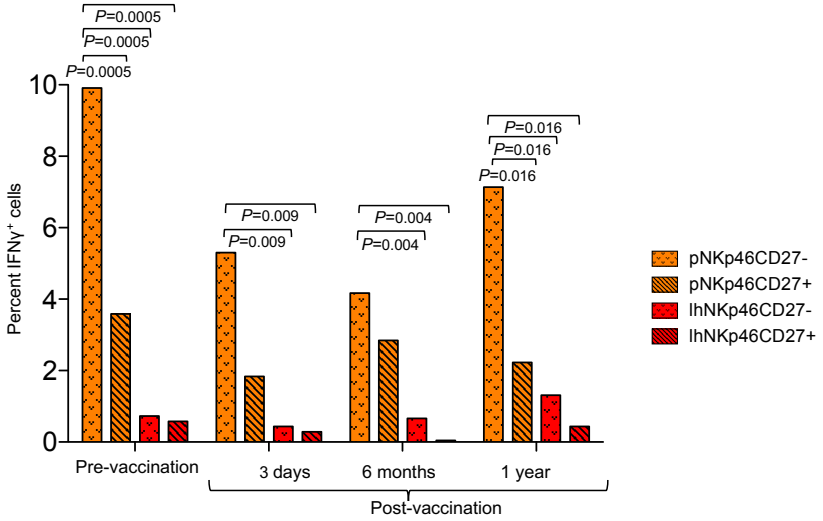


Figure 5.15: Differences in the magnitude of IFNγ producing cells between lymph homing and peripheral NKp46^{+} subphenotypes. Medians were calculated following corrections for background IFNγ responses and *P*-values represent comparisons between pNKp46CD27^{-} cells and pNKp46CD27^{+}, lhNKp46CD27^{-} and lhNKp46CD27^{+} subphenotypes. Paired comparisons were performed using Wilcoxon signed rank test and *P*-values of <0.05 were considered significant.

Taken together, peripheral NKp46 cells respond to influenza vaccine with enhanced IFNγ cytokine and CD107a degranulation responses compared to lymph homing cells. Importantly, CD27 co-expression functionally delineates peripheral NKp46 subphenotypes, as CD27 co-expression was associated with enhanced CD107a degranulation responses. Although the data was not as compelling for IFNγ responses, the lack of CD27 co-expression was largely associated with enhanced IFNγ responses.

5.3.4 CD56^{bright}CD16^{neg} NK cells are not polyfunctional

Polyfunctionality (ability to produce two or more cytokines/functions) is a feature of potent T cell responses to infection (Almeida et al., 2007; Betts et al., 2005; Bihl et al., 2009; Ciuffreda et al., 2008). To investigate if CD56^{bright}CD16^{neg} subsets are polyfunctional, quadrant gates were applied to CD27^{+} and CD27^{-} subphenotypes to determine levels of CD107a and IFNγ co-expression (**Figure 5.16**).

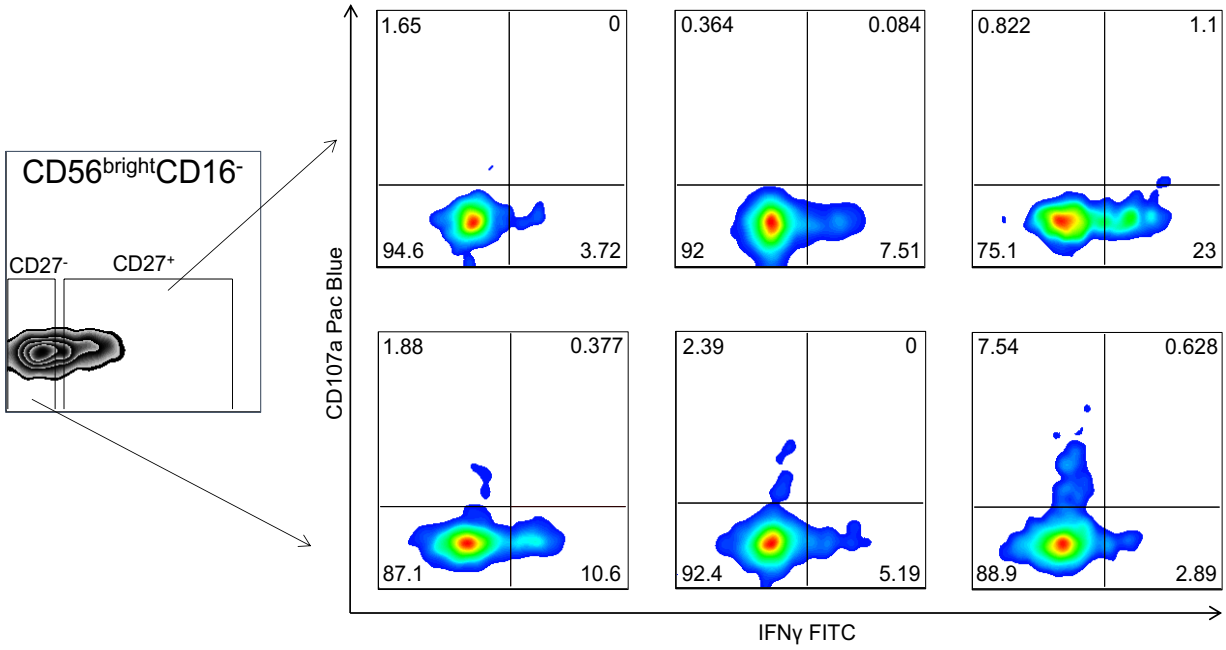


Figure 5.16: CD107a and IFNγ co-expression on CD56^{bright}CD16^{neg} NK cells. To assess if CD56^{bright}CD16^{neg} NK cells are polyfunctional, co-expression frequencies of CD107a and IFNγ responding cells were determined by applying quadrant gates to CD56^{bright}CD16^{neg} CD27^{+} (top row) and CD27^{-} (bottom row) flu-stimulated cells. Dot plots are representative examples of 3 participants with low, medium and high frequencies of IFNγ and CD107a responses. Numbers in dot plots represent percent expression for each quadrant as calculated by FlowJo^{TM} Software for Mac (version 9.9.4), Ashland.

No CD27^{+} or CD27^{-} CD56^{bright}CD16^{neg} NK cells capable of co-expressing CD107a and IFNγ were evident, in agreement with findings published by Juelke et al., (2010), who showed that unlike CD56^{dim} cells, CD56^{bright}CD16$^{dim/-}$ cells, are not polyfunctional (at least for the markers tested).

5.3.5 Influence of *ex vivo* flu-stimulation on NKp46 cell surface density

Since influenza vaccine driven changes in NKp46 and CD244 (2B4) expression, with accompanying functional responses, have been observed in human NK subsets following influenza vaccination (Jost et al., 2011), changes in NKp46 cell surface density were next investigated, by comparing NKp46 MFI of flu-stimulated cells with that of co-stimulated cells (**Figure 5.17**).

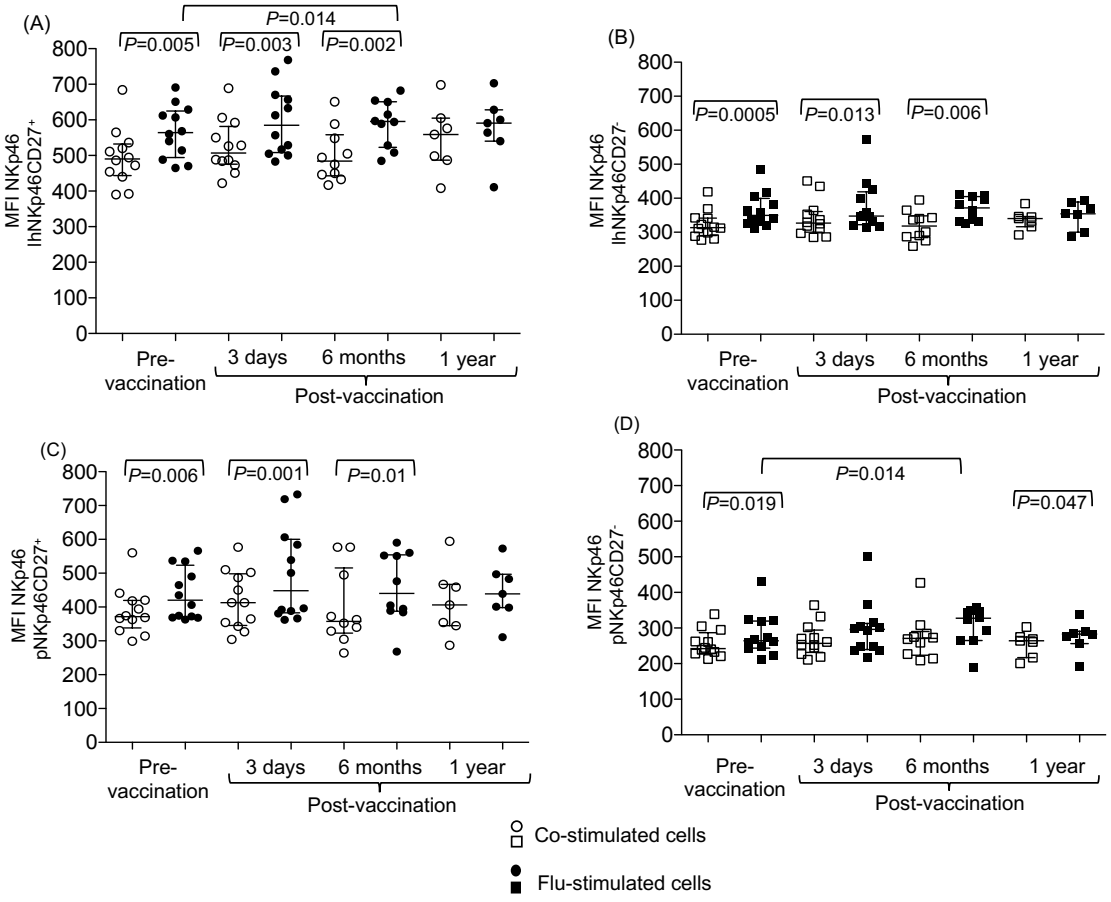


Figure 5.17: Effect of *ex vivo* flu-stimulation on NKp46 cell surface density. Median fluorescent intensities (MFI) of flu-stimulated cells were compared to co-stimulated cells for lhNKp46CD27^{+} (A); lhNKp46CD27^{-} (B); pNKp46CD27^{+} (C) and pNKp46CD27^{-} (D) subphenotypes. Paired comparisons were performed using Wilcoxon signed rank test and *P*-values of <0.05 were considered significant. Error bars represent medians with interquartile ranges.

In general, NKp46 cell surface density was significantly increased in response to *ex vivo* flu-stimulation compared to co-stimulated controls. This was significant prior to vaccination and up to 6 months post-vaccination for both lhNKp46CD27^{+} (**Figure 5.17A**) and lhNKp46CD27^{-} (**Figure 5.17B**) subphenotypes (P<0.05). Therefore, upregulated NKp46 surface expression occurred independently of CD27 co-expression, although to a greater extent on CD27^{+} cells. A similar significant upregulation of NKp46 surface density was observed on pNKp46CD27^{+} cells up to 6 months (**Figure 5.17C**). In contrast however, NKp46 surface density on pNKp46CD27^{-} cells was only upregulated pre-vaccination and 1 year post-vaccination (**Figure 5.17D**), which intriguingly coincided with the 2 time-points where the frequency of pNKp46CD27^{-} IFNγ producing cells was significantly greater than those of pNKp46CD27^{+} cells.

Changes attributed to *in vivo* vaccination were apparent for lhNKp46CD27^{+} and pNKp46CD27^{-} cells, as following vaccination, an enhanced upregulation of NKp46 surface expression was observed with flu re-challenge by 6 months post-vaccination for lhNKp46CD27^{+} cells (*P*=0.014) (**Figure 5.17A**) as well as pNKp46CD27^{-} cells (**Figure 5.17D**) compared with pre-vaccination flu-stimulated cells. This points to the existence of a pool of expanding vaccination primed or "trained" NKp46 cells within these 2 NKp46^{+} subphenotypes that by 6 months was larger than the pool of cells able to respond to flu-stimulation before vaccination.

5.4 Discussion

In the current study, CD56^{bright}CD16^{neg} lymph homing (CD62L^{+}) and peripheral (CD62L^{-}) NKp46 subphenotype responses to 2009-influenza vaccination were longitudinally investigated over a year, in order to establish if vaccination induced long term functional reprogramming of any CD56^{bright}CD16^{neg} NK subphenotypes. Associations between CD27 expression and NKp46 surface density were investigated, and subphenotype cytolytic and intracellular cytokine response was assessed by measuring CD107a degranulation and intracellular IFNγ production, respectively.

Accumulating evidence, suggests that NK cells have features characteristic of adaptive immunity. There are reports in mice of enhanced secondary responses by NK cells to MCMV (Sun et al., 2009) and in humans, evidence of adaptive NK memory-like recall responses to viruses includes specificity to antigen (Hammer et al., 2018; Nikzad et al., 2019), the presence of long lived memory cells (Geary and Sun, 2017; Hammer et al., 2018; Nikzad et al., 2019), the expansion of specific memory responses (Guma et al., 2006; Lopez-Verges et al., 2011) and enhanced functional responses (Foley et al., 2012). Vaccination of macaques with modified MVA vaccination leads to long term "imprinting" of NK cells with subsequent changes in NK phenotype, homing characteristics, cell adhesion and cytolytic responses (Palgen et al., 2019), yet, murine NK cells can also exhibit a "trained immunity" response as they produce higher amounts of IFNγ upon re-exposure to cytokines (Cooper et al., 2009; Keppel et al., 2013; Ni et al., 2012; Romee et al., 2012) which does not require antigen specificity. The fact that NK cells exhibit elements of adaptive recall responses, trained responses and long term vaccination induced functional reprogramming, reveals a potential role for NK cells in the development of improved vaccines.

In the current study, complex post-vaccination increases and decreases in proportions of NKp46 subphenotypes in response to *ex vivo* 2009-vaccine challenge, and which persisted for up 6 months post-vaccination, were observed for all NKp46 subphenotypes. These data

indicated long term vaccination induced functional reprogramming on NKp46 subphenotypes of which the lhNKp46CD27^{+} subphenotype showed four elements of an adaptive recall response.

1. As there was no pre-vaccination expansion of lhNKp46CD27^{+} subphenotype proportions in response to *ex vivo* flu-stimulation compared to co-stimulated cells, this indicated that changes in post-vaccination responses were due to *in vivo* vaccination.
2. The proportion of lhNKp46CD27^{+} cells increased significantly (P=0.012) in magnitude in response to influenza vaccine antigen re-challenge 6 months post-vaccination. This suggests the presence of a pool of specific cells that had undergone epigenetic changes and that expanded rapidly (within an *in vitro* setting) upon antigen re-challenge.
3. Responses were specific. There was no change in the proportion of post-vaccination co-stimulated cells indicating that changes in subphenotype proportions were not a reflection of nonspecific co-stimulation, but rather specific cells responding to antigen.
4. Responses were long lived. Although at 3 days post-vaccination there was no significant increase in 2009- influenza vaccine antigen responding cells, by 6 months the proportions of lhNKp46CD27^{+} cells were significantly greater than prior to vaccination, indicative of the presence of long-lived cells able to respond to antigen re-exposure.

It is known that during viral infection there can be a cytokine-mediated activation of NK cells, however MCMV-memory NK cells become less responsive to bystander cytokine NK cell activation and more antigen specific, which is dependent on the Ly49H receptor (Min-Oo and Lanier, 2014). Also, MCMV memory NK cells generated by Ly49H activation and expansion in response to MCMV is dependent on specific recognition of the m157 antigen and it has been suggested that one of the underlying mechanisms of MCMV induced memory NK cells involves an increase in Ly49H surface density (Min-Oo and Lanier, 2014). Following vaccination, lhNKp46CD27^{+} cells, with the highest NKp46 surface density (**Figure 4.9** in section 4.2.5 of Chapter 4) was the only subset that responded with an increase in proportion to *ex vivo* flu-stimulation but remained unchanged with co-stimulation. It is therefore conceivable that lhNKp46CD27^{+} cells are responding to influenza antigen in a manner similar to MCMV m157 antigen interactions with Ly49H as described by Min-Oo and Lanier (2014), hence an enhanced 2009- influenza vaccine antigen induced response and lack of response to CD28/CD49d co-stimulation.

In contrast, following vaccination, changes in proportions were observed in both control (co-stimulated) as well as flu-stimulated cells for lhNKp46CD27^{-} (which increased in proportion) and peripheral NKp46 subphenotypes (which decreased in poportion). Integrating and interpreting the data between *ex vivo* flu-stimulations and vaccination induced responses is complex with the data either being i) a reflection of up- and downregulation of CD27 and CD62L on the same subset and therefore either representing different stages of a trained recall response, or post-vaccination "imprinting" on CD62L^{+} cells as described by (Palgen et al., 2019) or ii) a reflection of differential responses to stimulatory influences by four distinct subphenotypes or iii) those of two subphenotypes, i.e. lymph homing and peripheral. But the varying influences driving the dynamics of response is beyond the scope of the current study. What the results from this study have established though, is that *in vivo* 2009- influenza vaccination "trained" (or sensitised) specific CD56^{bright}CD16^{neg} subphenotypes sufficiently that they are able to respond to both 2009-influenza vaccine antigen and CD28/CD49d co-stimulation.

The unexpected expansions in proportion of CD28/CD49d co-stimulated (lh)NKp46CD27^{-} NK cells could be attributed to bystander activation by T cells, but would need to be confirmed with T cell depletion experiments. The costimulatory requirements of CMV-specific memory CD4 T cells vary, are heterogeneous in their activation thresholds for antigen induced cytokine production and the costimulatory pathways (CD28, CD49d and CD5) can affect memory/effector T cell responses (Waldrop et al., 1998). During viral infection in mice, cell surface expression of CD49d (and CD11a) is upregulated on murine antigen specific CD4 T cells (McDermott and Varga, 2011) while in humans the frequency of CD49d^{+} (and CD11a) antigen-specific CD4 and CD8 T cells increases for up to 6 months following vaccination with *Leishmania* vaccine (Christiaansen et al., 2017). The α4β1 integrin (CD49d) is also expressed on NK cells (Gandoglia et al., 2017; Macias et al., 2000) and on innate memory NK-like CD8^{+} T cells (Barbarin et al., 2017). Similarly then, CD49d may play a role in trained immunity of NK cells, but synergy between co-receptors on resting NK cells is required for cell activation (Bryceson et al., 2006b) and whether mutual co-operation exists between CD49d and NKp46 is not known. It would therefore need to be ascertained if direct engagement of CD49d accounts for the observed responses.

As blocking CD80 and CD86 (the ligands for CD28) inhibits expansion of NK cells, a role for CD80/86 co-stimulation in IL-12 dependant lipopolysaccharide (LPS) expansion of NK cells has been suggested (Goodier and Londei, 2000) but this may be a consequence of T and dendritic cell blockade rather than a direct effect on NK cells per se (Goodier and Londei,

2004), as there is little evidence that CD28 is expressed on NK cells (Goodier and Londei, 2004; Lang et al., 1998; Wilson et al., 1999). Yet, even though there is no evidence of CD28 surface expression on NK cells, an unidentified CD28 homolog has been found to be a potent activator of NK cells as shown by their lytic response to B7H7^{+} tumour cells (Zhuang and Long, 2019). Thus, the role, if any, of CD28 and/or CD49d in changes of subphenotype proportions therefore remains unclear. Although a possible role of CD28 and CD49d in the observed changes in post-vaccination responses cannot be discounted, recognition of 2009- H1N1 by NKp46 leads to the direct killing of 2009- H1N1 influenza infected cells both *in vitro* and *in vivo* (Achdout et al., 2010). Importantly, in the current study, CD56^{bright}CD16^{neg} cells that did not express NKp46 remained unchanged following vaccination and did not respond to stimulation with flu antigen. This indicated that the observed responses (whether flu-stimulated or co-stimulated) were mediated by changes in NKp46^{+} cells following vaccination.

Although all NKp46^{+} subphenotypes responded to flu-stimulation with an increase in suface density, both lymph homing and peripheral subhenotypes that co-expressed CD27 responded with a greater increase in NKp46 MFI (P<0.05). These findings are significant, given the critical role of NKp46 in protection against influenza infection, for which influenza virus has developed an evasion mechanism that involves NA mediated removal of NKp46 sialic acid residues (Bar-On et al., 2013). By increasing the number of NKp46 receptors on the NK cell surface, CD27 may provide a mechanism to help counteract the NA mediated removal of NKp46 sialic acid residues which are so essential for NK cell interactions with influenza HA and furthermore, may lower the stimulation threshold for these cells.

CD56^{dim} and CD56^{bright} NK cells have different functional capacities (Cooper et al., 2001b; Frey et al., 1998; Sedlmayr et al., 1996) and in their resting state, CD56^{dim} NK cells are more cytotolytic against NK sensitive targets than the CD56^{bright} subset (Nagler et al., 1989), but following activation with IL-12 or IL-2, CD56^{bright} NK cells acquire similar cytolytic ability (Ellis and Fisher, 1989; Nagler et al., 1989). A role for CD27 as a co-activator for NKp46 function is also suggested, as NKp46 surface density is heterogeneous requiring a threshold for activation which impacts on NK cell function (Sivori et al., 1999) and in *vitro* blocking of CD27 with an anti-CD27 mAb inhibits cytolytic activity of IL-2 activated NK cells (Sugita et al., 1992). Peripheral NK cells that express CD27 are mostly of a CD56^{bright} phenotype (Vossen et al., 2008) and differences in receptor expression and cytotoxic responses between human CD27^{high} and CD27^{low} NK cells have been shown (Fu et al., 2011; Silva et al., 2008). In the current study all NKp46^{+} subphenotypes responded to 2009- influenza vaccine antigen stimulation with degranulation, but following vaccination, there was no increase in CD107a

degranulation with re-challenge. Thus, CD56^{bright}CD16^{neg} NK cell cytolytic activity remained unaffected by vaccination which indicated that responding cells showed no further enhanced cytolytic activity when re-challenged with 2009- influenza vaccine antigen. NK activation responses to 2009- H1N1 are reduced compared to those triggered by H5N1 and 1918-H1N1 pseudotyped particles (Du et al., 2010), which is consistent with a milder pathogenesis of the 2009- H1N1 influenza pandemic compared to the H5N1 and 1918-H1N1 pandemics, that were associated with a more severe pathogenesis caused by enhanced inflammation and cell death (Kash et al., 2006; Katz et al., 2000). Furthermore, evidence of enhanced degranulation responses of "memory-like" NK cells remains controversial. Increased secondary CD107a degranulation responses have been shown in Ly49H^{+} memory-like NK cells in response to MCMV re-challenge (Sun et al., 2009), however there was no difference between control and cytokine induced memory-like recall responses in a Rag-1$^{-/-}$ mouse model (Keppel et al., 2013) and hepatic resident CD49^{+}DX5^{-} cells, which have hapten specific CHS responses produce less CD107a than CD49^{-}DX5^{+} cells (Peng et al., 2013b). Taken together these studies suggest that enhanced CD107a degranulation during secondary NK responses is subject to stimulation, cell type and phenotype and could explain the degranulation responses observed in this study as subtle recall responses may have been masked by the innate degranulation activity of NK cells with flu antigen.

Despite the fact that cells degranulated above background there was no difference (P>0.05) in CD107a expression between lhNKp46CD27^{-} and lhNKp46CD27^{+} subphenotypes after adjustments were made for background responses, unlike pNKp46CD27^{+} cells, which degranulated, at all time-points (P<0.05), with a greater magnitude than the CD27^{-} pNKp46 subphenotype and both lymph homing NKp6 subphenotypes. The data from the current study therefore indicates that cytolytic responses of peripheral NKp46 subphenotypes could be delineated by CD27 expression but does not play a role as a marker of enhanced cytolytic responses for lymph homing NKp46 subphenotypes. This supports the idea that CD27 co-regulates NKp46 cytolytic responses to influenza antigen on activated peripheral NK cells and also reveals previously unreported differences of NKp46 mediated degranulation responses, based on NK homing capability and CD27 co-expression.

Enhanced vaccine induced IFNγ NK responses to influenza (Long et al., 2008) as well as other pathogens (White et al., 2014) have been shown, however conflicting data on IFNγ production by NK cells in human responses to influenza vaccination is also reported (He et al., 2006; Long et al., 2008). In the current study, distinct differences in IFNγ production between lymph homing and peripheral NKp46^{+} subphenotypes was observed. Lymph homing NKp46+ cells

produced very little IFNγ with lhNKp46CD27^{+} cells in particular, only reaching levels above background 3 days after vaccination. Although lhNKp46CD27^{-} cells responded above background for most time-points, the magnitude of response was subdued compared to those observed for peripheral NKp46 cells. Following migration to the LNs CD56^{bright} NK cells provide an early source of IFNγ which is essential for Th1 polarization of naïve CD4 T cells (Martin-Fontecha et al., 2004). Complex cellular interactions and local microenvironment modify NK cells (Mamessier et al., 2011; Mavilio et al., 2005) and the requirement for additional signals, such as priming by LN resident dendritic cells (Lucas et al., 2007), could explain why lhNKp46 cells isolated from the peripheral circulation produced low frequencies of IFNγ. Indeed, lymph homing IFNγ producing cells may have started migrating to the LNs following sensitisation at vaccination, as the proportion of IFNγ producing cells responding to *ex vivo* stimulation was reduced thereafter.

Although both peripheral NKp46 subphenotypes produced significant IFNγ (P<0.05) in response to flu-stimulation for all time-points, pNKp46CD27^{-} cells in particular, proved to produce more IFNγ than the other NKp46 subphenotypes. But following vaccination, there was a decline in the number pNKp46CD27^{-} IFNγ responding cells and by 6 months significantly fewer cells responded to re-challenge. These data are in contrast to results from other studies which have found that CD27^{+} NK cells are able to produce IFNγ with a greater magnitude than CD27^{-} cells (Fu et al., 2011; Silva et al., 2008), but it could be speculated that following vaccination, reduced pNKp46CD27^{-} IFNγ responding cells was a consequence of migration to the lungs. Murine lungs comprise of mainly CD27^{-} NK cells and following influenza infection, murine NK cells are rapidly recruited to the lungs from other sites (Stein-Streilein et al., 1988; Wang et al., 2012). Also, NK cells isolated from lung pleural effusion of patients infected with *Mycobacterium tuberculosis* are of a CD56^{bright}CD16^{neg} phenotype and although they have low degranulation capability, they are able to produce abundant IFNγ (Schierloh et al., 2005).

Overall, flu-stimulated peripheral NKp46^{+} cells elicited significant CD107a degranulation and IFNγ cytokine responses which remained robust for up to a year but wide differences in the frequency of CD107a and IFNγ producing cells were observed between individuals. As with other studies there was no apparent correlation to age or gender (Schapiro et al., 1990) and differences in functional responses most likely reflect previous immune activity unique to each individual which in turn shapes NK heterogeneity (Horowitz et al., 2013). In this study it was shown that neither CD27^{+} nor CD27^{-} CD56^{bright}CD16^{neg} NK cells were polyfunctional in their response to flu-antigen and this pertained to individuals with robust responses as well as to

those with a low frequency of responsive cells. This is in contrast to a study (Pelletier et al., 2010) that reported co-expression of IFNγ and CD107a on CD56^{bright}CD16^{neg} NK cells isolated from PBMCs from HCV patients (acute, chronic and exposed uninfected) and healthy controls and co-cultured with K562 cells. The contrasting results could be attributable to the difference in activation methods used by the studies. Also, K562 cells do not express human leukocyte antigen (HLA) class I and II (MHC antigens) (Klein et al., 1976; Lozzio and Lozzio, 1975) and are not able to engage NK cell inhibitory KIRs, thus the stimulatory potential and responses to K562 cells is determined by expression of ligands for activating NK cell receptors including NKp46 (Tremblay-McLean et al., 2019). Even though CD56^{bright} NK cells do not express inhibitory KIRs (Michel et al., 2016), NKp46 directly recognizes and engages with 2009-H1N1 and H5 influenza antigens (Achdout et al., 2010). Recognition and interactions of NKp46 with 2009- H1N1 leads to direct killing of virus whereas NKp46 interactions with 2009- H5 are mediated via a different binding site which does not elicit direct killing of virally infected cells (Achdout et al., 2010). The stimulatory signals received by NK cells and downstream responses are therefore dependent on the nature of NKp46 binding to target cells. The differences between this study and that of Pelletier *et. al.* (2010) could be explained by the different functional profiles induced in NK cells by K562 stimulation and NK cell response to stimulation by a subunit 2009-influenza vaccine antigen since K562 cell lines represent transformed cells targeted for destruction by NK cells via unknown ligands. It cannot be ruled out that a) similar to T cells (Han et al., 2012) CD56^{bright}CD16$^{dim/-}$ cells are polyfunctional, but release different cytokines in a sequential manner, or b) represent the same cell which at the time of stimulation, are responding to different microenvironment signals. These data however provide further evidence that as with mice, human NK cells can be functionally differentiated by CD27^{+} and CD27^{-} phenotypes (Fu et al., 2011; Silva et al., 2008; Vossen et al., 2008).

In conclusion, vaccination with 2009-influenza vaccine induced long term “training” of NKp46^{+} subphenotypes and these data reveal a complex scenario that contributes to emerging insights into NK heterogeneity and indicate that peripheral and lymph homing CD56^{bright}CD16^{neg} NKp46 subphenotypes respond differentially to vaccination.

CHAPTER 6:
Circulating soluble factors and T cell responses to influenza vaccination

6.1 Introduction

NK cells play a pivotal role in the initiation and regulation of immune defense against viral infections via reciprocal interactions with endogenous T-cell derived IL-2 (Fehniger et al., 2003) which include vaccination induced responses to influenza A (He et al., 2004), malaria and rabies (Horowitz et al., 2010a; Horowitz et al., 2012; Horowitz et al., 2010b; McCall et al., 2010). In mice, two subpopulations of $CD8^+$ cytotoxic T lymphocyte (CTL) are generated against influenza A virus (Braciale, 1977a, b) following immunization, viz. a virus specific population and a cross reactive population able to recognise other influenza A subtypes. NK cells are required to generate virus specific $CD8^+$ T cell responses to influenza infection (Kos and Engleman, 1996), mediated by IFNγ and perforin-dependant recruitment of $CD8^+$ T cells (and dendritic cells) to the lymph nodes (Ge et al., 2012). Initial viral clearance by CTLs is mediated through degranulation (Topham et al., 1997) but CTL recall responses to a previously encountered antigen requires CD4 T cell help during priming for the development of memory responses (Shedlock and Shen, 2003; Sun and Bevan, 2003) and the presence of CD4 T cells are required for recruitment of influenza specific CD8 T cells to the lungs (Riberdy et al., 2000). T cell derived IL-21 cytokines play a role in the generation of B cell memory responses to H1N1 influenza vaccine (Pallikkuth et al., 2011b) and T cell help is critical in shaping B cell responses through secretion of IFNγ and IL-4 (Snapper and Paul, 1987). Following activation by T cells, mature B cells proliferate and develop into memory or Ig-secreting cells (Parker, 1993) which are able to respond rapidly upon secondary encounter to specific antigen.

The induction of strong neutralizing antibody responses is an important component of an effective influenza vaccine (Gerhard et al., 1997). Following vaccination with inactivated influenza vaccine, specific IgG antibodies are induced within 6 days of administration and up to 90% of vaccinees show protective titres by 2 weeks post-vaccination (Cox et al., 1994). Secreted IgM (sIgM) is the earliest isotype to be expressed during the development of an immune response. Natural IgM (secreted by B-1 cells) is the predominant IgM within the circulation and does not require antigen stimulation (Casali and Schettino, 1996; Coutinho et al., 1995) whereas IgM produced by B-2 cells is antigen specific (Baumgarth et al., 1999). As both natural IgM and antigen specific IgM are polymeric, they are able to be transported via the poly-Ig receptor to mucosal surfaces allowing both to provide protection against pathogens (Gerhard et al., 1997). Furthermore, in mice, both B-1 and B-2 derived IgM have non-redundant functions against influenza infection (Baumgarth et al., 2000) and are necessary for induction of virus specific IgG responses. Soluble B cell-activating factor (BAFF) and “a

proliferation-inducing ligand" (APRIL) are innate factors belonging to the tumour necrosis factor family and are involved in B cell class switch recombination, survival and B-lineage differentiation (Castigli et al., 2005; Mackay et al., 2010; Mackay et al., 2003; Martin-Fontecha et al., 2004; Schiemann et al., 2001; Thompson et al., 2000). Serum BAFF and APRIL levels are increased in healthy controls and HIV^+ 2009-H1N1 vaccine responders, whereas impaired B cell responses to 2009-H1N1 vaccine are associated with deficiencies in serum BAFF and APRIL plasma levels (Pallikkuth et al., 2011a) revealing a role for these two soluble factors in effective anti-influenza vaccine responses.

Immune cell responses to influenza antigen are therefore dependant on multiple intrinsic and extrinsic factors mediated via reciprocal cell/cell interactions and soluble factors. The main aim of this chapter therefore, was to monitor the development of CD4 and CD8 T cell responses and to investigate *in vivo* changes of circulating soluble factors by measuring plasma cytokines, IgM, BAFF and APRIL responses, prior to and following influenza vaccination.

6.2 Materials and methods

6.2.1. Influenza vaccination participants

Twelve participants were vaccinated and venous blood collected as described in Materials and Methods (Chapter 2, section 2.1.1).

6.2.2 Cryopreservation and thawing of PBMCs

PBMCs from participants were isolated and cryopreserved as described in Chapter 2, section 2.3.1 and thawed and rested as described in Chapter 2, section 2.5.

6.2.3 Freezing of plasma samples

Plasma was collected and stored from pre-vaccination and 3 days, 6 months and 1 year post-vaccination as described in Chapter 2, section 2.4.

6.2.4 *Ex vivo* flu-stimulations

Ex vivo flu-stimulations were performed as described in Chapter 2, section 2.6.1.

6.2.5 Staining protocols

Cells were prepared for staining as described in Chapter 2, section 2.7. The staining protocol that was used is described in Chapter 2, section 2.8. Briefly, cells were stained to eliminate

dead cells (Chapter 2, section 2.8.1), stained for expression of surface receptors (Chapter 2, section 2.8.2) and for intracellular CD3 receptor expression to identify T cells (Chapter 2, section 2.8.3) (CD3 can be downregulated upon antigen stimulation).

6.2.6 Acquisition of cells and statistical analysis

Stimulated and stained cells were acquired and data collected on an LSRFortessa. Data was analysed by calculating proportions of gated cells as a percent (%) of the parent population using FlowJo™ Software for Mac (version 9.9.4), Ashland. Prism software (version 5) was used to calculate medians and interquartile ranges and nonparametric Wilcoxin signed rank test to determine differences between matched samples. $P<0.05$ was considered significant.

6.2.7 Measurement of influenza-specific antibodies and proteins (ligands and cytokines) by enzyme linked immunosorbent assay

6.2.7.1 Qualitative determination of anti-influenza virus A IgM

The qualitative measurement of anti-influenza virus A IgM antibodies was determined by enzyme linked immunosorbent assay (ELISA; Abcam, United Kingdom, cat no ab108747). The assay was performed as per manufacturer's instructions. Briefly, thawed plasma samples were diluted 1:100 in IgM sample diluent and run in duplicate. The substrate blank, negative and cut-off controls were run in triplicate and the cut-off value calculated as per manufacturer's instructions (Calculation of Results: **Appendix H**). The sensitivity for this assay is >95% and is defined as the probability of the assay scoring positive in the presence of the specific analyte.

6.2.7.2 Quantitative determination of B-cell activating factor

B-cell activating factor (BAFF) measurement was performed using the human BAFF ELISA kit (R&D Systems, USA, cat no DBLYS0B) as per manufacturer's instructions. Thawed plasma samples were diluted 1:2 in sample diluent and run in duplicate. Standard curves were run in duplicate and a standard curve generated. The minimum detectable dose of human BAFF ranged from 1.01 - 6.44 pg/ml with a mean of 2.68 pg/ml.

6.2.7.3 Quantitative determination of A-proliferation inducing ligand

Measurement of A-proliferation inducing ligand (APRIL) was performed using the human ELISA kit (R&D Systems, USA, cat no DAPR00) as per manufacturer's instructions without any deviation from the protocol. Thawed plasma samples were diluted 1:2 in sample diluent and run in duplicate. Standard curves were run in duplicate and a standard curve generated.

The minimum detectable dose of human APRIL ranged from 0.003 - 0.015 ng/ml with a mean of 0.007 ng/ml.

6.2.7.4 Cytometric Bead Array

A BD™ cytometric bead array (CBA) Th1/Th2/Th17 kit (Becton Dickinson Biosciences, San Jose, cat no 560484) was used to quantitatively measure soluble levels of IL-2, IL-4, IL-6, IL-10, IL17A, IFNγ and TNF. Thawed plasma samples were run in duplicate and the assay performed as per manufacturer's instructions. Data were acquired on an LSRFortessa and analysed using FCAP Array™ software (Becton Dickinson Biosciences, San Jose). The limits of detection were as follows: IL-2, 2.6 pg/ml; IL-4, 4.9 pg/ml; IL-6, 2.4 pg/ml; IL-10, 4.5 pg/ml; IL-17A, 18.9 pg/ml; IFNγ, 3.7pg/ml and TNF, 3.8 pg/ml .

6.3 Results

6.3.1 IgM levels at baseline and post-influenza vaccination

Structurally IgM is the largest of the immunoglobulins and the first to be secreted in an immune response. Monomers of IgM bind together to form a pentameric structure increasing its avidity and since this antibody can be secreted at mucosal surfaces and interact with complement it plays a key role in anti-influenza virus immunity. An anti-influenza IgM ELISA was used to confirm that participants did not have an active influenza infection (IgM levels above the cut-off; >10 SU) at baseline (pre-vaccination). In light of the fact that IgM (and IgG) influenza-specific antibodies increase after vaccination in healthy controls (Skountzou et al., 2014) the IgM levels measured after vaccination (3 days, 6 months and 1 year) were indicative of vaccine specific IgM responses. With the exception of one participant, whose baseline IgM levels gave an inconclusive result, falling slightly above the absorbance cut-off value, (10.9 SU), all other participants at baseline, had IgM levels well below the cut-off of detection (**Figure 6.1A**). Although a qualitative assay the unit measure was used to assess if any longitudinal quantitative differences were evident as a result of vaccination, even though strictly below the cut-off. Thus, when the baseline (pre-vaccination) plasma IgM levels were compared to time-points post-vaccination a slight increase in IgM antibody levels was detected as early as 3 days after vaccination (median of 4.16 standard units pre-vaccination versus 5.09 3 days post-vaccination) reaching a peak at 6 months post-vaccination (P=0.012) (**Figure 6.1A**).

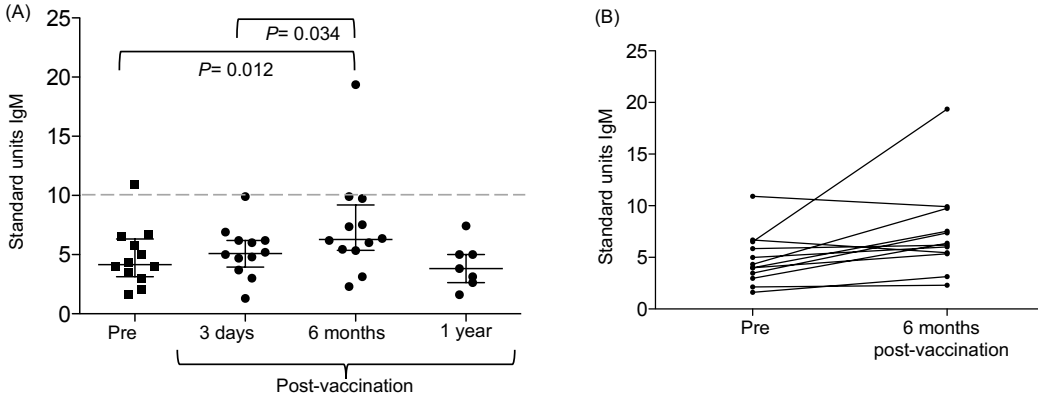


Figure 6.1: Circulating plasma IgM levels following influenza vaccination. Vaccination induced anti-influenza A plasma IgM levels were measured using a commercially available anti-influenza A IgM ELISA assay. Baseline pre-vaccination plasma IgM were compared to 3 days, 6 months and 1 year post-vaccination IgM levels (A). Anti-influenza A IgM plasma levels increased in 10 of 12 participants by 6 months post-vaccination (B). Wilcoxon signed rank test was used to compare paired samples and *P*-values of <0.05 were considered significant. Error bars represent medians with interquartile ranges. Cut-off = 10 standard units (SU) and is depicted by the dotted line in (A). Results are determined as: Positive: >11 SU; Negative <9 SU; Inconclusive: 9-11 SU. Abbreviations: Pre = Pre -vaccination.

Ten of the 12 participants showed an increase in circulating IgM (**Figure 6.1B**), and most exhibited a decline to pre-vaccination levels by one year (**Figure 6.1A**). When the data from the participant with the high baseline IgM level was excluded and the results re-analysed, statistical significance was still maintained (*P*=0.024 pre- versus 6 months post-vaccination) indicating that most participants had mounted IgM responses that persisted for at least 6 months post-vaccination.

6.3.2 Post-vaccination changes in plasma BAFF and APRIL levels

Concentrations of the soluble forms of the two ligands BAFF and APRIL, that comprise the BAFF system molecules, and play a role in B-lineage class switch recombination (Castigli et al., 2005) and lymphocyte activation (Schneider, 2005) were determined in plasma samples from the pre-vaccination and 3 days post-vaccination time-points by ELISA. BAFF levels increased significantly within 3 days of vaccination (*P*=0.045) (**Figure 6.2A**) in 9 of the 12 participants (**Figure 6.2B**).

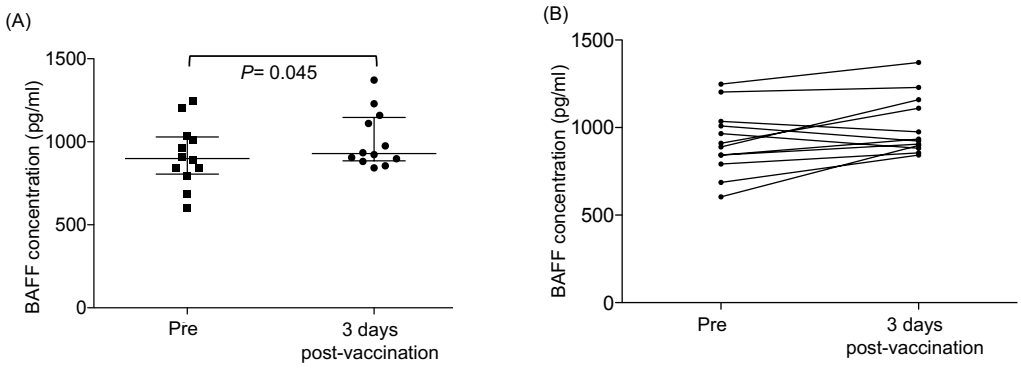


Figure 6.2: Circulating plasma BAFF levels following influenza vaccination. B cell activating factor (BAFF) plasma levels were measured using a commercially available BAFF ELISA assay and pre-vaccination levels compared to 3 days post-vaccination levels (A). BAFF plasma levels increased in 9 of 12 participants 3 days after vaccination with influenza vaccine (B). Wilcoxon signed rank test was used to compare related samples and *P*-values of <0.05 were considered significant. Error bars represent medians with interquartile ranges. Abbreviations: Pre = Pre- vaccination.

Soluble levels of APRIL on the other hand were barely measurable with optical density readings not being measured above background at 3 days post-vaccination. Another study showed an increase in plasma levels of APRIL at 28 days following vaccination with a monovalent 2009- influenza vaccine (Pallikkuth et al., 2011a). It is therefore possible that an increase in APRIL may have occurred later than 3 days post-vaccination.

6.3.3 Influence of vaccination on plasma cytokines

Cytokines are critical for defense against pathogens, mediate communication between various arms of the immune system and early cytokine responses are responsible for local inflammatory reactions as well as having systemic effects (Tisoncik et al., 2012). To ascertain the effect of influenza vaccination on cytokine production, a Th1/Th2/Th17 CBA kit was used to measure IL-2, IL-4, IL-6, IL-10, IL-17A, IFNγ and TNFα concentrations in pre-vaccination and 3 day post-vaccination plasma samples (**Figure 6.3**).

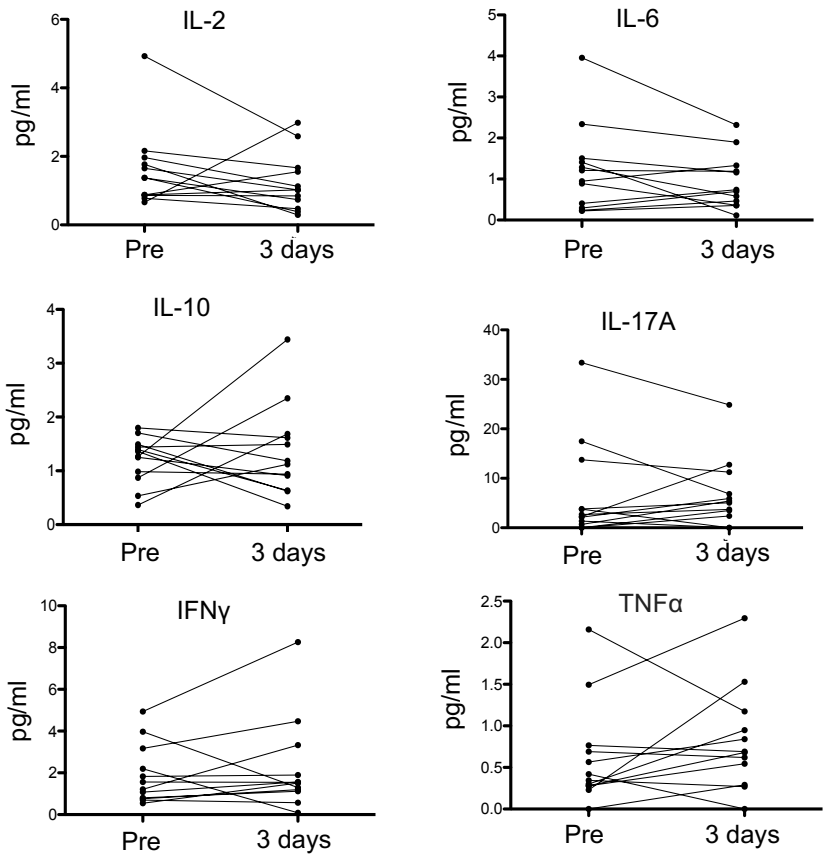


Figure 6.3: Effect of influenza vaccination on secreted cytokines. Secreted cytokine plasma levels were measured using a commercially available BD™ cytometric bead array (CBA) Th1/Th2/Th17 cytokine kit (Becton Dickinson Biosciences San Jose). Pre-vaccination plasma IL-2, IL-4*, IL-6, IL-10, IL-17A, IFNγ and TNFα, concentrations were compared to 3 days post-vaccination using Wilcoxon signed rank test. All *P*-values were not significant (*P*>0.05). Data were acquired on an LSRFortessa and analysed using FCAP Array™ software (Becton Dickinson Biosciences, San Jose). *Data for IL-4 are not shown as plasma levels were below the detection limit. Abbreviations: Pre = Pre-vaccination.

At 3 days following vaccination, the levels of the pro-inflammatory cytokines TNFα, IL-6 or IFNγ, the anti-inflammatory cytokine IL-10 or the cytokines involved in adaptive immunity, IL-2 or IL-17A, were not significantly different from pre-vaccination levels (*P*>0.05). However, IL-2 concentrations decreased in 9 of 12 (75%) participants post-vaccination and IFNγ levels increased in 8 of the participants (67%), suggesting that these 8 participants responded to vaccination, as activated T cells and NK cells produce IFNγ in response to antigen. In contrast, responses varied widely for TNFα, IL-6, IL-10 and IL-17, whereas IL-4 plasma levels were undetectable (0 pg/ml) for the majority of participants and the data therefore not presented. Overall, despite the trends for IL-2 and IFNγ these results indicate that 3 days following vaccination, circulating levels of the cytokines tested are not appreciably affected. As with

APRIL, it cannot be ruled out that differences in cytokine levels may be more notable beyond the timepoint tested.

6.3.4 CD45RO expression on memory T cell subsets in response to *ex vivo* flu-stimulation

During development of the flow cytometry panel (Chapter 3), cells from a healthy donor buffy coat (Chapter 2, section 2.1.2) were used to validate the panel. Following *ex vivo* flu-stimulation, decreased proportions of $CD45RO^+$ cells were observed on CD4 and CD8 Tcm and Tem memory subsets and in order to establish whether this was characteristic of all participants, flu-stimulated cells were compared to co-stimulated cells at pre- and post-vaccination time-points (**Figure 6.4**).

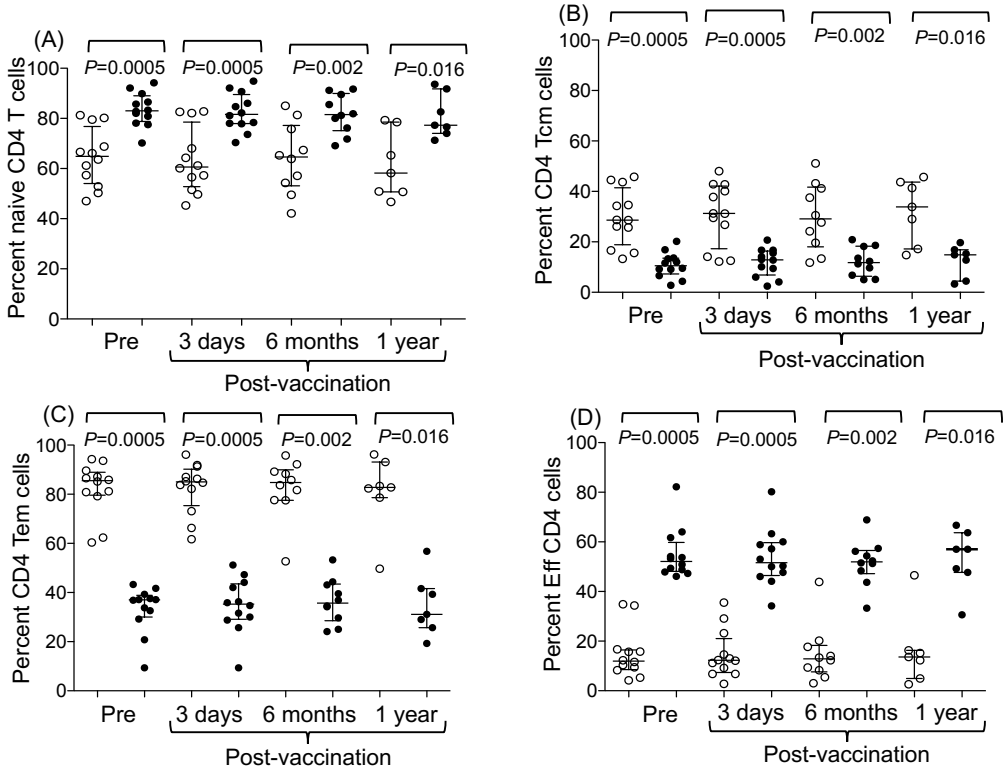


Figure 6.4: Effect of vaccination on expression of CD45RO on memory CD4 T cell subsets. CD4 naïve (A) Tcm (B), Tem (C) and effector (D) subsets, in co-stimulated and flu-stimulated, PBMCs were compared prior to vaccination and at 3 days, 6 months and 1 year post-vaccination. Wilcoxon signed rank test was used to compare related samples and *P*-values of <0.05 were considered significant. Error bars represent medians with interquartile ranges. Open symbols represent co-stimulated cells and closed symbols represent flu-stimulated cells. Abbreviations: Tcm = central memory; Tem = effector memory; Eff = effector cells; Pre = Pre -vaccination.

The proportion of flu- stimulated CD4 Tcm (**Figure 6.4B**) and Tem (**Figure 6.4C**) subsets were substantially decreased compared to co-stimulated cells which suggests that a universal

downregulation of the CD45RO receptor had occurred upon engagement with influenza antigen on these memory ($CD45RO^+$) cells. In contrast, as expected, $CD45RO^-$ effector (**Figure 6.4D**) and naïve (**Figure 6.4A**) subset proportions increased with stimulation, as this does not represent a proliferation of cells following antigen recognition, but rather a consequence of changing proportions of gated cells. Furthermore, following *in vivo* vaccination there was no demonstrable expansion of any CD4 T cell subset, as the number of cells responding to flu-stimulation at the pre-vaccination timepoint were similar to all post-vaccination timepoints ($P>0.05$).

The downregulation of CD45RO surface expression was also reflected in changes of CD8 subset proportions. Overall, *ex vivo* stimulated CD8 Tcm and Tem ($CD45RO^+$) cells were reduced in proportion compared to co-stimulated cells, whereas ($CD45RO^-$) effector and naive cell proportions were increased in comparison to co-stimulated cells (**Figure 6.5**).

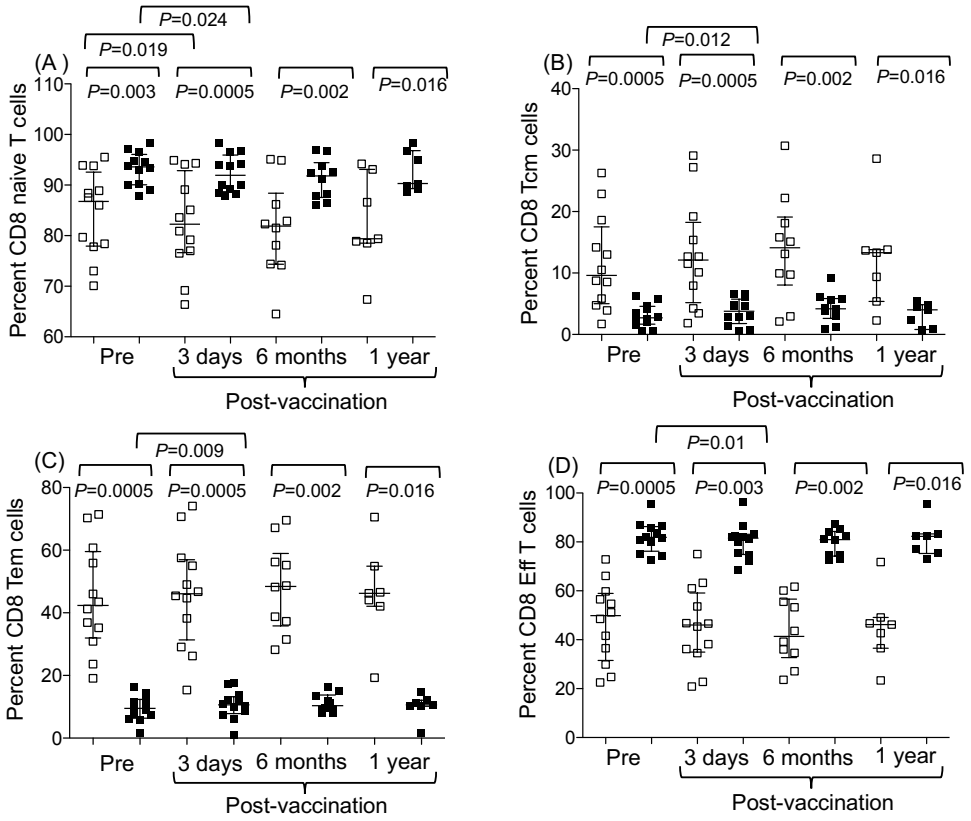


Figure 6.5: Effect of vaccination on expression of CD45RO on memory CD8 T cell subsets. CD8 naïve (A) Tcm (B), Tem (C) and effector (D) subsets, in co-stimulated and flu-stimulated, PBMCs were compared prior to vaccination and at 3 days, 6 months and 1 year post-vaccination. Wilcoxon signed rank test was used to compare related samples and *P*-values of <0.05 were considered significant. Error bars represent medians with interquartile ranges. Open symbols represent co-stimulated cells and closed symbols represent flu-stimulated cells. Abbreviations: Tcm = central memory; Tem = effector memory; Eff = effector cells; Pre = Pre -vaccination

In contrast to CD4 T cells, within 3 days of vaccination, changes in CD8 T cell subset proportions were observed. Both flu-stimulated CD8 Tcm (**Figure 6.5B**) and CD8 Tem (**Figure 6.5C**) subsets increased with flu-antigen re-challenge (*P*=0.012 and *P*=0.009, respectively), indicating that memory cells expanded in response to a previously encountered antigen whereas effector (**Figure 6.5D**) and naïve (**Figure 6.5A**) cells decreased (*P*=0.01 and *P*=0.024, respectively).

6.3.5 CD4 and CD8 T cell cytokine (IFNγ) responses to influenza vaccination

Murine virus specific CD4 T cells regulate the early innate response to influenza infection through upregulation of various innate cytokines(Strutt et al., 2010), and play an important role in heterosubtypic protection to influenza (Benton et al., 2001; Guo et al., 2011). To evaluate peripheral CD4 T cell IFNγ responses to *ex vivo* flu-stimulation, comparisons were made between stimulated and co-stimulated cells (**Figure 6.6**).

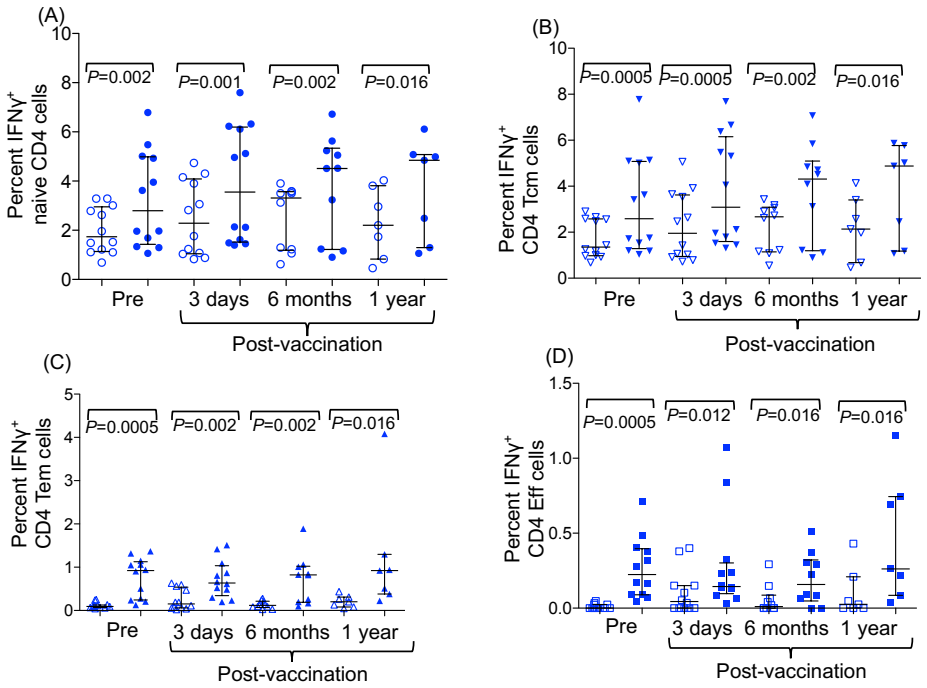


Figure 6.6: CD4 IFNγ responses to vaccination and *ex vivo* flu-stimulation. Flu-stimulated cells were compared to co-stimulated cells to determine intracellular IFNγ responses for CD4 naïve (A) Tcm (B), Tem (C) and effector (D) subsets. Wilcoxon signed rank test was used to compare related samples and *P*-values of <0.05 were considered significant. Error bars represent medians with interquartile ranges. Open symbols represent co-stimulated cells and closed symbols represent flu-stimulated cells. Abbreviations: Tcm = central memory; Tem = effector memory; Eff = effector cells; Pre = Pre -vaccination.

CD4 subsets responded above background controls for all time-points (P<0.05) (**Figure 6.6**), with the Tcm subset (**Figure 6.6B**) responding with a greater magnitude to flu-stimulation than the other 3 subsets. Yet, overall, similar to another study (Jost et al., 2011), the frequency of responding IFNγ cells was relatively low for all subsets, particularly after adjustments were made for background responses. Furthermore, IFNγ responses did not increase with flu-antigen re-challenge following vaccination (P>0.05).

IFNγ-responding CD8 T cells were next investigated (**Figure 6.7**). Some variation in the frequency of CD8 T cell IFNγ responses was observed and at 6 months one participant in particular, presented with an extremely high magnitude of IFNγ-responding naive, Tem and effector co-stimulated and flu-stimulated cells. Effector cells (**Figure 6.7D**) produced significantly more IFNγ than co-stimulated cells for all time-points whereas IFNγ responses varied for the naive, Tcm and Tem CD8 T cell subsets. However, similar to CD4 T cells, there was no increase in post-vaccination IFNγ responses for any CD8 subset with flu-antigen re-challenge (P>0.05).

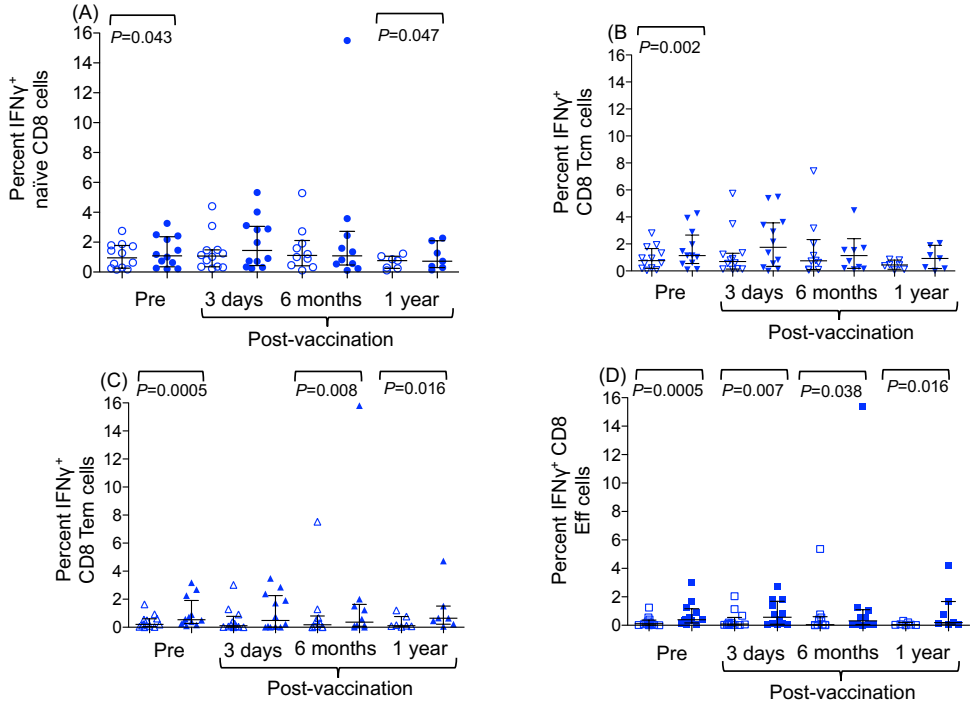


Figure 6.7: CD8 IFNγ responses to vaccination and *ex vivo* flu-stimulation. Flu-stimulated cells were compared to co-stimulated cells to determine intracellular IFNγ responses for CD8 naïve (A) Tcm (B), Tem (C) and effector (D) subsets. Wilcoxon signed rank test was used to compare related samples and P-values of <0.05 were considered significant. Error bars represent medians with interquartile ranges. Open symbols represent co-stimulated cells and closed symbols represent 2009- influenza vaccine antigen stimulated cells. Abbreviations: Tcm = central memory; Tem = effector memory; Eff = effector cells; Pre = Pre -vaccination.

6.3.6 Evaluation of CD4 and CD8 T cell cytolytic (CD107a) responses to influenza vaccination

During antiviral responses, CD4 T cells are generally considered to perform a "helper" role through enhancing CD8 T cell cytotoxic function. However, cytotoxic CD4 T cells have also been described (reviewed in (Marshall and Swain, 2011) so CD4 T cell degranulation responses (CD107a+) were investigated (**Figure 6.8**).

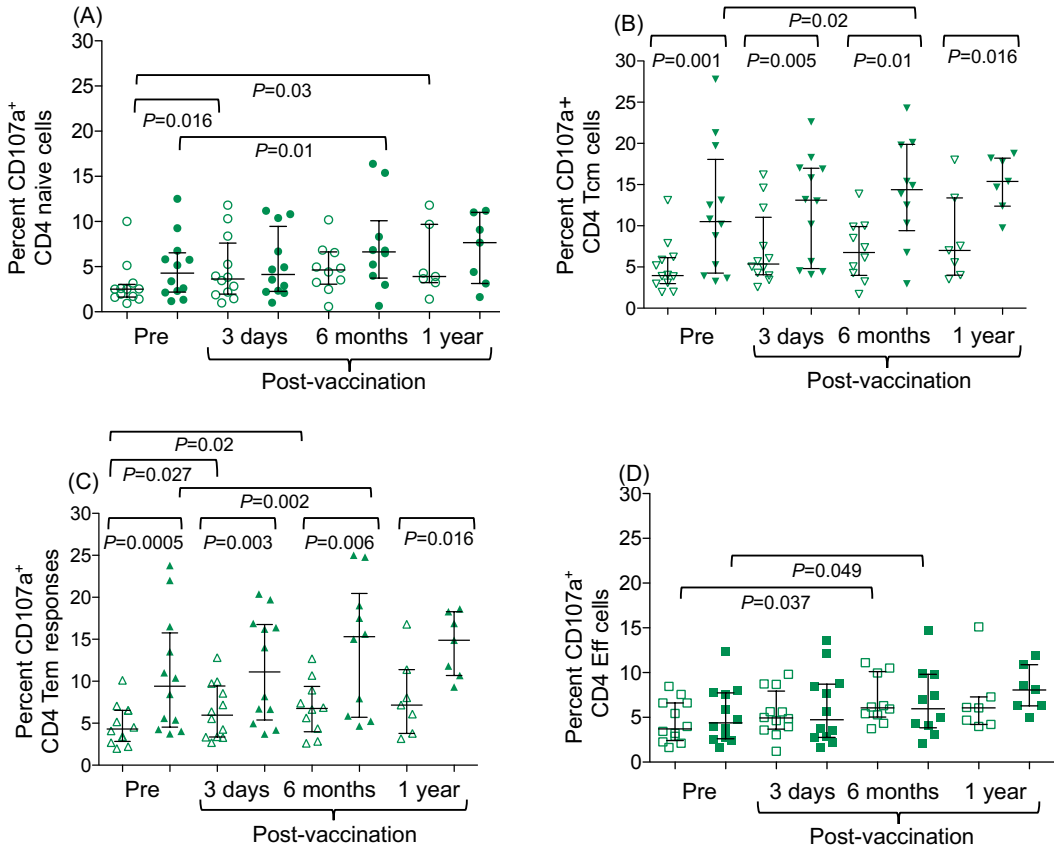


Figure 6.8: CD4 degranulation ($CD107a^+$) responses to vaccination and *ex vivo* flu-stimulation. Degranulation responses were determined by comparing flu-stimulated cells to co-stimulated cells for CD4 naïve (A) Tcm (B), Tem (C) and effector (D) subsets. Wilcoxon signed rank test was used to compare related samples and *P*-values of <0.05 were considered significant. Error bars represent medians with interquartile ranges. Open symbols represent co-stimulated cells and closed symbols flu-stimulated cells. Abbreviations: Tcm = central memory; Tem = effector memory; Eff = effector cells; Pre = Pre-vaccination.

CD4 $CD107a^+$ degranulation responses were more robust than IFNγ responses and differed between Tcm, Tem, effector, and naive subsets. Memory subsets ($CD45RO^+$) responded in a similar manner to *ex vivo* flu-stimulation, with CD4 Tcm (**Figure 6.8B**) and CD4 Tem (**Figure 6.8C**) memory subsets responding significantly above background, prior to and following vaccination ($P<0.05$), however both naive (**Figure 6.8A**) and effector (**Figure 6.8D**) cells degranulated with a similar magnitude to that of co-stimulated cells ($P>0.05$). *In vivo*

vaccination had a significant influence on CD4 degranulation by 6 months post-vaccination, with an increased magnitude of degranulation for naive cells (*P*=0.01) (**Figure 6.8A**) Tcm (*P*=0.02); (**Figure 6.8B**); Tem (*P*=0.002) (**Figure 6.8C**) and effector cells (*P*=0.049) (**Figure 6.8D**) with antigen re-challenge. Degranulation responses were also significantly increased in co-stimulated Tem (*P*=0.02) and effector cells (*P*=0.037) at 6 months, and in naive cells at 1 year (*P*=0.03).

Flu-stimulated CD107a CD8 memory subset responses were significantly above background for all time-points, including at pre-vaccination (**Figure 6.9B and 6C**). In contrast, effector cells (**Figure 6.9D**) were above background only at the pre-vaccination time-point (*P*=0.025) whereas naive cells (**Figure 6.9A**) degranulated significantly above background for all time-points except at 1 year (*P*>0.05)

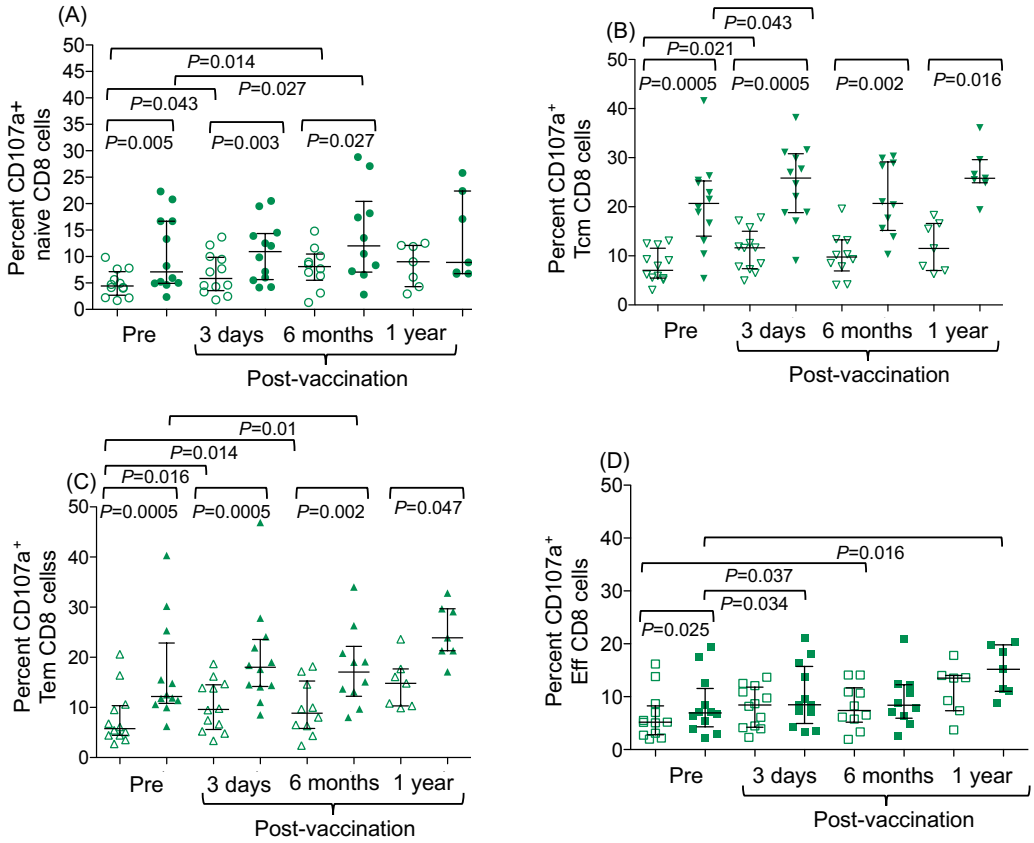


Figure 6.9: CD8 degranulation ($CD107a^+$) responses to vaccination and *ex vivo* flu-stimulation. Degranulation responses were determined by comparing flu-stimulated cells to co-stimulated cells for CD8 naïve (A) Tcm (B), Tem (C) and effector (D) subsets. Wilcoxon signed rank test was used to compare related samples and *P*-values of <0.05 were considered significant. Error bars represent medians with interquartile ranges. Open symbols represent co-stimulated cells and closed symbols flu-stimulated cells. Abbreviations: Tcm = central memory; Tem = effector memory; Eff = effector cells; Pre = Pre-vaccination.

With flu re-challenge, increased degranulation (P<0.05) occurred at all post-vaccination time-points. At 3 days post-vaccination, Tcm (**Figure 6.9B**) and effector (**Figure 6.9D**) cells degranulated significantly more than pre-vaccination cells, while naive, Tcm and Tem subsets degranulated at 6 months and effector cells at 1 year. Co-stimulated cells also degranulated at a greater magnitude than pre-vaccination at varying time-points for CD8 T cell subsets.

Finally, to assess which memory compartment degranulated with a greater magnitude, adjustments were made for background responses and Tcm CD107a expression compared to that of Tem for both CD4 and CD8 subsets. There were no differences between CD107 expression levels on CD4 Tcm and CD4 Tem cells (**Figure 6.10A**) but in contrast, CD107a expression on CD8 Tcm cells was significantly greater than on CD8 Tem cells for up to 6 months post-vaccination (P=0.027; P=0.043 and P=0.01 for pre-, 3 days and 6 months post-vaccination) (**Figure 6.10B**).

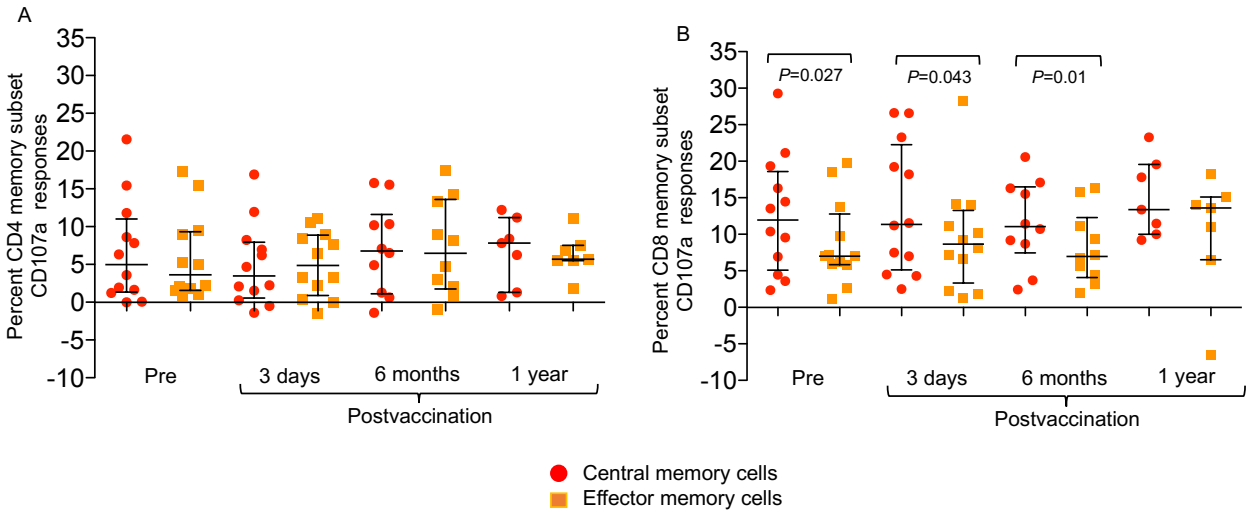


Figure 6.10: Differences in CD107a expression between central and effector memory subsets for CD4 and CD8 T cells. To determine which memory subset degranulated with a greater magnitude, differences in CD107a expression for Tcm and Tem memory subsets were assessed after adjustments were made for background responses for CD4 (A) and CD8 (B) T cells. Wilcoxon signed rank test was used to compare related samples and P-values of <0.05 were considered significant. Error bars represent medians with interquartile ranges. Open symbols represent co-stimulated cells and closed symbols represent flu-stimulated cells. Abbreviations: Pre = Pre-vaccination.

Tcm responses were more varied between individuals, probably reflecting differences in exposure to previously encountered flu antigens and despite the lack of definitive T cell

phenotypic markers in the current panel that are used to define T cell memory, naive and effector subsets, functional differences between various T cell subsets were apparent.

In summary, therefore, no post-vaccination increases in IFNγ-producing cells were found for CD4 and CD8 T cells. Furthermore, CD4 and CD8 T cell subsets were not polyfunctional for IFNγ production and $CD107a^+$ degranulation. Degranulation responses where however, enhanced following vaccination, with CD4 T cells degranulating significantly more at 6 months for all subsets and CD8 subsets responding at various time-points with flu re-stimulation. Data are summarised in **Table 6.1**.

Table 6.1: Post-vaccination IFNγ and CD107a responses for CD4 and CD8 T cells with flu re-challenge

	IFNγ			**CD107a**		
	3 days	6 months	1 year	3 days	6 months	1 year
	CD4					
Central memory	-	-	-	-	+	-
Effector memory	-	-	-	-	+	-
Effector	-	-	-	-	+	-
Naive	-	-	-	-	+	-
	CD8					
Central memory	-	-	-	+	-	-
Effector memory	-	-	-	-	+	-
Effector	-	-	-	+	-	+
Naive	-	-	-	-	+	-

+ = Significant increase with flu re-challenge compared to pre-vaccination cells.
Central memory: $CD27^+CD45RO^+CD62L^+$
Effector memory: $CD27^-CD45RO^+CD62L^-$
Naïve: $CD27^+CD45RO^-CD62L^+$
Effector: $CD27^-CD45RO^-CD62L^-$

6.3.7 Comparison between post-vaccination soluble factors, T cell and $CD56^{bright}CD16^{neg}$ NK cells responses

Within 3 days of vaccination BAFF plasma levels were elevated. Furthermore, at this time-point, CD8 Tcm and Tem proportions increased, whereas CD8 naive and effector cells decreased. Furthermore, CD8 T effector cells degranulated significantly more with flu antigen re-challenge. However, 6 months after vaccination multiple responses by various arms of the immune system occurred. With flu-antigen re-challenge, dynamic alterations of $CD56^{bright}CD16^{neg}$ NK cell subphenotype proportions were observed, with both lymph homing subphenotypes increasing in proportion and peripheral subphenoytypes decreasing. There was also a significant loss in the frequency of $pNKp46CD27^-$ $IFN\gamma^+$ cells. Degranulation

responses were greater for CD8 Tcm cells as well as for CD4 Tcm, Tem and effector cells and plasma IgM levels were elevated. (Summarised in more detail in **Figure 6.11**).

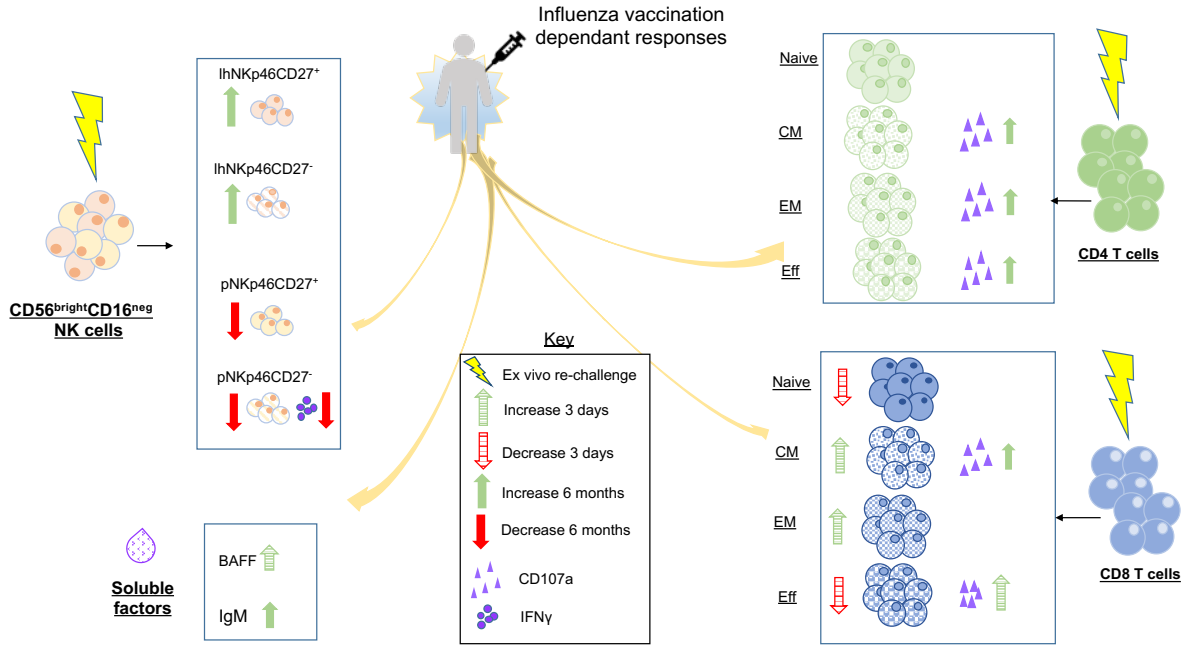


Figure 6.11 Key findings at 3 days and 6 months post-vaccination following intramuscular influenza vaccination. Comparisons were made between flu-stimulated pre-vaccination and post-vaccination cells using Wilcoxon signed rank test. Significant (P<0.05) post-vaccination responses are indicated for $CD56^{bright}CD16^{neg}$ NK cells and soluble factors (left panels) and CD4 and CD8 T cells (right panels). The figure key shows the symbols used to illustrate functional markers of cells (CD107a and IFNγ), and significant changes observed as a consequence of influenza vaccination: directional striated or solid coloured arrows for 3 days and 6 months, respectively; green = increased, red = decreased.

6.4 Discussion

Influenza virus evades the immune system through multiple processes that include seasonal mutations in the surface epitopes (antigenic drift) and gene segment re-assortment from distinct strains (antigenic shift) (Webster and Govorkova, 2014). Despite the long history of influenza research, key correlates of natural immune protection remain poorly understood (Allen and Thomas, 2015). The current study analysed the $CD56^{bright}CD16^{neg}$ NK subset and revealed multiple *in vivo* and *ex vivo* responses to flu vaccine antigen (Chapter 5). Since reciprocal interactions take place between NK cells, B cells, CD4 and CD8 T cells, changes in naïve, effector and memory CD4 and CD8 T cell responses were evaluated and *in vivo* responses assessed by measuring plasma concentrations of IFNγ, IL-6, IL-2, IL-10, TNFα, IL-17A and IL-4, BAFF, APRIL as well as anti-influenza virus A IgM antibody levels.

The BAFF system molecules comprise of the ligands BAFF and APRIL, and three receptors (BAFF receptor, calcium-modulating cyclophilin ligand interactor and B cell maturation antigen). BAFF provides critical signals for the development, survival and maturation of B cells (Mackay et al., 2010; Mackay et al., 2003; Schiemann et al., 2001) and the BAFF receptor, which is expressed on B cells, transduce signals that result in isotype switching (Castigli et al., 2005). Data from clinical studies has suggested that expression levels of the BAFF system molecules correlate with B cell responses (Sakai and Akkoyunlu, 2017). In the current study, BAFF plasma levels increased 3 days after vaccination in 75% (9/12) of the participants and decreased in 25% of the participants. Although samples numbers are too small for correlation studies, the 9 participants whose BAFF levels increased with vaccination, also had increased IgM levels at 6 months, whereas of the 3 participants whose BAFF levels had decreased after vaccination, 2 had reduced plasma IgM at 6 months. IgM antibodies are required to provide optimal immune protection against influenza, through positive regulation of the magnitude of IgG virus-specific responses (Baumgarth et al., 2000). Even though IgG levels were not measured in the current study these data suggests that the 9 participants with increased BAFF and IgM levels are more responsive to the vaccine; a study has shown that 2009- influenza vaccine responders have increased frequencies of IgG memory cells, which coincides with increased plasma BAFF levels, whereas vaccine non-responders have deficiencies in plasma BAFF levels and B cell receptors (Pallikkuth et al., 2011a). Interestingly, the one participant with decreased BAFF plasma levels was also the same participant who, at 6 months presented with an IgM value just above the cut-off (an outlier) for active infection, although this individual did not present with clinical symptoms.

With 75% of the participants in the current study having increased BAFF and IgM levels, which suggested that they were vaccine responders, it would therefore be expected that secreted cytokines, which are implicated in immune cell interactions and responses to viral antigen, would have been observed following vaccination. The commercial CBA kit used in the current study included IL-2, IL-4, IL-6, IL-10, IFNγ and TNFα, which are produced by various immune cells during interactions with antigen (Biron, 1997; Biron et al., 1999; Cooper et al., 2001a; Couper et al., 2008; Lauder et al., 2013; Schopf et al., 1998; Trinchieri, 1997). Although certain trends were noted for IFNγ and IL-2 responses, plasma cytokine concentrations did not significantly increase or decrease by 3 days post-vaccination. Secretion of cytokines is complex and tightly controlled and is dependent on cell type and the stimulus received by the cell (Lacy and Stow, 2011). Since upregulation of innate cytokine mRNA can be rapid (Hoadley and Hopkins, 2003) the lack of significant changes in cytokine responses in the current study

could be a consequence of the time delay between vaccination and first post-vaccination time-point. It would be interesting therefore to carry out studies that use alternate methods with different sensitivities, as well as to investigate the kinetics of soluble cytokines after 2009-influenza vaccination in order to understand if cytokines are secreted at an earlier time-point or if the lack of responses are due to assay detection limits.

The downregulation of CD45RO in response to the flu stimulus was profound for both CD4 and CD8 T cell memory subsets which express this receptor. Downregulation of the TCR occurs after engagement with MHC and activation of T cells (Krangel, 1987) and similarly downregulation of the NK cell 2B4 co-activating receptor occurs following engagement with its ligand CD48 (Mathew et al., 2007). Therefore in keeping with an activated cell, degranulation responses by $CD45RO^+$ CD4 and CD8 (memory) T cells were more robust than those of the naive and effector subsets (without CD45RO expression) and although there were no differences in $CD107^+$ cell frequencies between CD4 memory compartments, CD8 Tcm cells degranulated with a greater frequency than CD8 Tem cells. Tcm cells provide better long term protection and are able to proliferate rapidly (Wherry et al., 2003) but preferentially locate in lymphoid tissue, whereas Tem cells are found in non-lymphoid tissue (Masopust et al., 2014). Interpretation of T cell data however, is treated with caution with regards to assigning certain characteristics to T cell subsets in the current study, as T cell phenotypes were not properly characterized with a full panel of markers such as CCR7 which are required to accurately identify Tcm ($CD45RO^+CCR7^+CD62L^+$) and Tem ($CD45RO^+CCR7^-CD62L^-$) cells (Sallusto and Lanzavecchia, 2011).

Following vaccination, CD4 T cells and CD8 Tem cells degranulated significantly more than pre-vaccination cells which is in keeping with a specific recall response that requires time to develop. However increased CD8 degranulation responses occurred 3 days after vaccination. Although the H1N1 component of the vaccine was novel, participants may have been previously exposed to the H3N2 and subtype B antigens present in the formulation and therefore had pre-existing immune memory at the time of vaccination, hence the early response and even though influenza vaccination induced immunity wanes over time, data from this study indicated that effector CD8 degranulation responses were significantly enhanced for up to a year after vaccination. Degranulation responses were therefore relatively long-lived and could be specific or heterosubtypic, as innate-like properties have been ascribed to CD8 T cells in humans (reviewed in Barbarin et al., 2017). Furthermore, cross reactivity as a feature of T cells has been recognised for some time (Mason, 1998) and includes reactivity between

viruses (Aslan et al., 2017; Selin et al., 1998; Welsh and Selin, 2002) as well as bacteria and viruses ((Mathurin et al., 2009) and reviewed in (Welsh et al., 2010)) and cross reactive T cell responses to H1N1 pandemic influenza have also been shown in nonhuman primates which help mediate early clearance of virus (Weinfurter et al., 2011).

An unexpected result in increased degranulation responses was observed for cells that were only co-stimulated with CD28 and CD49d co-stimulatory molecules. These were added to stimulation mixes to allow for optimal responses under experimental conditions (Udagawa et al., 1996; Waldrop et al., 1998) but cytokine responses should not be detectable without co-engagement of CD3 with antigen (Waldrop et al., 1998). In keeping with these studies, there were no increases in IFNγ cytokine responses with CD28/CD49d co-stimulation for either CD4 or CD8 T cells but CD107a degranulation responses were noted for CD8 in particular. CD107a is a protein present in the lipid bilayer surrounding pre-formed cytolytic granules present in the cytoplasm (Peters et al., 1991) and low levels of CD107a surface expression are detectable on PBMCs, which is thought to enhance lymphocyte vascular adhesion (Kannan et al., 1996). These preformed lysosomal granules cycle to the cell surface during cell activation and the degranulation assay that was used in the current study measures the cumulative exposure of CD107a on the cell surface (Betts et al., 2003). Increased expression of CD107a was observed with CD28/CD49d co-stimulation for CD4 and CD8 T cells at various time-points after vaccination, and as there would not have been any engagement of the T cell receptor, this implies a non-specific response, possibly due to an increase in vaccine primed cells that are more responsive to costimulatory signals.

In conclusion, it was shown (Chapter 5) that influenza vaccination induces innate and NK trained immune responses as indicated by dynamic changes in $CD56^{bright}CD16^{neg}$ subphenotype proportions and a loss in the frequency of $IFN\gamma^{+}$ pNKp46$CD27^{-}$ cells. In this chapter, following vaccination, BAFF and IgM plasma levels were elevated and with flu-antigen re-challenge, proportions of CD8 memory cells increased and CD4 and CD8 T cells responded by degranulating. Although some vaccination induced responses occurred 3 days after vaccination, a co-ordinated response by multiple arms of the immune system occurred at 6 months. Together, these findings contribute to further understanding developing immune responses in the context of influenza vaccination.

CHAPTER 7:
Phenotypic characterization of $CD56^{bright}CD16^{neg}$ hepatic NK cells

7.1 Introduction

In contrast to peripheral blood, human hepatic derived lymphocytes can comprise 30-60% of NK cells (Doherty and O'Farrelly, 2000) that preferentially reside within the hepatic sinusoids (Hudspeth et al., 2016). Similar to conventional NK cells (cNK) human hepatic NK cells (hpNK) can be distinguished into $CD56^{bright}CD16^{pos/neg}$ and $CD56^{dim}CD16^{pos/neg}$ subsets, however the liver is enriched for $CD56^{bright}$ NK cells (Carrega et al., 2014; Harmon et al., 2016; Jonsson et al., 1997) which are phenotypically different from those in other tissues (Carrega et al., 2014) and those isolated from peripheral blood (Cosgrove et al., 2014; Hudspeth et al., 2016). It is generally accepted that $CD56^{bright}$ NK cells represent a precursor to more mature $CD16^{pos}CD16^{neg/dim}$ NK cells (Caligiuri, 2008) however, there is evidence that they may arise from separate lineages (Wu et al., 2014).

A high frequency of $CD56^{bright}$ NK cells are present in various solid tissues (Carrega et al., 2014) including the liver. With NK cells comprising heterogeneous populations and having distinct tissue distribution, they also express a broad range of adhesion molecules that are largely responsible for the redistribution of NK cells between organs and tissues enabling them to exert their effector functions during infection or inflammation (Gregoire et al., 2007). Hepatic $CD56^{bright}$ NK cells have been shown to express higher levels of the natural cytotoxicity receptors NKG2D, NKp44 and NKp46 which recognise viral and tumour-associated antigens and stress ligands (Harmon et al., 2016). Liver-resident $CD56^{bright}$ NK cells also express the C-type lectin CD161 (an activation and homing marker) (Podhorzer et al., 2018) and the tissue residency marker CD69 known to inhibit surface expression of sphingosine-1-phosphate receptor 1 (S1PR1) which promotes the movement of lymphocytes out of tissues (Shiow et al., 2006). More recently, $CD56^{bright}$ NK cells that constitutively express markers of tissue residency which include CD69, CCR5, and CXCR6 have been characterised making these chemokine receptors functionally important for their migration to hepatic sinusoids (Hudspeth et al., 2016). Emerging data from mouse studies suggests that there are 2 populations of liver NK cells, distinguished by CD49a and DX5 expression. $CD49a^{-}DX5^{+}$ are conventional (circulating) NK cells that are of splenic origin and $CD49a^{+}DX5^{-}$ liver resident NK cells that have memory potential and appear to originate from hepatic progenitor cells (Peng et al., 2013a). A further study proposes that murine tissue resident NK cells found in the liver have a distinct lineage maturing independently from NK cells found in the spleen or thymus and as they utilize different transcription factors, the authors suggest that they have tissue specific homeostatic functions by providing innate defense different to that of conventional NK cells (Sojka et al., 2014a).

CHAPTER 7:
Phenotypic characterization of CD56^{bright}CD16^{neg} hepatic NK cells

CD56^{bright} NK cells play a unique role in innate responses and are the primary source of NK cell derived immunoregulatory cytokines (Cooper et al., 2001b). Immune cells found in the liver are exposed to a high antigen load and therefore need to maintain a fine balance between tolerance and activation. Intriguingly, donor leucocytes can be detected in recipients' peripheral blood early after transplant, but these leucocyte numbers vary (Lukomska et al., 1997) and those recipients with a higher level of chimerism are less likely to acutely reject the liver (Jonsson et al., 1997). Furthermore, recipients of other solid organ transplants are less likely to reject these organs if co-transplanted with a liver allograft (Rasmussen et al., 1995), highlighting the importance of understanding the CD56^{bright} NK cell phenotype resident in healthy liver. As mentioned in Chapter 3, polychromatic flow cytometry provides a powerful tool to immunophenotype cell receptors at a single cell level however, when investigating rare populations within phenotypic subsets large numbers of cells are required. Investigating the liver-derived CD56^{bright} NK phenotype is difficult due to the small number of NK cells obtained from biopsies of healthy human liver. In addition, digestion of tissue using collagenase has been shown to downregulate CD56 expression and interfere with the surface expression of receptors (Abuzakouk et al., 1996; Hudspeth et al., 2016). Before human orthotopic transplantation, a donor liver is perfused to remove excess blood, with CD56^{bright} CD69^{pos} NK cells comprising a large proportion of NK cells that detach from liver grafts during this process (Moroso et al., 2010) making liver perfusate an ideal source of hepatic derived lymphocytes.

In Chapter 5 it was shown that CD27 is only expressed on NKp46^{+} cells and represents a bi-functional phenotype associated with a memory-like response to influenza vaccine antigen. Additionally, the peripheral NKp46^{+} cells showed increased cytolytic function (CD107a degranulaton) and increased NKp46 cells surface density. In humans, CD27^{+} CD56^{bright} NK cells are implicated in clearance of acute HCV infection in HIV-positive patients (Eisenhardt et al., 2014) and HIV patients co-infected with HCV have a reduced frequency of CD56^{bright} NK cells co-expressing CD27 with impaired cytolytic and cytotoxic function (Doherty et al., 1999; Kaczmarek et al., 2017; Norris et al., 1998). Given that CD56^{bright} cells are the predominant NK subset found in the liver and the importance of CD27 in hepatic pathology, surprisingly little phenotyping information is available on co-expression patterns of CD27^{+} with CD56^{bright} hepatic NK receptors under normal homeostatic conditions. To this end, CD27 co-expression patterns of NKp46^{+}, CD69^{+} and CD161^{+} liver perfusate-derived healthy NK cells as well as those from a single acute liver failure (ALF) case were investigated in relation to circulating (conventional) NK cells.

CHAPTER 7:
Phenotypic characterization of $CD56^{bright}CD16^{neg}$ hepatic NK cells

Note: In Chapter 4, $CD56^{bright}CD16^{neg}$ NK cells isolated from venous blood were described as either lymph homing ($CD62L^{+}$) or peripheral ($CD62L^{-}$) NK cells. In this Chapter, NK cells isolated from blood circulating in the periphery will be described as conventional NK cells (cNK) as they comprise both $CD62L^{+}$ and $CD62L^{-}$ subphenotypes and are cells that originate in the bone marrow and move through the circulation to organs or tissues (Sojka et al., 2014b; Yokoyama et al., 2013).

7.2 Materials and Methods

7.2.1 Liver transplant perfusate and isolation of mononuclear cells

Liver perfusate was collected (n=9 for flow cytometry panel 1 and n=8 for panel 2) as described in Chapter 2, section 2.1.3 and processed as described in Chapter 2, section 2.3.

7.2.2 Thawing and resting of perfusate mononuclear cells

Aliquots of donor derived mononuclear cells were thawed and rested as described in Chapter 2, section 2.5.

7.2.3 Immunophenotyping of liver perfusate derived NK cells

7.2.3.1 Staining protocols

Cells were prepared for staining as described in Chapter 2, section 2.7 and stained to eliminate dead cells (Chapter 2, section 2.8.1) and for surface (Chapter 2, section 2.8.2) and intracellular (Chapter 2, section 2.8.3) expression of receptors.

7.2.3.2 Development of polychromatic flow cytometry panel for perfusate NK cells

The flow cytometric panel developed and described in detail in Chapter 3, sections 3.2.5.1 to 3.2.6 formed the backbone to the flow panels used for immunophenotyping liver perfusate with a few minor modifications. Two 10 colour flow cytometry panels were developed to include a dump channel comprising CD14 APC Cy7, CD19 APC Cy7 (BD Pharmingen) and a near infra-red amine LIVE/DEAD® (Invitrogen Molecular Probes) discriminator with the anchor markers CD3 PECy7, CD4 PECy5.5 and CD8 Brilliant Violet 705 (BioLegend), CD16 FITC and CD56 Brilliant Violet 605 (Biolegend), and the cell subset phenotypic markers, CD45RO ECD (Beckman Coulter), with CD27 PECy5 (Biolegend), CD62L APC and NKp46 PE (BD Pharmingen) comprising panel 1 and CD161PE and CD69 V450 (Biolegend) panel 2. Between one and two million cells were stained, fixed and acquired within 24 hrs using a LSRFortessa (Becton-Dickinson, La Jolla, CA, USA) flow cytometer.

An “anchor” gating strategy was applied to exclude doublets. Singlets were selected by plotting FSC-H against FSC-A and lymphocytes selected based on SSC-A and FSC-A parameters. Monocytes (CD14^{+}), B cells (CD19^{+}) and dead cells were excluded in a dump channel. Live CD3^{-} cells defined 4 NK subsets based on CD56 and CD16 expression namely, CD56^{bright}CD16^{neg}; CD56^{bright}CD16^{pos}; CD56^{dim}CD16^{pos} and CD56^{dim}CD16^{neg}.

7.2.4 Statistical analysis

Proportions of gated cells were calculated as a percent (%) of the parent population using FlowJo^{TM} Software for Mac (version 9.9.4), Ashland and Mann Whitney *U* test (Prism, version 5) to compare differences between 2 independent groups. $P<0.05$ was considered significant. 50th percentile, minimum, maximum, 25th and 75th percentiles were calculated using Prism (version 5).

7.3 Results

7.3.1 Evaluation of hepatic perfusate derived and conventional CD56^{bright}CD16^{neg} and CD56^{bright}CD16^{dim} NK subsets

With several studies reporting that the liver is enriched for lymphocytes compared to the peripheral circulation (Doherty et al., 1999; Doherty and O'Farrelly, 2000; Norris et al., 1998) the proportions of CD3^{-} lymphocytes in hepatic perfusate were compared to PBMCs. When hepatic perfusate derived cells and PBMCs were gated to define live CD3^{-} lymphocytes **(Figure 7.1A)** hepatic perfusate was found to be significantly enriched for CD3^{-} lymphocytes compared to PBMCs (median 32.3% vs 11.9%; P= 0.0003) **(Figure 7.1B)**.

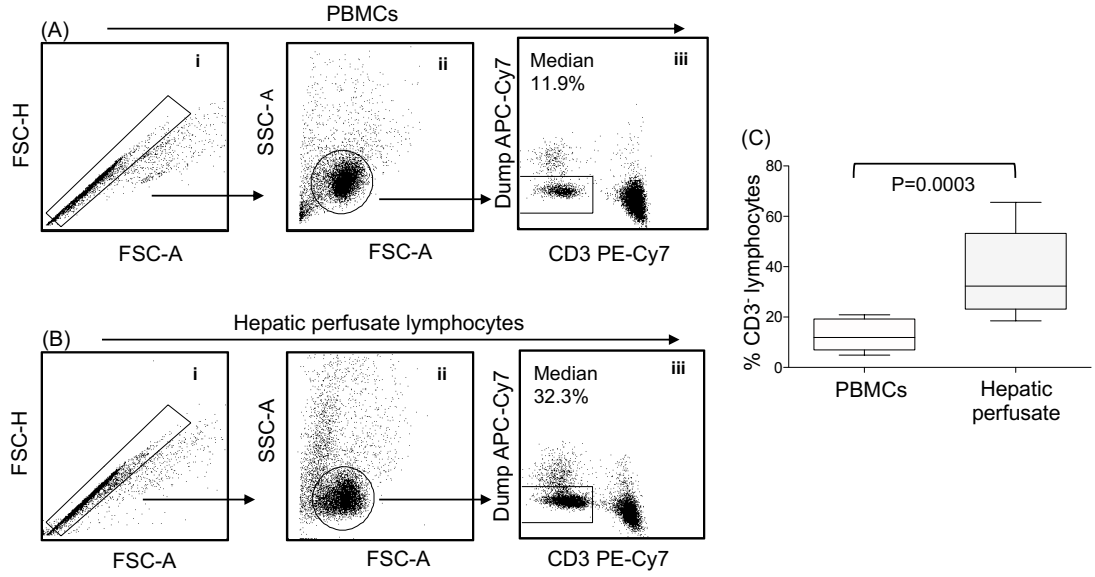


Figure 7.1: Differences in CD3^{-} lymphocyte proportions between PBMCs and hepatic perfusate. PBMCs (A) and hepatic derived perfusate (B) were gated for singlets (i) and lymphocytes (ii). Monocytes, B lymphocytes and dead cells were excluded in a dump channel and live CD3^{-} lymphocytes gated (iii). Liver derived perfusate is significantly enriched for CD3^{-} lymphocytes (C). Mann Whitney *U* test was used to compare differences between 2 independent groups and $P<0.05$ was considered significant. Data are presented as box and whiskers plots showing medians (50th percentile), minimum, maximum, 25th and 75th percentiles.

Since NK cells are phenotyped based on bright or dim expression of CD56 with CD16 co-expression, FMO experiments as described in Chapter 3, section 3.2.5.2 were performed for CD56 and CD16 expression to differentiate between CD56^{bright} (blue gates in **Figures 7.2A** and **7.2B**) and CD56^{dim} NK cells as well as establish the 4 NK subsets defined as CD56^{bright}CD16^{neg}; CD56^{bright}CD16^{dim}, CD56^{dim}CD16^{bright} and CD56^{dim}CD16^{neg} (red gates in **Figures 7.2A** and **7.2B**), but for the purposes of this study the focus is on CD56^{bright}CD16^{neg} NK subset.

As several other researchers (Carrega et al., 2014; Jonsson et al., 1997) have shown, it was found that a greater proportion of hepatic-derived NK cells (hpNK) cells were CD56^{bright} (median 34% hpNK cells vs 13.8% for cNK cells (P=0.0008) **(Figure 7.2C)**. This held true for both CD56^{bright}CD16^{neg} and CD56^{bright}CD16^{dim} subsets (P=0.038 and P=0.0008, respectively) **(Figure 7.2D)**.

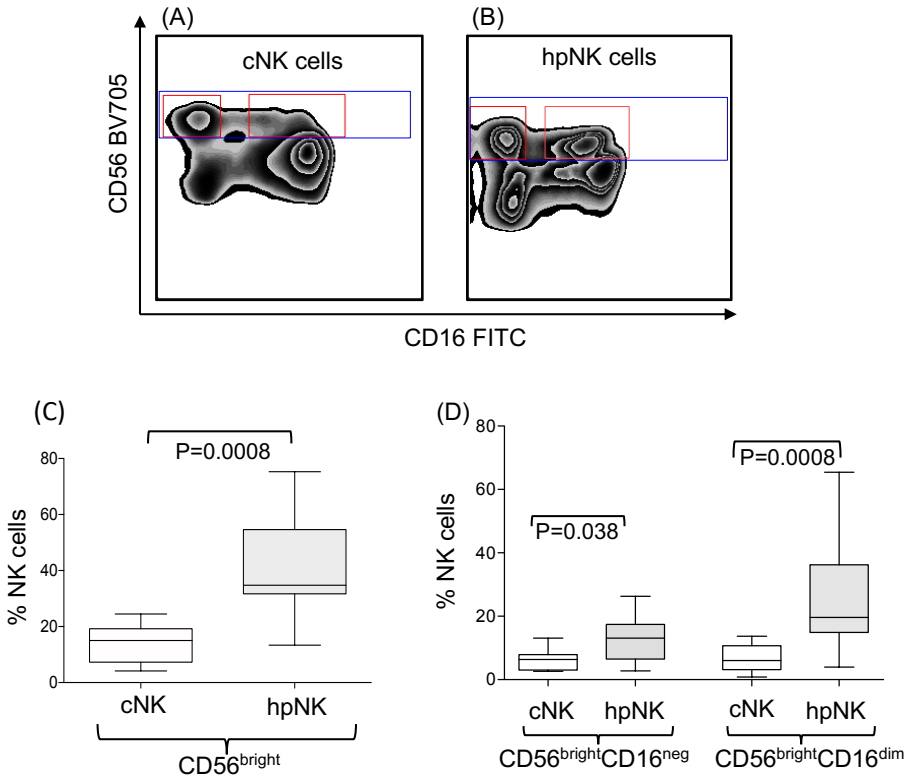


Figure 7.2: Differences in CD56^{bright} subset proportions between circulating and hepatic-derived NK cells. cNK (A) and hpNK (B) cells were gated for CD56^{bright} cells (blue gates) based on fluorescent intensity of CD56 and further defined (red gates) as CD56^{bright}CD16^{neg} and CD56^{bright}CD16^{dim} based on co-expression of CD16. Comparisons were made between cNK and hpNK CD56^{bright} subsets (C) and CD56^{bright}CD16^{neg} and CD56^{bright}CD16^{dim} NK cells (D). Mann Whitney *U* test was used to compare differences between the 2 independent groups and $P<0.05$ was considered significant. Data are presented as box and whiskers plots showing medians (50th percentile), minimum, maximum, 25th and 75th percentiles.

7.3.2 Evaluation of CD56^{bright}CD16^{neg} liver-derived NK cells for the lymph homing receptor CD62L

In the absence of a definitive marker for human liver resident NK cells in the flow cytometry panel used in the current study, the proportion of CD62L expressing CD56^{bright}CD16^{neg} hpNK cells was first examined as liver NK cells are not enriched for CD62L surface expression under steady state conditions (Peng et al., 2013b) whereas peripheral CD56^{bright}CD16^{neg} NK cells are enriched for this homing receptor. Few hpNK cells expressed CD62L (median 2.73%) as opposed to the high frequency of CD62L expression on cNK cells (median 66.2%; $P=0.0006$) **(Figure 7.3).** Thus, hepatic-derived NK cells from healthy liver perfusate, which were enriched for CD3^{-} lymphocytes, a predominant CD56^{bright} NK subset distribution and little expression of CD62L therefore closely resembles the phenotypic profile of tissue resident NK cells,

consistent with immunophenotyping data obtained from studies on intrahepatic lymphocytes (Hudspeth et al., 2016; Tu et al., 2007).

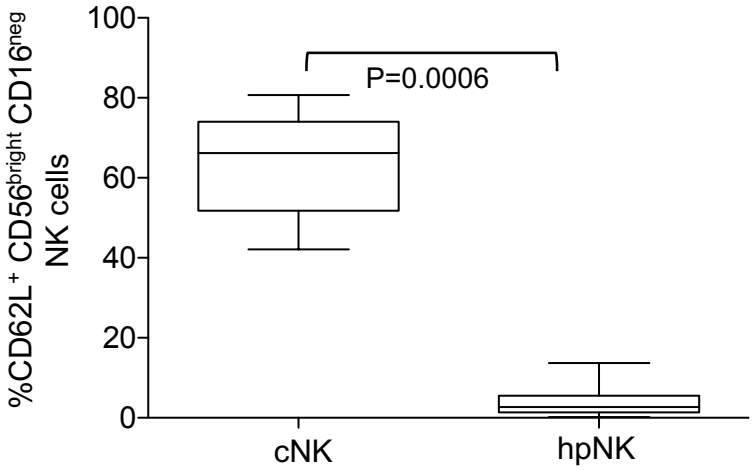


Figure 7.3: Differences in frequency distribution of CD62L proportions between circulating and hepatic CD56^{bright}CD16^{neg} subsets. CD56^{bright}CD16^{neg} NK cells were gated for CD62L^{+} cells to determine differences in the proportions between CD56^{bright}CD16^{neg} cNK and hpNK subsets. Mann Whitney *U* test was used to compare differences between the 2 independent groups and $P<0.05$ was considered significant. Data are presented as box and whiskers plots showing medians (50th percentile), minimum, maximum, 25th and 75th percentiles.

7.3.3 Phenotypic comparisons between cNK and hpNK CD56^{bright}CD16^{neg} and CD56^{bright}CD16^{dim} subsets

There are no published data investigating the phenotypic differences between cNK and hpNK CD56^{bright}CD16^{neg} and CD56^{bright}CD16^{pos} subsets, so the expression of CD27 (known to distinguish human NK subsets) as well as the activating receptor NKp46, inhibitory receptor CD161 and marker of early cell activation and tissue-resident marker CD69 **(Figure 7.4)** were next investigated on these subsets.

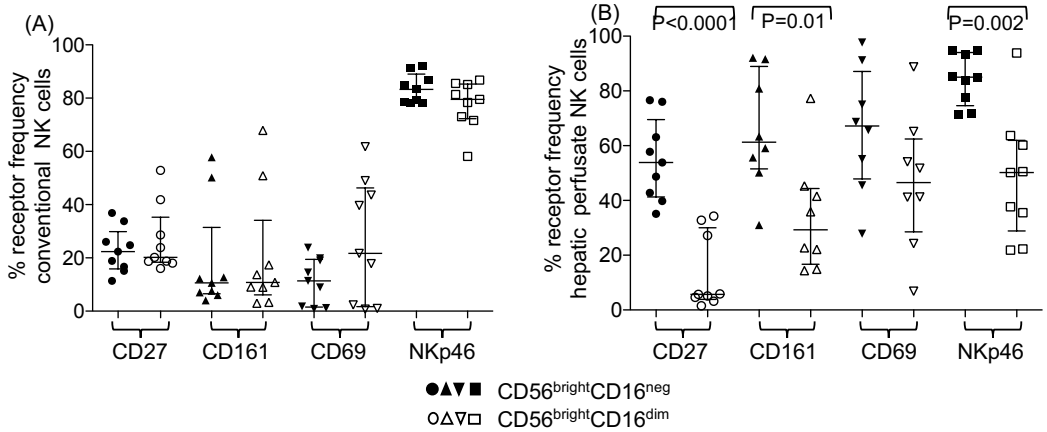


Figure 7.4: Differences in frequency distribution of CD27, CD161, CD69 and NKp46 between CD56^{bright}CD16^{neg} and CD56^{bright}CD16^{dim} cNK and hpNK subsets. To determine the frequency of the surface expression of receptors on cNK (A) and hpNK (B) cells, cells were gated for CD27 (n=9), CD161 (n=8), CD69 (n=8) and NKp46 (n=9). CD56^{bright}CD16^{neg} data is represented by solid symbols and CD56^{bright}CD16^{dim} by open symbols. Mann Whitney *U* test was used to compare differences between the 2 independent groups and $P<0.05$ was considered significant and error bars represent medians with interquartile ranges.

Striking differences in receptor frequency distribution were observed between the conventional and hepatic CD56^{bright}CD16^{neg} and CD56^{bright}CD16^{dim} NK subsets. Although there were differences in receptor magnitude in the cNK subsets, there were no differences in the distribution frequency of the receptors between CD56^{bright}CD16^{neg} and CD56^{bright}CD16^{dim} cNK subsets indicating that neither NK subset was enriched for any particular receptor (**Figure 7.4A**) suggesting that CD16 co-expression phenotypically distinguishes peripheral CD56^{bright} NK subsets more clearly than the other three receptors included in the flow panel.

In contrast, the CD56^{bright}CD16^{neg} hpNK subset was highly enriched for CD27 ($P<0.0001$), CD161 ($P=0.014$) and NKp46 ($P=0.002$) compared to the CD56^{bright}CD16^{dim} hpNK subset **(Figure 7.4B)**. Expression of the C-type lectin receptor CD69, induced by activation of NK cells and tissue resident marker, was however not significantly different between the CD56^{bright}CD16^{neg} and CD56^{bright}CD16^{dim} hpNK subsets ($P=0.083$). Although, some donors expressed a higher CD69 frequency in the CD56^{bright}CD16^{neg} subset compared to the CD56^{bright}CD16^{pos} subset there was no clear pattern of distribution between these subsets. As CD69 is associated with tissue residency the CD69 findings therefore, suggest that both CD56^{bright}CD16^{neg} and CD56^{bright}CD16^{pos} hpNK subsets have a similar capacity to be retained within the liver.

Overall, these data indicate that hpNK cells display frequency differences in CD27, CD161 and NKp46 distribution between CD56^{bright}CD16^{neg} and CD56^{bright}CD16^{dim} subsets not observed in cNK cells. Interestingly, the CD56^{bright}CD16^{dim} subset made up a larger proportion of hpNK subsets, unlike that observed in conventional NK cell subsets where they only made up a very small proportion of the NK subsets. Therefore, given the phenotypic differences observed between the two CD56^{bright} hpNK subsets, care should be taken in gating liver-derived CD56^{bright} NK cells as a single subset, as they may more accurately represent two functionally distinct subsets.

7.3.4 Differences in NKp46, CD27, CD69 and CD161 frequency distributions between CD56^{bright}CD16^{neg} cNK and hpNK subsets

For this Chapter, 2 flow cytometry panels were used - the first, to determine NKp46 and CD27 co-expression and the second to determine CD27, CD69 and CD161 co-expression. Having shown distinct differences between CD56^{bright}CD16^{neg} and CD56^{bright}CD16^{dim} NK subsets for each of the biological compartments, the frequency distribution of CD27, CD69, CD161 and NKp46 receptors between cNK and hpNK CD56^{bright}CD16^{neg} cells was firstly determined. **(Figure 7.5).** Compared to cNK cells, the hpNK subset was significantly enriched for CD27 (P<0.0001), CD161 (P=0.003) and CD69 (P<0.0001) but both biological compartments were equally enriched for the NK activating receptor NKp46. Although NKp46 was expressed on the majority of both cNK and hpNK CD56^{bright}CD16^{neg} cells, a large variance in the frequency of expression of CD27, CD69 and CD161 was noted for both cNK and hpNK CD56^{bright}CD16^{neg} cells (summarised in **Table 7.1**). Similarities therefore existed in the frequency distributions of CD27, CD69 and CD161 receptors in that both cNK and hpNK cells expressed all receptors under investigation, however the CD56^{bright}CD16^{neg} hpNK subset is highly enriched for surface expression of CD27, CD69 and CD161 receptors compared to the CD56^{bright}CD16^{neg} cNK subset.

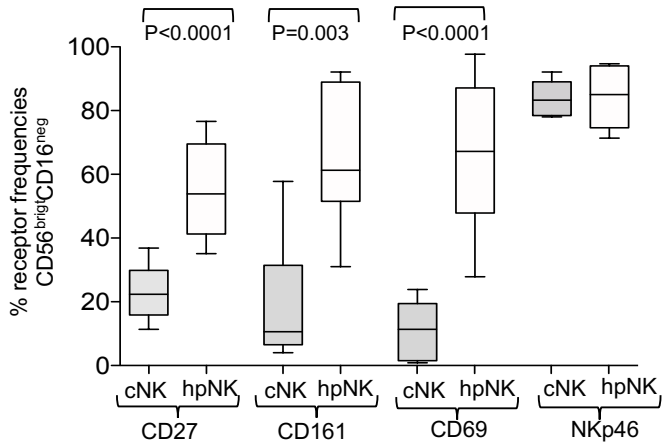


Figure 7.5: Phenotypic comparisons between cNK and hpNKCD56^{bright}CD16^{neg} subsets. Differences in the frequency and distribution of NKp46, CD27, CD69 and CD161 between CD56^{bright}CD16^{neg} cNK and hpNK subsets. Data are presented as box and whiskers plots showing medians, minimum, maximum, 25th and 75th percentiles. Mann Whitney *U* test was used to compare differences between the 2 independent groups and *P*<0.05 was considered significant.

Table 7.1: Median frequencies and distribution of NKp46, CD27, CD69 and CD161 receptors for CD56^{bright}CD16^{neg} cNK and hpNK subsets

	NKp46		**CD27**		**CD69**		**CD161**	
	Median	Range	Median	Range	Median	Range	Median	Range
cNK	83.3	78-92.1	22.4	11.4-36.9	11.4	0.87-23.9	10.6	6-57.8
hpNK	85	71.4-94.7	53.9	35.1-76.6	67.2	27.9-97.7	61.25	31-92.1

Co-expression of CD27 with NKp46, CD69 and CD161 were next investigated. The phenotyping data (Chapter 4, section 4.2.2) showed that CD27 is only expressed on NKp46^{+} cells of the CD56^{bright}CD16^{neg} cNK subset. Similarly, in this chapter, but using perfusate from liver transplants, very few CD56^{bright}CD16^{neg} hpNK cells expressed CD27 as a single population with the majority of CD27^{+} cells co-expressing NKp46 (median 96.4% for cNK cells and 94.2% for hpNK cells (**Figure 7.6**), pointing to the importance of CD27 co-expression on a subset of NKp46^{+} CD56^{bright}CD16^{neg} cells for both biological compartments.

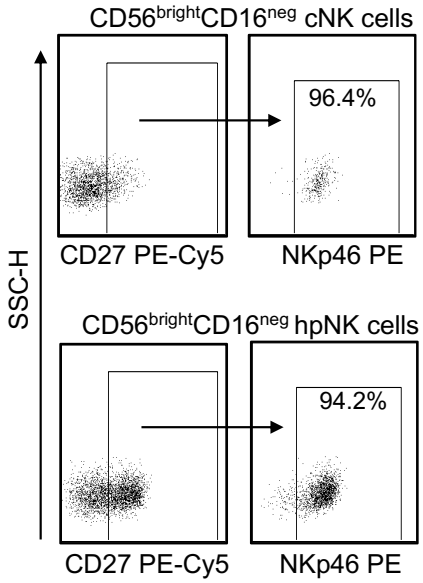


Figure 7.6: NKp46 co-expression on CD27^{+}CD56^{bright}CD16^{neg} cNK and hpNK cells. To determine what proportion of CD27^{+} cells co-express NKp46, CD27^{+} CD56^{bright}CD16^{neg} subsets were gated for NKp46 co-expression on cNK (top panels) and pNK cells (bottom panels). Percentages (median value) of CD27^{+}NKp46^{+} cells within the CD56^{bright}CD16^{neg} cNK and hpNK cells are shown within the dot plots.

The function of the C-type lectin-like receptor, CD161, on NK cells is still not completely understood, although a study has shown that CD161 expression defines pro-inflammatory NK cells with a high capacity to respond to cytokines (Kurioka et al., 2018). Both CD27 (Silva et al., 2008) and CD161 (Kurioka et al., 2018) have been shown to define NK cells into 2 functionally distinct subsets however, to the best of our knowledge there are no published immunophenotyping data comparing CD27/CD161 and CD27/CD69 co-expression patterns between conventional and hepatic CD56^{bright}CD16^{neg} NK cells. To understand the significance, if any, of CD69 and CD161 co-expression on CD27^{+} CD56^{bright}CD16^{neg} cNK and hpNK subsets, CD27^{+} cells were gated for CD69 and CD161 co-expression. Only a minority of CD27^{+} cNK co-expressed CD69 and CD161 (median of 10.9% and 9.14%, respectively) **(Figure 7.7A)** whereas CD27^{+} hpNK cells were highly enriched for CD69 (median 80.3%) and CD161 (75.1%) co-expression **(Figure 7.7B)**. The proportion of CD56^{bright}CD16^{neg} hpNK cells were therefore significantly enriched for CD27 cells co-expressing CD69 (P=0.0006) and CD161 (P=0.002) compared to CD56^{bright}CD16^{neg} cNK cells (**Figure 7.7C**).

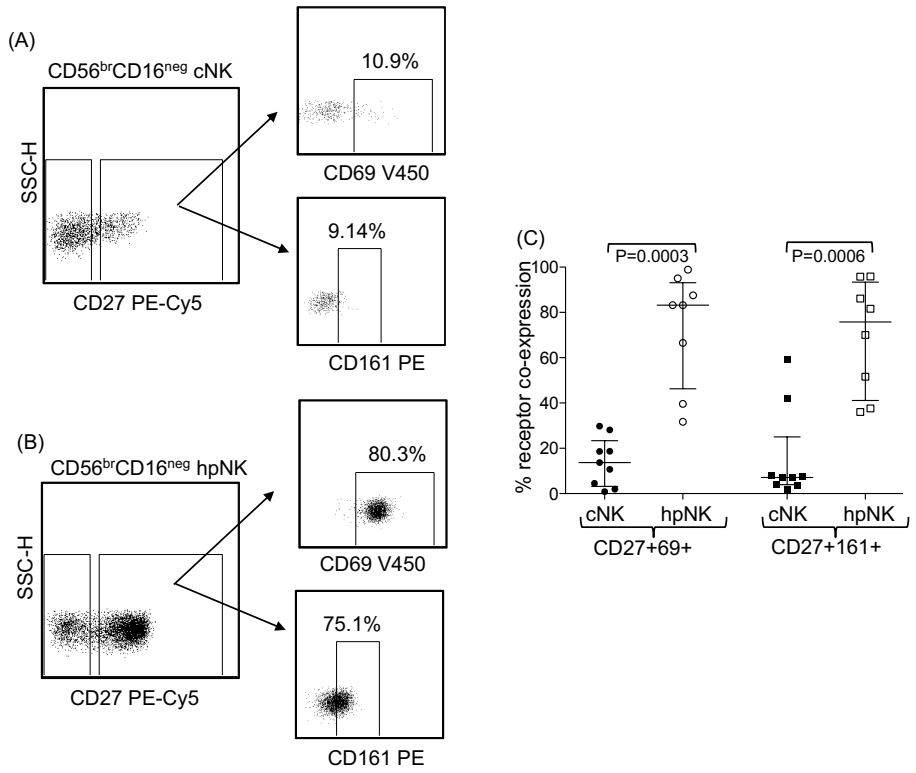


Figure 7.7: Representative dot plot of CD69 and CD161 co-expression on CD27$^+$ circulating and hepatic CD56^{bright}CD16^{neg} NK cells. CD27$^+$ cNK cells (A) and hpNK cells (B) were gated for CD69 and CD161 co-expression to determine receptor expression. Differences between biological compartments, were made by comparing CD27$^+$CD69$^+$ and CD27$^+$CD161$^+$ cNK and hpNK subphenotypes (C). Mann Whitney *U* test was used to compare differences between the 2 independent groups and $P<0.05$ was considered significant and error bars represent medians with interquartile ranges.

Despite the significant difference in proportions between cNK and hpNK CD27$^+$ subphenotypes, the variance in CD27$^+$ cNK and CD27$^+$ hpNK cells that co-express CD69 or CD161 was large, ranging from 1.77% to 39.7% and 24.5% to 99.4% for CD69 on CD27$^+$ cNK and CD27$^+$ hpNK cells, respectively, and 4.09% to 9.14% and 34.8% to 96.3% for CD161, respectively. Therefore, to appreciate the distribution differences between CD56^{bright}CD16^{neg} cNK and hpNK subphenotypes at a multidimensional level and to determine the predominant subphenotypes for each biological compartment, Boolean gates were applied to CD27, CD69 and CD161 cells. This analysis resulted in 8 subphenotypes (shown as different coloured in **Figure 7.8**) Striking differences in predominant subphenotyes were apparent between cNK cells (**Figure 7.8A**) and hpNK cells (**Figure 7.8B**). Unlike cNK cells with a mean of 0.89%, a large proportion (mean 29.6%) of CD56^{bright}CD16^{neg} hpNK cells co-expressed all 3 receptors (Segment 1**, Figure 7.8**). CD27 was expressed on 57.2% of hpNK Boolean defined subphenotypes compared to only 30.5% on cNK cells. Although 22.4% of

cNK Boolean subpopulations expressed CD27^{+} as a single population it can be assumed that this CD27^{+} subphenotype co-expressed NKp46, given that CD27 was shown to be almost exclusively expressed on NKp46^{+} cells. In keeping with tissue residency, 62% of hpNK Boolean defined subphenotypes expressed CD69 unlike cNK cells with only 14.7%.

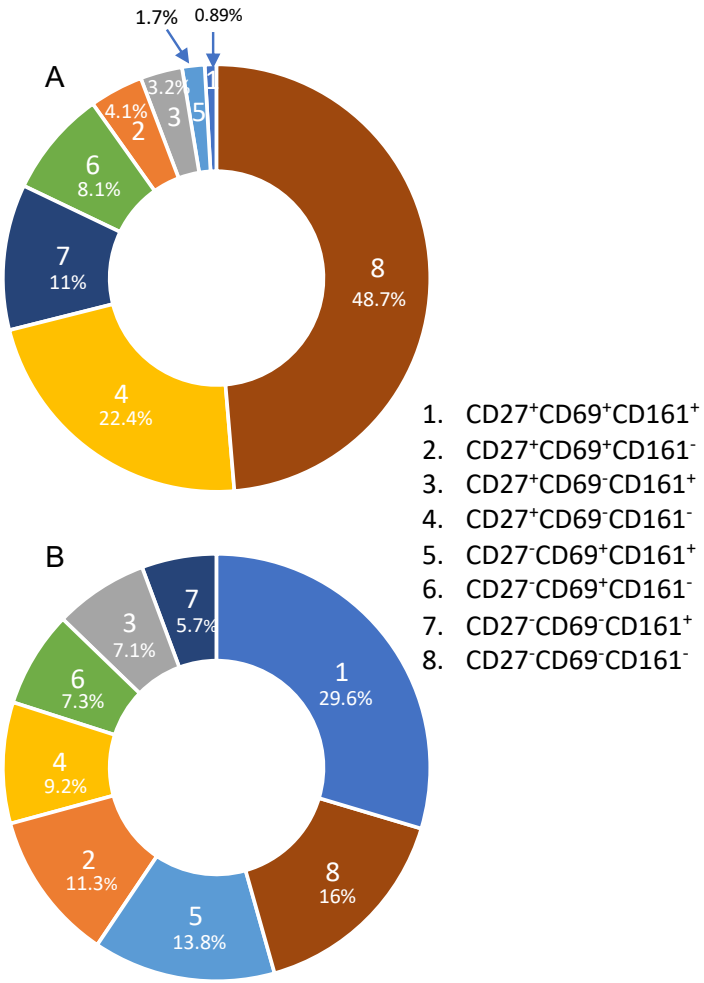


Figure 7.8: Differences between circulating and liver CD56^{bright}CD16^{neg} Boolean calculated CD27, CD69, CD161 NK subphenotypes. To determine differences between cNK (A) and hpNK (B) subphenotypes, a Boolean algorithm was applied to gated CD27, CD69 and CD161 cells, using FlowJo^{TM} software for Mac (version 9.9.4), Ashland. Charts were generated using Excel, Windows 365. Proportions for CD56^{bright}CD16^{neg} NK subphenotype are presented within each segment of the pie chart.

Taken together, differences between conventional and hepatic perfusate derived CD56^{bright}CD16^{neg} NK cells, were apparent not only in co-expression patterns of the receptors under investigation, but also in the predominance of subphenotypes.

7.3.5 Influence of CD27 co-expression on NKp46^{+} conventional and liver perfusate derived NK CD56^{bright}CD16^{neg} subsets.

In vitro studies have shown that NKp46 expression on cNK cells correlates with anti-HCV activity (Golden-Mason et al., 2012). It has also been shown that NK cells with high expression of NK46 and that co-express CD27 play an important role not only in controlling HCV replication but also modulate HCV associated liver damage (Kramer et al., 2012). Data presented in Chapter 4, section 4.2.5, revealed how co-expression of CD27 on NKp46^{+} cells influences NKp46 surface density and presents as a bi-functional phenotype impacting on the frequency of degranulating and IFNγ producing cells (Chapter 5, sections 5.3.2.1 and 5.3.3.1).

Cell surface density of NKp46 was significantly greater with CD27 co-expression for CD56^{bright}CD16^{neg} cNK cells (P=0.004) (**Figure 7.9A**), and was consistently seen amongst all individual participants (**Figure 7.9B**). This indicates that CD27 co-expression on NKp46^{+} delineates cNK cells into 2 sub-populations. However, this was not the case for CD56^{bright}CD16^{neg} hpNK cells where there was no difference (P=0.3) between CD27 co-expression or lack thereof and NKp46 surface density and at an individual level there were nominal differences in MFI between NKp46^{+} cells with or without CD27 co-expression (**Figure 7.9C**). Overall, these data indicate that there are substantial differences in the surface density of activating receptors such as NKp46 on CD56^{bright}CD16^{neg} NK cells that co-express CD27 between the conventional and hepatic circulatory compartments. Notably, a study has shown that after adoptive transfer splenic cells more closely resemble a liver NK phenotype and become functionally hypo-responsive indicating that the liver can modify NK receptor expression (Lassen et al., 2010). However, *in vivo* studies would need to be performed to understand if this is true for receptors with CD27 co-expression.

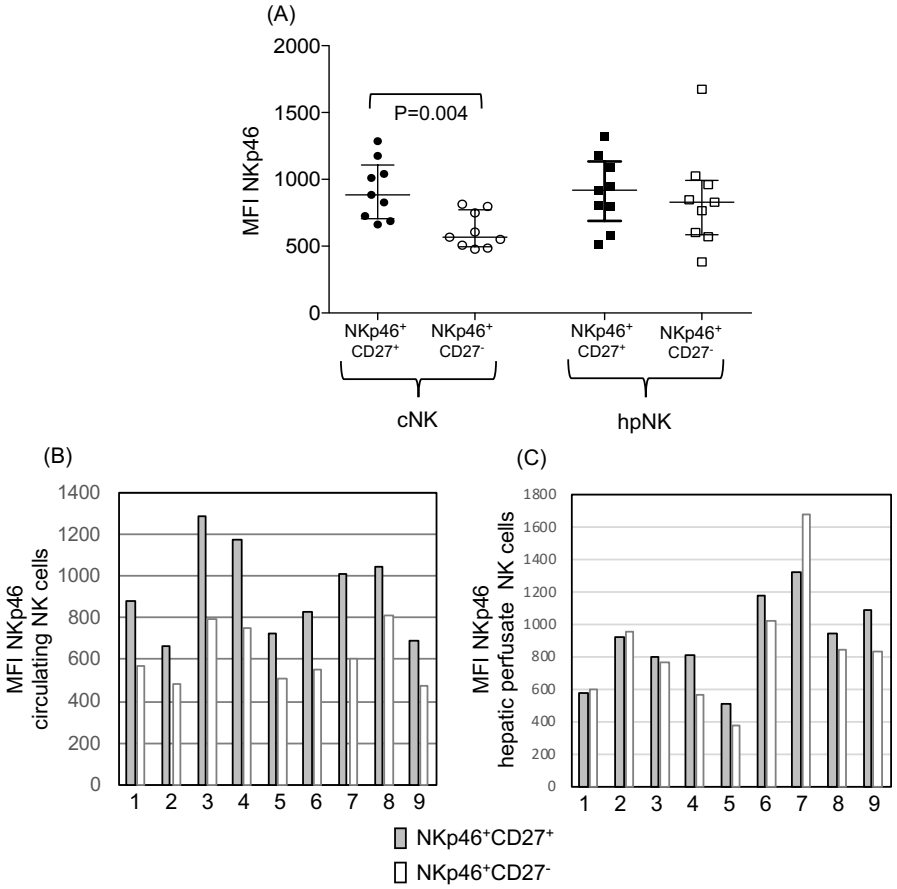


Figure 7.9: Influence of CD27 co-expression on NKp46 cell surface density for CD56^{bright}CD16^{neg} circulating and hepatic NK subsets. NKp46^{+} cells were gated for CD27^{+} and CD27^{-} cells and NKp46 cell surface density determined using MFI statistics (FlowJo^{TM} software for Mac (version 9.9.4), Ashland. (A) The MFI of NKp46^{+} cells that co-express CD27 (solid symbols) was compared to the MFI of NKp46^{+} cells that do not co-express CD27 (open symbols) for cNK and hpNK cells. Paired comparisons were performed using Wilcoxon signed rank t-test and *P*-values of <0.05 were considered significant. Error bars represent medians with interquartile ranges. Graphs (B) and (C) depict comparisons between NKp46^{+}CD27^{+} and NKp46^{+}CD27^{-} cells for individual data points for circulating cells and hepatic cells, respectively. Bar charts of individual data was generated using Excel (Windows 365).

Finally, co-expression of CD27 on CD69 and CD161 cells was analysed to understand the influence, if any, on receptor surface density for these 2 receptors. Although co-expression of CD27 did not increase surface density of CD161^{+} cells (*P*=0.23 for cNK and *P*=1 for hpNK) or CD69^{+} cells (*P*=1 for cNK and *P*=0.38 for hpNK), overall surface density of these 2 receptors was significantly greater for hpNK cells compared to cNK cells (**Figure 7.10;** CD161: *P*=0.011 for CD161^{+}CD27^{+} and *P*=0.008 for CD161^{+}CD27^{-} and CD69: *P*=0.011 for CD69^{+}CD27^{+} and *P*=0.008 for CD69^{+}CD27^{-} cells).

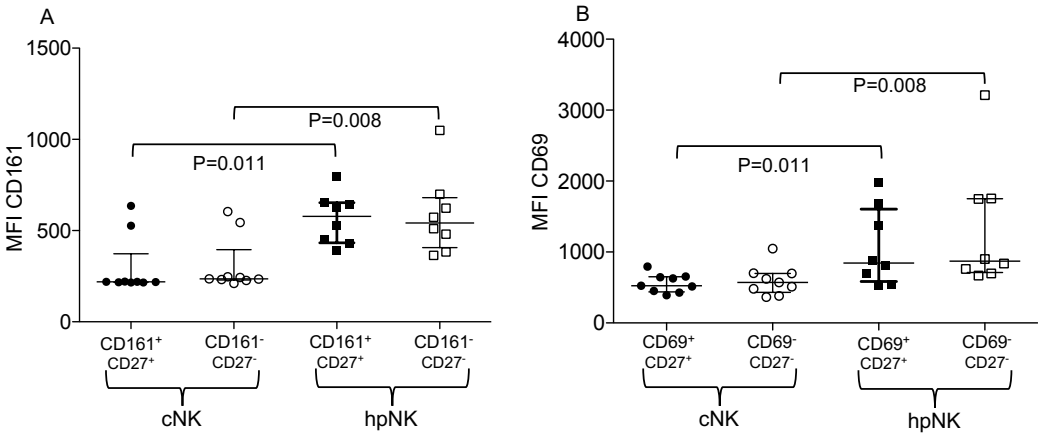


Figure 7.10: Influence of CD27 co-expression on CD161 and CD69 cell surface density for CD56^{bright}CD16^{neg} circulating and hepatic perfusate derived NK subsets. To investigate the influence of CD27 co-expression on receptor cell surface density, CD161^{+} cells and CD69^{+} cells were gated for CD27^{+} and CD27^{-} cells and receptor cell surface density determined using MFI statistics (FlowJo^{TM} software for Mac (version 9.9.4), Ashland. The MFI of CD161^{+} cells that co-express CD27 (solid symbols) was compared to the MFI of CD161^{+} cells that do not co-express CD27 (open symbols) for CD56^{bright}CD16^{neg} cNK and hpNK cells (A). The MFI of CD69^{+} cells that co-express CD27 (solid symbols) was compared to the MFI of CD69^{+} cells that do not co-express CD27 (open symbols) for CD56^{bright}CD16^{neg} cNK and hpNK cells (B). Mann Whitney *U* test was used to compare differences between the 2 independent groups and $P<0.05$ was considered significant. Error bars represent medians with interquartile ranges.

7.3.6 Acute liver failure case study

Hepatic perfusate from an ALF patient became available during the course of the study. The 46 year old female patient had no clinical history of liver problems or alcohol or drug abuse, but started becoming ill a month after consuming a globally available weight loss herbal supplement. Similar to other reported case studies (Chen et al., 2010), the patient's condition deteriorated into fulminant liver failure which is believed to have been a consequence of drug induced liver injury caused by an ingredient of the supplement. CD56^{bright}CD16^{neg} hpNK cell phenotypes from the ALF patient were therefore examined and compared to those of healthy liver donors (**Figure 7.11**).

The proportion of ALF NKp46^{+} CD56^{bright}CD16^{neg} cells was in keeping with that observed in healthy liver perfusate (93.1% versus a median of 85%) and similar to healthy liver perfusate, the majority of CD27^{+} cells also co-expressed NKp46 (95% versus a median of 94.2%). There was however, a dramatic loss in the proportion of CD56^{bright}CD16^{neg} cells that expressed CD27 (14.3%) in comparison to NK cells from healthy livers (median 53.9%) (**Figure 7.11A**) which

was also reflected in the proportion of NKp46 cells that co-express CD27 (14.6% versus a median of 57.2%).

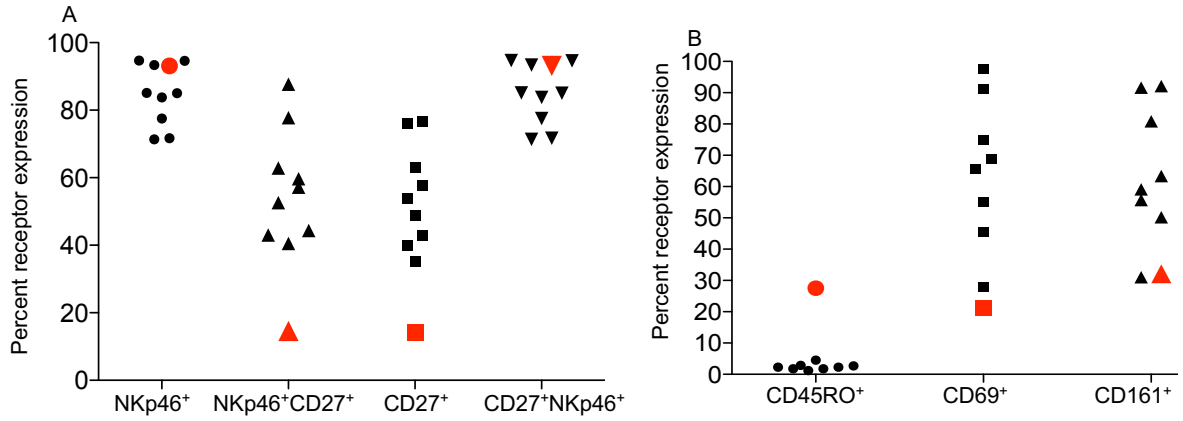


Figure 7.11: Differences in receptor expression between healthy liver and acute liver failure CD56^{bright}CD16^{neg} cells. Proportions of CD56^{bright}CD16^{neg} cells from healthy livers (black symbols) and acute liver failure case (red symbols) expressing NKp46^{+}, NKp46^{+}CD27^{+}, CD27^{+} CD27^{+}NKp46^{+} cells (healthy livers: n=9) (A) and CD45RO^{+}, CD69^{+} and CD161^{+} cells (healthy livers: n=8) (B).

Furthermore, in contrast to NK cells from healthy donors, which had minimal surface expression of CD45RO (median of 2.32%), a large proportion of CD56^{bright}CD16^{neg} cells from the ALF patient expressed this receptor (27.5%) (**Figure 7.11B**). CD56^{bright}CD16^{neg} phenotypic changes for the ALF patient were therefore marked by aberrant expression of CD45RO and under-expression of CD27. Surface expression of both CD69 and CD161 varied widely for the healthy livers and although surface expression of these markers in the liver from the ALF patient was low (21.2% versus a median of 67.2% for CD69 and 32.1% versus 61.25% for CD161), proportions in the ALF patient were not dissimilar to the lowest value found in healthy livers. However, when Boolean gated CD27, CD69 and CD161 subphenotypes were examined, there was aberrant co-expression patterns for these receptors was also apparent in comparison to healthy cells. As shown in **Figure 7.8B**, the largest proportion of Boolean gated healthy NK cells expressed all 3 receptors (mean 29.6%) yet strikingly, the proportion of cells from the ALF patient that co-expressed all 3 receptors was minimal (1.84%) (**Figure 7.12**) and the largest proportion of ALF cells were negative for all 3 receptors (38.2%) compared to 16% for healthy CD56^{bright}CD16^{neg} cells. These novel findings are novel and significant. As CD27^{+} is only co-expressed on NKp46^{+} cells, this indicates that the ALF patient lacks the largest NKp46^{+} subphenotype that is present in healthy donor livers.

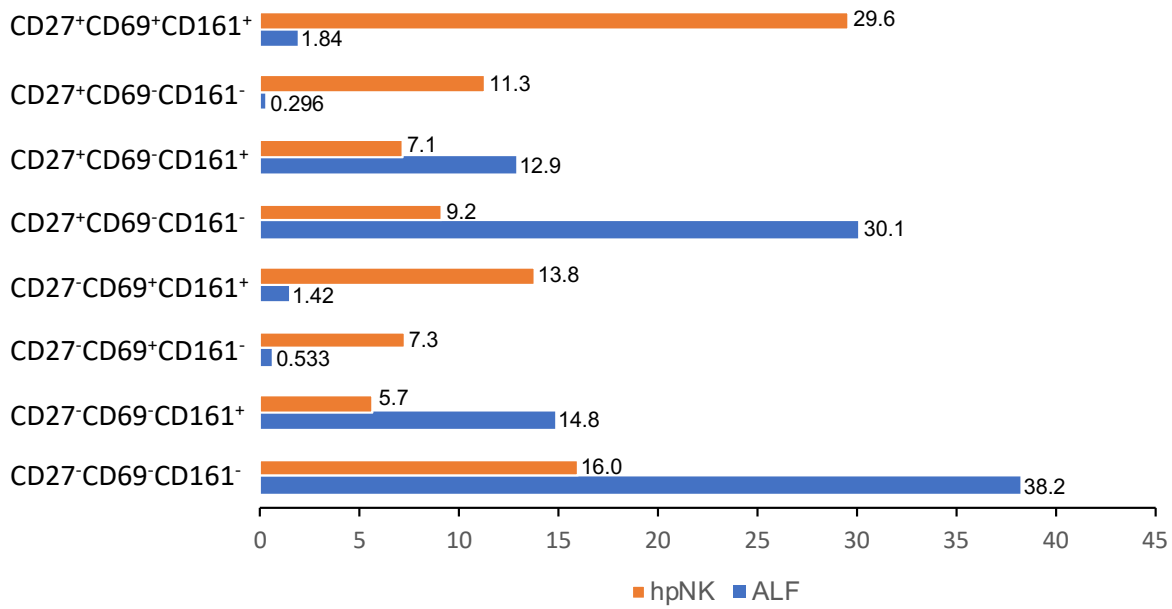


Figure 7.12: Boolean gated CD27, CD69, CD161 subphenotypes of acute liver failure case and healthy liver CD56^{bright}CD16^{neg} NK cells. Differences between Boolean gated CD56^{bright}CD16^{neg} ALF and healthy (n=8) NK subphenotype proportions were calculated using FlowJo^{TM} software for Mac (version 9.9.4), Ashland. The chart was generated in Excel, Windows 365. Numbers in the chart represent the mean. ALF= acute liver failure cells (blue bars), hpNK=hepatic perfusate NK cells (orange bars).

Furthermore, the proportion of ALF cells that expressed CD27 in the absence of CD69 and CD161 represented the 2nd largest Boolean population (30.1%), whereas an average of only 9.2% of healthy cells were CD27^{+}CD69^{-}CD161^{-}, suggesting that a loss of receptors occurred on NKp46 cells.

CD4 and CD8 T cells were next gated for CD27 and CD45RO surface expression to determine if any surface receptor differences were obvious on these lymphocytes. Although the dot plots (FlowJo^{TM} software for Mac version 9.9.4, Ashland) indicated that there was no apparent difference in surface expression of CD27 on ALF CD4 and CD8 T cells compared to healthy liver T cells (data not shown), there were 2 clearly defined CD45RO populations on ALF CD4 and CD8 T cells not evident on healthy liver T cells with the one population expressed at a similar level to that of healthy cells and a 2nd bright population not observed on healthy cells (**Figure 7.13**). Furthermore, a small population of CD45RO^{+} CD4 and CD8 T cells displayed changes in granularity (evident by SSC on y-axis of dot plots) not seen in healthy cells.

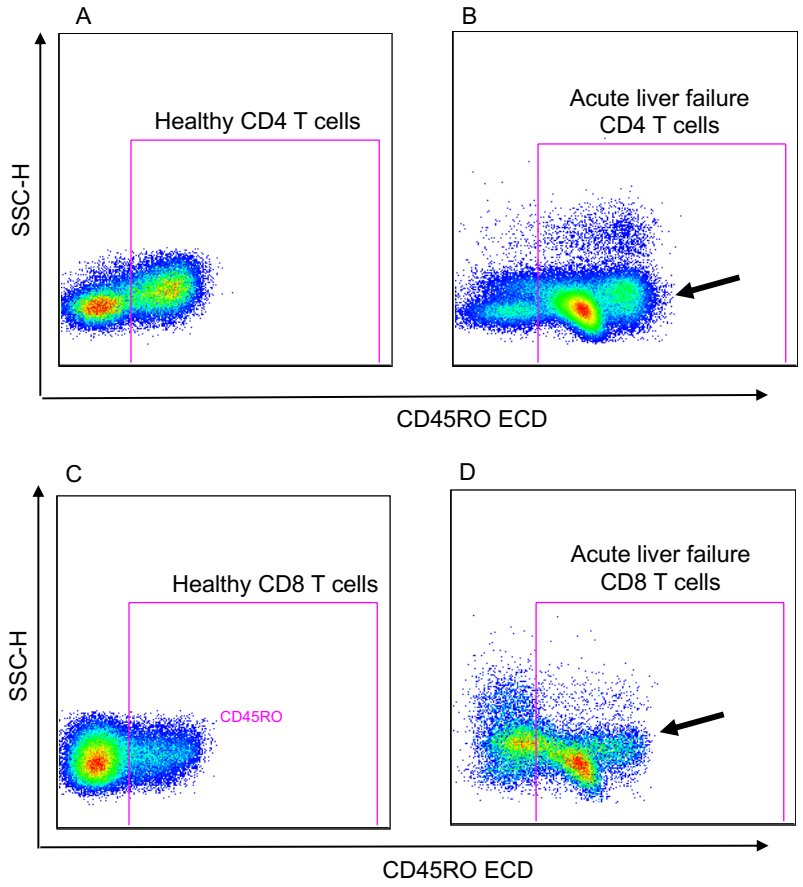


Figure 7.13: CD45RO surface expression on healthy liver and acute liver failure CD4 and CD8 T cells. CD4 (top panel) and CD8 (bottom panel) cells were gated for CD45RO to compare surface expression between healthy (A) and (C) and acute liver failure cells (B) and (D). Black arrows indicate bright expression of CD45RO on acute liver failure T cells not found on healthy T cells.

Interestingly, although the NK cells from the ALF patient showed a substantial loss of CD27^{+} cells, CD27 and CD45RO expression on CD4 and CD8 T cells fell well within the ranges determined for the healthy liver samples with CD27 expression falling in the upper limit of that for healthy CD4 T cells (93.4% versus a median of 74.7%; range: 54.4% to 97.7%) but similar to those of healthy CD8 T cells (64.3% versus a median of 66.35%). Similarly, despite the bright expression of a 2nd CD45RO population, CD45RO^{+} cell frequencies on CD4 and CD8 T cells (although at the upper limit of healthy donor cells) were not much greater than healthy cells (81.5% versus a median of 59.15%; upper limit of 78.1% for healthy donor CD4 T cells and 52.9% versus a median of 35.85%; upper limit of 57.4% for healthy donor CD8 T cells) (**Figure 7.14A**).

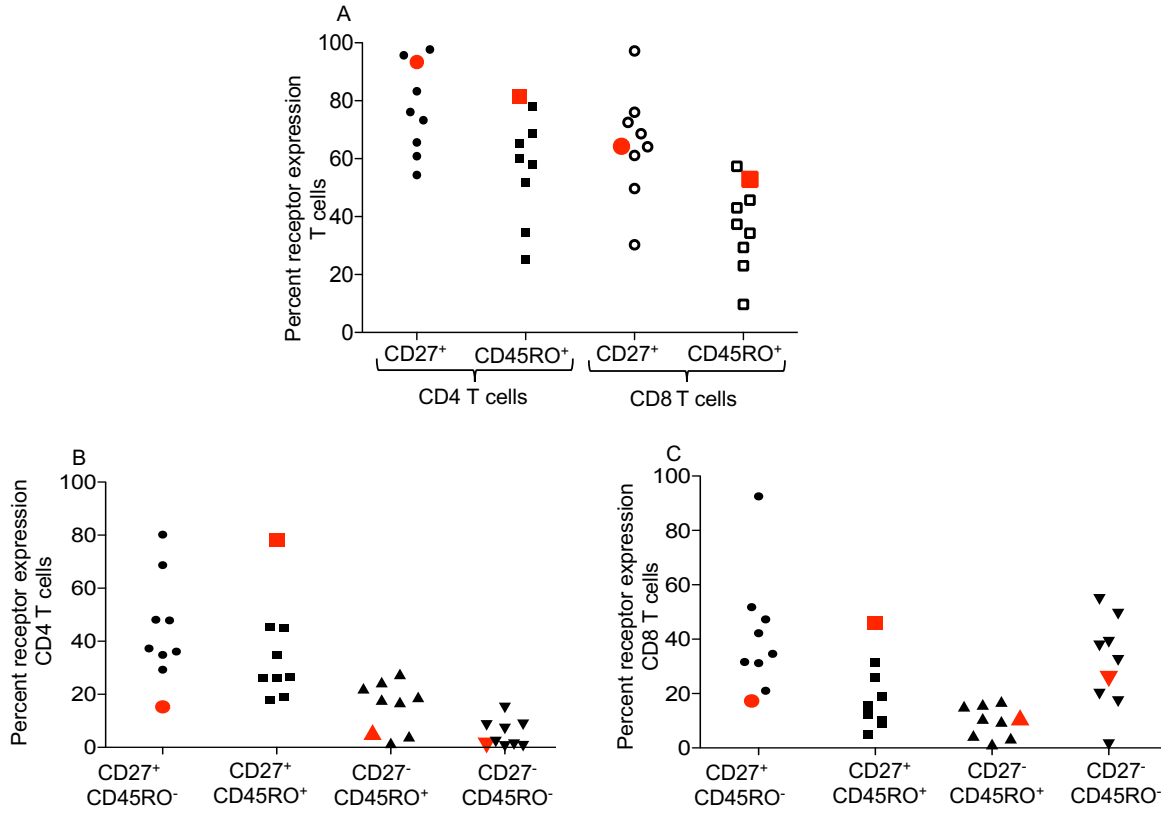


Figure 7.14: Differences in CD27 and CD45RO receptor expression for healthy liver and acute liver failure CD4 and CD8 T cells. Percentage of CD4 and CD8 T expressing CD27 or CD45RO expression (A). Quadrant gates were applied to CD27 and CD45RO and percentage of CD4 T cells (B) and CD8 T cells (C) singly or co-expressing CD27 and CD45RO determined. Healthy livers (n=8; black symbols) and acute liver failure case (red symbols).

When CD27 and CD45RO were quadrant gated for co-expression strikingly there was a skewing for ALF CD4 T cells (**Figure 7.14B**) towards a CD27^{+}CD45RO^{+} phenotype (78.2% versus a median of 26.35% for healthy donors) and a loss of the CD27^{+}CD45RO^{-} phenotype (15.3% versus a median of 42.6% for healthy donors) which suggested a loss of naive CD4 T cells and a gain of CD4 Tcm cells. Although the CD8 T cells showed a similar trend (46% versus 14% for healthy CD27^{+}CD45RO^{+} phenotype and 17.3% versus 38.4% for healthy CD27^{+}CD45RO^{-} phenotype), the changes were not as substantial (**Figure 7.14C**) as those of CD4 T cells. Intriguingly, factors inducing liver failure in this particular patient affected both the CD4 T cells and the CD56^{bright}CD16^{neg} hpNK cells characterized by a substantial loss of CD27 and overexpression of CD45RO.

7.4 Discussion

One of the key factors that determines the divergent and heterogeneous functions of NK cells is their tissue residency and evolving knowledge on NK cells indicates that these cells not only develop in the bone marrow but also develop and differentiate in tissues (Marquardt et al., 2015; Sojka et al., 2014a; Victorino et al., 2015). Tissue-resident NK cells are not only developmentally less mature but also express different surface markers (reviewed in (Peng and Tian, 2017)). The phenotype, functions and transcription factor requirements of these NK cells differ suggesting that complex interactions within the tissue microenvironment shape the functional phenotype of tissue resident NK cells (Shi et al., 2011). This challenges the manner in which we view and can study NK cells.

With this in mind, a secondary objective of the current study was to ascertain whether sufficient numbers of NK cells could be isolated from hepatic perfusate and importantly if they were of hepatic origin. Hepatic perfusate could therefore provide an alternative source of liver NK cells for phenotyping and functional studies as human liver NK cells studies are limited by the availability of suitable material. Unlike enzymatic digestion of liver biopsies, which alters lymphocyte phenotype and function, liver associated leucocytes, predominantly located in the hepatic sinusoids, can be isolated during donor liver harvesting when the organ is perfused with HTK solution. This solution is physiologically not harmful to hepatic tissue, as integrity of the liver cells is required for transplant purposes. A drawback though of this method is that the liver is highly vascularized, receiving approximately 75% of its blood supply from the portal vein and 25% from the hepatic artery, so not all blood collected during perfusion of the liver will be of hepatic origin. Yet, the descriptive phenotyping data presented in this Chapter indicated that there were sufficient differences between cNK and hpNK cells to imply the presence of liver specific CD56^{bright}CD16^{neg} cells. Also, as a few litres of perfusate are collected, sufficiently large numbers of cells can be isolated to allow for rare populations to be phenotypically differentiated during flow cytometric data acquisition. Therefore, in principle, the data generated in this Chapter provides proof that hepatic perfusate (which is discarded) is an abundant source of lymphocytes and suitable for studying liver resident NK cells.

CD56^{bright} human NK cells are broadly divided into two subsets based on their co-expression of CD16, namely CD56^{bright}CD16^{neg} and CD56^{bright}CD16^{pos}. As reported in the literature, NK cells isolated from hepatic perfusate were abundant in CD56^{bright} cells and on average, hpNK cells were highly enriched for the CD56^{bright}CD16^{dim} subset (mean 25.3%) compared to the CD56^{bright}CD16^{neg} subset (mean 13.1%). This is distinct from peripheral cNK cells where the

proportion of CD56^{bright}CD16^{dim} NK cells was less than that of the CD56^{bright}CD16^{neg} NK cells (4.6% versus 6.49%, respectively). Furthermore, cNK cells showed similar subphenotype characteristics with no difference in proportions of the two CD56^{bright} subsets expressing receptors CD27, CD69, CD161 and NKp46 between. This was in stark contrast to the CD56^{bright}CD16^{neg} hpNK subset which was highly enriched for CD27, CD161 and NKp46 compared to the CD56^{bright}CD16^{dim} hpNK subset, but not for CD69 expression. Egress of lymphocytes from secondary lymphoid organs is mediated by a sphingosine-1-phosphate (SIP1) gradient at exit sites (Schwab and Cyster, 2007) and CD69 is known to prevent egress from the tissue environment (Shiow et al., 2006). This is supported by a study reporting that liver resident CD56^{bright} NK cells which express CD69, CCR5 and CXCR6 are retained within the hepatic sinusoids (Hudspeth et al., 2016). As the phenotyping data showed that both CD56^{bright} hpNK subsets were equally enriched for CD69^{+} cells, this strongly suggests that both subsets are equally retained in the hepatic environment. Further studies would however need to be done to understand if the CD56^{bright}CD16^{dim} subset represents a group of cells still undergoing differentiation within the hepatic environment, or whether they represent an ontologically distinct subset as has been shown in clonal tracking studies in macaques (Wu et al., 2014).

Although CD69 is considered a marker of tissue residency it is rapidly upregulated on most lymphocytes (including NK cells) following activation, playing an important immune regulatory role by controlling the inflammatory response through inhibition of CD4 Th17 differentiation (Gonzalez-Amaro et al., 2013). The CD56^{bright} CD16^{neg} hpNK subset was enriched at high frequencies for CD69 (median 67.2%), but with 80.3% (median) of CD56^{bright} CD16^{neg} hpNK cells expressing a CD27^{+}CD69^{+} subphenotype, this indicated that the majority of CD69^{+} cells were co-expressed with CD27, compared to cNK cells with a median of only 10.9%. These results identify a preferential co-expression of CD69 and CD27 within the hepatic environment. The significance of these findings is not clear, as the multiple roles of CD69 expression on lymphocytes has not been studied, but as the liver is enriched for CD27^{+} cells and a large proportion of CD27^{+} cells co-express CD69, CD27^{+} cells are therefore likely to be retained in the liver possibly mediated by CD69/SIP1 interactions (Shiow et al., 2006).

CD161^{+} NK cells are highly responsive to pro-inflammatory cytokines (Kurioka et al., 2018) and CD27^{+} CD56^{bright} NK cells produce high levels of pro-inflammatory IFNγ and TNFα cytokines suggesting that they could be an early source of NK cell derived cytokines able to help modify the immune response. CD161 expression has been shown to define NK cells into

2 functionally distinct subsets that are highly proliferative (Kurioka et al., 2018) and reduced CD161^{+} NK frequencies are found in viremic HIV patients (Alter et al., 2004) and peripheral blood of patients able to clear acute HCV infection (Alter et al., 2011), implicating them in control and clearance of viral infections. Many factors influence the human immune response and following HCV infection, some patients develop chronic HCV whereas others are able to clear the infection during the acute phase (Shepard et al., 2005), possibly mediated by innate immune cells before the development of an adaptive immune response (Guidotti and Chisari, 2006). In the current study, the CD56^{bright}CD16^{neg} hpNK subset was significantly enriched for CD161^{+} cells compared to cNK, yet both hpNK and cNK CD56^{bright}CD16^{neg} cells showed a wide variation in CD161 expression which was also reflected in the CD27^{+}CD161^{+} subphenotype proportions (range 4.1% to 52.5% for cNK cells and 34% to 96.3% for hpNK cells) indicating that in some individuals a very high proportion of CD161 cells are co-expressed with CD27. In Chapter 5 it was shown that CD56^{bright}CD16^{neg} CD27^{+} NK cells (which are also NKp46^{+}) are more cytolytic than CD27^{-} NK cells, yet NK CD107a degranulation and IFNγ production is inhibited upon engagement of CD161 with its ligand (Rosen et al., 2008), so it would be of interest to understand the functional response differences between CD161^{+} NK cells that co-express CD27 and CD161 cells without CD27 expression and to ascertain if variations in CD27/CD161 co-expression play a role (if any) in the differential outcomes observed in HCV infection.

The role of NK cells expressing CD27 has been investigated under various pathological conditions (Eisenhardt et al., 2014; Kaczmarek et al., 2017; Viegas et al., 2013; Zhang et al., 2017) and studies indicate that NK cell functional responses can be modulated via the co-stimulatory effects of CD27 (De Colvenaer et al., 2010; Hayakawa and Smyth, 2006). CD56^{bright} NK cells that express CD27 are involved in spontaneous clearance of acute HCV in HIV-infected patients (Eisenhardt et al., 2014) and reduced frequencies of CD27 in HIV/HCV co-infected patients may be involved in the rapid progression of liver disease (Kaczmarek et al., 2017). However, patients with chronic HCV infection have altered NK receptor expression (Kaczmarek et al., 2017; Nattermann et al., 2006) suggesting that chronic HCV infection could become established as a result of virus-induced changes of NK receptors. Importantly, in this study it was found that a significant majority of CD27^{+} cells for both cNK and hpNK CD56^{bright}CD16^{neg} subsets, co-express NKp46 (median 96.4% for cNK cells and 94.2% for hpNK cells) and that very few cells express CD27 in the absence of NKp46, which strongly indicates that expression of CD27 may be dependent on NKp46. This suggests that CD27 plays a crucial role in NKp46 function given the importance of NKp46 in various pathological

conditions. As not all CD56^{bright}CD16^{neg} NKp46^{+} cells co-express CD27 it can be proposed that the CD56^{bright}CD16^{neg} subset comprises of 2 NKp46 populations and so studies that link CD27 to various pathological conditions most likely also reflect its co-stimulatory effects on NKp46 function.

NK cells require a balance of signals from various cell surface receptors to become activated and as a major activating receptor, NKp46 is involved in natural cytotoxicity (Mandelboim et al., 2001; Sivori et al., 1999), being expressed on both resting and activated NK cells (although its cellular ligand has still not been identified), with differences in natural cytotoxicity against target cells correlating with a high NKp46 surface density (Sivori et al., 1999). Critically, cell surface density of NKp46 for the CD56^{bright}CD16^{neg} pNK subset was significantly greater when co-expressed with CD27 which held true for each participant. Interestingly, HIV-infected patients, despite effective prolonged use of HAART, do not fully recover surface expression of NKp46 (amongst other NK receptors) compared to healthy controls and undetectable viral load has been associated with higher NKp46 expression (Frias et al., 2015). Yet the percentage of CD27^{+} cells is increased in patients chronically infected with HIV (Titanji 2007) It would therefore be of interest to determine if the NKp46^{+}CD27^{+} subphenotype (as found in healthy controls for this study) is present in HIV patients, or if the proportion of CD27^{+} cells that do not express NKp46 is increased.

There was however, no associaton of higher NKp46 cell surface density with CD27 co-expression on CD56^{bright}CD16^{neg} hpNK cells. Although NK cells in the current study were isolated from healthy hepatic tissue and represent cell phenotypes under normal homeostatic conditions, venous blood circulates in a sterile environment, unlike that found in the liver, in which large volumes of antigen are derived from the intestines and brought to the liver for processing. A balance between activating and inhibitory receptors is required to reach a threshold for NK cells to become activated (Narni-Mancinelli et al., 2013) and as NKp46 is an activating receptor, its activation requirements in the liver therefore are likely to be more strictly controlled, requiring additional co-stimulatory signals from co-receptors. Indeed, the largest Boolean gated subphenotype from hepatic derived CD56^{bright}CD16^{neg} cells co-expressed CD27, CD69 and CD161, with a mean of 29.6% as opposed to 0.89% for conventional NK cells and given that 94.2% of CD27^{+} hpNK cells co-expressed NKp46, it can be assumed that this triple positive population also included NKp46 surface expression.

This study is the first to present data on phenotypic alterations of the CD56^{bright}CD16^{neg} NK subset in a case of acute liver failure believed to be a consequence of consuming a herbal weight loss product. NK cells are critical in maintaining homeostasis within the liver as depletion of NK cells results in liver fibrosis (Radaeva et al., 2006; Robinson et al., 2016) and drugs or their metabolites that are intrinsic hepatotoxins cause hepatocellular damage in a dose dependant manner, whereas idiosyncratic hepatotoxicity is a hypersensitivity reaction to the drug following a previous exposure. Idiosyncratic hepatotoxicity is accompanied by inflammation, unlike intrinsic hepatotoxicity which manifests as hepatic necrosis with little inflammation (Reviewed in (Ramachandran and Kakar, 2009)). Although NK cells have been studied within the context of hepatocellular carcinoma, there appears to be little published data on changes in NK cells phenotypes following drug induced acute liver damage (Liu et al., 2018a). In the ALF case, proportions of NKp46-expressing cells were similar to those of healthy cells (93.1% versus 85%, respectively) as were the proportion of CD27 cells that co-express NKp46 (95.4% versus 94.2%, respectively). Yet, there was a general overall loss of CD27 cells (14.3% versus a median of 53.9%) that was reflected by CD27 co-expression on NKp46^{+} cells (14.6% versus a median of 57.2%) which points to a loss of CD27 on NKp46^{+} cells. This loss (or downregulation) was more apparent when co-expressed with other receptors, as the ALF patient had a severe loss of the triple positive Boolean gated population which comprised 1.84% of cells unlike healthy cells with a mean of 29.6%. These novel data are significant given the importance of co-receptors for normal functioning of NK cells and as CD69 is considered a marker of tissue residency, the loss of CD69^{+} cells also suggest that liver resident cells were severely depleted.

In addition to the loss of cells expressing NKp46 co-receptors, the ALF patient also had aberrant expression of CD45RO on CD56^{bright}CD16^{neg} NK cells (27.5%), which was not found on healthy donors. Although there are limited reports of CD45RO expression on NK cells, a study has reported low levels of dim expression on both healthy CD56^{bright} and CD56^{dim} NK cells (Lima et al., 2001). Furthermore, T cells and CD4 T cells in particular, reflected a skewing towards a CD27^{+}CD45RO^{+} phenotype which may be suggestive of the acquisition of a memory phenotype and loss of naive cells (CD27^{+}CD45RO^{-}). Increases in T memory phenotypes have been reported in various autoimmune conditions including multiple sclerosis (Bhargava and Calabresi, 2015), type 1 diabetes (Matteucci et al., 2011), psoriasis (Hayashi et al., 2013) and in the inflammatory conditions of lichen planus and lichenoid mucositis (Devi et al., 2017). Yet, although CD4 T cells mediate hepatocellular damage in autoimmune hepatitis (Rosen, 2003) and demonstrate antigen specific responses (Yoshizawa et al., 1999)

to liver specific antigens (Vergani and Mieli-Vergani, 2004; Zachou et al., 2004), the exact phenotypes (memory or otherwise) are not well described and the significance of the alterations in T cell phenotypes observed in the ALF patient in the current study remains to be established.

Limitations: Proportions of contaminating cNK cells likely differed between donors which would affect data analysis of cell proportions. The hepatic perfusate was collected from patients who up until the time of their demise (through a traumatic event) were healthy. Some of the donors received no drugs or blood transfusions, whereas others received drugs such as low dose adrenalin and vasodilators and/or packed blood cells during resuscitation attempts. The presence of these drugs and cells, as well as the effects of traumatic death on NK cell and T cell phenotypes are unknown and cannot be discounted.

In summary, advances in flow cytometry enable powerful multicolour approaches to be used to investigate and characterize cell types and their subpopulations. The use of hepatic perfusate provides an excellent source of liver NK cells which has enabled novel characteristics to be identified. *Ex vivo* immunophenotyping data revealed that NK cells derived from hepatic perfusate are significantly enriched for CD56^{bright}CD16^{neg} cells that co-express CD27 with CD69 and CD161 and importantly, that CD27 is not expressed in the absence of NKp46 for either cNK or hpNK cells. Although surface density of NKp46 remained unchanged with CD27 co-expression for hpNK cells, the importance of CD27 surface expression within the hepatic environment was indicated by an ALF patient, who had an overall loss of CD27^{+} cell frequencies and alterations in co-expression patterns with CD69 and CD161.

CHAPTER 8
Discussion and concluding remarks

8.1 Discussion

$CD56^{bright}CD16^{neg}$ NK cells are major producers of cytokines, playing a functional role as an innate immunoregulator in early immune responses to pathogens. Lymph nodes are the site of developing adaptive immune responses, and high expression levels of L-selectin and CCR7 on $CD56^{bright}CD16^{neg}$ NK cells, mediates their trafficking to the lymph nodes where they interact dynamically with antigen presenting cells and T cells. Studies into this important NK subset are limited and given the importance of $CD56^{bright}CD16^{neg}$ NK cells not only as an immunoregulator, but also in the maintenance of homeostasis in certain solid organs, further studies are warranted. In this study, an influenza vaccination model was used to monitor functional responses and developing alterations in $CD56^{bright}CD16^{neg}$ lymph homing and peripheral subphenotypes in a cohort of healthy vaccinated individuals. Furthermore, liver-derived NK cells were immunophenotypically characterized using a liver perfusate model, to provide insights into tissue resident $CD56^{bright}CD16^{neg}$ NK cells.

A brief summary of the significant findings from each Chapter are as follows:

From **Chapter 3:**

1. A 12 colour polychromatic flow cytometry panel was developed to simultaneously immunophenotype NK and T cells and measure intracellular IFNγ responses and CD107a expression. CV's of the immunophenotyped control sample indicated that data were consistent across experiments.
2. CD56 and CD16 NK cell subsets and subphenotypes were clearly distinguished on flow cytometry dot plots as were CD4 and CD8 T memory cells.
3. The flow cytometry panel identified the 4 major NK subsets: $CD56^{bright}CD16^{neg}$, $CD56^{bright}CD16^{bright}$, $CD56^{dim}CD16^{bright}$ and $CD56^{dim}CD16^{neg}$ subsets and co-expression analyses of NKp46, CD27 and CD62L identified NK subphenotypes.
4. Central memory (Tcm) ($CD27^{+}CD62L^{+}CD45RO^{+}$), effector memory (Tem) ($CD27^{-}CD62L^{-}CD45RO^{+}$), effector cells ($CD27^{-}CD62L^{-}CD45RO^{-}$) and naive ($CD27^{+}CD62L^{+}CD45RO^{-}$) CD4 and CD8 T cells could be phenotyped.

From **Chapter 4**:

1. Boolean gating of $CD56^{bright}CD16^{neg}$ cells for CD27, CD62L and NKp46 expression defined 4 subphenotypes based on lymph homing capability and CD27 co-expression. The 4 subphenotypes were described as $lhNKp46CD27^{+}$; $lhNKp46CD27^{-}$; $pNKp46CD27^{+}$ and $pNKp46CD27^{-}$.
2. CD27 and CD62L proportions varied widely between individuals and was shown to be almost exclusively expressed on $NKp46^{+}$ cells.

3. NKp46 cell surface density was shown to be increased with co-expression of CD27 and CD62L.
4. Although CD27 surface expression varied widely between individuals it remained stable for up to 1 year suggesting that unique antigen interactions with NKp46 influences expression of this receptor.

From **Chapter 5**:

1. Six months post-vaccination, lymph homing $CD56^{bright}CD16^{neg}$ subphenotypes expanded in proportion to 2009- influenza antigen re-challenge whereas peripheral $CD56^{bright}CD16^{neg}$ subphenotypes decreased.
2. Unexpected changes in proportions of CD28/CD49d co-stimulated cells occurred following vaccination. Notably, an expansion of lhNKp46$CD27^-$ cells and decreases in both pNKp46$CD27^-$ and pNKp46$CD27^+$ subphenotypes.
3. The lhNKp46$CD27^+$ subphenotype was putatively identified as providing an antigen trained immune response as it expanded in proportion to antigen re-challenge 6 months post-vaccination but not to co-stimulatory signals.
4. Peripheral functional (IFNγ and CD107a) responses were more robust than lymph homing subphenotypes thereby functionally defining $CD56^{bright}CD16^{neg}$ cells based on migratory patterns.
5. Functionally responding $CD56^{bright}CD16^{neg}$ cells were not polyfunctional (ie did not co-express IFNγ and CD107a) and CD27 broadly delineated NKp46 into 2 functional phenotypes with $CD27^-$ cells producing more IFNγ and $CD27^+$ cells being more cytolytic.
6. There was a loss of IFNγ-responding pNKp46$CD27^-$cells following vaccination, which might suggest a migration of these cells to the lungs.

From **Chapter 6**:

1. With flu-stimulation, CD45RO was downregulated on CD4 and CD8 memory cells.
2. CD4 and CD8 memory subsets and CD4 effector cells degranulated with a greater frequency 6 months post-vaccination.
3. CD8 Tcm ($CD45RO^+CD62L^+CD27^+$) degranulated with a greater magnitude than CD8 Tem ($CD45RO^+CD62L^-CD27^-$).
4. In general, BAFF plasma levels were increased by 3 days post-vaccination and plasma IgM levels by 6 months. Elevated levels of BAFF and IgM in some participants but reduced levels in others suggests there is an association between these plasma proteins.

CHAPTER 8
Discussion and concluding remarks

From **Chapter 7**

1. Comparisons between hepatic perfusate derived and circulating lymphocytes indicated that hepatic perfusate provides a suitable source of liver resident NK cells.
2. Unlike circulating NK $CD56^{bright}CD16^{neg}$ subset with similar receptor frequency distributions to that of circulating $CD56^{bright}CD16^{dim}$ cells, hepatic perfusate derived $CD56^{bright}CD16^{neg}$ cells were distinctly different in frequency distributions of CD27, CD69 and CD161 compared to hepatic perfusate derived $CD56^{bright}CD16^{dim}$ cells.
3. CD27 surface expression was only evident on $NKp46^{+}$ cells for both circulating and hepatic $CD56^{bright}CD16^{neg}$ subsets.
4. Boolean CD27/CD69/CD161 subphenotypes varied signficantly between hepatic and circulating $CD56^{bright}CD16^{neg}$ subsets.
5. Unlike circulating $CD56^{bright}CD16^{neg}$ $NKp46^{+}$ cells, co-expression of CD27 was not associated with increased cell surface density of $NKp46^{+}$ hepatic perfusate cells.
6. Altered co-expression patterns of Boolean CD27/CD69/CD161 subphenotypes was observed in a single ALF case compared to healthy liver donor NK cells. Furthermore, the ALF case was characterised by a striking reduction in CD27 surface expression and aberrant expression of CD45RO on $CD56^{bright}CD16^{neg}$ cells (which was also noted to a lesser extent on CD8 T memory phenotypes).

Overall, a number of *in vivo* immunological changes occurred 6 months following influenza vaccination, indicative of a co-ordinated response by multiple arms of the immune system. Plasma BAFF was elevated (P=0.045) by 3 days (the only time-point measured post-vaccination) and by 6 months, plasma IgM was elevated (P=0.034) (although below the cut-off for active infection in 11 participants, with 1 participant at the border of cut-off). This may suggest that participants with elevated BAFF and IgM were more efficient vaccine responders as both B-1 (natural) and B-2 (antigen specific) derived IgM have non-redundant functions against influenza infection and are necessary for induction of virus specific IgG responses (Baumgarth et al., 2000). Around the same time-point, all CD4 T cell subsets degranulated significantly more than pre-vaccination cells (P<0.05) as did CD8 Tem (P=0.01) and naive (P=0.027) subsets. It was also at this time-point that $CD56^{bright}CD16^{neg}$ subphenotype proportions were dynamically altered (P<0.05) and the number of $pNKp46CD27^{-}$ IFNγ-responding cells decreased (P=0.037).

CHAPTER 8
Discussion and concluding remarks

The current paradigm is that $CD56^{bright}$ NK cells represent an earlier stage of NK development than $CD56^{dim}$ cells and give rise to $CD56^{dim}$ NK cells. NK cell functional responses to influenza vaccination have therefore largely focused on the $CD56^{dim}$ subset (Riese et al., 2020) or with the exception of a single study (Jost et al., 2011), have not clearly delineated NK cells by subset (Long et al., 2008; Schapiro et al., 1990). Yet there is gathering evidence challenging the paradigm that $CD56^{bright}$ NK cells are precursors to $CD56^{dim}$ NK cells (Mace et al., 2013; Parrish-Novak et al., 2000; Wu et al., 2014) and rather, that $CD56^{bright}$ NK cells represent a functionally distinct mature NK phenotype with important immunoregulatory properties (Cooper et al., 2001b). Data from the current study indicated that indeed, $CD56^{bright}CD16^{neg}$ NK cells do respond to flu-stimulation and vaccination and collectively this study provides novel insights into the functional and phenotypic alterations of $CD56^{bright}CD16^{neg}$ NK cells in response to influenza antigen as well as vaccination.

In recent years a number of studies have provided evidence that immunological memory is found not only in vertebrates (Gourbal et al., 2018; Hirano et al., 2011), but also in plants (Reimer-Michalski and Conrath, 2016) and invertebrates (Melillo et al., 2018; Milutinovic and Kurtz, 2016) and an initial infection can lead to a priming event of the immune system providing protection against a secondary encounter (Conrath et al., 2015; Cooper and Alder, 2006). Even though this response may not be specific, the principal function of immune protection is similar, in that, an enhanced and more rapid response provides an improved chance of survival for the host. Therefore the concept of “trained” immunity for innate cells has expanded beyond that of vertebrates and is indicative of an evolutionary conserved mechanism involving multiple organisms and cells. Data from this study could point to a “trained” response, as witnessed by changes in subphenotype proportions and post-vaccination $IFN\gamma^{+}$ cell frequencies 6 months following vaccination. However, these post-vaccination alterations could also represent cells undergoing an education process, as various studies reveal that NK cell licensing is proving to be more fluid than previously thought (Elliott et al., 2010; Joncker et al., 2010) and reviewed in (Orr and Lanier, 2010; Tu et al., 2016) and does not necessarily occur only in the bone marrow. Although a deeper understanding of NK cell education is developing, there are 3 different opposing models (licensing, disarming and rheostat) that currently prevail. There is consensus however, on the requirement of inhibitory receptors during the education process, so a limitation of this study is that expression levels of inhibitory receptors are unknown, as no markers were included for these receptors. Furthermore, the methodology used in this study does not allow for the differentiation between a “trained” NK cell that has been altered through epigenetic influences and an NK cell that has undergone an education process which would lead to an altered response to the same stimulus. But whether the

alterations in $CD56^{bright}CD16^{neg}$ NK cells following vaccination represent a "trained" response or an education process, the data in this study is novel and adds further insight into the $CD56^{bright}CD16^{neg}$ NK subset.

Using a Boolean gating strategy $NKp46^{+}$ $CD56^{bright}CD16^{neg}$ NK cells were defined as either lymph homing or peripheral subphenotypes. Following vaccination and flu antigen re-challenge, subphenotypes displayed time adjusted dynamics that were particularly evident 6 months after influenza vaccination. NKp46 directly recognises influenza HA (Mandelboim et al., 2001) and the only changes in proportions were found among the $NKp46^{+}$ subphenotypes, so it is likely these responses were mediated by interactions between NKp46 and the haemagglutinin antigen present in the vaccine preparation. The proportion of lymph homing $CD56^{bright}CD16^{neg}$ NK cells increased in response to *ex vivo* re-challenge with flu-antigen, whereas proportions of peripheral subphenotypes decreased, following which, proportions returned to levels similar to those of pre-vaccination responding cells. These dynamic changes in proportions could be attributable to peripheral cells responding to vaccination by the upregulation of CD62L surface expression, as both $CD27^{+}$ and $CD27^{-}$ ($CD62L^{-}$) peripheral subphenotypes decreased in proportion whereas the proportion of $CD27^{+}$ and $CD27^{-}$ lymph homing ($CD62L^{+}$) cells increased **(Figure 8.1**) These changes in subphenotype proportions were therefore independent of CD27 co-expression.

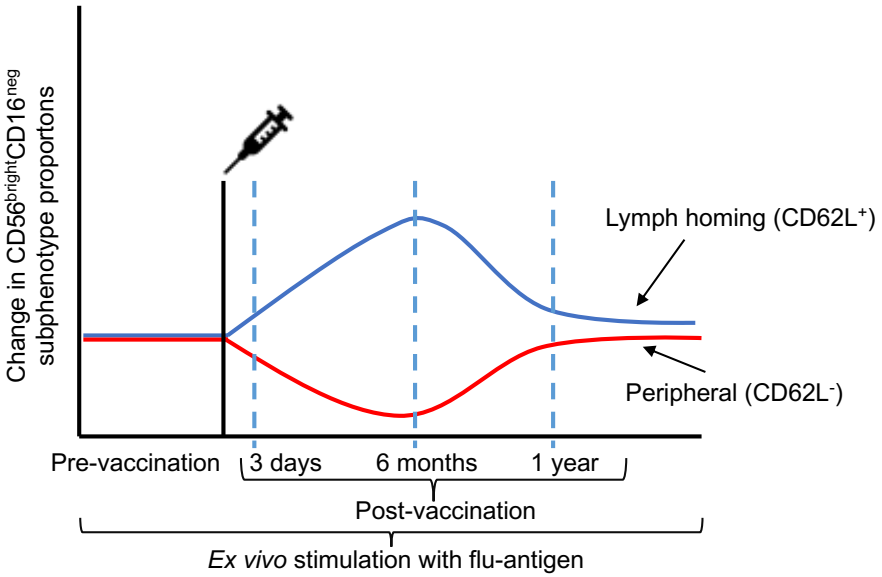


Figure 8.1: Graph depicting dynamic changes of $CD56^{bright}CD16^{neg}$ subphenotype proportions following influenza vaccination. Changes in subphenotype proportions were determined by comparing flu-stimulated pre-vaccination cells to post-vaccination cells. Proportions of lymph homing ($lhNKp46CD27^{+}$ and $lhNKp46CD27^{-}$) cells increase, whereas peripheral ($pNKp46CD27^{+}$ and $pNKp46CD27^{-}$) cells decrease significantly by 6 months with re-challenge and returning to pre-vaccination proportions by 1 year.

With vaccination and flu re-challenge, there was a remarkable fluidity in the changes of IFNγ^{+} cell frequencies. Prior to vaccination and compared to the other 3 subphenotypes, pNKp46CD27^{-} cells were the major producer of IFNγ (*P*=0.0005), but following vaccination, IFNγ cell frequencies started declining and by 6 months were significantly less than pre-vaccination levels. This coincided with a decrease in the overall proportion of pNKp46CD27^{-} cells, suggesting that the loss in frequency of IFNγ^{+} cells did not necessarily reflect an altered response to *ex vivo* flu-stimulation, but rather a loss in the proportion of IFNγ^{+} producing pNKp46CD27^{-} cells. Marquardt et al., (2017) have shown that the majority of NK cells move dynamically between the lungs and blood and it has also been reported that NK cells are rapidly recruited to the lungs from other sites following influenza infection (Wang et al., 2012). Therefore it cannot be discounted that with vaccination, certain cells of the pNKp46CD27^{-} subphenotype were "trained" and IFNγ producing cells had migrated to the lungs. However, licensed IFNγ producing NK cells have been shown to migrate to the lungs in a mouse model (Zamora et al., 2017), so this could represent the migration of cells that, with vaccination, had undergone an education process and moved from the periphery to the lungs rather than a "trained" response.

The lhNKp46CD27^{-} subphenotype represented the largest of the 8 Boolean CD56^{bright}CD16^{neg} subset populations, indicating that the predominant subphenotype has lymph node migratory potential, the site of DC/NK interactions and development of T cell memory responses. Pre-activation of NK cells by DCs is required for an efficient response against viral infections (Andrews et al., 2003; Kassim et al., 2006; Lucas et al., 2007) and the SLOs are also the site where DCs primarily interact with CD56^{bright}CD16^{neg} cells, promoting proliferation and IFNγ secretion by this NK subset (Vitale et al., 2004b). Lymph homing IFNγ and CD107a cell frequencies were less robust compared to those of peripheral cells and this could mean that they require additional or unique signals within the LN environment to reach an activation threshold, or require further signals (education) to acquire full functional maturation as unlicensed NK cells are functionally hyporesponsive (Bix et al., 1991; Brodin et al., 2009b; Joncker et al., 2009; Liao et al., 1991) and preferentially localise to the draining LNs (Zamora et al., 2017).

Given that both lymph homing subphenotypes expanded in proportions whereas their peripheral counterparts decreased, it could be postulated that with vaccination, specific cells of CD56^{bright}CD16^{neg} subphenotypes are altered and characterised by an upregulation of CD62L by NKp46 and following vaccination, a dynamic movement of cells between the periphery, lungs and lymph nodes occurs (summarised below and depicted graphically in **Figure 8.2)**.

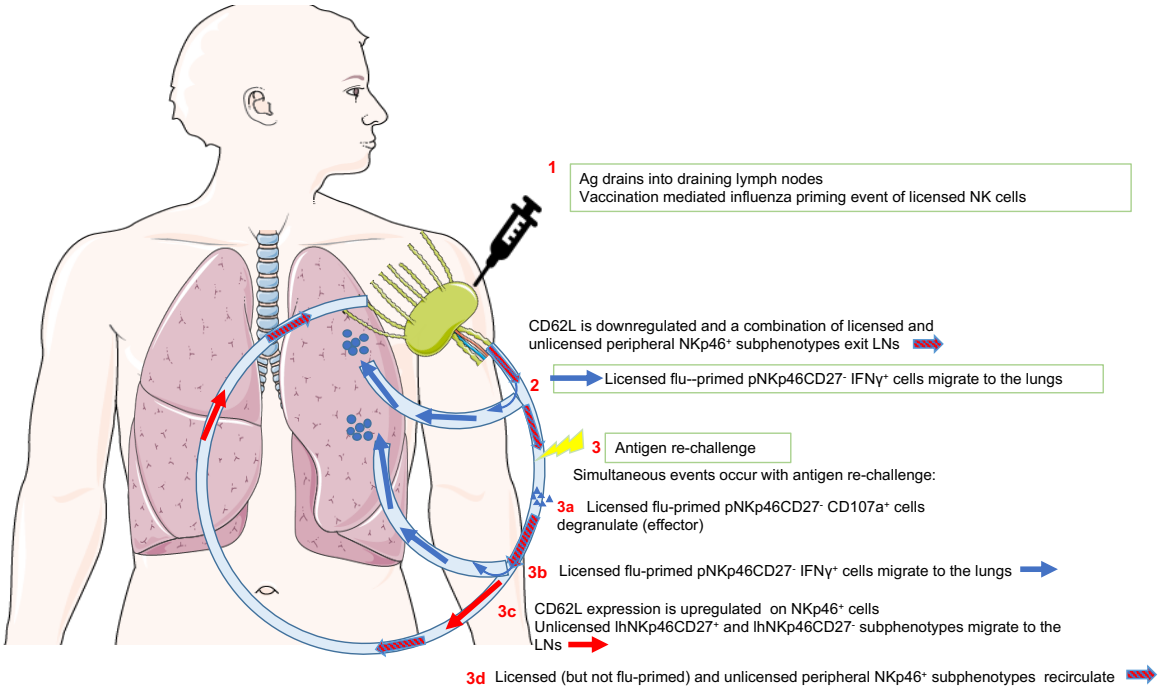


Figure 8.2: Schematic outline of proposed trafficking of CD56^{bright}CD16^{neg} lymph homing and peripheral NKp46 cells following influenza. Numbers in red depict the sequence of immune responses from time of vaccination. Coloured arrows depict trafficking of CD56^{bright}CD16^{neg} subphenotypes. Abbreviation: Ag = antigen. Some elements of the schematic are created from drawings available on Smart.servier.com Creative Commons Attribution 3.0 Unported License.

1. Following intramuscular vaccination, antigen drains into regional lymph nodes and acts as an influenza antigen priming event for CD56^{bright}CD16^{neg} cells mediated by NK/DC cell interactions.
2. Similar to T cells in the lymph nodes, CD56^{bright}CD16^{neg} NK cells lose CD62L surface expression to allow egress from the LNs. CD62L^{-} cells comprising both educated (licensed) and uneducated (unlicensed) cells exit the LNs and licensed influenza primed IFNγ producing cells (now defined as pNKp46CD27^{-}) move to reside in the lungs, whereas influenza primed CD107a producing pNKp46CD27^{+} cells recirculate (immune surveillance).
3. Upon re-stimulation signals which are mediated by NKp46 interactions with influenza antigen, simultaneous events occur:

   3a. the influenza primed pNK46CD27^{+} subset responds by degranulation (acting as licensed effector cells).

   3b. influenza primed licensed pNK46CD27^{-} IFNγ producing proportions are reduced as responding cells migrate from the periphery to the lungs.

3c. CD62L is upregulated and a subset of unlicensed lhNKp46CD27^{-} and lhNKp46CD27^{+} migrate to the lymph nodes.

3d. Licensed (but not influenza antigen primed) and unlicensed peripheral NKp46 CD62L^{-} cells continue recirculating through the lymph nodes and periphery.

Therefore, peripheral subphenotypes may represent a combination of licensed cells of which some have been flu-antigen primed and unlicensed cells awaiting further priming/education. Licensed flu-antigen primed peripheral cells degranulate and produce more IFNγ and unlicensed (or possibly licensed but not flu-antigen primed) peripheral cells upon receiving the correct signals, upregulate CD62L, and migrate to the LNs where they either receive further signals or education before returning to the periphery. Some of the cells that have migrated to the LNs remain as mature fully functional cells able to participate in immunoregulatory interactions with other cells of the immune system. The movement of CD56^{bright}CD16^{neg} subphenotypes between the peripheral circulation, lungs and LNs is likely an ongoing dynamic process, thereby providing continual immune surveillance and protection. Indeed, the data from this study has similarities to that of the influenza infection mouse study by Zamora (2017). In their study, unlicensed NK cells were functionally subdued and preferentially located to the LNs (similar to the lymph homing subphenotypes in this study) and licensed IFNγ producing cells located to the lungs (similar to the IFNγ^{+} NKp46CD27^{-} subphenotype in this study).

Although there is no evidence that CD28 is expressed on NK cells, it acts as a co-receptor for T cells and is required for T cell receptor initiated recognition of antigen during memory formation (Boomer and Green, 2010). CD49d however, is expressed on CD4 T and CD8 T cells as well as NK cells and has recently been used to define innate-like CD8 T cells (Barbarin et al., 2017). With the exception of lhNKp46CD27^{+} cells, for which proportions of co-stimulated remained unchanged, most notably, cells from the other 3 subphenotypes exhibited dynamic changes in proportion for CD28/CD49d co-stimulated proportions that mimicked the same pattern as that of flu-stimulated cells. However, both degranulation and the frequency of IFNγ producing cells for flu-stimulated cells were consistently greater, particularly for the peripheral subphenotypes, which indicated that the functional capacity of co-stimulated cells did not match that of flu-stimulated cells. Changes in co-stimulated proportions (mediated by alterations in CD62L expression), could therefore represent a heterologous immune response (Selin et al., 2006; Welsh and Selin, 2002) by cells that had been sensitised prior to vaccination, either through interactions with influenza antigens or unrelated pathogens, but also require additional antigen mediated signals to respond in a fully functional manner.

This study also highlighted a previously under-appreciated role for CD27 expression on human $CD56^{bright}CD16^{neg}$ NK cells. Although NKp46 is constitutively expressed on most NK cells (Sivori et al., 1997), it is expressed more brightly on $CD56^{bright}$ cells (Alter & Altfeld, 2009) and NKp46 deficiency prevents migration of NK cells to the LNs in MCMV infected mice (Miletic et al., 2017). The expression of CD27 (as well as CD62L) was almost exclusively confined to $NKp46^{+}$ NK cells and that NKp46 surface density is greater when co-expressed with CD27, suggesting that CD27 may act as a co-receptor or co-regulator for human NKp46 mediated function, as increased NKp46 cell surface density correlates with NK cell cytotoxicity against HLA-class I allogeneic or xenogeneic cells (Sivori et al., 1999). A study by Sugita et al., (1992) found that with IL-2 stimulation, CD27 is upregulated on NK cells and that the cytolytic activity of activated but not resting NK cells is inhibited by anti-CD27 mAb. There are only a few studies that have investigated co-expression of CD27 on human NK cells and its impact on functional responses (Fu et al., 2011; Silva et al., 2008), but they suggest that CD27 functionally delineates NK cells. This study showed that $CD27^{+}$ NK cells were more cytolytic than $CD27^{-}$ cells, whether lymph homing or peripheral, whereas $CD27^{-}$ cells produced more IFNγ. Furthermore, there was no evidence of polyfunctionality by either $CD27^{+}$ or $CD27^{-}$ cells, which may suggest that a differentiation in functional capacity of NKp46 takes place during development and that function is related to a specific subphenotype or that function is influenced by the antigenic signals that the cell receives. Similar to cNK cells, CD27 expression on $CD56^{bright}CD16^{neg}$ hepatic NK cells was almost exclusively co-expressed on $NKp46^{+}$ cells. Although functional activity of hpNK cells wasn't investigated in this study, $CD56^{bright}CD16^{neg}$ NK cells isolated from hepatic perfusate of an ALF patient revealed a severe loss of CD27 on NK cells suggesting that $NKp46^{+}$ cells (for which proportions remained unchanged) now comprised largely of $CD27^{-}$ IFNγ producing cells. Depletion of NK cells in hepatic models enhances liver fibrosis and the role of NK cells in liver homeostasis is mediated by prevention of fibrosis development through killing of activated stellate cells (Radaeva et al., 2006; Robinson et al., 2016), therefore the loss of CD27 on NKp46 cells implies a reduction in NK cells involved in cytolytic activity necessary for direct killing of cells and a critical role for expression of CD27 on $NKp46^{+}$ cells.

Whether the $CD56^{bright}CD16^{neg}$ subset represents developing NK cells or a functional subset within their own right, an understanding of the normal homeostatic mechanisms and processes are required, as aberrations or alterations in the $CD56^{bright}CD16^{neg}$ subset would lead to defective $CD56^{dim}CD16^{bright}$ cells or impairment in $CD56^{bright}CD16^{neg}$ immunoregulatory interactions with other cells of the immune system. In conclusion, this thesis has contributed and expanded our knowledge of human $CD56^{bright}CD16^{neg}$ heterogeneity and NK

subphenotypes found in the peripheral circulation. By characterising $CD56^{bright}CD16^{neg}$ cells based on lymph homing properties, this study has offered novel insights into NK subphenotypes that respond to influenza vaccination, as well as functional differences between subphenotypes which are characterised by CD27 expression.

8.2 Concluding remarks

Unfortunately, a limitation of this study was the availability of patient and participant samples. Increasing the sample numbers could help confirm the multiple responses observed in this study, particularly within the broader context of a universal vaccine which ultimately is dependent on a better understanding of the complex elements of the immune system that contribute towards heterologous immunity.

The methodology used in the current study was also not able to elucidate the dynamic changes in $CD56^{bright}CD16^{neg}$ subphenotype proportions after vaccination, necessitating that the inference be made that $NKp46^{+}$ cells that do not express CD62L respond to *ex vivo* flu-stimulation by upregulating CD62L and that the results represent a trafficking of specific cells. The use of animal models would help to track the movement of cells and identify potential sites of NK immune training.

Based on the data from this study the following warrant further investigation:

1. Further clonal tracking studies are required to understand if indeed $CD56^{dim}$ are more mature NK cells that have developed from $CD56^{bright}CD16^{neg}$, so as to provide a better understanding of NK cell development pathways. Of interest, would be the characterisation of the $CD56^{bright}CD16^{bright}$ subset (for which very little data are available), to understand if it represents an intermediate stage between $CD56^{bright}$ and $CD56^{dim}$ cells.
2. The CD4, CD8 and NK cell phenotypes of cells showing expansions and contractions of CD28/CD49d co-stimulated cells need to be ascertained to understand if these are vaccination primed cells that are more responsive to co-stimulatory signals but require specific antigen signals to become fully functional or may indeed be innate-like cells that have yet to be defined.
3. A deeper understanding of what stimuli induce $CD56^{bright}CD16^{neg}$ cells with lymph homing potential to traffic from the periphery to the lymph nodes and other solid organs.
4. Studies on heathy human liver NK cells are limited by material availability. Hepatic perfusate was found to provide an abundant source of NK cells and $CD56^{bright}CD16^{neg}$ cells in particular, but sample collection took longer than anticipated, so time constraints

did not allow for further flow cytometry panel development. Flow cytometry panels that include markers for liver resident NK phenotypes, as well as functional markers would be helpful in the further investigation differences between healthy liver resident and peripheral NK cells.

5. Similar to healthy liver NK cells, CD27 surface expression was confined to NKp46^{+} NK cells from the acute liver failure patient. Yet there was a severe loss of CD27 surface expression, so the proportion of NKp46^{+}CD27^{-} NK cells was a predominant phenotypic feature of the patient's hepatic CD56^{bright}CD16^{neg} NK cells. Further studies are required to understand if the loss of CD27 is a common feature of drug induced liver pathology and if this differs from other liver pathologies, particularly as NK cells are critical in maintaining homeostasis within the hepatic environment.

The findings from this study could be considered within the context of the global emergence of respiratory viruses that are novel to humans since the role of NK cells during viral infection of the lungs is still not well characterised. During vaccinia virus infection (VACV), NK cells provide an early source of IFNγ in the lungs contributing to both innate and adaptive VACV antiviral responses (Abboud et al., 2016). Furthermore, not only does IFNγ act as a pro-inflammatory cytokine but also is important for regulation of neutrophil expansion and helps to limit neutrophil mediated tissue injury as has been shown in tuberculous infected mice (Nandi and Behar, 2011). A dual role for NK cells has been found in murine influenza infection models and with a medium-dose influenza infection, depletion of either lung or systemic NK cells during early infection increases mortality and morbidity (Nogusa et al., 2008; Stein-Streilein and Guffee, 1986), whereas depletion of systemic NK cells in high-dose infection improves mortality as a consequence in reduction of lung pathology (Abdul-Careem et al., 2012; Zhou et al., 2013). The world is currently in the grips of a global pandemic which emerged in 2019 and is caused by the severe acute respiratory syndrome coronavirus 2 (SARS-CoV-2). Similar to influenza viruses (Weinheimer et al., 2012), coronaviruses replicate in alveolar type 2 cells of the lung (Mossel et al., 2008). During infection with SARS-CoV-2, most patients present with mild to moderate symptoms but in some patients, pulmonary infiltration of immune cells occurs following viral replication and may ultimately lead to death from acute respiratory failure (Huang et al., 2020). The cause of death is believed to be the consequence of an uncontrolled cytokine storm (Jose and Manuel, 2020; Mangalmurti and Hunter, 2020) resulting from severe inflammation which leads to multi-organ failure.

There is an early increase in cytokines in all patients with COVID-19 infection (Lucas et al., 2020) but dysregulation of the immune system occurs as clinical disease worsens in certain

patients. Patients with ongoing severe disease maintain a strong antiviral (type-1) cytokine response whereas this subsides in patients with moderate clinical disease (Lucas et al., 2020). The role of NK cells in the pathogenesis of COVID-19 is not known but using a vaccinated macaque study (Manickam et al., 2020; Yu et al., 2020) it has been shown that NK cells not only respond to COVID-19 infected cells but replication of COVID-19 in the lungs is similar to that observed in the 2009- influenza H1N1 pandemic (Hui et al., 2020). NK cells may contribute to the cytokine storm witnessed in some individuals during COVID-19 infection since cNK cells have reduced expression of various cytokines including IFNγ (Kuri-Cervantes et al., 2020) and the spike proteins of SARS-CoV-2 mediates migration of NK cells, thereby acting as a chemo-attractant as well as influencing IFNγ secretion and modifying CD107a expression when presented by lung epithelial (Bortolotti et al., 2020). Furthermore NK cell proportions are reduced in COVID-19 patients (Giamarellos-Bourboulis et al., 2020; Wan et al., 2020) including $CD56^{bright}$ NK cells (Varchetta et al., 2020) which may suggest a migration of NK cells out of the peripheral circulation occurs. Therefore a study on COVID patients, defining $CD56^{bright}CD16^{neg}$ subphenotypes based on lymph homing and CD27 properties, could be relevant to understanding if the loss of $CD56^{bright}$ NK cells witnessed in such patients represents a loss of IFNγ producing $pNKp46CD27^{-}$ cells, due to migration of these cells to the lungs where they may contribute to a cytokine storm. Within the context of the findings from the current study it can therefore be postulated that during ongoing COVID-19 infection, IFNγ producing $pNKp46CD27^{-}$ $CD56^{bright}CD16^{neg}$ cells are constantly recruited to the lungs from the periphery through signals received from other immune cells or as NK cells become exhausted (Market et al., 2020) and are retained in the lungs through NKG2A interactions with HLA-E expressed on lung epithelium (Bortolotti et al., 2020).

Most importantly, the novel findings in the current study, using a virus that infects the same cells as those of other respiratory tract viruses, could contribute to a deeper understanding of differential contributions of $CD56^{bright}CD16^{neg}$ subphenotypes to the immune dysfunction that is mediated by such viral infections. This may be of significance particularly within the context of heterologous immunity for the development not only of vaccines but also immunoregulatory therapies.

REFERENCES

Abboud, G., Tahiliani, V., Desai, P., Varkoly, K., Driver, J., Hutchinson, T.E., Salek-Ardakani, S., 2016. Natural Killer Cells and Innate Interferon Gamma Participate in the Host Defense against Respiratory Vaccinia Virus Infection. J Virol 90, 129-141.

Abdul-Careem, M.F., Mian, M.F., Yue, G., Gillgrass, A., Chenoweth, M.J., Barra, N.G., Chew, M.V., Chan, T., Al-Garawi, A.A., Jordana, M., Ashkar, A.A., 2012. Critical role of natural killer cells in lung immunopathology during influenza infection in mice. J Infect Dis 206, 167-177.

Abel, A.M., Yang, C., Thakar, M.S., Malarkannan, S., 2018. Natural Killer Cells: Development, Maturation, and Clinical Utilization. Front Immunol 9, 1869.

Abuzakouk, M., Feighery, C., O'Farrelly, C., 1996. Collagenase and Dispase enzymes disrupt lymphocyte surface molecules. J Immunol Methods 194, 211-216.

Achdout, H., Arnon, T.I., Markel, G., Gonen-Gross, T., Katz, G., Lieberman, N., Gazit, R., Joseph, A., Kedar, E., Mandelboim, O., 2003. Enhanced recognition of human NK receptors after influenza virus infection. J Immunol 171, 915-923.

Achdout, H., Meningher, T., Hirsh, S., Glasner, A., Bar-On, Y., Gur, C., Porgador, A., Mendelson, M., Mandelboim, M., Mandelboim, O., 2010. Killing of avian and Swine influenza virus by natural killer cells. J Virol 84, 3993-4001.

Ahmed, R., Oldstone, M.B., Palese, P., 2007. Protective immunity and susceptibility to infectious diseases: lessons from the 1918 influenza pandemic. Nat Immunol 8, 1188-1193.

Akbar, A.N., Terry, L., Timms, A., Beverley, P.C., Janossy, G., 1988. Loss of CD45R and gain of UCHL1 reactivity is a feature of primed T cells. J Immunol 140, 2171-2178.

Allen, E.K., Thomas, P.G., 2015. Immunity to influenza. Preventing infection and regulating disease. Am J Respir Crit Care Med 191, 248-251.

Almeida-Oliveira, A., Smith-Carvalho, M., Porto, L.C., Cardoso-Oliveira, J., Ribeiro Ados, S., Falcao, R.R., Abdelhay, E., Bouzas, L.F., Thuler, L.C., Ornellas, M.H., Diamond, H.R., 2011. Age-related changes in natural killer cell receptors from childhood through old age. Hum Immunol 72, 319-329.

Almeida, J.R., Price, D.A., Papagno, L., Arkoub, Z.A., Sauce, D., Bornstein, E., Asher, T.E., Samri, A., Schnuriger, A., Theodorou, I., Costagliola, D., Rouzioux, C., Agut, H., Marcelin, A.G., Douek, D., Autran, B., Appay, V., 2007. Superior control of HIV-1 replication by CD8+ T cells is reflected by their avidity, polyfunctionality, and clonal turnover. J Exp Med 204, 2473-2485.

Alter, G., Altfeld, M., 2009. NK cells in HIV-1 infection: evidence for their role in the control of HIV-1 infection. J Intern Med 265, 29-42.

Alter, G., Jost, S., Rihn, S., Reyor, L.L., Nolan, B.E., Ghebremichael, M., Bosch, R., Altfeld, M., Lauer, G.M., 2011. Reduced frequencies of NKp30+NKp46+, CD161+, and NKG2D+ NK cells in acute HCV infection may predict viral clearance. J Hepatol 55, 278-288.

Alter, G., Malenfant, J.M., Delabre, R.M., Burgett, N.C., Yu, X.G., Lichterfeld, M., Zaunders, J., Altfeld, M., 2004. Increased natural killer cell activity in viremic HIV-1 infection. J Immunol 173, 5305-5311.

Ambrose, C.S., Levin, M.J., Belshe, R.B., 2011. The relative efficacy of trivalent live attenuated and inactivated influenza vaccines in children and adults. Influenza Other Respir Viruses 5, 67-75.

Andrews, D.M., Scalzo, A.A., Yokoyama, W.M., Smyth, M.J., Degli-Esposti, M.A., 2003. Functional interactions between dendritic cells and NK cells during viral infection. Nat Immunol 4, 175-181.

Anfossi, N., Andre, P., Guia, S., Falk, C.S., Roetynck, S., Stewart, C.A., Breso, V., Frassati, C., Reviron, D., Middleton, D., Romagne, F., Ugolini, S., Vivier, E., 2006. Human NK cell education by inhibitory receptors for MHC class I. Immunity 25, 331-342.

Angelo, L.S., Banerjee, P.P., Monaco-Shawver, L., Rosen, J.B., Makedonas, G., Forbes, L.R., Mace, E.M., Orange, J.S., 2015. Practical NK cell phenotyping and variability in healthy adults. Immunol Res 62, 341-356.

REFERENCES

Arad, U., Tzadok, S., Amir, S., Mandelboim, M., Mendelson, E., Wigler, I., Sarbagil-Maman, H., Paran, D., Caspi, D., Elkayam, O., 2011. The cellular immune response to influenza vaccination is preserved in rheumatoid arthritis patients treated with rituximab. Vaccine 29, 1643-1648.

Arlettaz, L., Degermann, S., De Rham, C., Roosnek, E., Huard, B., 2004a. Expression of inhibitory KIR is confined to CD8+ effector T cells and limits their proliferative capacity. Eur J Immunol 34, 3413-3422.

Arlettaz, L., Villard, J., de Rham, C., Degermann, S., Chapuis, B., Huard, B., Roosnek, E., 2004b. Activating CD94:NKG2C and inhibitory CD94:NKG2A receptors are expressed by distinct subsets of committed CD8+ TCR alphabeta lymphocytes. Eur J Immunol 34, 3456-3464.

Arnon, T.I., Achdout, H., Levi, O., Markel, G., Saleh, N., Katz, G., Gazit, R., Gonen-Gross, T., Hanna, J., Nahari, E., Porgador, A., Honigman, A., Plachter, B., Mevorach, D., Wolf, D.G., Mandelboim, O., 2005. Inhibition of the NKp30 activating receptor by pp65 of human cytomegalovirus. Nat Immunol 6, 515-523.

Arnon, T.I., Achdout, H., Lieberman, N., Gazit, R., Gonen-Gross, T., Katz, G., Bar-Ilan, A., Bloushtain, N., Lev, M., Joseph, A., Kedar, E., Porgador, A., Mandelboim, O., 2004. The mechanisms controlling the recognition of tumor- and virus-infected cells by NKp46. Blood 103, 664-672.

Arnon, T.I., Lev, M., Katz, G., Chernobrov, Y., Porgador, A., Mandelboim, O., 2001. Recognition of viral hemagglutinins by NKp44 but not by NKp30. Eur J Immunol 31, 2680-2689.

Ashkar, A.A., Black, G.P., Wei, Q., He, H., Liang, L., Head, J.R., Croy, B.A., 2003. Assessment of requirements for IL-15 and IFN regulatory factors in uterine NK cell differentiation and function during pregnancy. J Immunol 171, 2937-2944.

Ashkar, A.A., Di Santo, J.P., Croy, B.A., 2000. Interferon gamma contributes to initiation of uterine vascular modification, decidual integrity, and uterine natural killer cell maturation during normal murine pregnancy. J Exp Med 192, 259-270.

Aslan, N., Watkin, L.B., Gil, A., Mishra, R., Clark, F.G., Welsh, R.M., Ghersi, D., Luzuriaga, K., Selin, L.K., 2017. Severity of Acute Infectious Mononucleosis Correlates with Cross-Reactive Influenza CD8 T-Cell Receptor Repertoires. mBio 8.

Assarsson, E., Kambayashi, T., Persson, C.M., Chambers, B.J., Ljunggren, H.G., 2005. 2B4/CD48-mediated regulation of lymphocyte activation and function. J Immunol 175, 2045-2049.

Aw Yeang, H.X., Piersma, S.J., Lin, Y., Yang, L., Malkova, O.N., Miner, C., Krupnick, A.S., Chapman, W.C., Yokoyama, W.M., 2017. Cutting Edge: Human CD49e- NK Cells Are Tissue Resident in the Liver. J Immunol 198, 1417-1422.

Bajenoff, M., Breart, B., Huang, A.Y., Qi, H., Cazareth, J., Braud, V.M., Germain, R.N., Glaichenhaus, N., 2006. Natural killer cell behavior in lymph nodes revealed by static and real-time imaging. J Exp Med 203, 619-631.

Ballas, Z.K., Buchta, C.M., Rosean, T.R., Heusel, J.W., Shey, M.R., 2013. Role of NK cell subsets in organ-specific murine melanoma metastasis. PLoS One 8, e65599.

Bar-Ephraim, Y.E., Koning, J.J., Burniol Ruiz, E., Konijn, T., Mourits, V.P., Lakeman, K.A., Boon, L., Bogels, M., van Maanen, J.P., Den Haan, J.M.M., van Egmond, M., Bouma, G., Reijmers, R.M., Mebius, R.E., 2019. CD62L Is a Functional and Phenotypic Marker for Circulating Innate Lymphoid Cell Precursors. J Immunol 202, 171-182.

Bar-On, Y., Glasner, A., Meningher, T., Achdout, H., Gur, C., Lankry, D., Vitenshtein, A., Meyers, A.F.A., Mandelboim, M., Mandelboim, O., 2013. Neuraminidase-mediated, NKp46-dependent immune-evasion mechanism of influenza viruses. Cell Rep 3, 1044-1050.

Barbarin, A., Cayssials, E., Jacomet, F., Nunez, N.G., Basbous, S., Lefevre, L., Abdallah, M., Piccirilli, N., Morin, B., Lavoue, V., Catros, V., Piaggio, E., Herbelin, A., Gombert, J.M., 2017. Phenotype of NK-Like CD8(+) T Cells with Innate Features in Humans and Their Relevance in Cancer Diseases. Front Immunol 8, 316.

REFERENCES

Barnaba, V., Franco, A., Alberti, A., Benvenuto, R., Balsano, F., 1990. Selective killing of hepatitis B envelope antigen-specific B cells by class I-restricted, exogenous antigen-specific T lymphocytes. Nature 345, 258-260.

Baumgarth, N., Herman, O.C., Jager, G.C., Brown, L., Herzenberg, L.A., Herzenberg, L.A., 1999. Innate and acquired humoral immunities to influenza virus are mediated by distinct arms of the immune system. Proc Natl Acad Sci U S A 96, 2250-2255.

Baumgarth, N., Herman, O.C., Jager, G.C., Brown, L.E., Herzenberg, L.A., Chen, J., 2000. B-1 and B-2 cell-derived immunoglobulin M antibodies are nonredundant components of the protective response to influenza virus infection. J Exp Med 192, 271-280.

Beck, S., Barrell, B.G., 1988. Human cytomegalovirus encodes a glycoprotein homologous to MHC class-I antigens. Nature 331, 269-272.

Bedford, T., Suchard, M.A., Lemey, P., Dudas, G., Gregory, V., Hay, A.J., McCauley, J.W., Russell, C.A., Smith, D.J., Rambaut, A., 2014. Integrating influenza antigenic dynamics with molecular evolution. Elife 3, e01914.

Ben-Moshe, S., Itzkovitz, S., 2019. Spatial heterogeneity in the mammalian liver. Nat Rev Gastroenterol Hepatol 16, 395-410.

Bender, J.R., Pardi, R., Karasek, M.A., Engleman, E.G., 1987. Phenotypic and functional characterization of lymphocytes that bind human microvascular endothelial cells in vitro. Evidence for preferential binding of natural killer cells. J Clin Invest 79, 1679-1688.

Bennett, I.M., Zatsepina, O., Zamai, L., Azzoni, L., Mikheeva, T., Perussia, B., 1996. Definition of a natural killer NKR-P1A+/CD56-/CD16- functionally immature human NK cell subset that differentiates in vitro in the presence of interleukin 12. J Exp Med 184, 1845-1856.

Benton, K.A., Misplon, J.A., Lo, C.Y., Brutkiewicz, R.R., Prasad, S.A., Epstein, S.L., 2001. Heterosubtypic immunity to influenza A virus in mice lacking IgA, all Ig, NKT cells, or gamma delta T cells. J Immunol 166, 7437-7445.

Bernstein, E., Kaye, D., Abrutyn, E., Gross, P., Dorfman, M., Murasko, D.M., 1999. Immune response to influenza vaccination in a large healthy elderly population. Vaccine 17, 82-94.

Berrien-Elliott, M.M., Wagner, J.A., Fehniger, T.A., 2015. Human Cytokine-Induced Memory-Like Natural Killer Cells. J Innate Immun 7, 563-571.

Betts, M.R., Brenchley, J.M., Price, D.A., De Rosa, S.C., Douek, D.C., Roederer, M., Koup, R.A., 2003. Sensitive and viable identification of antigen-specific CD8+ T cells by a flow cytometric assay for degranulation. J Immunol Methods 281, 65-78.

Betts, M.R., Exley, B., Price, D.A., Bansal, A., Camacho, Z.T., Teaberry, V., West, S.M., Ambrozak, D.R., Tomaras, G., Roederer, M., Kilby, J.M., Tartaglia, J., Belshe, R., Gao, F., Douek, D.C., Weinhold, K.J., Koup, R.A., Goepfert, P., Ferrari, G., 2005. Characterization of functional and phenotypic changes in anti-Gag vaccine-induced T cell responses and their role in protection after HIV-1 infection. Proc Natl Acad Sci U S A 102, 4512-4517.

Beutler, B., 2004. Innate immunity: an overview. Mol Immunol 40, 845-859.

Beziat, V., Dalgard, O., Asselah, T., Halfon, P., Bedossa, P., Boudifa, A., Hervier, B., Theodorou, I., Martinot, M., Debre, P., Bjorkstrom, N.K., Malmberg, K.J., Marcellin, P., Vieillard, V., 2012. CMV drives clonal expansion of NKG2C+ NK cells expressing self-specific KIRs in chronic hepatitis patients. Eur J Immunol 42, 447-457.

Bhargava, P., Calabresi, P.A., 2015. Novel therapies for memory cells in autoimmune diseases. Clin Exp Immunol 180, 353-360.

Bianchi, G., Sironi, M., Ghibaudi, E., Selvaggini, C., Elices, M., Allavena, P., Mantovani, A., 1993. Migration of natural killer cells across endothelial cell monolayers. J Immunol 151, 5135-5144.

Bigos, M., Baumgarth, N., Jager, G.C., Herman, O.C., Nozaki, T., Stovel, R.T., Parks, D.R., Herzenberg, L.A., 1999. Nine color eleven parameter immunophenotyping using three laser flow cytometry. Cytometry 36, 36-45.

Bihl, F., Berger, C., Chisholm, J.V., 3rd, Henry, L.M., Bertisch, B., Trojan, A., Nadal, D., Speck, R.F., Flepp, M., Brander, C., Mueller, N.J., Swiss, H.I.V.C.S., 2009. Cellular immune responses and disease control in acute AIDS-associated Kaposi's sarcoma. AIDS 23, 1918-1922.

REFERENCES

Bird, L., 2017. Immune regulation: Immune cell social networks. Nat Rev Immunol 17, 216.

Biron, C.A., 1997. Activation and function of natural killer cell responses during viral infections. Curr Opin Immunol 9, 24-34.

Biron, C.A., Byron, K.S., Sullivan, J.L., 1989. Severe herpesvirus infections in an adolescent without natural killer cells. N Engl J Med 320, 1731-1735.

Biron, C.A., Nguyen, K.B., Pien, G.C., Cousens, L.P., Salazar-Mather, T.P., 1999. Natural killer cells in antiviral defense: function and regulation by innate cytokines. Annu Rev Immunol 17, 189-220.

Bix, M., Liao, N.S., Zijlstra, M., Loring, J., Jaenisch, R., Raulet, D., 1991. Rejection of class I MHC-deficient haemopoietic cells by irradiated MHC-matched mice. Nature 349, 329-331.

Bjorkstrom, N.K., Beziat, V., Cichocki, F., Liu, L.L., Levine, J., Larsson, S., Koup, R.A., Anderson, S.K., Ljunggren, H.G., Malmberg, K.J., 2012. CD8 T cells express randomly selected KIRs with distinct specificities compared with NK cells. Blood 120, 3455-3465.

Bjorkstrom, N.K., Lindgren, T., Stoltz, M., Fauriat, C., Braun, M., Evander, M., Michaelsson, J., Malmberg, K.J., Klingstrom, J., Ahlm, C., Ljunggren, H.G., 2011. Rapid expansion and long-term persistence of elevated NK cell numbers in humans infected with hantavirus. J Exp Med 208, 13-21.

Bjorkstrom, N.K., Riese, P., Heuts, F., Andersson, S., Fauriat, C., Ivarsson, M.A., Bjorklund, A.T., Flodstrom-Tullberg, M., Michaelsson, J., Rottenberg, M.E., Guzman, C.A., Ljunggren, H.G., Malmberg, K.J., 2010. Expression patterns of NKG2A, KIR, and CD57 define a process of CD56dim NK-cell differentiation uncoupled from NK-cell education. Blood 116, 3853-3864.

Blum, K.S., Pabst, R., 2007. Lymphocyte numbers and subsets in the human blood. Do they mirror the situation in all organs? Immunol Lett 108, 45-51.

Boomer, J.S., Green, J.M., 2010. An enigmatic tail of CD28 signaling. Cold Spring Harb Perspect Biol 2, a002436.

Borges, L., Hsu, M.L., Fanger, N., Kubin, M., Cosman, D., 1997. A family of human lymphoid and myeloid Ig-like receptors, some of which bind to MHC class I molecules. J Immunol 159, 5192-5196.

Borghesi, L., Hsu, L.Y., Miller, J.P., Anderson, M., Herzenberg, L., Herzenberg, L., Schlissel, M.S., Allman, D., Gerstein, R.M., 2004. B lineage-specific regulation of V(D)J recombinase activity is established in common lymphoid progenitors. J Exp Med 199, 491-502.

Bortolotti, D., Gentili, V., Rizzo, S., Rotola, A., Rizzo, R., 2020. SARS-CoV-2 Spike 1 Protein Controls Natural Killer Cell Activation via the HLA-E/NKG2A Pathway. Cells 9.

Bottino, C., Biassoni, R., Millo, R., Moretta, L., Moretta, A., 2000. The human natural cytotoxicity receptors (NCR) that induce HLA class I-independent NK cell triggering. Hum Immunol 61, 1-6.

Braciale, T.J., 1977a. Immunologic recognition of influenza virus-infected cells. I. Generation of a virus-strain specific and a cross-reactive subpopulation of cytotoxic T cells in the response to type A influenza viruses of different subtypes. Cell Immunol 33, 423-436.

Braciale, T.J., 1977b. Immunologic recognition of influenza virus-infected cells. II. Expression of influenza A matrix protein on the infected cell surface and its role in recognition by cross-reactive cytotoxic T cells. J Exp Med 146, 673-689.

Brandstadter, J.D., Yang, Y., 2011. Natural killer cell responses to viral infection. J Innate Immun 3, 274-279.

Brandt, C.S., Baratin, M., Yi, E.C., Kennedy, J., Gao, Z., Fox, B., Haldeman, B., Ostrander, C.D., Kaifu, T., Chabannon, C., Moretta, A., West, R., Xu, W., Vivier, E., Levin, S.D., 2009. The B7 family member B7-H6 is a tumor cell ligand for the activating natural killer cell receptor NKp30 in humans. J Exp Med 206, 1495-1503.

Brodin, P., Hoglund, P., 2008. Beyond licensing and disarming: a quantitative view on NK-cell education. Eur J Immunol 38, 2934-2937.

Brodin, P., Karre, K., Hoglund, P., 2009a. NK cell education: not an on-off switch but a tunable rheostat. Trends Immunol 30, 143-149.

REFERENCES

Brodin, P., Lakshmikanth, T., Johansson, S., Karre, K., Hoglund, P., 2009b. The strength of inhibitory input during education quantitatively tunes the functional responsiveness of individual natural killer cells. Blood 113, 2434-2441.

Bruno, A., Focaccetti, C., Pagani, A., Imperatori, A.S., Spagnoletti, M., Rotolo, N., Cantelmo, A.R., Franzi, F., Capella, C., Ferlazzo, G., Mortara, L., Albini, A., Noonan, D.M., 2013. The proangiogenic phenotype of natural killer cells in patients with non-small cell lung cancer. Neoplasia 15, 133-142.

Bryceson, Y.T., Ljunggren, H.G., Long, E.O., 2009. Minimal requirement for induction of natural cytotoxicity and intersection of activation signals by inhibitory receptors. Blood 114, 2657-2666.

Bryceson, Y.T., March, M.E., Ljunggren, H.G., Long, E.O., 2006a. Activation, coactivation, and costimulation of resting human natural killer cells. Immunol Rev 214, 73-91.

Bryceson, Y.T., March, M.E., Ljunggren, H.G., Long, E.O., 2006b. Synergy among receptors on resting NK cells for the activation of natural cytotoxicity and cytokine secretion. Blood 107, 159-166.

Bubenik, J., 2003. Tumour MHC class I downregulation and immunotherapy (Review). Oncol Rep 10, 2005-2008.

Butcher, E.C., Picker, L.J., 1996. Lymphocyte homing and homeostasis. Science 272, 60-66.

Caligiuri, M.A., 2008. Human natural killer cells. Blood 112, 461-469.

Caligiuri, M.A., Murray, C., Robertson, M.J., Wang, E., Cochran, K., Cameron, C., Schow, P., Ross, M.E., Klumpp, T.R., Soiffer, R.J., et al., 1993. Selective modulation of human natural killer cells in vivo after prolonged infusion of low dose recombinant interleukin 2. J Clin Invest 91, 123-132.

Caligiuri, M.A., Zmuidzinas, A., Manley, T.J., Levine, H., Smith, K.A., Ritz, J., 1990. Functional consequences of interleukin 2 receptor expression on resting human lymphocytes. Identification of a novel natural killer cell subset with high affinity receptors. J Exp Med 171, 1509-1526.

Camerini, D., Walz, G., Loenen, W.A., Borst, J., Seed, B., 1991. The T cell activation antigen CD27 is a member of the nerve growth factor/tumor necrosis factor receptor gene family. J Immunol 147, 3165-3169.

Camous, X., Pera, A., Solana, R., Larbi, A., 2012. NK cells in healthy aging and age-associated diseases. J Biomed Biotechnol 2012, 195956.

Campbell, J.J., Qin, S., Unutmaz, D., Soler, D., Murphy, K.E., Hodge, M.R., Wu, L., Butcher, E.C., 2001. Unique subpopulations of CD56+ NK and NK-T peripheral blood lymphocytes identified by chemokine receptor expression repertoire. J Immunol 166, 6477-6482.

Cantoni, C., Verdiani, S., Falco, M., Pessino, A., Cilli, M., Conte, R., Pende, D., Ponte, M., Mikaelsson, M.S., Moretta, L., Biassoni, R., 1998. p49, a putative HLA class I-specific inhibitory NK receptor belonging to the immunoglobulin superfamily. Eur J Immunol 28, 1980-1990.

Cantor, H., Simpson, E., Sato, V.L., Fathman, C.G., Herzenberg, L.A., 1975. Characterization of subpopulations of T lymphocytes. I. Separation and functional studies of peripheral T-cells binding different amounts of fluorescent anti-Thy 1.2 (theta) antibody using a fluorescence-activated cell sorter (FACS). Cell Immunol 15, 180-196.

Carrega, P., Bonaccorsi, I., Di Carlo, E., Morandi, B., Paul, P., Rizzello, V., Cipollone, G., Navarra, G., Mingari, M.C., Moretta, L., Ferlazzo, G., 2014. CD56(bright)perforin(low) noncytotoxic human NK cells are abundant in both healthy and neoplastic solid tissues and recirculate to secondary lymphoid organs via afferent lymph. J Immunol 192, 3805-3815.

Carrega, P., Morandi, B., Costa, R., Frumento, G., Forte, G., Altavilla, G., Ratto, G.B., Mingari, M.C., Moretta, L., Ferlazzo, G., 2008. Natural killer cells infiltrating human nonsmall-cell lung cancer are enriched in CD56 bright CD16(-) cells and display an impaired capability to kill tumor cells. Cancer 112, 863-875.

Casali, P., Schettino, E.W., 1996. Structure and function of natural antibodies. Curr Top Microbiol Immunol 210, 167-179.

REFERENCES

Castigli, E., Wilson, S.A., Scott, S., Dedeoglu, F., Xu, S., Lam, K.P., Bram, R.J., Jabara, H., Geha, R.S., 2005. TACI and BAFF-R mediate isotype switching in B cells. J Exp Med 201, 35-39.

Catalina, M.D., Carroll, M.C., Arizpe, H., Takashima, A., Estess, P., Siegelman, M.H., 1996. The route of antigen entry determines the requirement for L-selectin during immune responses. J Exp Med 184, 2341-2351.

Catalina, M.D., Estess, P., Siegelman, M.H., 1999. Selective requirements for leukocyte adhesion molecules in models of acute and chronic cutaneous inflammation: participation of E- and P- but not L-selectin. Blood 93, 580-589.

Cella, M., Fuchs, A., Vermi, W., Facchetti, F., Otero, K., Lennerz, J.K., Doherty, J.M., Mills, J.C., Colonna, M., 2009. A human natural killer cell subset provides an innate source of IL-22 for mucosal immunity. Nature 457, 722-725.

Cerwenka, A., Lanier, L.L., 2001. Natural killer cells, viruses and cancer. Nat Rev Immunol 1, 41-49.

Chattopadhyay, P.K., Betts, M.R., Price, D.A., Gostick, E., Horton, H., Roederer, M., De Rosa, S.C., 2009. The cytolytic enzymes granyzme A, granzyme B, and perforin: expression patterns, cell distribution, and their relationship to cell maturity and bright CD57 expression. J Leukoc Biol 85, 88-97.

Chen, H., Chen, Y., Deng, M., John, S., Gui, X., Kansagra, A., Chen, W., Kim, J., Lewis, C., Wu, G., Xie, J., Zhang, L., Huang, R., Liu, X., Arase, H., Huang, Y., Yu, H., Luo, W., Xia, N., Zhang, N., An, Z., Zhang, C.C., 2020. Antagonistic anti-LILRB1 monoclonal antibody regulates antitumor functions of natural killer cells. J Immunother Cancer 8.

Chen, K.C., Stanton, R.J., Banat, J.J., Wills, M.R., 2016. Leukocyte Immunoglobulin-Like Receptor 1-Expressing Human Natural Killer Cell Subsets Differentially Recognize Isolates of Human Cytomegalovirus through the Viral Major Histocompatibility Complex Class I Homolog UL18. J Virol 90, 3123-3137.

Chen, S., Kawashima, H., Lowe, J.B., Lanier, L.L., Fukuda, M., 2005. Suppression of tumor formation in lymph nodes by L-selectin-mediated natural killer cell recruitment. J Exp Med 202, 1679-1689.

Ching, C., Lopez, C., 1979. Natural killing of herpes simplex virus type 1-infected target cells: normal human responses and influence of antiviral antibody. Infect Immun 26, 49-56.

Christiaansen, A.F., Dixit, U.G., Coler, R.N., Marie Beckmann, A., Reed, S.G., Winokur, P.L., Zimmerman, M.B., Varga, S.M., Wilson, M.E., 2017. CD11a and CD49d enhance the detection of antigen-specific T cells following human vaccination. Vaccine 35, 4255-4261.

Chuang, S.S., Kim, M.H., Johnson, L.A., Albertsson, P., Kitson, R.P., Nannmark, U., Goldfarb, R.H., Mathew, P.A., 2000. 2B4 stimulation of YT cells induces natural killer cell cytolytic function and invasiveness. Immunology 100, 378-383.

Cichocki, F., Cooley, S., Davis, Z., DeFor, T.E., Schlums, H., Zhang, B., Brunstein, C.G., Blazar, B.R., Wagner, J., Diamond, D.J., Verneris, M.R., Bryceson, Y.T., Weisdorf, D.J., Miller, J.S., 2016. CD56dimCD57+NKG2C+ NK cell expansion is associated with reduced leukemia relapse after reduced intensity HCT. Leukemia 30, 456-463.

Cichocki, F., Miller, J.S., Anderson, S.K., Bryceson, Y.T., 2013. Epigenetic regulation of NK cell differentiation and effector functions. Front Immunol 4, 55.

Ciuffreda, D., Comte, D., Cavassini, M., Giostra, E., Buhler, L., Perruchoud, M., Heim, M.H., Battegay, M., Genne, D., Mulhaupt, B., Malinverni, R., Oneta, C., Bernasconi, E., Monnat, M., Cerny, A., Chuard, C., Borovicka, J., Mentha, G., Pascual, M., Gonvers, J.J., Pantaleo, G., Dutoit, V., 2008. Polyfunctional HCV-specific T-cell responses are associated with effective control of HCV replication. Eur J Immunol 38, 2665-2677.

Clark, I.A., 2001. Heterologous immunity revisited. Parasitology 122 Suppl, S51-59.

Cohen, M., Zhang, X.Q., Senaati, H.P., Chen, H.W., Varki, N.M., Schooley, R.T., Gagneux, P., 2013. Influenza A penetrates host mucus by cleaving sialic acids with neuraminidase. Virol J 10, 321.

Colonna, M., Navarro, F., Bellon, T., Llano, M., Garcia, P., Samaridis, J., Angman, L., Cella, M., Lopez-Botet, M., 1997. A common inhibitory receptor for major histocompatibility

complex class I molecules on human lymphoid and myelomonocytic cells. J Exp Med 186, 1809-1818.
Colonna, M., Samaridis, J., 1995. Cloning of immunoglobulin-superfamily members associated with HLA-C and HLA-B recognition by human natural killer cells. Science 268, 405-408.
Colucci, F., Caligiuri, M.A., Di Santo, J.P., 2003. What does it take to make a natural killer? Nat Rev Immunol 3, 413-425.
Conrath, U., Beckers, G.J., Langenbach, C.J., Jaskiewicz, M.R., 2015. Priming for enhanced defense. Annu Rev Phytopathol 53, 97-119.
Cooper, G.E., Ostridge, K., Khakoo, S.I., Wilkinson, T.M.A., Staples, K.J., 2018. Human CD49a(+) Lung Natural Killer Cell Cytotoxicity in Response to Influenza A Virus. Front Immunol 9, 1671.
Cooper, M.A., Bush, J.E., Fehniger, T.A., VanDeusen, J.B., Waite, R.E., Liu, Y., Aguila, H.L., Caligiuri, M.A., 2002. In vivo evidence for a dependence on interleukin 15 for survival of natural killer cells. Blood 100, 3633-3638.
Cooper, M.A., Elliott, J.M., Keyel, P.A., Yang, L., Carrero, J.A., Yokoyama, W.M., 2009. Cytokine-induced memory-like natural killer cells. Proc Natl Acad Sci U S A 106, 1915-1919.
Cooper, M.A., Fehniger, T.A., Caligiuri, M.A., 2001a. The biology of human natural killer-cell subsets. Trends Immunol 22, 633-640.
Cooper, M.A., Fehniger, T.A., Fuchs, A., Colonna, M., Caligiuri, M.A., 2004. NK cell and DC interactions. Trends Immunol 25, 47-52.
Cooper, M.A., Fehniger, T.A., Turner, S.C., Chen, K.S., Ghaheri, B.A., Ghayur, T., Carson, W.E., Caligiuri, M.A., 2001b. Human natural killer cells: a unique innate immunoregulatory role for the CD56(bright) subset. Blood 97, 3146-3151.
Cooper, M.D., Alder, M.N., 2006. The evolution of adaptive immune systems. Cell 124, 815-822.
Cosgrove, C., Berger, C.T., Kroy, D.C., Cheney, P.C., Ghebremichael, M., Aneja, J., Tomlinson, M., Kim, A.Y., Lauer, G.M., Alter, G., 2014. Chronic HCV infection affects the NK cell phenotype in the blood more than in the liver. PLoS One 9, e105950.
Cosman, D., Fanger, N., Borges, L., Kubin, M., Chin, W., Peterson, L., Hsu, M.L., 1997. A novel immunoglobulin superfamily receptor for cellular and viral MHC class I molecules. Immunity 7, 273-282.
Costanzo, M.C., Kim, D., Creegan, M., Lal, K.G., Ake, J.A., Currier, J.R., Streeck, H., Robb, M.L., Michael, N.L., Bolton, D.L., Steers, N.J., Eller, M.A., 2018. Transcriptomic signatures of NK cells suggest impaired responsiveness in HIV-1 infection and increased activity post-vaccination. Nat Commun 9, 1212.
Costello, R.T., Sivori, S., Marcenaro, E., Lafage-Pochitaloff, M., Mozziconacci, M.J., Reviron, D., Gastaut, J.A., Pende, D., Olive, D., Moretta, A., 2002. Defective expression and function of natural killer cell-triggering receptors in patients with acute myeloid leukemia. Blood 99, 3661-3667.
Couper, K.N., Blount, D.G., Riley, E.M., 2008. IL-10: the master regulator of immunity to infection. J Immunol 180, 5771-5777.
Coutinho, A., Kazatchkine, M.D., Avrameas, S., 1995. Natural autoantibodies. Curr Opin Immunol 7, 812-818.
Cox, R.J., Brokstad, K.A., Zuckerman, M.A., Wood, J.M., Haaheim, L.R., Oxford, J.S., 1994. An early humoral immune response in peripheral blood following parenteral inactivated influenza vaccination. Vaccine 12, 993-999.
Crinier, A., Milpied, P., Escaliere, B., Piperoglou, C., Galluso, J., Balsamo, A., Spinelli, L., Cervera-Marzal, I., Ebbo, M., Girard-Madoux, M., Jaeger, S., Bollon, E., Hamed, S., Hardwigsen, J., Ugolini, S., Vely, F., Narni-Mancinelli, E., Vivier, E., 2018. High-Dimensional Single-Cell Analysis Identifies Organ-Specific Signatures and Conserved NK Cell Subsets in Humans and Mice. Immunity 49, 971-986 e975.
Crispe, I.N., 2009. The liver as a lymphoid organ. Annu Rev Immunol 27, 147-163.

REFERENCES

Crotty, S., 2015. A brief history of T cell help to B cells. Nat Rev Immunol 15, 185-189.

Cuff, A.O., Robertson, F.P., Stegmann, K.A., Pallett, L.J., Maini, M.K., Davidson, B.R., Male, V., 2016. Eomeshi NK Cells in Human Liver Are Long-Lived and Do Not Recirculate but Can Be Replenished from the Circulation. J Immunol 197, 4283-4291.

Culley, F.J., Johnson, M., Evans, J.H., Kumar, S., Crilly, R., Casasbuenas, J., Schnyder, T., Mehrabi, M., Deonarain, M.P., Ushakov, D.S., Braud, V., Roth, G., Brock, R., Kohler, K., Davis, D.M., 2009. Natural killer cell signal integration balances synapse symmetry and migration. PLoS Biol 7, e1000159.

De Colvenaer, V., Taveirne, S., Hamann, J., de Bruin, A.M., De Smedt, M., Taghon, T., Vandekerckhove, B., Plum, J., van Lier, R., Leclercq, G., 2010. Continuous CD27 triggering in vivo strongly reduces NK cell numbers. Eur J Immunol 40, 1107-1117.

De Jong, R., Brouwer, M., Hooibrink, B., Van der Pouw-Kraan, T., Miedema, F., Van Lier, R.A., 1992. The CD27- subset of peripheral blood memory CD4+ lymphocytes contains functionally differentiated T lymphocytes that develop by persistent antigenic stimulation in vivo. Eur J Immunol 22, 993-999.

De Maria, A., Fogli, M., Costa, P., Murdaca, G., Puppo, F., Mavilio, D., Moretta, A., Moretta, L., 2003. The impaired NK cell cytolytic function in viremic HIV-1 infection is associated with a reduced surface expression of natural cytotoxicity receptors (NKp46, NKp30 and NKp44). Eur J Immunol 33, 2410-2418.

De Maria, A., Moretta, L., 2011. Revisited function of human NK cell subsets. Cell Cycle 10, 1178-1179.

De Rosa, S.C., Roederer, M., 2001. Eleven-color flow cytometry. A powerful tool for elucidation of the complex immune system. Clin Lab Med 21, 697-712, vii.

Della Chiesa, M., Falco, M., Podesta, M., Locatelli, F., Moretta, L., Frassoni, F., Moretta, A., 2012. Phenotypic and functional heterogeneity of human NK cells developing after umbilical cord blood transplantation: a role for human cytomegalovirus? Blood 119, 399-410.

Delobel, P., Sandres-Saune, K., Cazabat, M., L'Faqihi, F.E., Aquilina, C., Obadia, M., Pasquier, C., Marchou, B., Massip, P., Izopet, J., 2005. Persistence of distinct HIV-1 populations in blood monocytes and naive and memory CD4 T cells during prolonged suppressive HAART. AIDS 19, 1739-1750.

Denney, L., Aitken, C., Li, C.K., Wilson-Davies, E., Kok, W.L., Clelland, C., Rooney, K., Young, D., Dong, T., McMichael, A.J., Carman, W.F., Ho, L.P., 2010. Reduction of natural killer but not effector CD8 T lymphocytes in three consecutive cases of severe/lethal H1N1/09 influenza A virus infection. PLoS One 5, e10675.

Devi, M., Vijayalakshmi, D., Dhivya, K., Janane, M., 2017. Memory T Cells (CD45RO) Role and Evaluation in Pathogenesis of Lichen Planus and Lichenoid Mucositis. J Clin Diagn Res 11, ZC84-ZC86.

Di Santo, J.P., 2006. Natural killer cell developmental pathways: a question of balance. Annu Rev Immunol 24, 257-286.

Di Santo, J.P., 2009. A defining factor for natural killer cell development. Nat Immunol 10, 1051-1052.

Diab, M., Glasner, A., Isaacson, B., Bar-On, Y., Drori, Y., Yamin, R., Duev-Cohen, A., Danziger, O., Zamostiano, R., Mandelboim, M., Jonjic, S., Bacharach, E., Mandelboim, O., 2017. NK-cell receptors NKp46 and NCR1 control human metapneumovirus infection. Eur J Immunol 47, 692-703.

Diacovo, T.G., Catalina, M.D., Siegelman, M.H., von Andrian, U.H., 1998. Circulating activated platelets reconstitute lymphocyte homing and immunity in L-selectin-deficient mice. J Exp Med 187, 197-204.

Diefenbach, A., Colonna, M., Koyasu, S., 2014. Development, differentiation, and diversity of innate lymphoid cells. Immunity 41, 354-365.

Dogra, P., Rancan, C., Ma, W., Toth, M., Senda, T., Carpenter, D.J., Kubota, M., Matsumoto, R., Thapa, P., Szabo, P.A., Li Poon, M.M., Li, J., Arakawa-Hoyt, J., Shen, Y., Fong, L.,

Lanier, L.L., Farber, D.L., 2020. Tissue Determinants of Human NK Cell Development, Function, and Residence. Cell 180, 749-763 e713.
Doherty, D.G., Norris, S., Madrigal-Estebas, L., McEntee, G., Traynor, O., Hegarty, J.E., O'Farrelly, C., 1999. The human liver contains multiple populations of NK cells, T cells, and CD3+CD56+ natural T cells with distinct cytotoxic activities and Th1, Th2, and Th0 cytokine secretion patterns. J Immunol 163, 2314-2321.
Doherty, D.G., O'Farrelly, C., 2000. Innate and adaptive lymphoid cells in the human liver. Immunol Rev 174, 5-20.
Dohring, C., Scheidegger, D., Samaridis, J., Cella, M., Colonna, M., 1996. A human killer inhibitory receptor specific for HLA-A1,2. J Immunol 156, 3098-3101.
Doisne, J.M., Balmas, E., Boulenouar, S., Gaynor, L.M., Kieckbusch, J., Gardner, L., Hawkes, D.A., Barbara, C.F., Sharkey, A.M., Brady, H.J., Brosens, J.J., Moffett, A., Colucci, F., 2015. Composition, Development, and Function of Uterine Innate Lymphoid Cells. J Immunol 195, 3937-3945.
Dokun, A.O., Kim, S., Smith, H.R., Kang, H.S., Chu, D.T., Yokoyama, W.M., 2001. Specific and nonspecific NK cell activation during virus infection. Nat Immunol 2, 951-956.
Dou, D., Revol, R., Ostbye, H., Wang, H., Daniels, R., 2018. Influenza A Virus Cell Entry, Replication, Virion Assembly and Movement. Front Immunol 9, 1581.
Douagi, I., Colucci, F., Di Santo, J.P., Cumano, A., 2002. Identification of the earliest prethymic bipotent T/NK progenitor in murine fetal liver. Blood 99, 463-471.
Du, N., Zhou, J., Lin, X., Zhang, Y., Yang, X., Wang, Y., Shu, Y., 2010. Differential activation of NK cells by influenza A pseudotype H5N1 and 1918 and 2009 pandemic H1N1 viruses. J Virol 84, 7822-7831.
Eick, A.A., Wang, Z., Hughes, H., Ford, S.M., Tobler, S.K., 2009. Comparison of the trivalent live attenuated vs. inactivated influenza vaccines among U.S. military service members. Vaccine 27, 3568-3575.
Eisenhardt, M., Glassner, A., Wolter, F., Kramer, B., Kokordelis, P., Nischalke, H.D., Boesecke, C., Rockstroh, J.K., Spengler, U., Nattermann, J., 2014. CD27(+)CD56Bright natural killer cells may be involved in spontaneous clearance of acute hepatitis C in HIV-positive patients. AIDS 28, 1879-1884.
Eissens, D.N., Spanholtz, J., van der Meer, A., van Cranenbroek, B., Dolstra, H., Kwekkeboom, J., Preijers, F.W., Joosten, I., 2012. Defining early human NK cell developmental stages in primary and secondary lymphoid tissues. PLoS One 7, e30930.
Elliott, J.M., Wahle, J.A., Yokoyama, W.M., 2010. MHC class I-deficient natural killer cells acquire a licensed phenotype after transfer into an MHC class I-sufficient environment. J Exp Med 207, 2073-2079.
Ellis, T.M., Fisher, R.I., 1989. Functional heterogeneity of Leu 19"bright"+ and Leu 19"dim"+ lymphokine-activated killer cells. J Immunol 142, 2949-2954.
Elmaagacli, A.H., Steckel, N.K., Koldehoff, M., Hegerfeldt, Y., Trenschel, R., Ditschkowski, M., Christoph, S., Gromke, T., Kordelas, L., Ottinger, H.D., Ross, R.S., Horn, P.A., Schnittger, S., Beelen, D.W., 2011. Early human cytomegalovirus replication after transplantation is associated with a decreased relapse risk: evidence for a putative virus-versus-leukemia effect in acute myeloid leukemia patients. Blood 118, 1402-1412.
Epstein, M.M., Di Rosa, F., Jankovic, D., Sher, A., Matzinger, P., 1995. Successful T cell priming in B cell-deficient mice. J Exp Med 182, 915-922.
Eriksson, M., Meadows, S.K., Wira, C.R., Sentman, C.L., 2004. Unique phenotype of human uterine NK cells and their regulation by endogenous TGF-beta. J Leukoc Biol 76, 667-675.
Etzioni, A., Eidenschenk, C., Katz, R., Beck, R., Casanova, J.L., Pollack, S., 2005. Fatal varicella associated with selective natural killer cell deficiency. J Pediatr 146, 423-425.
Farrell, H.E., Vally, H., Lynch, D.M., Fleming, P., Shellam, G.R., Scalzo, A.A., Davis-Poynter, N.J., 1997. Inhibition of natural killer cells by a cytomegalovirus MHC class I homologue in vivo. Nature 386, 510-514.
Farsakoglu, Y., Palomino-Segura, M., Latino, I., Zanaga, S., Chatziandreou, N., Pizzagalli, D.U., Rinaldi, A., Bolis, M., Sallusto, F., Stein, J.V., Gonzalez, S.F., 2019. Influenza

Vaccination Induces NK-Cell-Mediated Type-II IFN Response that Regulates Humoral Immunity in an IL-6-Dependent Manner. Cell Rep 26, 2307-2315 e2305.

Fawaz, L.M., Sharif-Askari, E., Menezes, J., 1999. Up-regulation of NK cytotoxic activity via IL-15 induction by different viruses: a comparative study. J Immunol 163, 4473-4480.

Fehniger, T.A., Cooper, M.A., Nuovo, G.J., Cella, M., Facchetti, F., Colonna, M., Caligiuri, M.A., 2003. CD56bright natural killer cells are present in human lymph nodes and are activated by T cell-derived IL-2: a potential new link between adaptive and innate immunity. Blood 101, 3052-3057.

Ferlazzo, G., Morandi, B., 2014. Cross-Talks between Natural Killer Cells and Distinct Subsets of Dendritic Cells. Front Immunol 5, 159.

Ferlazzo, G., Pack, M., Thomas, D., Paludan, C., Schmid, D., Strowig, T., Bougras, G., Muller, W.A., Moretta, L., Munz, C., 2004. Distinct roles of IL-12 and IL-15 in human natural killer cell activation by dendritic cells from secondary lymphoid organs. Proc Natl Acad Sci U S A 101, 16606-16611.

Fernandez, N.C., Lozier, A., Flament, C., Ricciardi-Castagnoli, P., Bellet, D., Suter, M., Perricaudet, M., Tursz, T., Maraskovsky, E., Zitvogel, L., 1999. Dendritic cells directly trigger NK cell functions: cross-talk relevant in innate anti-tumor immune responses in vivo. Nat Med 5, 405-411.

Fernandez, N.C., Treiner, E., Vance, R.E., Jamieson, A.M., Lemieux, S., Raulet, D.H., 2005. A subset of natural killer cells achieves self-tolerance without expressing inhibitory receptors specific for self-MHC molecules. Blood 105, 4416-4423.

Fielding, C.A., Aicheler, R., Stanton, R.J., Wang, E.C., Han, S., Seirafian, S., Davies, J., McSharry, B.P., Weekes, M.P., Antrobus, P.R., Prod'homme, V., Blanchet, F.P., Sugrue, D., Cuff, S., Roberts, D., Davison, A.J., Lehner, P.J., Wilkinson, G.W., Tomasec, P., 2014. Two novel human cytomegalovirus NK cell evasion functions target MICA for lysosomal degradation. PLoS Pathog 10, e1004058.

Filipovic, I., Sonnerborg, I., Strunz, B., Friberg, D., Cornillet, M., Hertwig, L., Ivarsson, M.A., Bjorkstrom, N.K., 2019. 29-Color Flow Cytometry: Unraveling Human Liver NK Cell Repertoire Diversity. Front Immunol 10, 2692.

Foley, B., Cooley, S., Verneris, M.R., Curtsinger, J., Luo, X., Waller, E.K., Anasetti, C., Weisdorf, D., Miller, J.S., 2012. Human cytomegalovirus (CMV)-induced memory-like NKG2C(+) NK cells are transplantable and expand in vivo in response to recipient CMV antigen. J Immunol 189, 5082-5088.

Fox, A., Le, N.M., Horby, P., van Doorn, H.R., Nguyen, V.T., Nguyen, H.H., Nguyen, T.C., Vu, D.P., Nguyen, M.H., Diep, N.T., Bich, V.T., Huong, H.T., Taylor, W.R., Farrar, J., Wertheim, H., Nguyen, V.K., 2012. Severe pandemic H1N1 2009 infection is associated with transient NK and T deficiency and aberrant CD8 responses. PLoS One 7, e31535.

Frankel, T.L., Burns, W., Riley, J., Morgan, R.A., Davis, J.L., Hanada, K., Quezado, M., Rosenberg, S.A., Royal, R.E., 2010. Identification and characterization of a tumor infiltrating CD56(+)/CD16 (-) NK cell subset with specificity for pancreatic and prostate cancer cell lines. Cancer Immunol Immunother 59, 1757-1769.

Freud, A.G., Becknell, B., Roychowdhury, S., Mao, H.C., Ferketich, A.K., Nuovo, G.J., Hughes, T.L., Marburger, T.B., Sung, J., Baiocchi, R.A., Guimond, M., Caligiuri, M.A., 2005. A human CD34(+) subset resides in lymph nodes and differentiates into CD56bright natural killer cells. Immunity 22, 295-304.

Freud, A.G., Caligiuri, M.A., 2006. Human natural killer cell development. Immunol Rev 214, 56-72.

Freud, A.G., Yokohama, A., Becknell, B., Lee, M.T., Mao, H.C., Ferketich, A.K., Caligiuri, M.A., 2006. Evidence for discrete stages of human natural killer cell differentiation in vivo. J Exp Med 203, 1033-1043.

Frey, M., Packianathan, N.B., Fehniger, T.A., Ross, M.E., Wang, W.C., Stewart, C.C., Caligiuri, M.A., Evans, S.S., 1998. Differential expression and function of L-selectin on CD56bright and CD56dim natural killer cell subsets. J Immunol 161, 400-408.

Frias, M., Rivero-Juarez, A., Gordon, A., Camacho, A., Cantisan, S., Cuenca-Lopez, F., Torre-Cisneros, J., Pena, J., Rivero, A., 2015. Persistence of pathological distribution of NK cells in HIV-infected patients with prolonged use of HAART and a sustained immune response. PLoS One 10, e0121019.

Fu, B., Tian, Z., Wei, H., 2014. Subsets of human natural killer cells and their regulatory effects. Immunology 141, 483-489.

Fu, B., Wang, F., Sun, R., Ling, B., Tian, Z., Wei, H., 2011. CD11b and CD27 reflect distinct population and functional specialization in human natural killer cells. Immunology 133, 350-359.

Gambaryan, A.S., Tuzikov, A.B., Piskarev, V.E., Yamnikova, S.S., Lvov, D.K., Robertson, J.S., Bovin, N.V., Matrosovich, M.N., 1997. Specification of receptor-binding phenotypes of influenza virus isolates from different hosts using synthetic sialylglycopolymers: non-egg-adapted human H1 and H3 influenza A and influenza B viruses share a common high binding affinity for 6'-sialyl(N-acetyllactosamine). Virology 232, 345-350.

Gamblin, S.J., Skehel, J.J., 2010. Influenza hemagglutinin and neuraminidase membrane glycoproteins. J Biol Chem 285, 28403-28409.

Gandoglia, I., Ivaldi, F., Carrega, P., Armentani, E., Ferlazzo, G., Mancardi, G., Kerlero de Rosbo, N., Uccelli, A., Laroni, A., 2017. In vitro VLA-4 blockade results in an impaired NK cell-mediated immune surveillance against melanoma. Immunol Lett 181, 109-115.

Garcia-Peydro, M., de Yebenes, V.G., Toribio, M.L., 2006. Notch1 and IL-7 receptor interplay maintains proliferation of human thymic progenitors while suppressing non-T cell fates. J Immunol 177, 3711-3720.

Garten, R.J., Davis, C.T., Russell, C.A., Shu, B., Lindstrom, S., Balish, A., Sessions, W.M., Xu, X., Skepner, E., Deyde, V., Okomo-Adhiambo, M., Gubareva, L., Barnes, J., Smith, C.B., Emery, S.L., Hillman, M.J., Rivailler, P., Smagala, J., de Graaf, M., Burke, D.F., Fouchier, R.A., Pappas, C., Alpuche-Aranda, C.M., Lopez-Gatell, H., Olivera, H., Lopez, I., Myers, C.A., Faix, D., Blair, P.J., Yu, C., Keene, K.M., Dotson, P.D., Jr., Boxrud, D., Sambol, A.R., Abid, S.H., St George, K., Bannerman, T., Moore, A.L., Stringer, D.J., Blevins, P., Demmler-Harrison, G.J., Ginsberg, M., Kriner, P., Waterman, S., Smole, S., Guevara, H.F., Belongia, E.A., Clark, P.A., Beatrice, S.T., Donis, R., Katz, J., Finelli, L., Bridges, C.B., Shaw, M., Jernigan, D.B., Uyeki, T.M., Smith, D.J., Klimov, A.I., Cox, N.J., 2009. Antigenic and genetic characteristics of swine-origin 2009 A(H1N1) influenza viruses circulating in humans. Science 325, 197-201.

Gascoyne, D.M., Long, E., Veiga-Fernandes, H., de Boer, J., Williams, O., Seddon, B., Coles, M., Kioussis, D., Brady, H.J., 2009. The basic leucine zipper transcription factor E4BP4 is essential for natural killer cell development. Nat Immunol 10, 1118-1124.

Gazit, R., Gruda, R., Elboim, M., Arnon, T.I., Katz, G., Achdout, H., Hanna, J., Qimron, U., Landau, G., Greenbaum, E., Zakay-Rones, Z., Porgador, A., Mandelboim, O., 2006. Lethal influenza infection in the absence of the natural killer cell receptor gene Ncr1. Nat Immunol 7, 517-523.

Ge, M.Q., Ho, A.W., Tang, Y., Wong, K.H., Chua, B.Y., Gasser, S., Kemeny, D.M., 2012. NK cells regulate CD8+ T cell priming and dendritic cell migration during influenza A infection by IFN-gamma and perforin-dependent mechanisms. J Immunol 189, 2099-2109.

Geary, C.D., Sun, J.C., 2017. Memory responses of natural killer cells. Semin Immunol 31, 11-19.

Gerhard, W., Mozdzanowska, K., Furchner, M., Washko, G., Maiese, K., 1997. Role of the B-cell response in recovery of mice from primary influenza virus infection. Immunol Rev 159, 95-103.

Giamarellos-Bourboulis, E.J., Netea, M.G., Rovina, N., Akinosoglou, K., Antoniadou, A., Antonakos, N., Damoraki, G., Gkavogianni, T., Adami, M.E., Katsaounou, P., Ntaganou, M., Kyriakopoulou, M., Dimopoulos, G., Koutsodimitropoulos, I., Velissaris, D., Koufargyris, P., Karageorgos, A., Katrini, K., Lekakis, V., Lupse, M., Kotsaki, A., Renieris, G., Theodoulou, D., Panou, V., Koukaki, E., Koulouris, N., Gogos, C., Koutsoukou, A.,

2020. Complex Immune Dysregulation in COVID-19 Patients with Severe Respiratory Failure. Cell Host Microbe 27, 992-1000 e1003.

Gineau, L., Cognet, C., Kara, N., Lach, F.P., Dunne, J., Veturi, U., Picard, C., Trouillet, C., Eidenschenk, C., Aoufouchi, S., Alcais, A., Smith, O., Geissmann, F., Feighery, C., Abel, L., Smogorzewska, A., Stillman, B., Vivier, E., Casanova, J.L., Jouanguy, E., 2012. Partial MCM4 deficiency in patients with growth retardation, adrenal insufficiency, and natural killer cell deficiency. J Clin Invest 122, 821-832.

Glassner, A., Eisenhardt, M., Kramer, B., Korner, C., Coenen, M., Sauerbruch, T., Spengler, U., Nattermann, J., 2012. NK cells from HCV-infected patients effectively induce apoptosis of activated primary human hepatic stellate cells in a TRAIL-, FasL- and NKG2D-dependent manner. Lab Invest 92, 967-977.

Golden-Mason, L., Stone, A.E., Bambha, K.M., Cheng, L., Rosen, H.R., 2012. Race- and gender-related variation in natural killer p46 expression associated with differential anti-hepatitis C virus immunity. Hepatology 56, 1214-1222.

Gonzalez-Amaro, R., Cortes, J.R., Sanchez-Madrid, F., Martin, P., 2013. Is CD69 an effective brake to control inflammatory diseases? Trends Mol Med 19, 625-632.

Gonzalez, S.F., Lukacs-Kornek, V., Kuligowski, M.P., Pitcher, L.A., Degn, S.E., Kim, Y.A., Cloninger, M.J., Martinez-Pomares, L., Gordon, S., Turley, S.J., Carroll, M.C., 2010. Capture of influenza by medullary dendritic cells via SIGN-R1 is essential for humoral immunity in draining lymph nodes. Nat Immunol 11, 427-434.

Gonzalez, V.D., Falconer, K., Bjorkstrom, N.K., Blom, K.G., Weiland, O., Ljunggren, H.G., Alaeus, A., Sandberg, J.K., 2009. Expansion of functionally skewed CD56-negative NK cells in chronic hepatitis C virus infection: correlation with outcome of pegylated IFN-alpha and ribavirin treatment. J Immunol 183, 6612-6618.

Goodier, M.R., Londei, M., 2000. Lipopolysaccharide stimulates the proliferation of human CD56+CD3- NK cells: a regulatory role of monocytes and IL-10. J Immunol 165, 139-147.

Goodier, M.R., Londei, M., 2004. CD28 is not directly involved in the response of human CD3-CD56+ natural killer cells to lipopolysaccharide: a role for T cells. Immunology 111, 384-390.

Goodwin, K., Viboud, C., Simonsen, L., 2006. Antibody response to influenza vaccination in the elderly: a quantitative review. Vaccine 24, 1159-1169.

Gordon, S.M., Chaix, J., Rupp, L.J., Wu, J., Madera, S., Sun, J.C., Lindsten, T., Reiner, S.L., 2012. The transcription factors T-bet and Eomes control key checkpoints of natural killer cell maturation. Immunity 36, 55-67.

Gourbal, B., Pinaud, S., Beckers, G.J.M., Van Der Meer, J.W.M., Conrath, U., Netea, M.G., 2018. Innate immune memory: An evolutionary perspective. Immunol Rev 283, 21-40.

Green, M.L., Leisenring, W.M., Xie, H., Walter, R.B., Mielcarek, M., Sandmaier, B.M., Riddell, S.R., Boeckh, M., 2013. CMV reactivation after allogeneic HCT and relapse risk: evidence for early protection in acute myeloid leukemia. Blood 122, 1316-1324.

Gregoire, C., Chasson, L., Luci, C., Tomasello, E., Geissmann, F., Vivier, E., Walzer, T., 2007. The trafficking of natural killer cells. Immunol Rev 220, 169-182.

Gretz, J.E., Anderson, A.O., Shaw, S., 1997. Cords, channels, corridors and conduits: critical architectural elements facilitating cell interactions in the lymph node cortex. Immunol Rev 156, 11-24.

Gross, P.A., Hermogenes, A.W., Sacks, H.S., Lau, J., Levandowski, R.A., 1995. The efficacy of influenza vaccine in elderly persons. A meta-analysis and review of the literature. Ann Intern Med 123, 518-527.

Guidotti, L.G., Chisari, F.V., 2006. Immunobiology and pathogenesis of viral hepatitis. Annu Rev Pathol 1, 23-61.

Guma, M., Angulo, A., Vilches, C., Gomez-Lozano, N., Malats, N., Lopez-Botet, M., 2004. Imprint of human cytomegalovirus infection on the NK cell receptor repertoire. Blood 104, 3664-3671.

REFERENCES

Guma, M., Cabrera, C., Erkizia, I., Bofill, M., Clotet, B., Ruiz, L., Lopez-Botet, M., 2006. Human cytomegalovirus infection is associated with increased proportions of NK cells that express the CD94/NKG2C receptor in aviremic HIV-1-positive patients. J Infect Dis 194, 38-41.

Guo, H., Kumar, P., Moran, T.M., Garcia-Sastre, A., Zhou, Y., Malarkannan, S., 2009. The functional impairment of natural killer cells during influenza virus infection. Immunol Cell Biol 87, 579-589.

Guo, H., Santiago, F., Lambert, K., Takimoto, T., Topham, D.J., 2011. T cell-mediated protection against lethal 2009 pandemic H1N1 influenza virus infection in a mouse model. J Virol 85, 448-455.

Hadad, U., Thauland, T.J., Martinez, O.M., Butte, M.J., Porgador, A., Krams, S.M., 2015. NKp46 Clusters at the Immune Synapse and Regulates NK Cell Polarization. Front Immunol 6, 495.

Hamilton, B.S., Whittaker, G.R., Daniel, S., 2012. Influenza virus-mediated membrane fusion: determinants of hemagglutinin fusogenic activity and experimental approaches for assessing virus fusion. Viruses 4, 1144-1168.

Hammer, Q., Ruckert, T., Borst, E.M., Dunst, J., Haubner, A., Durek, P., Heinrich, F., Gasparoni, G., Babic, M., Tomic, A., Pietra, G., Nienen, M., Blau, I.W., Hofmann, J., Na, I.K., Prinz, I., Koenecke, C., Hemmati, P., Babel, N., Arnold, R., Walter, J., Thurley, K., Mashreghi, M.F., Messerle, M., Romagnani, C., 2018. Peptide-specific recognition of human cytomegalovirus strains controls adaptive natural killer cells. Nat Immunol 19, 453-463.

Han, Q., Bagheri, N., Bradshaw, E.M., Hafler, D.A., Lauffenburger, D.A., Love, J.C., 2012. Polyfunctional responses by human T cells result from sequential release of cytokines. Proc Natl Acad Sci U S A 109, 1607-1612.

Hanna, J., Bechtel, P., Zhai, Y., Youssef, F., McLachlan, K., Mandelboim, O., 2004. Novel insights on human NK cells' immunological modalities revealed by gene expression profiling. J Immunol 173, 6547-6563.

Harmon, C., Robinson, M.W., Fahey, R., Whelan, S., Houlihan, D.D., Geoghegan, J., O'Farrelly, C., 2016. Tissue-resident Eomes(hi) T-bet(lo) CD56(bright) NK cells with reduced proinflammatory potential are enriched in the adult human liver. Eur J Immunol 46, 2111-2120.

Hayakawa, Y., Sato-Matsushita, M., Takeda, K., Iwakura, Y., Tahara, H., Irimura, T., 2011. Early activation and interferon-gamma production of tumor-infiltrating mature CD27 high natural killer cells. Cancer Sci 102, 1967-1971.

Hayakawa, Y., Smyth, M.J., 2006. CD27 dissects mature NK cells into two subsets with distinct responsiveness and migratory capacity. J Immunol 176, 1517-1524.

Hayashi, M., Furuhashi, T., Nishida, E., Saito, C., Torii, K., Morita, A., 2013. Increased population of central memory T cells in circulating peripheral blood of psoriasis patients. J Dermatol Sci 70, 61-64.

He, X.S., Draghi, M., Mahmood, K., Holmes, T.H., Kemble, G.W., Dekker, C.L., Arvin, A.M., Parham, P., Greenberg, H.B., 2004. T cell-dependent production of IFN-gamma by NK cells in response to influenza A virus. J Clin Invest 114, 1812-1819.

He, X.S., Holmes, T.H., Zhang, C., Mahmood, K., Kemble, G.W., Lewis, D.B., Dekker, C.L., Greenberg, H.B., Arvin, A.M., 2006. Cellular immune responses in children and adults receiving inactivated or live attenuated influenza vaccines. J Virol 80, 11756-11766.

Helft, J., Manicassamy, B., Guermonprez, P., Hashimoto, D., Silvin, A., Agudo, J., Brown, B.D., Schmolke, M., Miller, J.C., Leboeuf, M., Murphy, K.M., Garcia-Sastre, A., Merad, M., 2012. Cross-presenting CD103+ dendritic cells are protected from influenza virus infection. J Clin Invest 122, 4037-4047.

Hendriks, J., Gravestein, L.A., Tesselaar, K., van Lier, R.A., Schumacher, T.N., Borst, J., 2000. CD27 is required for generation and long-term maintenance of T cell immunity. Nat Immunol 1, 433-440.

Hendriks, J., Xiao, Y., Borst, J., 2003. CD27 promotes survival of activated T cells and complements CD28 in generation and establishment of the effector T cell pool. J Exp Med 198, 1369-1380.

Hengel, R.L., Nicholson, J.K., 2001. An update on the use of flow cytometry in HIV infection and AIDS. Clin Lab Med 21, 841-856.

Hervier, B., Russick, J., Cremer, I., Vieillard, V., 2019. NK Cells in the Human Lungs. Front Immunol 10, 1263.

Hibbs, M.L., Selvaraj, P., Carpen, O., Springer, T.A., Kuster, H., Jouvin, M.H., Kinet, J.P., 1989. Mechanisms for regulating expression of membrane isoforms of Fc gamma RIII (CD16). Science 246, 1608-1611.

Hiby, S.E., Regan, L., Lo, W., Farrell, L., Carrington, M., Moffett, A., 2008. Association of maternal killer-cell immunoglobulin-like receptors and parental HLA-C genotypes with recurrent miscarriage. Hum Reprod 23, 972-976.

Hirano, M., Das, S., Guo, P., Cooper, M.D., 2011. The evolution of adaptive immunity in vertebrates. Adv Immunol 109, 125-157.

Hoadley, M.E., Hopkins, S.J., 2003. Simple, quantitative measurement of cytokine gene expression using an immunometric reverse transcriptase-polymerase chain reaction. J Immunol Methods 282, 135-145.

Holmberg, L.A., Springer, T.A., Ault, K.A., 1981. Natural killer activity in the peritoneal exudates of mice infected with Listeria monocytogenes: characterization of the natural killer cells by using a monoclonal rat anti-murine macrophage antibody (M1/70). J Immunol 127, 1792-1799.

Hong, H.A., Paximadis, M., Gray, G.E., Kuhn, L., Tiemessen, C.T., 2013. KIR2DS4 allelic variants: Differential effects on in utero and intrapartum HIV-1 mother-to-child transmission. Clin Immunol 149, 498-508.

Horinaka, M., Yoshida, T., Kishi, A., Akatani, K., Yasuda, T., Kouhara, J., Wakada, M., Sakai, T., 2010. Lactobacillus strains induce TRAIL production and facilitate natural killer activity against cancer cells. FEBS Lett 584, 577-582.

Horowitz, A., Behrens, R.H., Okell, L., Fooks, A.R., Riley, E.M., 2010a. NK cells as effectors of acquired immune responses: effector CD4+ T cell-dependent activation of NK cells following vaccination. J Immunol 185, 2808-2818.

Horowitz, A., Hafalla, J.C., King, E., Lusingu, J., Dekker, D., Leach, A., Moris, P., Cohen, J., Vekemans, J., Villafana, T., Corran, P.H., Bejon, P., Drakeley, C.J., von Seidlein, L., Riley, E.M., 2012. Antigen-specific IL-2 secretion correlates with NK cell responses after immunization of Tanzanian children with the RTS,S/AS01 malaria vaccine. J Immunol 188, 5054-5062.

Horowitz, A., Newman, K.C., Evans, J.H., Korbel, D.S., Davis, D.M., Riley, E.M., 2010b. Cross-talk between T cells and NK cells generates rapid effector responses to Plasmodium falciparum-infected erythrocytes. J Immunol 184, 6043-6052.

Horowitz, A., Strauss-Albee, D.M., Leipold, M., Kubo, J., Nemat-Gorgani, N., Dogan, O.C., Dekker, C.L., Mackey, S., Maecker, H., Swan, G.E., Davis, M.M., Norman, P.J., Guethlein, L.A., Desai, M., Parham, P., Blish, C.A., 2013. Genetic and environmental determinants of human NK cell diversity revealed by mass cytometry. Sci Transl Med 5, 208ra145.

Horst, D., Verweij, M.C., Davison, A.J., Ressing, M.E., Wiertz, E.J., 2011. Viral evasion of T cell immunity: ancient mechanisms offering new applications. Curr Opin Immunol 23, 96-103.

Houchins, J.P., Yabe, T., McSherry, C., Bach, F.H., 1991. DNA sequence analysis of NKG2, a family of related cDNA clones encoding type II integral membrane proteins on human natural killer cells. J Exp Med 173, 1017-1020.

Huang, C., Wang, Y., Li, X., Ren, L., Zhao, J., Hu, Y., Zhang, L., Fan, G., Xu, J., Gu, X., Cheng, Z., Yu, T., Xia, J., Wei, Y., Wu, W., Xie, X., Yin, W., Li, H., Liu, M., Xiao, Y., Gao, H., Guo, L., Xie, J., Wang, G., Jiang, R., Gao, Z., Jin, Q., Wang, J., Cao, B., 2020. Clinical features of patients infected with 2019 novel coronavirus in Wuhan, China. Lancet 395, 497-506.

Hudspeth, K., Donadon, M., Cimino, M., Pontarini, E., Tentorio, P., Preti, M., Hong, M., Bertoletti, A., Bicciato, S., Invernizzi, P., Lugli, E., Torzilli, G., Gershwin, M.E., Mavilio, D., 2016. Human liver-resident CD56(bright)/CD16(neg) NK cells are retained within hepatic sinusoids via the engagement of CCR5 and CXCR6 pathways. J Autoimmun 66, 40-50.

Hudspeth, K., Pontarini, E., Tentorio, P., Cimino, M., Donadon, M., Torzilli, G., Lugli, E., Della Bella, S., Gershwin, M.E., Mavilio, D., 2013. The role of natural killer cells in autoimmune liver disease: a comprehensive review. J Autoimmun 46, 55-65.

Hui, K.P.Y., Cheung, M.C., Perera, R., Ng, K.C., Bui, C.H.T., Ho, J.C.W., Ng, M.M.T., Kuok, D.I.T., Shih, K.C., Tsao, S.W., Poon, L.L.M., Peiris, M., Nicholls, J.M., Chan, M.C.W., 2020. Tropism, replication competence, and innate immune responses of the coronavirus SARS-CoV-2 in human respiratory tract and conjunctiva: an analysis in ex-vivo and in-vitro cultures. Lancet Respir Med 8, 687-695.

Hulett, H.R., Bonner, W.A., Barrett, J., Herzenberg, L.A., 1969. Cell sorting: automated separation of mammalian cells as a function of intracellular fluorescence. Science 166, 747-749.

Huntington, N.D., Vosshenrich, C.A., Di Santo, J.P., 2007. Developmental pathways that generate natural-killer-cell diversity in mice and humans. Nat Rev Immunol 7, 703-714.

Igarashi, H., Gregory, S.C., Yokota, T., Sakaguchi, N., Kincade, P.W., 2002. Transcription from the RAG1 locus marks the earliest lymphocyte progenitors in bone marrow. Immunity 17, 117-130.

Ikawa, T., Kawamoto, H., Fujimoto, S., Katsura, Y., 1999. Commitment of common T/Natural killer (NK) progenitors to unipotent T and NK progenitors in the murine fetal thymus revealed by a single progenitor assay. J Exp Med 190, 1617-1626.

Imai, K., Matsuyama, S., Miyake, S., Suga, K., Nakachi, K., 2000. Natural cytotoxic activity of peripheral-blood lymphocytes and cancer incidence: an 11-year follow-up study of a general population. Lancet 356, 1795-1799.

Ivarsson, M.A., Loh, L., Marquardt, N., Kekalainen, E., Berglin, L., Bjorkstrom, N.K., Westgren, M., Nixon, D.F., Michaelsson, J., 2013. Differentiation and functional regulation of human fetal NK cells. J Clin Invest 123, 3889-3901.

Jameson, S.C., Lee, Y.J., Hogquist, K.A., 2015. Innate memory T cells. Adv Immunol 126, 173-213.

Janeway, C.A., Jr., Medzhitov, R., 2002. Innate immune recognition. Annu Rev Immunol 20, 197-216.

Jarahian, M., Watzl, C., Fournier, P., Arnold, A., Djandji, D., Zahedi, S., Cerwenka, A., Paschen, A., Schirrmacher, V., Momburg, F., 2009. Activation of natural killer cells by newcastle disease virus hemagglutinin-neuraminidase. J Virol 83, 8108-8121.

Jefferson, T., Rivetti, D., Rivetti, A., Rudin, M., Di Pietrantonj, C., Demicheli, V., 2005. Efficacy and effectiveness of influenza vaccines in elderly people: a systematic review. Lancet 366, 1165-1174.

Jegaskanda, S., Job, E.R., Kramski, M., Laurie, K., Isitman, G., de Rose, R., Winnall, W.R., Stratov, I., Brooks, A.G., Reading, P.C., Kent, S.J., 2013. Cross-reactive influenza-specific antibody-dependent cellular cytotoxicity antibodies in the absence of neutralizing antibodies. J Immunol 190, 1837-1848.

Joncas, J., Monczak, Y., Ghibu, F., Alfieri, C., Bonin, A., Ahronheim, G., Rivard, G., 1989. Brief report: killer cell defect and persistent immunological abnormalities in two patients with chronic active Epstein-Barr virus infection. J Med Virol 28, 110-117.

Joncker, N.T., Fernandez, N.C., Treiner, E., Vivier, E., Raulet, D.H., 2009. NK cell responsiveness is tuned commensurate with the number of inhibitory receptors for self-MHC class I: the rheostat model. J Immunol 182, 4572-4580.

Joncker, N.T., Shifrin, N., Delebecque, F., Raulet, D.H., 2010. Mature natural killer cells reset their responsiveness when exposed to an altered MHC environment. J Exp Med 207, 2065-2072.

Jonsson, J.R., Hogan, P.G., Balderson, G.A., Ooi, L.L., Lynch, S.V., Strong, R.W., Powell, E.E., 1997. Human liver transplant perfusate: an abundant source of donor liver-associated leukocytes. Hepatology 26, 1111-1114.

Jose, R.J., Manuel, A., 2020. COVID-19 cytokine storm: the interplay between inflammation and coagulation. Lancet Respir Med 8, e46-e47.

Joshi, S.R., Shaw, A.C., Quagliarello, V.J., 2009. Pandemic influenza H1N1 2009, innate immunity, and the impact of immunosenescence on influenza vaccine. Yale J Biol Med 82, 143-151.

Jost, S., Altfeld, M., 2013. Control of human viral infections by natural killer cells. Annu Rev Immunol 31, 163-194.

Jost, S., Reardon, J., Peterson, E., Poole, D., Bosch, R., Alter, G., Altfeld, M., 2011. Expansion of 2B4+ natural killer (NK) cells and decrease in NKp46+ NK cells in response to influenza. Immunology 132, 516-526.

Juelke, K., Killig, M., Luetke-Eversloh, M., Parente, E., Gruen, J., Morandi, B., Ferlazzo, G., Thiel, A., Schmitt-Knosalla, I., Romagnani, C., 2010. CD62L expression identifies a unique subset of polyfunctional CD56dim NK cells. Blood 116, 1299-1307.

Kaczmarek, D.J., Kokordelis, P., Kramer, B., Glassner, A., Wolter, F., Goeser, F., Lutz, P., Schwarze-Zander, C., Boesecke, C., Strassburg, C.P., Rockstroh, J.K., Spengler, U., Nattermann, J., 2017. Alterations of the NK cell pool in HIV/HCV co-infection. PLoS One 12, e0174465.

Kamizono, S., Duncan, G.S., Seidel, M.G., Morimoto, A., Hamada, K., Grosveld, G., Akashi, K., Lind, E.F., Haight, J.P., Ohashi, P.S., Look, A.T., Mak, T.W., 2009. Nfil3/E4bp4 is required for the development and maturation of NK cells in vivo. J Exp Med 206, 2977-2986.

Kannan, K., Stewart, R.M., Bounds, W., Carlsson, S.R., Fukuda, M., Betzing, K.W., Holcombe, R.F., 1996. Lysosome-associated membrane proteins h-LAMP1 (CD107a) and h-LAMP2 (CD107b) are activation-dependent cell surface glycoproteins in human peripheral blood mononuclear cells which mediate cell adhesion to vascular endothelium. Cell Immunol 171, 10-19.

Karlhofer, F.M., Ribaudo, R.K., Yokoyama, W.M., 1992. MHC class I alloantigen specificity of Ly-49+ IL-2-activated natural killer cells. Nature 358, 66-70.

Kash, J.C., Tumpey, T.M., Proll, S.C., Carter, V., Perwitasari, O., Thomas, M.J., Basler, C.F., Palese, P., Taubenberger, J.K., Garcia-Sastre, A., Swayne, D.E., Katze, M.G., 2006. Genomic analysis of increased host immune and cell death responses induced by 1918 influenza virus. Nature 443, 578-581.

Kassim, S.H., Rajasagi, N.K., Zhao, X., Chervenak, R., Jennings, S.R., 2006. In vivo ablation of CD11c-positive dendritic cells increases susceptibility to herpes simplex virus type 1 infection and diminishes NK and T-cell responses. J Virol 80, 3985-3993.

Katz, J.M., Lu, X., Frace, A.M., Morken, T., Zaki, S.R., Tumpey, T.M., 2000. Pathogenesis of and immunity to avian influenza A H5 viruses. Biomed Pharmacother 54, 178-187.

Kay, A.W., Fukuyama, J., Aziz, N., Dekker, C.L., Mackey, S., Swan, G.E., Davis, M.M., Holmes, S., Blish, C.A., 2014. Enhanced natural killer-cell and T-cell responses to influenza A virus during pregnancy. Proc Natl Acad Sci U S A 111, 14506-14511.

Ke, Y., Kapp, J.A., 1996. Exogenous antigens gain access to the major histocompatibility complex class I processing pathway in B cells by receptor-mediated uptake. J Exp Med 184, 1179-1184.

Kennedy, M.K., Glaccum, M., Brown, S.N., Butz, E.A., Viney, J.L., Embers, M., Matsuki, N., Charrier, K., Sedger, L., Willis, C.R., Brasel, K., Morrissey, P.J., Stocking, K., Schuh, J.C., Joyce, S., Peschon, J.J., 2000. Reversible defects in natural killer and memory CD8 T cell lineages in interleukin 15-deficient mice. J Exp Med 191, 771-780.

Keppel, M.P., Yang, L., Cooper, M.A., 2013. Murine NK cell intrinsic cytokine-induced memory-like responses are maintained following homeostatic proliferation. J Immunol 190, 4754-4762.

Kiessling, R., Klein, E., Pross, H., Wigzell, H., 1975. "Natural" killer cells in the mouse. II. Cytotoxic cells with specificity for mouse Moloney leukemia cells. Characteristics of the killer cell. Eur J Immunol 5, 117-121.

Kim, S., Iizuka, K., Kang, H.S., Dokun, A., French, A.R., Greco, S., Yokoyama, W.M., 2002. In vivo developmental stages in murine natural killer cell maturation. Nat Immunol 3, 523-528.

Kim, S., Poursine-Laurent, J., Truscott, S.M., Lybarger, L., Song, Y.J., Yang, L., French, A.R., Sunwoo, J.B., Lemieux, S., Hansen, T.H., Yokoyama, W.M., 2005. Licensing of natural killer cells by host major histocompatibility complex class I molecules. Nature 436, 709-713.

Klein, E., Ben-Bassat, H., Neumann, H., Ralph, P., Zeuthen, J., Polliack, A., Vanky, F., 1976. Properties of the K562 cell line, derived from a patient with chronic myeloid leukemia. Int J Cancer 18, 421-431.

Klein Wolterink, R.G., Serafini, N., van Nimwegen, M., Vosshenrich, C.A., de Bruijn, M.J., Fonseca Pereira, D., Veiga Fernandes, H., Hendriks, R.W., Di Santo, J.P., 2013. Essential, dose-dependent role for the transcription factor Gata3 in the development of IL-5+ and IL-13+ type 2 innate lymphoid cells. Proc Natl Acad Sci U S A 110, 10240-10245.

Kondo, M., Maruoka, T., Otsuka, N., Kasamatsu, J., Fugo, K., Hanzawa, N., Kasahara, M., 2010. Comparative genomic analysis of mammalian NKG2D ligand family genes provides insights into their origin and evolution. Immunogenetics 62, 441-450.

Kos, F.J., Engleman, E.G., 1996. Role of natural killer cells in the generation of influenza virus-specific cytotoxic T cells. Cell Immunol 173, 1-6.

Kottilil, S., Shin, K., Planta, M., McLaughlin, M., Hallahan, C.W., Ghany, M., Chun, T.W., Sneller, M.C., Fauci, A.S., 2004. Expression of chemokine and inhibitory receptors on natural killer cells: effect of immune activation and HIV viremia. J Infect Dis 189, 1193-1198.

Kouro, T., Kumar, V., Kincade, P.W., 2002. Relationships between early B- and NK-lineage lymphocyte precursors in bone marrow. Blood 100, 3672-3680.

Kramer, B., Korner, C., Kebschull, M., Glassner, A., Eisenhardt, M., Nischalke, H.D., Alexander, M., Sauerbruch, T., Spengler, U., Nattermann, J., 2012. Natural killer p46High expression defines a natural killer cell subset that is potentially involved in control of hepatitis C virus replication and modulation of liver fibrosis. Hepatology 56, 1201-1213.

Krangel, M.S., 1987. Endocytosis and recycling of the T3-T cell receptor complex. The role of T3 phosphorylation. J Exp Med 165, 1141-1159.

Kubin, M.Z., Parshley, D.L., Din, W., Waugh, J.Y., Davis-Smith, T., Smith, C.A., Macduff, B.M., Armitage, R.J., Chin, W., Cassiano, L., Borges, L., Petersen, M., Trinchieri, G., Goodwin, R.G., 1999. Molecular cloning and biological characterization of NK cell activation-inducing ligand, a counterstructure for CD48. Eur J Immunol 29, 3466-3477.

Kumar, B.V., Ma, W., Miron, M., Granot, T., Guyer, R.S., Carpenter, D.J., Senda, T., Sun, X., Ho, S.H., Lerner, H., Friedman, A.L., Shen, Y., Farber, D.L., 2017. Human Tissue-Resident Memory T Cells Are Defined by Core Transcriptional and Functional Signatures in Lymphoid and Mucosal Sites. Cell Rep 20, 2921-2934.

Kuri-Cervantes, L., Pampena, M.B., Meng, W., Rosenfeld, A.M., Ittner, C.A.G., Weisman, A.R., Agyekum, R., Mathew, D., Baxter, A.E., Vella, L., Kuthuru, O., Apostolidis, S., Bershaw, L., Dougherty, J., Greenplate, A.R., Pattekar, A., Kim, J., Han, N., Gouma, S., Weirick, M.E., Arevalo, C.P., Bolton, M.J., Goodwin, E.C., Anderson, E.M., Hensley, S.E., Jones, T.K., Mangalmurti, N.S., Luning Prak, E.T., Wherry, E.J., Meyer, N.J., Betts, M.R., 2020. Immunologic perturbations in severe COVID-19/SARS-CoV-2 infection. bioRxiv.

Kurioka, A., Cosgrove, C., Simoni, Y., van Wilgenburg, B., Geremia, A., Bjorkander, S., Sverremark-Ekstrom, E., Thurnheer, C., Gunthard, H.F., Khanna, N., Swiss, H.I.V.C.S., Oxford, I.B.D.C.I., Walker, L.J., Arancibia-Carcamo, C.V., Newell, E.W., Willberg, C.B., Klenerman, P., 2018. CD161 Defines a Functionally Distinct Subset of Pro-Inflammatory Natural Killer Cells. Front Immunol 9, 486.

REFERENCES

Kurtz, J., 2005. Specific memory within innate immune systems. Trends Immunol 26, 186-192.

Lacy, P., Stow, J.L., 2011. Cytokine release from innate immune cells: association with diverse membrane trafficking pathways. Blood 118, 9-18.

Lamoreaux, L., Roederer, M., Koup, R., 2006. Intracellular cytokine optimization and standard operating procedure. Nat Protoc 1, 1507-1516.

Lang, S., Vujanovic, N.L., Wollenberg, B., Whiteside, T.L., 1998. Absence of B7.1-CD28/CTLA-4-mediated co-stimulation in human NK cells. Eur J Immunol 28, 780-786.

Lanier, L.L., 2005. NK cell recognition. Annu Rev Immunol 23, 225-274.

Lanier, L.L., 2008. Evolutionary struggles between NK cells and viruses. Nat Rev Immunol 8, 259-268.

Lanier, L.L., Le, A.M., Phillips, J.H., Warner, N.L., Babcock, G.F., 1983. Subpopulations of human natural killer cells defined by expression of the Leu-7 (HNK-1) and Leu-11 (NK-15) antigens. J Immunol 131, 1789-1796.

Lanier, L.L., Phillips, J.H., Hackett, J., Jr., Tutt, M., Kumar, V., 1986. Natural killer cells: definition of a cell type rather than a function. J Immunol 137, 2735-2739.

Lanier, L.L., Testi, R., Bindl, J., Phillips, J.H., 1989a. Identity of Leu-19 (CD56) leukocyte differentiation antigen and neural cell adhesion molecule. J Exp Med 169, 2233-2238.

Lanier, L.L., Yu, G., Phillips, J.H., 1989b. Co-association of CD3 zeta with a receptor (CD16) for IgG Fc on human natural killer cells. Nature 342, 803-805.

Lassen, M.G., Lukens, J.R., Dolina, J.S., Brown, M.G., Hahn, Y.S., 2010. Intrahepatic IL-10 maintains NKG2A+Ly49- liver NK cells in a functionally hyporesponsive state. J Immunol 184, 2693-2701.

Lauder, S.N., Jones, E., Smart, K., Bloom, A., Williams, A.S., Hindley, J.P., Ondondo, B., Taylor, P.R., Clement, M., Fielding, C., Godkin, A.J., Jones, S.A., Gallimore, A.M., 2013. Interleukin-6 limits influenza-induced inflammation and protects against fatal lung pathology. Eur J Immunol 43, 2613-2625.

Lazetic, S., Chang, C., Houchins, J.P., Lanier, L.L., Phillips, J.H., 1996. Human natural killer cell receptors involved in MHC class I recognition are disulfide-linked heterodimers of CD94 and NKG2 subunits. J Immunol 157, 4741-4745.

Lepin, E.J., Bastin, J.M., Allan, D.S., Roncador, G., Braud, V.M., Mason, D.Y., van der Merwe, P.A., McMichael, A.J., Bell, J.I., Powis, S.H., O'Callaghan, C.A., 2000. Functional characterization of HLA-F and binding of HLA-F tetramers to ILT2 and ILT4 receptors. Eur J Immunol 30, 3552-3561.

Liao, N.S., Bix, M., Zijlstra, M., Jaenisch, R., Raulet, D., 1991. MHC class I deficiency: susceptibility to natural killer (NK) cells and impaired NK activity. Science 253, 199-202.

Lima, M., Teixeira, M.A., Queiros, M.L., Leite, M., Santos, A.H., Justica, B., Orfao, A., 2001. Immunophenotypic characterization of normal blood CD56+lo versus CD56+hi NK-cell subsets and its impact on the understanding of their tissue distribution and functional properties. Blood Cells Mol Dis 27, 731-743.

Lisnic, V.J., Krmpotic, A., Jonjic, S., 2010. Modulation of natural killer cell activity by viruses. Curr Opin Microbiol 13, 530-539.

Little, T.J., Kraaijeveld, A.R., 2004. Ecological and evolutionary implications of immunological priming in invertebrates. Trends Ecol Evol 19, 58-60.

Litwin, V., Gumperz, J., Parham, P., Phillips, J.H., Lanier, L.L., 1994. NKB1: a natural killer cell receptor involved in the recognition of polymorphic HLA-B molecules. J Exp Med 180, 537-543.

Liu, B., Mori, I., Hossain, M.J., Dong, L., Takeda, K., Kimura, Y., 2004. Interleukin-18 improves the early defence system against influenza virus infection by augmenting natural killer cell-mediated cytotoxicity. J Gen Virol 85, 423-428.

Liu, P., Chen, L., Zhang, H., 2018a. Natural Killer Cells in Liver Disease and Hepatocellular Carcinoma and the NK Cell-Based Immunotherapy. J Immunol Res 2018, 1206737.

Liu, Y., Zheng, J., Liu, Y., Wen, L., Huang, L., Xiang, Z., Lam, K.T., Lv, A., Mao, H., Lau, Y.L., Tu, W., 2018b. Uncompromised NK cell activation is essential for virus-specific CTL activity during acute influenza virus infection. Cell Mol Immunol 15, 827-837.

Ljunggren, H.G., Karre, K., 1990. In search of the 'missing self': MHC molecules and NK cell recognition. Immunol Today 11, 237-244.

Long, B.R., Michaelsson, J., Loo, C.P., Ballan, W.M., Vu, B.A., Hecht, F.M., Lanier, L.L., Chapman, J.M., Nixon, D.F., 2008. Elevated frequency of gamma interferon-producing NK cells in healthy adults vaccinated against influenza virus. Clin Vaccine Immunol 15, 120-130.

Long, E.O., 1999. Regulation of immune responses through inhibitory receptors. Annu Rev Immunol 17, 875-904.

Lopez-Verges, S., Milush, J.M., Schwartz, B.S., Pando, M.J., Jarjoura, J., York, V.A., Houchins, J.P., Miller, S., Kang, S.M., Norris, P.J., Nixon, D.F., Lanier, L.L., 2011. Expansion of a unique CD57(+)NKG2Chi natural killer cell subset during acute human cytomegalovirus infection. Proc Natl Acad Sci U S A 108, 14725-14732.

Loza, M.J., Zamai, L., Azzoni, L., Rosati, E., Perussia, B., 2002. Expression of type 1 (interferon gamma) and type 2 (interleukin-13, interleukin-5) cytokines at distinct stages of natural killer cell differentiation from progenitor cells. Blood 99, 1273-1281.

Lozzio, C.B., Lozzio, B.B., 1975. Human chronic myelogenous leukemia cell-line with positive Philadelphia chromosome. Blood 45, 321-334.

Lu, X., Kondo, Y., Takamatsu, H., Ohata, K., Yamazaki, H., Takami, A., Akatsuka, Y., Nakao, S., 2008. CD16+ CD56- NK cells in the peripheral blood of cord blood transplant recipients: a unique subset of NK cells possibly associated with graft-versus-leukemia effect. Eur J Haematol 81, 18-25.

Lucas, C., Wong, P., Klein, J., Castro, T.B.R., Silva, J., Sundaram, M., Ellingson, M.K., Mao, T., Oh, J.E., Israelow, B., Takahashi, T., Tokuyama, M., Lu, P., Venkataraman, A., Park, A., Mohanty, S., Wang, H., Wyllie, A.L., Vogels, C.B.F., Earnest, R., Lapidus, S., Ott, I.M., Moore, A.J., Muenker, M.C., Fournier, J.B., Campbell, M., Odio, C.D., Casanovas-Massana, A., Yale, I.T., Herbst, R., Shaw, A.C., Medzhitov, R., Schulz, W.L., Grubaugh, N.D., Dela Cruz, C., Farhadian, S., Ko, A.I., Omer, S.B., Iwasaki, A., 2020. Longitudinal analyses reveal immunological misfiring in severe COVID-19. Nature 584, 463-469.

Lucas, M., Schachterle, W., Oberle, K., Aichele, P., Diefenbach, A., 2007. Dendritic cells prime natural killer cells by trans-presenting interleukin 15. Immunity 26, 503-517.

Lukomska, B., Winnock, M., Balabaud, C., Saric, J., Polanski, J., Olszewski, W.L., 1997. Human liver passenger cells suppress autologous and allogeneic blood lymphocytes proliferation. Transplant Proc 29, 1105-1107.

Ma, W., Kahn, R.E., Richt, J.A., 2008. The pig as a mixing vessel for influenza viruses: Human and veterinary implications. J Mol Genet Med 3, 158-166.

Mace, E.M., Hsu, A.P., Monaco-Shawver, L., Makedonas, G., Rosen, J.B., Dropulic, L., Cohen, J.I., Frenkel, E.P., Bagwell, J.C., Sullivan, J.L., Biron, C.A., Spalding, C., Zerbe, C.S., Uzel, G., Holland, S.M., Orange, J.S., 2013. Mutations in GATA2 cause human NK cell deficiency with specific loss of the CD56(bright) subset. Blood 121, 2669-2677.

Macias, C., Ballester, J.M., Hernandez, P., 2000. Expression and functional activity of the very late activation antigen-4 molecule on human natural killer cells in different states of activation. Immunology 100, 77-83.

Maciejewski-Duval, A., Meuris, F., Bignon, A., Aknin, M.L., Balabanian, K., Faivre, L., Pasquet, M., Barlogis, V., Fieschi, C., Bellanne-Chantelot, C., Donadieu, J., Schlecht-Louf, G., Marin-Esteban, V., Bachelerie, F., 2016. Altered chemotactic response to CXCL12 in patients carrying GATA2 mutations. J Leukoc Biol 99, 1065-1076.

Mackay, F., Figgett, W.A., Saulep, D., Lepage, M., Hibbs, M.L., 2010. B-cell stage and context-dependent requirements for survival signals from BAFF and the B-cell receptor. Immunol Rev 237, 205-225.

Mackay, F., Schneider, P., Rennert, P., Browning, J., 2003. BAFF AND APRIL: a tutorial on B cell survival. Annu Rev Immunol 21, 231-264.

Mackay, L.K., Minnich, M., Kragten, N.A., Liao, Y., Nota, B., Seillet, C., Zaid, A., Man, K., Preston, S., Freestone, D., Braun, A., Wynne-Jones, E., Behr, F.M., Stark, R., Pellicci, D.G., Godfrey, D.I., Belz, G.T., Pellegrini, M., Gebhardt, T., Busslinger, M., Shi, W., Carbone, F.R., van Lier, R.A., Kallies, A., van Gisbergen, K.P., 2016. Hobit and Blimp1 instruct a universal transcriptional program of tissue residency in lymphocytes. Science 352, 459-463.

Maecker, H.T., Rinfret, A., D'Souza, P., Darden, J., Roig, E., Landry, C., Hayes, P., Birungi, J., Anzala, O., Garcia, M., Harari, A., Frank, I., Baydo, R., Baker, M., Holbrook, J., Ottinger, J., Lamoreaux, L., Epling, C.L., Sinclair, E., Suni, M.A., Punt, K., Calarota, S., El-Bahi, S., Alter, G., Maila, H., Kuta, E., Cox, J., Gray, C., Altfeld, M., Nougarede, N., Boyer, J., Tussey, L., Tobery, T., Bredt, B., Roederer, M., Koup, R., Maino, V.C., Weinhold, K., Pantaleo, G., Gilmour, J., Horton, H., Sekaly, R.P., 2005. Standardization of cytokine flow cytometry assays. BMC Immunol 6, 13.

Magri, G., Muntasell, A., Romo, N., Saez-Borderias, A., Pende, D., Geraghty, D.E., Hengel, H., Angulo, A., Moretta, A., Lopez-Botet, M., 2011. NKp46 and DNAM-1 NK-cell receptors drive the response to human cytomegalovirus-infected myeloid dendritic cells overcoming viral immune evasion strategies. Blood 117, 848-856.

Male, V., Nisoli, I., Kostrzewski, T., Allan, D.S., Carlyle, J.R., Lord, G.M., Wack, A., Brady, H.J., 2014. The transcription factor E4bp4/Nfil3 controls commitment to the NK lineage and directly regulates Eomes and Id2 expression. J Exp Med 211, 635-642.

Mamessier, E., Sylvain, A., Thibult, M.L., Houvenaeghel, G., Jacquemier, J., Castellano, R., Goncalves, A., Andre, P., Romagne, F., Thibault, G., Viens, P., Birnbaum, D., Bertucci, F., Moretta, A., Olive, D., 2011. Human breast cancer cells enhance self tolerance by promoting evasion from NK cell antitumor immunity. J Clin Invest 121, 3609-3622.

Mandelboim, O., Lieberman, N., Lev, M., Paul, L., Arnon, T.I., Bushkin, Y., Davis, D.M., Strominger, J.L., Yewdell, J.W., Porgador, A., 2001. Recognition of haemagglutinins on virus-infected cells by NKp46 activates lysis by human NK cells. Nature 409, 1055-1060.

Mangalmurti, N., Hunter, C.A., 2020. Cytokine Storms: Understanding COVID-19. Immunity 53, 19-25.

Manicassamy, B., Manicassamy, S., Belicha-Villanueva, A., Pisanelli, G., Pulendran, B., Garcia-Sastre, A., 2010. Analysis of in vivo dynamics of influenza virus infection in mice using a GFP reporter virus. Proc Natl Acad Sci U S A 107, 11531-11536.

Manickam, C., Sugawara, S., Reeves, R.K., 2020. Friends or foes? The knowns and unknowns of natural killer cell biology in COVID-19 and other coronaviruses in July 2020. PLoS Pathog 16, e1008820.

Mao, H., Tu, W., Qin, G., Law, H.K., Sia, S.F., Chan, P.L., Liu, Y., Lam, K.T., Zheng, J., Peiris, M., Lau, Y.L., 2009. Influenza virus directly infects human natural killer cells and induces cell apoptosis. J Virol 83, 9215-9222.

Margolick, J.B., Munoz, A., Donnenberg, A.D., Park, L.P., Galai, N., Giorgi, J.V., O'Gorman, M.R., Ferbas, J., 1995. Failure of T-cell homeostasis preceding AIDS in HIV-1 infection. The Multicenter AIDS Cohort Study. Nat Med 1, 674-680.

Market, M., Angka, L., Martel, A.B., Bastin, D., Olanubi, O., Tennakoon, G., Boucher, D.M., Ng, J., Ardolino, M., Auer, R.C., 2020. Flattening the COVID-19 Curve With Natural Killer Cell Based Immunotherapies. Front Immunol 11, 1512.

Marquardt, N., Beziat, V., Nystrom, S., Hengst, J., Ivarsson, M.A., Kekalainen, E., Johansson, H., Mjosberg, J., Westgren, M., Lankisch, T.O., Wedemeyer, H., Ellis, E.C., Ljunggren, H.G., Michaelsson, J., Bjorkstrom, N.K., 2015. Cutting edge: identification and characterization of human intrahepatic CD49a+ NK cells. J Immunol 194, 2467-2471.

Marquardt, N., Kekalainen, E., Chen, P., Kvedaraite, E., Wilson, J.N., Ivarsson, M.A., Mjosberg, J., Berglin, L., Safholm, J., Manson, M.L., Adner, M., Al-Ameri, M., Bergman, P., Orre, A.C., Svensson, M., Dahlen, B., Dahlen, S.E., Ljunggren, H.G., Michaelsson, J., 2017. Human lung natural killer cells are predominantly comprised of highly differentiated hypofunctional CD69(-)CD56(dim) cells. J Allergy Clin Immunol 139, 1321-1330 e1324.

Marquardt, N., Kekalainen, E., Chen, P., Lourda, M., Wilson, J.N., Scharenberg, M., Bergman, P., Al-Ameri, M., Hard, J., Mold, J.E., Ljunggren, H.G., Michaelsson, J., 2019. Unique transcriptional and protein-expression signature in human lung tissue-resident NK cells. Nat Commun 10, 3841.

Marshall, N.B., Swain, S.L., 2011. Cytotoxic CD4 T cells in antiviral immunity. J Biomed Biotechnol 2011, 954602.

Martin-Fontecha, A., Thomsen, L.L., Brett, S., Gerard, C., Lipp, M., Lanzavecchia, A., Sallusto, F., 2004. Induced recruitment of NK cells to lymph nodes provides IFN-gamma for T(H)1 priming. Nat Immunol 5, 1260-1265.

Mason, D., 1998. A very high level of crossreactivity is an essential feature of the T-cell receptor. Immunol Today 19, 395-404.

Masopust, D., Soerens, A.G., 2019. Tissue-Resident T Cells and Other Resident Leukocytes. Annu Rev Immunol 37, 521-546.

Masopust, D., Vezys, V., Marzo, A.L., Lefrancois, L., 2014. Pillars article: preferential localization of effector memory cells in nonlymphoid tissue. Science. 2001. 291: 2413-2417. J Immunol 192, 845-849.

Mathew, S.O., Vaidya, S.V., Kim, J.R., Mathew, P.A., 2007. Human natural killer cell receptor 2B4 (CD244) down-regulates its own expression by reduced promoter activity at an Ets element. Biochem Biophys Res Commun 355, 483-487.

Mathurin, K.S., Martens, G.W., Kornfeld, H., Welsh, R.M., 2009. CD4 T-cell-mediated heterologous immunity between mycobacteria and poxviruses. J Virol 83, 3528-3539.

Matrosovich, M., Tuzikov, A., Bovin, N., Gambaryan, A., Klimov, A., Castrucci, M.R., Donatelli, I., Kawaoka, Y., 2000. Early alterations of the receptor-binding properties of H1, H2, and H3 avian influenza virus hemagglutinins after their introduction into mammals. J Virol 74, 8502-8512.

Matrosovich, M.N., Matrosovich, T.Y., Gray, T., Roberts, N.A., Klenk, H.D., 2004. Human and avian influenza viruses target different cell types in cultures of human airway epithelium. Proc Natl Acad Sci U S A 101, 4620-4624.

Matsuzaki, Y., Katsushima, N., Nagai, Y., Shoji, M., Itagaki, T., Sakamoto, M., Kitaoka, S., Mizuta, K., Nishimura, H., 2006. Clinical features of influenza C virus infection in children. J Infect Dis 193, 1229-1235.

Matteucci, E., Ghimenti, M., Di Beo, S., Giampietro, O., 2011. Altered proportions of naive, central memory and terminally differentiated central memory subsets among CD4+ and CD8 + T cells expressing CD26 in patients with type 1 diabetes. J Clin Immunol 31, 977-984.

Mavilio, D., Benjamin, J., Daucher, M., Lombardo, G., Kottilil, S., Planta, M.A., Marcenaro, E., Bottino, C., Moretta, L., Moretta, A., Fauci, A.S., 2003. Natural killer cells in HIV-1 infection: dichotomous effects of viremia on inhibitory and activating receptors and their functional correlates. Proc Natl Acad Sci U S A 100, 15011-15016.

Mavilio, D., Lombardo, G., Benjamin, J., Kim, D., Follman, D., Marcenaro, E., O'Shea, M.A., Kinter, A., Kovacs, C., Moretta, A., Fauci, A.S., 2005. Characterization of CD56-/CD16+ natural killer (NK) cells: a highly dysfunctional NK subset expanded in HIV-infected viremic individuals. Proc Natl Acad Sci U S A 102, 2886-2891.

McCall, M.B., Roestenberg, M., Ploemen, I., Teirlinck, A., Hopman, J., de Mast, Q., Dolo, A., Doumbo, O.K., Luty, A., van der Ven, A.J., Hermsen, C.C., Sauerwein, R.W., 2010. Memory-like IFN-gamma response by NK cells following malaria infection reveals the crucial role of T cells in NK cell activation by P. falciparum. Eur J Immunol 40, 3472-3477.

McDermott, D.S., Varga, S.M., 2011. Quantifying antigen-specific CD4 T cells during a viral infection: CD4 T cell responses are larger than we think. J Immunol 187, 5568-5576.

McIntyre, K.W., Welsh, R.M., 1986. Accumulation of natural killer and cytotoxic T large granular lymphocytes in the liver during virus infection. J Exp Med 164, 1667-1681.

Melhem, A., Muhanna, N., Bishara, A., Alvarez, C.E., Ilan, Y., Bishara, T., Horani, A., Nassar, M., Friedman, S.L., Safadi, R., 2006. Anti-fibrotic activity of NK cells in experimental liver injury through killing of activated HSC. J Hepatol 45, 60-71.

REFERENCES

Melillo, D., Marino, R., Italiani, P., Boraschi, D., 2018. Innate Immune Memory in Invertebrate Metazoans: A Critical Appraisal. Front Immunol 9, 1915.

Merino, F., Henle, W., Ramirez-Duque, P., 1986. Chronic active Epstein-Barr virus infection in patients with Chediak-Higashi syndrome. J Clin Immunol 6, 299-305.

Michel, T., Poli, A., Cuapio, A., Briquemont, B., Iserentant, G., Ollert, M., Zimmer, J., 2016. Human CD56bright NK Cells: An Update. J Immunol 196, 2923-2931.

Michie, A.M., Carlyle, J.R., Schmitt, T.M., Ljutic, B., Cho, S.K., Fong, Q., Zuniga-Pflucker, J.C., 2000. Clonal characterization of a bipotent T cell and NK cell progenitor in the mouse fetal thymus. J Immunol 164, 1730-1733.

Middleton, D., Curran, M., Maxwell, L., 2002. Natural killer cells and their receptors. Transpl Immunol 10, 147-164.

Miletic, A., Lenartic, M., Popovic, B., Brizic, I., Trsan, T., Miklic, K., Mandelboim, O., Krmpotic, A., Jonjic, S., 2017. NCR1-deficiency diminishes the generation of protective murine cytomegalovirus antibodies by limiting follicular helper T-cell maturation. Eur J Immunol 47, 1443-1456.

Miller, J.S., Alley, K.A., McGlave, P., 1994. Differentiation of natural killer (NK) cells from human primitive marrow progenitors in a stroma-based long-term culture system: identification of a CD34+7+ NK progenitor. Blood 83, 2594-2601.

Miller, J.S., McCullar, V., 2001. Human natural killer cells with polyclonal lectin and immunoglobulinlike receptors develop from single hematopoietic stem cells with preferential expression of NKG2A and KIR2DL2/L3/S2. Blood 98, 705-713.

Miller, J.S., Verfaillie, C., McGlave, P., 1992. The generation of human natural killer cells from CD34+/DR- primitive progenitors in long-term bone marrow culture. Blood 80, 2182-2187.

Milutinovic, B., Kurtz, J., 2016. Immune memory in invertebrates. Semin Immunol 28, 328-342.

Min-Oo, G., Lanier, L.L., 2014. Cytomegalovirus generates long-lived antigen-specific NK cells with diminished bystander activation to heterologous infection. J Exp Med 211, 2669-2680.

Moffett, A., Colucci, F., 2014. Uterine NK cells: active regulators at the maternal-fetal interface. J Clin Invest 124, 1872-1879.

Montalto, E., Mangraviti, S., Costa, G., Carrega, P., Morandi, B., Pezzino, G., Bonaccorsi, I., Cancellieri, A., Mingari, M.C., Mesiti, M., Ferlazzo, G., Melioli, G., 2010. Seroma fluid subsequent to axillary lymph node dissection for breast cancer derives from an accumulation of afferent lymph. Immunol Lett 131, 67-72.

Monteiro, J.M., Harvey, C., Trinchieri, G., 1998. Role of interleukin-12 in primary influenza virus infection. J Virol 72, 4825-4831.

Moretta, A., 2002. Natural killer cells and dendritic cells: rendezvous in abused tissues. Nat Rev Immunol 2, 957-964.

Moretta, A., Biassoni, R., Bottino, C., Mingari, M.C., Moretta, L., 2000. Natural cytotoxicity receptors that trigger human NK-cell-mediated cytolysis. Immunol Today 21, 228-234.

Moretta, A., Biassoni, R., Bottino, C., Pende, D., Vitale, M., Poggi, A., Mingari, M.C., Moretta, L., 1997. Major histocompatibility complex class I-specific receptors on human natural killer and T lymphocytes. Immunol Rev 155, 105-117.

Moretta, A., Bottino, C., Vitale, M., Pende, D., Cantoni, C., Mingari, M.C., Biassoni, R., Moretta, L., 2001. Activating receptors and coreceptors involved in human natural killer cell-mediated cytolysis. Annu Rev Immunol 19, 197-223.

Moretta, A., Moretta, L., 1997. HLA class I specific inhibitory receptors. Curr Opin Immunol 9, 694-701.

Moroso, V., Metselaar, H.J., Mancham, S., Tilanus, H.W., Eissens, D., van der Meer, A., van der Laan, L.J., Kuipers, E.J., Joosten, I., Kwekkeboom, J., 2010. Liver grafts contain a unique subset of natural killer cells that are transferred into the recipient after liver transplantation. Liver Transpl 16, 895-908.

Mosmann, T.R., Coffman, R.L., 1989. TH1 and TH2 cells: different patterns of lymphokine secretion lead to different functional properties. Annu Rev Immunol 7, 145-173.

REFERENCES

Mosmann, T.R., Li, L., Sad, S., 1997. Functions of CD8 T-cell subsets secreting different cytokine patterns. Semin Immunol 9, 87-92.

Mossel, E.C., Wang, J., Jeffers, S., Edeen, K.E., Wang, S., Cosgrove, G.P., Funk, C.J., Manzer, R., Miura, T.A., Pearson, L.D., Holmes, K.V., Mason, R.J., 2008. SARS-CoV replicates in primary human alveolar type II cell cultures but not in type I-like cells. Virology 372, 127-135.

Mrozek, E., Anderson, P., Caligiuri, M.A., 1996. Role of interleukin-15 in the development of human CD56+ natural killer cells from CD34+ hematopoietic progenitor cells. Blood 87, 2632-2640.

Nagler, A., Lanier, L.L., Cwirla, S., Phillips, J.H., 1989. Comparative studies of human FcRIII-positive and negative natural killer cells. J Immunol 143, 3183-3191.

Nakajima, H., Cella, M., Langen, H., Friedlein, A., Colonna, M., 1999. Activating interactions in human NK cell recognition: the role of 2B4-CD48. Eur J Immunol 29, 1676-1683.

Nandi, B., Behar, S.M., 2011. Regulation of neutrophils by interferon-gamma limits lung inflammation during tuberculosis infection. J Exp Med 208, 2251-2262.

Narni-Mancinelli, E., Ugolini, S., Vivier, E., 2013. Tuning the threshold of natural killer cell responses. Curr Opin Immunol 25, 53-58.

Nattermann, J., Feldmann, G., Ahlenstiel, G., Langhans, B., Sauerbruch, T., Spengler, U., 2006. Surface expression and cytolytic function of natural killer cell receptors is altered in chronic hepatitis C. Gut 55, 869-877.

Natuk, R.J., Welsh, R.M., 1987. Accumulation and chemotaxis of natural killer/large granular lymphocytes at sites of virus replication. J Immunol 138, 877-883.

Netea, M.G., Dominguez-Andres, J., Barreiro, L.B., Chavakis, T., Divangahi, M., Fuchs, E., Joosten, L.A.B., van der Meer, J.W.M., Mhlanga, M.M., Mulder, W.J.M., Riksen, N.P., Schlitzer, A., Schultze, J.L., Stabell Benn, C., Sun, J.C., Xavier, R.J., Latz, E., 2020. Defining trained immunity and its role in health and disease. Nat Rev Immunol 20, 375-388.

Newhook, N., Fudge, N., Grant, M., 2017. NK cells generate memory-type responses to human cytomegalovirus-infected fibroblasts. Eur J Immunol 47, 1032-1039.

Ni, F., Guo, C., Sun, R., Fu, B., Yang, Y., Wu, L., Ren, S., Tian, Z., Wei, H., 2015. MicroRNA transcriptomes of distinct human NK cell populations identify miR-362-5p as an essential regulator of NK cell function. Sci Rep 5, 9993.

Ni, J., Miller, M., Stojanovic, A., Garbi, N., Cerwenka, A., 2012. Sustained effector function of IL-12/15/18-preactivated NK cells against established tumors. J Exp Med 209, 2351-2365.

Nicholson, K.G., Wood, J.M., Zambon, M., 2003. Influenza. Lancet 362, 1733-1745.

Nikzad, R., Angelo, L.S., Aviles-Padilla, K., Le, D.T., Singh, V.K., Bimler, L., Vukmanovic-Stejic, M., Vendrame, E., Ranganath, T., Simpson, L., Haigwood, N.L., Blish, C.A., Akbar, A.N., Paust, S., 2019. Human natural killer cells mediate adaptive immunity to viral antigens. Sci Immunol 4.

Nogusa, S., Ritz, B.W., Kassim, S.H., Jennings, S.R., Gardner, E.M., 2008. Characterization of age-related changes in natural killer cells during primary influenza infection in mice. Mech Ageing Dev 129, 223-230.

Norris, S., Collins, C., Doherty, D.G., Smith, F., McEntee, G., Traynor, O., Nolan, N., Hegarty, J., O'Farrelly, C., 1998. Resident human hepatic lymphocytes are phenotypically different from circulating lymphocytes. J Hepatol 28, 84-90.

O'Leary, J.G., Goodarzi, M., Drayton, D.L., von Andrian, U.H., 2006. T cell- and B cell-independent adaptive immunity mediated by natural killer cells. Nat Immunol 7, 507-516.

O'Shea, J.J., Ma, A., Lipsky, P., 2002. Cytokines and autoimmunity. Nat Rev Immunol 2, 37-45.

Orange, J.S., 2006. Human natural killer cell deficiencies. Curr Opin Allergy Clin Immunol 6, 399-409.

Orange, J.S., 2008. Formation and function of the lytic NK-cell immunological synapse. Nat Rev Immunol 8, 713-725.

Orr, M.T., Lanier, L.L., 2010. Natural killer cell education and tolerance. Cell 142, 847-856.

REFERENCES

Palgen, J.L., Tchitchek, N., Huot, N., Elhmouzi-Younes, J., Lefebvre, C., Rosenbaum, P., Dereuddre-Bosquet, N., Martinon, F., Hocini, H., Cosma, A., Muller-Trutwin, M., Levy, Y., Le Grand, R., Beignon, A.S., 2019. NK cell immune responses differ after prime and boost vaccination. J Leukoc Biol 105, 1055-1073.

Pallikkuth, S., Kanthikeel, S.P., Silva, S.Y., Fischl, M., Pahwa, R., Pahwa, S., 2011a. Innate immune defects correlate with failure of antibody responses to H1N1/09 vaccine in HIV-infected patients. J Allergy Clin Immunol 128, 1279-1285.

Pallikkuth, S., Pilakka Kanthikeel, S., Silva, S.Y., Fischl, M., Pahwa, R., Pahwa, S., 2011b. Upregulation of IL-21 receptor on B cells and IL-21 secretion distinguishes novel 2009 H1N1 vaccine responders from nonresponders among HIV-infected persons on combination antiretroviral therapy. J Immunol 186, 6173-6181.

Pappas, C., Aguilar, P.V., Basler, C.F., Solorzano, A., Zeng, H., Perrone, L.A., Palese, P., Garcia-Sastre, A., Katz, J.M., Tumpey, T.M., 2008. Single gene reassortants identify a critical role for PB1, HA, and NA in the high virulence of the 1918 pandemic influenza virus. Proc Natl Acad Sci U S A 105, 3064-3069.

Parato, K.G., Kumar, A., Badley, A.D., Sanchez-Dardon, J.L., Chambers, K.A., Young, C.D., Lim, W.T., Kravcik, S., Cameron, D.W., Angel, J.B., 2002. Normalization of natural killer cell function and phenotype with effective anti-HIV therapy and the role of IL-10. AIDS 16, 1251-1256.

Parham, P., 2005. Influence of KIR diversity on human immunity. Adv Exp Med Biol 560, 47-50.

Parker, D.C., 1993. T cell-dependent B cell activation. Annu Rev Immunol 11, 331-360.

Parr, E.L., Young, L.H., Parr, M.B., Young, J.D., 1990. Granulated metrial gland cells of pregnant mouse uterus are natural killer-like cells that contain perforin and serine esterases. J Immunol 145, 2365-2372.

Parrish-Novak, J., Dillon, S.R., Nelson, A., Hammond, A., Sprecher, C., Gross, J.A., Johnston, J., Madden, K., Xu, W., West, J., Schrader, S., Burkhead, S., Heipel, M., Brandt, C., Kuijper, J.L., Kramer, J., Conklin, D., Presnell, S.R., Berry, J., Shiota, F., Bort, S., Hambly, K., Mudri, S., Clegg, C., Moore, M., Grant, F.J., Lofton-Day, C., Gilbert, T., Rayond, F., Ching, A., Yao, L., Smith, D., Webster, P., Whitmore, T., Maurer, M., Kaushansky, K., Holly, R.D., Foster, D., 2000. Interleukin 21 and its receptor are involved in NK cell expansion and regulation of lymphocyte function. Nature 408, 57-63.

Pasero, C., Gravis, G., Guerin, M., Granjeaud, S., Thomassin-Piana, J., Rocchi, P., Paciencia-Gros, M., Poizat, F., Bentobji, M., Azario-Cheillan, F., Walz, J., Salem, N., Brunelle, S., Moretta, A., Olive, D., 2016. Inherent and Tumor-Driven Immune Tolerance in the Prostate Microenvironment Impairs Natural Killer Cell Antitumor Activity. Cancer Res 76, 2153-2165.

Paust, S., Blish, C.A., Reeves, R.K., 2017. Redefining Memory: Building the Case for Adaptive NK Cells. J Virol 91.

Paust, S., Senman, B., von Andrian, U.H., 2010. Adaptive immune responses mediated by natural killer cells. Immunol Rev 235, 286-296.

Pelletier, S., Drouin, C., Bedard, N., Khakoo, S.I., Bruneau, J., Shoukry, N.H., 2010. Increased degranulation of natural killer cells during acute HCV correlates with the magnitude of virus-specific T cell responses. J Hepatol 53, 805-816.

Pende, D., Biassoni, R., Cantoni, C., Verdiani, S., Falco, M., di Donato, C., Accame, L., Bottino, C., Moretta, A., Moretta, L., 1996. The natural killer cell receptor specific for HLA-A allotypes: a novel member of the p58/p70 family of inhibitory receptors that is characterized by three immunoglobulin-like domains and is expressed as a 140-kD disulphide-linked dimer. J Exp Med 184, 505-518.

Pende, D., Falco, M., Vitale, M., Cantoni, C., Vitale, C., Munari, E., Bertaina, A., Moretta, F., Del Zotto, G., Pietra, G., Mingari, M.C., Locatelli, F., Moretta, L., 2019. Killer Ig-Like Receptors (KIRs): Their Role in NK Cell Modulation and Developments Leading to Their Clinical Exploitation. Front Immunol 10, 1179.

Pende, D., Parolini, S., Pessino, A., Sivori, S., Augugliaro, R., Morelli, L., Marcenaro, E., Accame, L., Malaspina, A., Biassoni, R., Bottino, C., Moretta, L., Moretta, A., 1999. Identification and molecular characterization of NKp30, a novel triggering receptor involved in natural cytotoxicity mediated by human natural killer cells. J Exp Med 190, 1505-1516.

Peng, H., Jiang, X., Chen, Y., Sojka, D.K., Wei, H., Gao, X., Sun, R., Yokoyama, W.M., Tian, Z., 2013a. Liver-resident NK cells confer adaptive immunity in skin-contact inflammation. J Clin Invest 123, 1444-1456.

Peng, H., Sun, R., Tang, L., Wei, H., Tian, Z., 2013b. CD62L is critical for maturation and accumulation of murine hepatic NK cells in response to viral infection. J Immunol 190, 4255-4262.

Peng, H., Tian, Z., 2017. Diversity of tissue-resident NK cells. Semin Immunol 31, 3-10.

Perfetto, S.P., Ambrozak, D., Nguyen, R., Chattopadhyay, P., Roederer, M., 2006a. Quality assurance for polychromatic flow cytometry. Nat Protoc 1, 1522-1530.

Perfetto, S.P., Chattopadhyay, P.K., Lamoreaux, L., Nguyen, R., Ambrozak, D., Koup, R.A., Roederer, M., 2006b. Amine reactive dyes: an effective tool to discriminate live and dead cells in polychromatic flow cytometry. J Immunol Methods 313, 199-208.

Perfetto, S.P., Chattopadhyay, P.K., Roederer, M., 2004. Seventeen-colour flow cytometry: unravelling the immune system. Nat Rev Immunol 4, 648-655.

Perussia, B., Acuto, O., Terhorst, C., Faust, J., Lazarus, R., Fanning, V., Trinchieri, G., 1983. Human natural killer cells analyzed by B73.1, a monoclonal antibody blocking Fc receptor functions. II. Studies of B73.1 antibody-antigen interaction on the lymphocyte membrane. J Immunol 130, 2142-2148.

Pessino, A., Sivori, S., Bottino, C., Malaspina, A., Morelli, L., Moretta, L., Biassoni, R., Moretta, A., 1998. Molecular cloning of NKp46: a novel member of the immunoglobulin superfamily involved in triggering of natural cytotoxicity. J Exp Med 188, 953-960.

Peters, P.J., Borst, J., Oorschot, V., Fukuda, M., Krahenbuhl, O., Tschopp, J., Slot, J.W., Geuze, H.J., 1991. Cytotoxic T lymphocyte granules are secretory lysosomes, containing both perforin and granzymes. J Exp Med 173, 1099-1109.

Petitdemange, C., Becquart, P., Wauquier, N., Beziat, V., Debre, P., Leroy, E.M., Vieillard, V., 2011. Unconventional repertoire profile is imprinted during acute chikungunya infection for natural killer cells polarization toward cytotoxicity. PLoS Pathog 7, e1002268.

Pham, L.N., Dionne, M.S., Shirasu-Hiza, M., Schneider, D.S., 2007. A specific primed immune response in Drosophila is dependent on phagocytes. PLoS Pathog 3, e26.

Picker, L.J., Singh, M.K., Zdraveski, Z., Treer, J.R., Waldrop, S.L., Bergstresser, P.R., Maino, V.C., 1995. Direct demonstration of cytokine synthesis heterogeneity among human memory/effector T cells by flow cytometry. Blood 86, 1408-1419.

Pilbeam, K., Basse, P., Brossay, L., Vujanovic, N., Gerstein, R., Vallejo, A.N., Borghesi, L., 2008. The ontogeny and fate of NK cells marked by permanent DNA rearrangements. J Immunol 180, 1432-1441.

Pinola, M., Saksela, E., Tiisala, S., Renkonen, R., 1994. Human NK cells expressing alpha 4 beta 1/beta 7 adhere to VCAM-1 without preactivation. Scand J Immunol 39, 131-136.

Podhorzer, A., Machicote, A., Belen, S., Lauferman, L., Imventarza, O., Montal, S., Marciano, S., Galdame, O., Podesta, L.G., Fainboim, L., 2018. Intrahepatic and peripheral blood phenotypes of natural killer and T cells: differential surface expression of killer cell immunoglobulin-like receptors. Immunology 154, 261-273.

Pogge von Strandmann, E., Simhadri, V.R., von Tresckow, B., Sasse, S., Reiners, K.S., Hansen, H.P., Rothe, A., Boll, B., Simhadri, V.L., Borchmann, P., McKinnon, P.J., Hallek, M., Engert, A., 2007. Human leukocyte antigen-B-associated transcript 3 is released from tumor cells and engages the NKp30 receptor on natural killer cells. Immunity 27, 965-974.

Poli, A., Michel, T., Theresine, M., Andres, E., Hentges, F., Zimmer, J., 2009. CD56bright natural killer (NK) cells: an important NK cell subset. Immunology 126, 458-465.

Pons, M.W., 1971. Isolation of influenza virus ribonucleoprotein from infected cells. Demonstration of the presence of negative-stranded RNA in viral RNP. Virology 46, 149-160.

REFERENCES

Prlic, M., Blazar, B.R., Farrar, M.A., Jameson, S.C., 2003. In vivo survival and homeostatic proliferation of natural killer cells. J Exp Med 197, 967-976.

Quinnan, G.V., Jr., Kirmani, N., Rook, A.H., Manischewitz, J.F., Jackson, L., Moreschi, G., Santos, G.W., Saral, R., Burns, W.H., 1982. Cytotoxic t cells in cytomegalovirus infection: HLA-restricted T-lymphocyte and non-T-lymphocyte cytotoxic responses correlate with recovery from cytomegalovirus infection in bone-marrow-transplant recipients. N Engl J Med 307, 7-13.

Radaeva, S., Sun, R., Jaruga, B., Nguyen, V.T., Tian, Z., Gao, B., 2006. Natural killer cells ameliorate liver fibrosis by killing activated stellate cells in NKG2D-dependent and tumor necrosis factor-related apoptosis-inducing ligand-dependent manners. Gastroenterology 130, 435-452.

Rajagopalan, S., Long, E.O., 1999. A human histocompatibility leukocyte antigen (HLA)-G-specific receptor expressed on all natural killer cells. J Exp Med 189, 1093-1100.

Rajalingam, R., 2012. Overview of the killer cell immunoglobulin-like receptor system. Methods Mol Biol 882, 391-414.

Ramachandran, R., Kakar, S., 2009. Histological patterns in drug-induced liver disease. J Clin Pathol 62, 481-492.

Ramos, H.C., Reyes, J., Abu-Elmagd, K., Zeevi, A., Reinsmoen, N., Tzakis, A., Demetris, A.J., Fung, J.J., Flynn, B., McMichael, J., et al., 1995. Weaning of immunosuppression in long-term liver transplant recipients. Transplantation 59, 212-217.

Ranson, T., Vosshenrich, C.A., Corcuff, E., Richard, O., Muller, W., Di Santo, J.P., 2003. IL-15 is an essential mediator of peripheral NK-cell homeostasis. Blood 101, 4887-4893.

Rasmussen, A., Davies, H.F., Jamieson, N.V., Evans, D.B., Calne, R.Y., 1995. Combined transplantation of liver and kidney from the same donor protects the kidney from rejection and improves kidney graft survival. Transplantation 59, 919-921.

Raulet, D.H., 2003. Roles of the NKG2D immunoreceptor and its ligands. Nat Rev Immunol 3, 781-790.

Raulet, D.H., 2004. Interplay of natural killer cells and their receptors with the adaptive immune response. Nat Immunol 5, 996-1002.

Raulet, D.H., Vance, R.E., 2006. Self-tolerance of natural killer cells. Nat Rev Immunol 6, 520-531.

Ravetch, J.V., Bolland, S., 2001. IgG Fc receptors. Annu Rev Immunol 19, 275-290.

Rawlins, E.L., Clark, C.P., Xue, Y., Hogan, B.L., 2009. The Id2+ distal tip lung epithelium contains individual multipotent embryonic progenitor cells. Development 136, 3741-3745.

Reimer-Michalski, E.M., Conrath, U., 2016. Innate immune memory in plants. Semin Immunol 28, 319-327.

Renoux, V.M., Zriwil, A., Peitzsch, C., Michaelsson, J., Friberg, D., Soneji, S., Sitnicka, E., 2015. Identification of a Human Natural Killer Cell Lineage-Restricted Progenitor in Fetal and Adult Tissues. Immunity 43, 394-407.

Ribeiro, V.S., Hasan, M., Wilson, A., Boucontet, L., Pereira, P., Lesjean-Pottier, S., Satoh-Takayama, N., Di Santo, J.P., Vosshenrich, C.A., 2010. Cutting edge: Thymic NK cells develop independently from T cell precursors. J Immunol 185, 4993-4997.

Riberdy, J.M., Christensen, J.P., Branum, K., Doherty, P.C., 2000. Diminished primary and secondary influenza virus-specific CD8(+) T-cell responses in CD4-depleted Ig(-/-) mice. J Virol 74, 9762-9765.

Rieckmann, J.C., Geiger, R., Hornburg, D., Wolf, T., Kveler, K., Jarrossay, D., Sallusto, F., Shen-Orr, S.S., Lanzavecchia, A., Mann, M., Meissner, F., 2017. Social network architecture of human immune cells unveiled by quantitative proteomics. Nat Immunol 18, 583-593.

Riese, P., Trittel, S., Pathirana, R.D., Klawonn, F., Cox, R.J., Guzman, C.A., 2020. Responsiveness to Influenza Vaccination Correlates with NKG2C-Expression on NK Cells. Vaccines (Basel) 8.

Ritz, J., Schmidt, R.E., Michon, J., Hercend, T., Schlossman, S.F., 1988. Characterization of functional surface structures on human natural killer cells. Adv Immunol 42, 181-211.

Roberti, M.P., Julia, E.P., Rocca, Y.S., Amat, M., Bravo, A.I., Loza, J., Colo, F., Loza, C.M., Fabiano, V., Maino, M., Podhorzer, A., Fainboim, L., Barrio, M.M., Mordoh, J., Levy, E.M., 2015. Overexpression of CD85j in TNBC patients inhibits Cetuximab-mediated NK-cell ADCC but can be restored with CD85j functional blockade. Eur J Immunol 45, 1560-1569.

Roberto, A., Di Vito, C., Zaghi, E., Mazza, E.M.C., Capucetti, A., Calvi, M., Tentorio, P., Zanon, V., Sarina, B., Mariotti, J., Bramanti, S., Tenedini, E., Tagliafico, E., Bicciato, S., Santoro, A., Roederer, M., Marcenaro, E., Castagna, L., Lugli, E., Mavilio, D., 2018. The early expansion of anergic NKG2A(pos)/CD56(dim)/CD16(neg) natural killer represents a therapeutic target in haploidentical hematopoietic stem cell transplantation. Haematologica 103, 1390-1402.

Robertson, M.J., Ritz, J., 1990. Biology and clinical relevance of human natural killer cells. Blood 76, 2421-2438.

Robinson, M.W., Harmon, C., O'Farrelly, C., 2016. Liver immunology and its role in inflammation and homeostasis. Cell Mol Immunol 13, 267-276.

Robson, A., Harris, L.K., Innes, B.A., Lash, G.E., Aljunaidy, M.M., Aplin, J.D., Baker, P.N., Robson, S.C., Bulmer, J.N., 2012. Uterine natural killer cells initiate spiral artery remodeling in human pregnancy. FASEB J 26, 4876-4885.

Roederer, M., 2001. Spectral compensation for flow cytometry: visualization artifacts, limitations, and caveats. Cytometry 45, 194-205.

Roederer, M., De Rosa, S., Gerstein, R., Anderson, M., Bigos, M., Stovel, R., Nozaki, T., Parks, D., Herzenberg, L., Herzenberg, L., 1997. 8 color, 10-parameter flow cytometry to elucidate complex leukocyte heterogeneity. Cytometry 29, 328-339.

Roederer, M., Dubs, J.G., Anderson, M.T., Raju, P.A., Herzenberg, L.A., Herzenberg, L.A., 1995. CD8 naive T cell counts decrease progressively in HIV-infected adults. J Clin Invest 95, 2061-2066.

Roederer, M., Nozzi, J.L., Nason, M.C., 2011. SPICE: exploration and analysis of post-cytometric complex multivariate datasets. Cytometry A 79, 167-174.

Romagnani, C., Juelke, K., Falco, M., Morandi, B., D'Agostino, A., Costa, R., Ratto, G., Forte, G., Carrega, P., Lui, G., Conte, R., Strowig, T., Moretta, A., Munz, C., Thiel, A., Moretta, L., Ferlazzo, G., 2007. CD56brightCD16- killer Ig-like receptor- NK cells display longer telomeres and acquire features of CD56dim NK cells upon activation. J Immunol 178, 4947-4955.

Romee, R., Schneider, S.E., Leong, J.W., Chase, J.M., Keppel, C.R., Sullivan, R.P., Cooper, M.A., Fehniger, T.A., 2012. Cytokine activation induces human memory-like NK cells. Blood 120, 4751-4760.

Rosen, D.B., Cao, W., Avery, D.T., Tangye, S.G., Liu, Y.J., Houchins, J.P., Lanier, L.L., 2008. Functional consequences of interactions between human NKR-P1A and its ligand LLT1 expressed on activated dendritic cells and B cells. J Immunol 180, 6508-6517.

Rosen, H.R., 2003. Hepatitis C pathogenesis: mechanisms of viral clearance and liver injury. Liver Transpl 9, S35-43.

Roth, O., Sadd, B.M., Schmid-Hempel, P., Kurtz, J., 2009. Strain-specific priming of resistance in the red flour beetle, Tribolium castaneum. Proc Biol Sci 276, 145-151.

Rouse, B.T., Sehrawat, S., 2010. Immunity and immunopathology to viruses: what decides the outcome? Nat Rev Immunol 10, 514-526.

Ruggeri, L., Capanni, M., Urbani, E., Perruccio, K., Shlomchik, W.D., Tosti, A., Posati, S., Rogaia, D., Frassoni, F., Aversa, F., Martelli, M.F., Velardi, A., 2002. Effectiveness of donor natural killer cell alloreactivity in mismatched hematopoietic transplants. Science 295, 2097-2100.

Sakai, J., Akkoyunlu, M., 2017. The Role of BAFF System Molecules in Host Response to Pathogens. Clin Microbiol Rev 30, 991-1014.

Sallusto, F., Lanzavecchia, A., 2011. Memory in disguise. Nat Med 17, 1182-1183.

Sallusto, F., Lenig, D., Forster, R., Lipp, M., Lanzavecchia, A., 1999. Two subsets of memory T lymphocytes with distinct homing potentials and effector functions. Nature 401, 708-712.

Sanchez, M.J., Muench, M.O., Roncarolo, M.G., Lanier, L.L., Phillips, J.H., 1994. Identification of a common T/natural killer cell progenitor in human fetal thymus. J Exp Med 180, 569-576.

Santourlidis, S., Trompeter, H.I., Weinhold, S., Eisermann, B., Meyer, K.L., Wernet, P., Uhrberg, M., 2002. Crucial role of DNA methylation in determination of clonally distributed killer cell Ig-like receptor expression patterns in NK cells. J Immunol 169, 4253-4261.

Sato, T., Furukawa, K., Autero, M., Gahmberg, C.G., Kobata, A., 1993. Structural study of the sugar chains of human leukocyte common antigen CD45. Biochemistry 32, 12694-12704.

Schapiro, J.M., Segev, Y., Rannon, L., Alkan, M., Rager-Zisman, B., 1990. Natural killer (NK) cell response after vaccination of volunteers with killed influenza vaccine. J Med Virol 30, 196-200.

Scharenberg, M., Vangeti, S., Kekalainen, E., Bergman, P., Al-Ameri, M., Johansson, N., Sonden, K., Falck-Jones, S., Farnert, A., Ljunggren, H.G., Michaelsson, J., Smed-Sorensen, A., Marquardt, N., 2019. Influenza A Virus Infection Induces Hyperresponsiveness in Human Lung Tissue-Resident and Peripheral Blood NK Cells. Front Immunol 10, 1116.

Scharton, T.M., Scott, P., 1993. Natural killer cells are a source of interferon gamma that drives differentiation of CD4+ T cell subsets and induces early resistance to Leishmania major in mice. J Exp Med 178, 567-577.

Schiemann, B., Gommerman, J.L., Vora, K., Cachero, T.G., Shulga-Morskaya, S., Dobles, M., Frew, E., Scott, M.L., 2001. An essential role for BAFF in the normal development of B cells through a BCMA-independent pathway. Science 293, 2111-2114.

Schierloh, P., Yokobori, N., Aleman, M., Musella, R.M., Beigier-Bompadre, M., Saab, M.A., Alves, L., Abbate, E., de la Barrera, S.S., Sasiain, M.C., 2005. Increased susceptibility to apoptosis of CD56dimCD16+ NK cells induces the enrichment of IFN-gamma-producing CD56bright cells in tuberculous pleurisy. J Immunol 175, 6852-6860.

Schmid-Hempel, P., 2005. Natural insect host-parasite systems show immune priming and specificity: puzzles to be solved. Bioessays 27, 1026-1034.

Schmiedel, D., Tai, J., Levi-Schaffer, F., Dovrat, S., Mandelboim, O., 2016. Human Herpesvirus 6B Downregulates Expression of Activating Ligands during Lytic Infection To Escape Elimination by Natural Killer Cells. J Virol 90, 9608-9617.

Schneider, P., 2005. The role of APRIL and BAFF in lymphocyte activation. Curr Opin Immunol 17, 282-289.

Schnittman, S.M., Lane, H.C., Greenhouse, J., Justement, J.S., Baseler, M., Fauci, A.S., 1990. Preferential infection of CD4+ memory T cells by human immunodeficiency virus type 1: evidence for a role in the selective T-cell functional defects observed in infected individuals. Proc Natl Acad Sci U S A 87, 6058-6062.

Schopf, L.R., Filutowicz, H., Bi, X.J., Mansfield, J.M., 1998. Interleukin-4-dependent immunoglobulin G1 isotype switch in the presence of a polarized antigen-specific Th1-cell response to the trypanosome variant surface glycoprotein. Infect Immun 66, 451-461.

Schwab, S.R., Cyster, J.G., 2007. Finding a way out: lymphocyte egress from lymphoid organs. Nat Immunol 8, 1295-1301.

Scoville, S.D., Freud, A.G., Caligiuri, M.A., 2017. Modeling Human Natural Killer Cell Development in the Era of Innate Lymphoid Cells. Front Immunol 8, 360.

Sedlmayr, P., Schallhammer, L., Hammer, A., Wilders-Truschnig, M., Wintersteiger, R., Dohr, G., 1996. Differential phenotypic properties of human peripheral blood CD56dim+ and CD56bright+ natural killer cell subpopulations. Int Arch Allergy Immunol 110, 308-313.

Selin, L.K., Brehm, M.A., Naumov, Y.N., Cornberg, M., Kim, S.K., Clute, S.C., Welsh, R.M., 2006. Memory of mice and men: CD8+ T-cell cross-reactivity and heterologous immunity. Immunol Rev 211, 164-181.

Selin, L.K., Varga, S.M., Wong, I.C., Welsh, R.M., 1998. Protective heterologous antiviral immunity and enhanced immunopathogenesis mediated by memory T cell populations. J Exp Med 188, 1705-1715.

REFERENCES

Serafini, N., Klein Wolterink, R.G., Satoh-Takayama, N., Xu, W., Vosshenrich, C.A., Hendriks, R.W., Di Santo, J.P., 2014. Gata3 drives development of RORgammat+ group 3 innate lymphoid cells. J Exp Med 211, 199-208.

Shedlock, D.J., Shen, H., 2003. Requirement for CD4 T cell help in generating functional CD8 T cell memory. Science 300, 337-339.

Shepard, C.W., Finelli, L., Alter, M.J., 2005. Global epidemiology of hepatitis C virus infection. Lancet Infect Dis 5, 558-567.

Shi, F.D., Ljunggren, H.G., La Cava, A., Van Kaer, L., 2011. Organ-specific features of natural killer cells. Nat Rev Immunol 11, 658-671.

Shibuya, A., Kojima, H., Shibuya, K., Nagayoshi, K., Nagasawa, T., Nakauchi, H., 1993. Enrichment of interleukin-2-responsive natural killer progenitors in human bone marrow. Blood 81, 1819-1826.

Shiow, L.R., Rosen, D.B., Brdickova, N., Xu, Y., An, J., Lanier, L.L., Cyster, J.G., Matloubian, M., 2006. CD69 acts downstream of interferon-alpha/beta to inhibit S1P1 and lymphocyte egress from lymphoid organs. Nature 440, 540-544.

Silva, A., Andrews, D.M., Brooks, A.G., Smyth, M.J., Hayakawa, Y., 2008. Application of CD27 as a marker for distinguishing human NK cell subsets. Int Immunol 20, 625-630.

Sivori, S., Parolini, S., Falco, M., Marcenaro, E., Biassoni, R., Bottino, C., Moretta, L., Moretta, A., 2000. 2B4 functions as a co-receptor in human NK cell activation. Eur J Immunol 30, 787-793.

Sivori, S., Pende, D., Bottino, C., Marcenaro, E., Pessino, A., Biassoni, R., Moretta, L., Moretta, A., 1999. NKp46 is the major triggering receptor involved in the natural cytotoxicity of fresh or cultured human NK cells. Correlation between surface density of NKp46 and natural cytotoxicity against autologous, allogeneic or xenogeneic target cells. Eur J Immunol 29, 1656-1666.

Sivori, S., Vacca, P., Del Zotto, G., Munari, E., Mingari, M.C., Moretta, L., 2019. Human NK cells: surface receptors, inhibitory checkpoints, and translational applications. Cell Mol Immunol 16, 430-441.

Sivori, S., Vitale, M., Morelli, L., Sanseverino, L., Augugliaro, R., Bottino, C., Moretta, L., Moretta, A., 1997. p46, a novel natural killer cell-specific surface molecule that mediates cell activation. J Exp Med 186, 1129-1136.

Skountzou, I., Satyabhama, L., Stavropoulou, A., Ashraf, Z., Esser, E.S., Vassilieva, E., Koutsonanos, D., Compans, R., Jacob, J., 2014. Influenza virus-specific neutralizing IgM antibodies persist for a lifetime. Clin Vaccine Immunol 21, 1481-1489.

Smith, G.J., Vijaykrishna, D., Bahl, J., Lycett, S.J., Worobey, M., Pybus, O.G., Ma, S.K., Cheung, C.L., Raghwani, J., Bhatt, S., Peiris, J.S., Guan, Y., Rambaut, A., 2009. Origins and evolutionary genomics of the 2009 swine-origin H1N1 influenza A epidemic. Nature 459, 1122-1125.

Smyth, M.J., Nutt, S.L., 2006. IL-7 and the thymus dictate the NK cell 'labor market'. Nat Immunol 7, 1134-1136.

Snapper, C.M., Paul, W.E., 1987. Interferon-gamma and B cell stimulatory factor-1 reciprocally regulate Ig isotype production. Science 236, 944-947.

Sojka, D.K., Plougastel-Douglas, B., Yang, L., Pak-Wittel, M.A., Artyomov, M.N., Ivanova, Y., Zhong, C., Chase, J.M., Rothman, P.B., Yu, J., Riley, J.K., Zhu, J., Tian, Z., Yokoyama, W.M., 2014a. Tissue-resident natural killer (NK) cells are cell lineages distinct from thymic and conventional splenic NK cells. Elife 3, e01659.

Sojka, D.K., Tian, Z., Yokoyama, W.M., 2014b. Tissue-resident natural killer cells and their potential diversity. Semin Immunol 26, 127-131.

Sojka, D.K., Yang, L., Plougastel-Douglas, B., Higuchi, D.A., Croy, B.A., Yokoyama, W.M., 2018a. Cutting Edge: Local Proliferation of Uterine Tissue-Resident NK Cells during Decidualization in Mice. J Immunol 201, 2551-2556.

Sojka, D.K., Yang, L., Yokoyama, W.M., 2018b. Uterine natural killer cells: To protect and to nurture. Birth Defects Res 110, 1531-1538.

Sojka, D.K., Yang, L., Yokoyama, W.M., 2019. Uterine Natural Killer Cells. Front Immunol 10, 960.

Spinner, M.A., Sanchez, L.A., Hsu, A.P., Shaw, P.A., Zerbe, C.S., Calvo, K.R., Arthur, D.C., Gu, W., Gould, C.M., Brewer, C.C., Cowen, E.W., Freeman, A.F., Olivier, K.N., Uzel, G., Zelazny, A.M., Daub, J.R., Spalding, C.D., Claypool, R.J., Giri, N.K., Alter, B.P., Mace, E.M., Orange, J.S., Cuellar-Rodriguez, J., Hickstein, D.D., Holland, S.M., 2014. GATA2 deficiency: a protean disorder of hematopoiesis, lymphatics, and immunity. Blood 123, 809-821.

Spits, H., Artis, D., Colonna, M., Diefenbach, A., Di Santo, J.P., Eberl, G., Koyasu, S., Locksley, R.M., McKenzie, A.N., Mebius, R.E., Powrie, F., Vivier, E., 2013. Innate lymphoid cells--a proposal for uniform nomenclature. Nat Rev Immunol 13, 145-149.

Spits, H., Cupedo, T., 2012. Innate lymphoid cells: emerging insights in development, lineage relationships, and function. Annu Rev Immunol 30, 647-675.

Spits, H., Lanier, L.L., Phillips, J.H., 1995. Development of human T and natural killer cells. Blood 85, 2654-2670.

Springer, T.A., 1995. Traffic signals on endothelium for lymphocyte recirculation and leukocyte emigration. Annu Rev Physiol 57, 827-872.

Stegmann, K.A., Robertson, F., Hansi, N., Gill, U., Pallant, C., Christophides, T., Pallett, L.J., Peppa, D., Dunn, C., Fusai, G., Male, V., Davidson, B.R., Kennedy, P., Maini, M.K., 2016. CXCR6 marks a novel subset of T-bet(lo)Eomes(hi) natural killer cells residing in human liver. Sci Rep 6, 26157.

Stein-Streilein, J., Guffee, J., 1986. In vivo treatment of mice and hamsters with antibodies to asialo GM1 increases morbidity and mortality to pulmonary influenza infection. J Immunol 136, 1435-1441.

Stein-Streilein, J., Guffee, J., Fan, W., 1988. Locally and systemically derived natural killer cells participate in defense against intranasally inoculated influenza virus. Reg Immunol 1, 100-105.

Strauss-Albee, D.M., Fukuyama, J., Liang, E.C., Yao, Y., Jarrell, J.A., Drake, A.L., Kinuthia, J., Montgomery, R.R., John-Stewart, G., Holmes, S., Blish, C.A., 2015. Human NK cell repertoire diversity reflects immune experience and correlates with viral susceptibility. Sci Transl Med 7, 297ra115.

Strutt, T.M., McKinstry, K.K., Dibble, J.P., Winchell, C., Kuang, Y., Curtis, J.D., Huston, G., Dutton, R.W., Swain, S.L., 2010. Memory CD4+ T cells induce innate responses independently of pathogen. Nat Med 16, 558-564, 551p following 564.

Sugita, K., Robertson, M.J., Torimoto, Y., Ritz, J., Schlossman, S.F., Morimoto, C., 1992. Participation of the CD27 antigen in the regulation of IL-2-activated human natural killer cells. J Immunol 149, 1199-1203.

Sun, J.C., Beilke, J.N., Lanier, L.L., 2009. Adaptive immune features of natural killer cells. Nature 457, 557-561.

Sun, J.C., Bevan, M.J., 2003. Defective CD8 T cell memory following acute infection without CD4 T cell help. Science 300, 339-342.

Takeda, K., Cretney, E., Hayakawa, Y., Ota, T., Akiba, H., Ogasawara, K., Yagita, H., Kinoshita, K., Okumura, K., Smyth, M.J., 2005. TRAIL identifies immature natural killer cells in newborn mice and adult mouse liver. Blood 105, 2082-2089.

Takenaka, K., Nishida, T., Asano-Mori, Y., Oshima, K., Ohashi, K., Mori, T., Kanamori, H., Miyamura, K., Kato, C., Kobayashi, N., Uchida, N., Nakamae, H., Ichinohe, T., Morishima, Y., Suzuki, R., Yamaguchi, T., Fukuda, T., 2015. Cytomegalovirus Reactivation after Allogeneic Hematopoietic Stem Cell Transplantation is Associated with a Reduced Risk of Relapse in Patients with Acute Myeloid Leukemia Who Survived to Day 100 after Transplantation: The Japan Society for Hematopoietic Cell Transplantation Transplantation-related Complication Working Group. Biol Blood Marrow Transplant 21, 2008-2016.

Taubenberger, J.K., Morens, D.M., 2006. 1918 Influenza: the mother of all pandemics. Emerg Infect Dis 12, 15-22.

Tayade, C., Fang, Y., Black, G.P., V, A.P., Jr., Erlebacher, A., Croy, B.A., 2005. Differential transcription of Eomes and T-bet during maturation of mouse uterine natural killer cells. J Leukoc Biol 78, 1347-1355.

Tesselaar, K., Arens, R., van Schijndel, G.M., Baars, P.A., van der Valk, M.A., Borst, J., van Oers, M.H., van Lier, R.A., 2003. Lethal T cell immunodeficiency induced by chronic costimulation via CD27-CD70 interactions. Nat Immunol 4, 49-54.

Thomas, M.L., Lefrancois, L., 1988. Differential expression of the leucocyte-common antigen family. Immunol Today 9, 320-326.

Thomas, R., Low, H.Z., Kniesch, K., Jacobs, R., Schmidt, R.E., Witte, T., 2012. NKG2C deletion is a risk factor of HIV infection. AIDS Res Hum Retroviruses 28, 844-851.

Thompson, J.S., Schneider, P., Kalled, S.L., Wang, L., Lefevre, E.A., Cachero, T.G., MacKay, F., Bixler, S.A., Zafari, M., Liu, Z.Y., Woodcock, S.A., Qian, F., Batten, M., Madry, C., Richard, Y., Benjamin, C.D., Browning, J.L., Tsapis, A., Tschopp, J., Ambrose, C., 2000. BAFF binds to the tumor necrosis factor receptor-like molecule B cell maturation antigen and is important for maintaining the peripheral B cell population. J Exp Med 192, 129-135.

Tiemessen, C.T., Shalekoff, S., Meddows-Taylor, S., Schramm, D.B., Papathanasopoulos, M., Gray, G., Sherman, G., Coovadia, A., Kuhn, L., 2010. Natural killer cells that respond to human immunodeficiency virus type 1 (HIV-1) peptides are associated with control of HIV-1 infection. J Infect Dis 202, 1444-1453.

Tiemessen, C.T., Shalekoff, S., Meddows-Taylor, S., Schramm, D.B., Papathanasopoulos, M.A., Gray, G.E., Sherman, G.G., Coovadia, A.H., Kuhn, L., 2009. Cutting Edge: Unusual NK cell responses to HIV-1 peptides are associated with protection against maternal-infant transmission of HIV-1. J Immunol 182, 5914-5918.

Tisoncik, J.R., Korth, M.J., Simmons, C.P., Farrar, J., Martin, T.R., Katze, M.G., 2012. Into the eye of the cytokine storm. Microbiol Mol Biol Rev 76, 16-32.

Tomasec, P., Braud, V.M., Rickards, C., Powell, M.B., McSharry, B.P., Gadola, S., Cerundolo, V., Borysiewicz, L.K., McMichael, A.J., Wilkinson, G.W., 2000. Surface expression of HLA-E, an inhibitor of natural killer cells, enhanced by human cytomegalovirus gpUL40. Science 287, 1031.

Topham, D.J., Tripp, R.A., Doherty, P.C., 1997. CD8+ T cells clear influenza virus by perforin or Fas-dependent processes. J Immunol 159, 5197-5200.

Tremblay-McLean, A., Coenraads, S., Kiani, Z., Dupuy, F.P., Bernard, N.F., 2019. Expression of ligands for activating natural killer cell receptors on cell lines commonly used to assess natural killer cell function. BMC Immunol 20, 8.

Trinchieri, G., 1997. Cytokines acting on or secreted by macrophages during intracellular infection (IL-10, IL-12, IFN-gamma). Curr Opin Immunol 9, 17-23.

Tu, M.M., Mahmoud, A.B., Makrigiannis, A.P., 2016. Licensed and Unlicensed NK Cells: Differential Roles in Cancer and Viral Control. Front Immunol 7, 166.

Tu, Z., Bozorgzadeh, A., Crispe, I.N., Orloff, M.S., 2007. The activation state of human intrahepatic lymphocytes. Clin Exp Immunol 149, 186-193.

Tumpey, T.M., Garcia-Sastre, A., Taubenberger, J.K., Palese, P., Swayne, D.E., Pantin-Jackwood, M.J., Schultz-Cherry, S., Solorzano, A., Van Rooijen, N., Katz, J.M., Basler, C.F., 2005. Pathogenicity of influenza viruses with genes from the 1918 pandemic virus: functional roles of alveolar macrophages and neutrophils in limiting virus replication and mortality in mice. J Virol 79, 14933-14944.

Tung, J.W., Heydari, K., Tirouvanziam, R., Sahaf, B., Parks, D.R., Herzenberg, L.A., Herzenberg, L.A., 2007. Modern flow cytometry: a practical approach. Clin Lab Med 27, 453-468, v.

Udagawa, T., Woodside, D.G., McIntyre, B.W., 1996. Alpha 4 beta 1 (CD49d/CD29) integrin costimulation of human T cells enhances transcription factor and cytokine induction in the absence of altered sensitivity to anti-CD3 stimulation. J Immunol 157, 1965-1972.

Van Kaer, L., 2015. Innate and virtual memory T cells in man. Eur J Immunol 45, 1916-1920.

van Lier, R.A., Borst, J., Vroom, T.M., Klein, H., Van Mourik, P., Zeijlemaker, W.P., Melief, C.J., 1987. Tissue distribution and biochemical and functional properties of Tp55 (CD27), a novel T cell differentiation antigen. J Immunol 139, 1589-1596.

Varchetta, S., Mele, D., Oliviero, B., Mantovani, S., Ludovisi, S., Cerino, A., Bruno, R., Castelli, A., Mosconi, M., Vecchia, M., Roda, S., Sachs, M., Klersy, C., Mondelli, M.U., 2020. Unique immunological profile in patients with COVID-19. Cell Mol Immunol.

Vargas-Inchaustegui, D.A., Ying, O., Demberg, T., Robert-Guroff, M., 2016. Evaluation of Functional NK Cell Responses in Vaccinated and SIV-Infected Rhesus Macaques. Front Immunol 7, 340.

Vargas, C.L., Poursine-Laurent, J., Yang, L., Yokoyama, W.M., 2011. Development of thymic NK cells from double negative 1 thymocyte precursors. Blood 118, 3570-3578.

Vergani, D., Mieli-Vergani, G., 2004. Mechanisms of autoimmune hepatitis. Pediatr Transplant 8, 589-593.

Victorino, F., Sojka, D.K., Brodsky, K.S., McNamee, E.N., Masterson, J.C., Homann, D., Yokoyama, W.M., Eltzschig, H.K., Clambey, E.T., 2015. Tissue-Resident NK Cells Mediate Ischemic Kidney Injury and Are Not Depleted by Anti-Asialo-GM1 Antibody. J Immunol 195, 4973-4985.

Viegas, N., Andzinski, L., Wu, C.F., Komoll, R.M., Gekara, N., Dittmar, K.E., Weiss, S., Jablonska, J., 2013. IFN-gamma production by CD27(+) NK cells exacerbates Listeria monocytogenes infection in mice by inhibiting granulocyte mobilization. Eur J Immunol 43, 2626-2637.

Vitale, C., Chiossone, L., Morreale, G., Lanino, E., Cottalasso, F., Moretti, S., Dini, G., Moretta, L., Mingari, M.C., 2004a. Analysis of the activating receptors and cytolytic function of human natural killer cells undergoing in vivo differentiation after allogeneic bone marrow transplantation. Eur J Immunol 34, 455-460.

Vitale, M., Bottino, C., Sivori, S., Sanseverino, L., Castriconi, R., Marcenaro, E., Augugliaro, R., Moretta, L., Moretta, A., 1998. NKp44, a novel triggering surface molecule specifically expressed by activated natural killer cells, is involved in non-major histocompatibility complex-restricted tumor cell lysis. J Exp Med 187, 2065-2072.

Vitale, M., Della Chiesa, M., Carlomagno, S., Romagnani, C., Thiel, A., Moretta, L., Moretta, A., 2004b. The small subset of CD56brightCD16- natural killer cells is selectively responsible for both cell proliferation and interferon-gamma production upon interaction with dendritic cells. Eur J Immunol 34, 1715-1722.

Vitale, M., Sivori, S., Pende, D., Augugliaro, R., Di Donato, C., Amoroso, A., Malnati, M., Bottino, C., Moretta, L., Moretta, A., 1996. Physical and functional independency of p70 and p58 natural killer (NK) cell receptors for HLA class I: their role in the definition of different groups of alloreactive NK cell clones. Proc Natl Acad Sci U S A 93, 1453-1457.

Vivier, E., Artis, D., Colonna, M., Diefenbach, A., Di Santo, J.P., Eberl, G., Koyasu, S., Locksley, R.M., McKenzie, A.N.J., Mebius, R.E., Powrie, F., Spits, H., 2018. Innate Lymphoid Cells: 10 Years On. Cell 174, 1054-1066.

Vossen, M.T., Matmati, M., Hertoghs, K.M., Baars, P.A., Gent, M.R., Leclercq, G., Hamann, J., Kuijpers, T.W., van Lier, R.A., 2008. CD27 defines phenotypically and functionally different human NK cell subsets. J Immunol 180, 3739-3745.

Vosshenrich, C.A., Garcia-Ojeda, M.E., Samson-Villeger, S.I., Pasqualetto, V., Enault, L., Richard-Le Goff, O., Corcuff, E., Guy-Grand, D., Rocha, B., Cumano, A., Rogge, L., Ezine, S., Di Santo, J.P., 2006. A thymic pathway of mouse natural killer cell development characterized by expression of GATA-3 and CD127. Nat Immunol 7, 1217-1224.

Vosshenrich, C.A., Samson-Villeger, S.I., Di Santo, J.P., 2005. Distinguishing features of developing natural killer cells. Curr Opin Immunol 17, 151-158.

Wagtmann, N., Biassoni, R., Cantoni, C., Verdiani, S., Malnati, M.S., Vitale, M., Bottino, C., Moretta, L., Moretta, A., Long, E.O., 1995. Molecular clones of the p58 NK cell receptor reveal immunoglobulin-related molecules with diversity in both the extra- and intracellular domains. Immunity 2, 439-449.

Waldrop, S.L., Davis, K.A., Maino, V.C., Picker, L.J., 1998. Normal human CD4+ memory T cells display broad heterogeneity in their activation threshold for cytokine synthesis. J Immunol 161, 5284-5295.

Wan, S., Yi, Q., Fan, S., Lv, J., Zhang, X., Guo, L., Lang, C., Xiao, Q., Xiao, K., Yi, Z., Qiang, M., Xiang, J., Zhang, B., Chen, Y., Gao, C., 2020. Relationships among lymphocyte subsets, cytokines, and the pulmonary inflammation index in coronavirus (COVID-19) infected patients. Br J Haematol 189, 428-437.

Wang, J., Li, F., Zheng, M., Sun, R., Wei, H., Tian, Z., 2012. Lung natural killer cells in mice: phenotype and response to respiratory infection. Immunology 137, 37-47.

Wang, Z., Tobler, S., Roayaei, J., Eick, A., 2009. Live attenuated or inactivated influenza vaccines and medical encounters for respiratory illnesses among US military personnel. JAMA 301, 945-953.

Warren, H.S., Rana, P.M., Rieger, D.T., Hewitt, K.A., Dahlstrom, J.E., Kent, A.L., 2006. CD8 T cells expressing killer Ig-like receptors and NKG2A are present in cord blood and express a more naive phenotype than their counterparts in adult blood. J Leukoc Biol 79, 1252-1259.

Watt, S.V., Andrews, D.M., Takeda, K., Smyth, M.J., Hayakawa, Y., 2008. IFN-gamma-dependent recruitment of mature CD27(high) NK cells to lymph nodes primed by dendritic cells. J Immunol 181, 5323-5330.

Webster, R.G., Govorkova, E.A., 2014. Continuing challenges in influenza. Ann N Y Acad Sci 1323, 115-139.

Weinfurter, J.T., Brunner, K., Capuano, S.V., 3rd, Li, C., Broman, K.W., Kawaoka, Y., Friedrich, T.C., 2011. Cross-reactive T cells are involved in rapid clearance of 2009 pandemic H1N1 influenza virus in nonhuman primates. PLoS Pathog 7, e1002381.

Weinheimer, V.K., Becher, A., Tonnies, M., Holland, G., Knepper, J., Bauer, T.T., Schneider, P., Neudecker, J., Ruckert, J.C., Szymanski, K., Temmesfeld-Wollbrueck, B., Gruber, A.D., Bannert, N., Suttorp, N., Hippenstiel, S., Wolff, T., Hocke, A.C., 2012. Influenza A viruses target type II pneumocytes in the human lung. J Infect Dis 206, 1685-1694.

Weis, W., Brown, J.H., Cusack, S., Paulson, J.C., Skehel, J.J., Wiley, D.C., 1988. Structure of the influenza virus haemagglutinin complexed with its receptor, sialic acid. Nature 333, 426-431.

Weiss, I.D., Wald, O., Wald, H., Beider, K., Abraham, M., Galun, E., Nagler, A., Peled, A., 2010. IFN-gamma treatment at early stages of influenza virus infection protects mice from death in a NK cell-dependent manner. J Interferon Cytokine Res 30, 439-449.

Welsh, R.M., Che, J.W., Brehm, M.A., Selin, L.K., 2010. Heterologous immunity between viruses. Immunol Rev 235, 244-266.

Welsh, R.M., Selin, L.K., 2002. No one is naive: the significance of heterologous T-cell immunity. Nat Rev Immunol 2, 417-426.

Wherry, E.J., Blattman, J.N., Murali-Krishna, K., van der Most, R., Ahmed, R., 2003. Viral persistence alters CD8 T-cell immunodominance and tissue distribution and results in distinct stages of functional impairment. J Virol 77, 4911-4927.

White, M.J., Nielsen, C.M., McGregor, R.H., Riley, E.H., Goodier, M.R., 2014. Differential activation of CD57-defined natural killer cell subsets during recall responses to vaccine antigens. Immunology 142, 140-150.

Wilkinson, G.W., Tomasec, P., Stanton, R.J., Armstrong, M., Prod'homme, V., Aicheler, R., McSharry, B.P., Rickards, C.R., Cochrane, D., Llewellyn-Lacey, S., Wang, E.C., Griffin, C.A., Davison, A.J., 2008. Modulation of natural killer cells by human cytomegalovirus. J Clin Virol 41, 206-212.

Williams, N.S., Moore, T.A., Schatzle, J.D., Puzanov, I.J., Sivakumar, P.V., Zlotnik, A., Bennett, M., Kumar, V., 1997. Generation of lytic natural killer 1.1+, Ly-49- cells from multipotential murine bone marrow progenitors in a stroma-free culture: definition of cytokine requirements and developmental intermediates. J Exp Med 186, 1609-1614.

Wilson, E.M., Sereti, I., 2013. Immune restoration after antiretroviral therapy: the pitfalls of hasty or incomplete repairs. Immunol Rev 254, 343-354.

Wilson, J.L., Charo, J., Martin-Fontecha, A., Dellabona, P., Casorati, G., Chambers, B.J., Kiessling, R., Bejarano, M.T., Ljunggren, H.G., 1999. NK cell triggering by the human costimulatory molecules CD80 and CD86. J Immunol 163, 4207-4212.

Wong, A.H., Williams, K., Reddy, S., Wilson, D., Giddy, J., Alter, G., Ghebremichael, M., Carrington, M.N., Ndung'u, T., Walker, B.D., Altfeld, M., Carr, W.H., 2010. Alterations in natural killer cell receptor profiles during HIV type 1 disease progression among chronically infected South African adults. AIDS Res Hum Retroviruses 26, 459-469.

Woodland, D.L., Kohlmeier, J.E., 2009. Migration, maintenance and recall of memory T cells in peripheral tissues. Nat Rev Immunol 9, 153-161.

Woodruff, M.C., Heesters, B.A., Herndon, C.N., Groom, J.R., Thomas, P.G., Luster, A.D., Turley, S.J., Carroll, M.C., 2014. Trans-nodal migration of resident dendritic cells into medullary interfollicular regions initiates immunity to influenza vaccine. J Exp Med 211, 1611-1621.

Wu, C., Li, B., Lu, R., Koelle, S.J., Yang, Y., Jares, A., Krouse, A.E., Metzger, M., Liang, F., Lore, K., Wu, C.O., Donahue, R.E., Chen, I.S.Y., Weissman, I., Dunbar, C.E., 2014. Clonal tracking of rhesus macaque hematopoiesis highlights a distinct lineage origin for natural killer cells. Cell Stem Cell 14, 486-499.

Xiong, S., Sharkey, A.M., Kennedy, P.R., Gardner, L., Farrell, L.E., Chazara, O., Bauer, J., Hiby, S.E., Colucci, F., Moffett, A., 2013. Maternal uterine NK cell-activating receptor KIR2DS1 enhances placentation. J Clin Invest 123, 4264-4272.

Yefenof, E., Zehavi-Feferman, R., Guy, R., 1990. Control of primary and secondary antibody responses by cytotoxic T lymphocytes specific for a soluble antigen. Eur J Immunol 20, 1849-1853.

Yokota, T., Kouro, T., Hirose, J., Igarashi, H., Garrett, K.P., Gregory, S.C., Sakaguchi, N., Owen, J.J., Kincade, P.W., 2003. Unique properties of fetal lymphoid progenitors identified according to RAG1 gene expression. Immunity 19, 365-375.

Yokota, Y., Mansouri, A., Mori, S., Sugawara, S., Adachi, S., Nishikawa, S., Gruss, P., 1999. Development of peripheral lymphoid organs and natural killer cells depends on the helix-loop-helix inhibitor Id2. Nature 397, 702-706.

Yokoyama, W.M., Kim, S., French, A.R., 2004. The dynamic life of natural killer cells. Annu Rev Immunol 22, 405-429.

Yokoyama, W.M., Sojka, D.K., Peng, H., Tian, Z., 2013. Tissue-resident natural killer cells. Cold Spring Harb Symp Quant Biol 78, 149-156.

Yoshizawa, K., Ota, M., Katsuyama, Y., Ichijo, T., Inada, H., Umemura, T., Tanaka, E., Kiyosawa, K., 1999. T cell repertoire in the liver of patients with autoimmune hepatitis. Hum Immunol 60, 806-815.

Yu, H., Fehniger, T.A., Fuchshuber, P., Thiel, K.S., Vivier, E., Carson, W.E., Caligiuri, M.A., 1998. Flt3 ligand promotes the generation of a distinct CD34(+) human natural killer cell progenitor that responds to interleukin-15. Blood 92, 3647-3657.

Yu, J., Freud, A.G., Caligiuri, M.A., 2013. Location and cellular stages of natural killer cell development. Trends Immunol 34, 573-582.

Yu, J., Mao, H.C., Wei, M., Hughes, T., Zhang, J., Park, I.K., Liu, S., McClory, S., Marcucci, G., Trotta, R., Caligiuri, M.A., 2010. CD94 surface density identifies a functional intermediary between the CD56bright and CD56dim human NK-cell subsets. Blood 115, 274-281.

Yu, J., Tostanoski, L.H., Peter, L., Mercado, N.B., McMahan, K., Mahrokhian, S.H., Nkolola, J.P., Liu, J., Li, Z., Chandrashekar, A., Martinez, D.R., Loos, C., Atyeo, C., Fischinger, S., Burke, J.S., Slein, M.D., Chen, Y., Zuiani, A., Lelis, F.J.N., Travers, M., Habibi, S., Pessaint, L., Van Ry, A., Blade, K., Brown, R., Cook, A., Finneyfrock, B., Dodson, A., Teow, E., Velasco, J., Zahn, R., Wegmann, F., Bondzie, E.A., Dagotto, G., Gebre, M.S., He, X., Jacob-Dolan, C., Kirilova, M., Kordana, N., Lin, Z., Maxfield, L.F., Nampanya, F., Nityanandam, R., Ventura, J.D., Wan, H., Cai, Y., Chen, B., Schmidt, A.G., Wesemann, D.R., Baric, R.S., Alter, G., Andersen, H., Lewis, M.G., Barouch, D.H., 2020. DNA vaccine protection against SARS-CoV-2 in rhesus macaques. Science 369, 806-811.

Zachou, K., Rigopoulou, E., Dalekos, G.N., 2004. Autoantibodies and autoantigens in autoimmune hepatitis: important tools in clinical practice and to study pathogenesis of the disease. J Autoimmune Dis 1, 2.

Zamai, L., Ahmad, M., Bennett, I.M., Azzoni, L., Alnemri, E.S., Perussia, B., 1998. Natural killer (NK) cell-mediated cytotoxicity: differential use of TRAIL and Fas ligand by immature and mature primary human NK cells. J Exp Med 188, 2375-2380.

Zamora, A.E., Aguilar, E.G., Sungur, C.M., Khuat, L.T., Dunai, C., Lochhead, G.R., Du, J., Pomeroy, C., Blazar, B.R., Longo, D.L., Venstrom, J.M., Baumgarth, N., Murphy, W.J., 2017. Licensing delineates helper and effector NK cell subsets during viral infection. JCI Insight 2.

Zhang, L.H., Shin, J.H., Haggadone, M.D., Sunwoo, J.B., 2016. The aryl hydrocarbon receptor is required for the maintenance of liver-resident natural killer cells. J Exp Med 213, 2249-2257.

Zhang, Q.F., Yin, W.W., Xia, Y., Yi, Y.Y., He, Q.F., Wang, X., Ren, H., Zhang, D.Z., 2017. Liver-infiltrating CD11b(-)CD27(-) NK subsets account for NK-cell dysfunction in patients with hepatocellular carcinoma and are associated with tumor progression. Cell Mol Immunol 14, 819-829.

Zhang, Y., Wallace, D.L., de Lara, C.M., Ghattas, H., Asquith, B., Worth, A., Griffin, G.E., Taylor, G.P., Tough, D.F., Beverley, P.C., Macallan, D.C., 2007. In vivo kinetics of human natural killer cells: the effects of ageing and acute and chronic viral infection. Immunology 121, 258-265.

Zhong, C., Cui, K., Wilhelm, C., Hu, G., Mao, K., Belkaid, Y., Zhao, K., Zhu, J., 2016. Group 3 innate lymphoid cells continuously require the transcription factor GATA-3 after commitment. Nat Immunol 17, 169-178.

Zhou, G., Juang, S.W., Kane, K.P., 2013. NK cells exacerbate the pathology of influenza virus infection in mice. Eur J Immunol 43, 929-938.

Zhuang, X., Long, E.O., 2019. CD28 Homolog Is a Strong Activator of Natural Killer Cells for Lysis of B7H7(+) Tumor Cells. Cancer Immunol Res 7, 939-951.

Zitvogel, L., 2002. Dendritic and natural killer cells cooperate in the control/switch of innate immunity. J Exp Med 195, F9-14.

APPENDIX A
Ethics

UNIVERSITY OF THE WITWATERSRAND, JOHANNESBURG

R49 Ms P Kaye

HUMAN RESEARCH ETHICS COMMITTEE (MEDICAL)
CLEARANCE CERTIFICATE NO. M2011137

NAME: (Principal Investigator)	Ms P Kaye
DEPARTMENT:	Centre for HIV and STI's National Institute for Communicable Diseases Sandringham
PROJECT TITLE:	Phenotypic and functional characterization of natural killer cell subsets within the context of influenza vaccination and HIV infection
DATE CONSIDERED:	Ad hoc
DECISION:	Approved unconditionally
CONDITIONS:	Formerly M130268 (expired on 25 April 2018)
SUPERVISOR:	Professor CT Tiemessen
APPROVED BY:	Dr CB Penny, Chairperson, HREC (Medical)
DATE OF APPROVAL:	8 December 2020

This Clearance Certificate is valid for 5 years from the date of approval. An extension may be applied for.

DECLARATION OF INVESTIGATORS

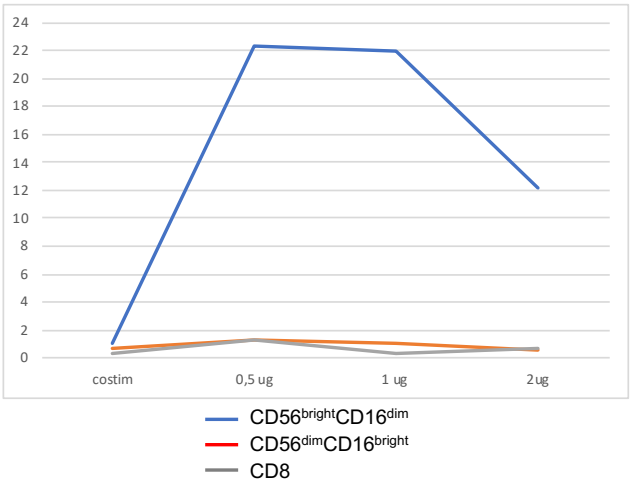
To be completed in duplicate and **ONE COPY** returned to the Research Office secretariat on the 3rd floor, Phillip Tobias Building, Parktown, University of the Witwatersrand, Johannesburg.

I/we fully understand the conditions under which I am/we are authorized to carry out the above-mentioned research and I/we undertake to ensure compliance with these conditions. Should any departure be contemplated from the research protocol as approved, I/we undertake to submit details to the Committee. **I agree to submit a yearly progress report**. When a funder requires annual re-certification, the application date will be one year after the date when the study was initially reviewed. In this case, the study was initially reviewed in **November** and therefore reports and re-certification will be due in the month of **November** each year. Unreported changes to the study may invalidate the clearance given by the HREC (Medical).

Signature of Principal Investigator _____ Date _____

APPENDIX B
Influenza antigen titration

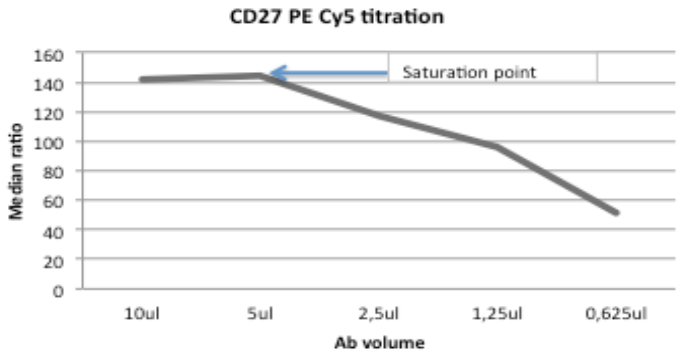
Doubling dilutions of Influvac® subunit inactivated influenza vaccine (Solvay Pharmaceuticals), containing 15 µg each haemaglutinin and neuraminidase antigen of strains A/California/7/2009(H1N1)-like virus; A/Perth/16/2009(H3N2)-like virus and B/Brisbane/60/2008 virus) to give final concentrations of 0.5 µg; 1 µg and 2 µg per ml. 2 x 10^6 PBMC aliquots were stimulated (**Section 2.6.1**) and stained as per the staining protocol used for test samples (**Sections 2.8.1; 2.8.2** and **2.8.3**). The concentration of antigen giving the best magnitude of degranulation response (CD107a$^+$) for CD56^{bright}CD16^{neg}, CD56^{dim}CD16^{bright} and CD8 T cells was deemed the optimal concentration.



APPENDIX C
Antibody titrations

The purpose of an antibody titration is to a) determine the optimal concentration of antibody that is required to give good separation between positive and negative populations and b) determine the position of the negative population on the axis.

Commercially available fluorescently labeled antibodies generally suggest a recommended volume for use in a flow cytometry panel, but as this may not be the optimum concentration for each panel, antibody titrations were performed.to obtain the desired result. Starting with the manufacturers recommended volume, doubling dilutions of fluorochrome conjugated antibody were made in PBS and 2 x 10^6 PBMC aliquots stained as per the staining protocol used for test samples. To ensure best separation between positive and negative populations with minimal interference from negative populations, the peak signal-to-noise ratio was calculated as $\frac{positive\ MFI}{negative\ MFI}$ and graphed against antibody concentrations. The point where the minimum antibody volume gave the greatest signal to noise ratio was determined as the optimal concentration point and used for all experimental protocols. A representative example using CD27 PE Cy5 stained cells to determine optimal antibody concentration is given below.



Monoclonal antibody titrations using anchor markers

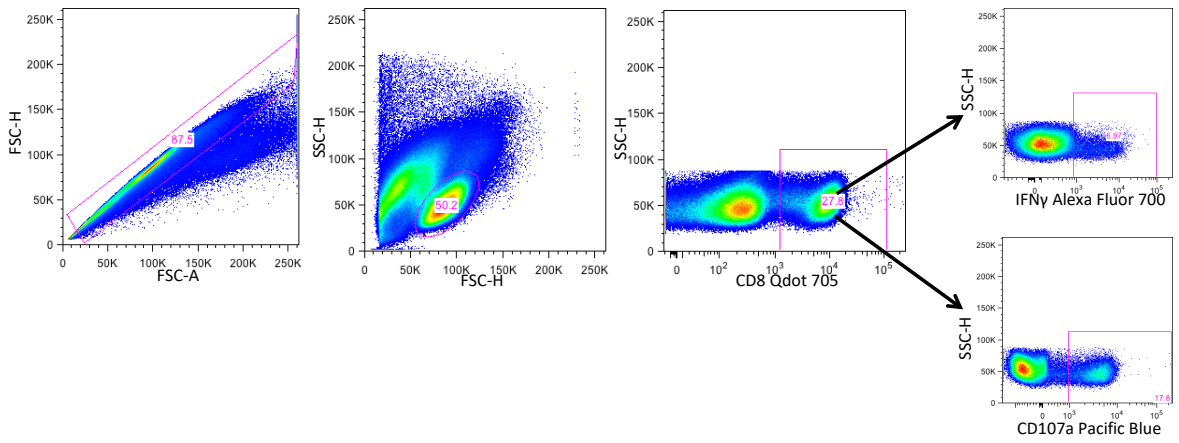
Flow analysis software programs present data as a percentage of the gated parent population, the interference of inherent background noise with measurement accuracies makes it difficult to determine antibody saturation point when a cell population represents a small fraction of the parent population. Therefore, anchor markers were included for titrations of CD56, CD16, IFNγ and CD107a antibodies (summarized below).

APPENDIX C
Antibody titrations

Anchor marker	Antibody for titration
CD3 PE Cy7 (for negative gating)	CD56 brilliant violet 605
	CD16 FITC
CD8 Qdot 705	IFNγ Alexa fluor 700
	CD107a Pacific blue

The same staining protocols that were used for test samples were followed. 2 x 10^6 PBMC cell pellets were surface stained (Chapter 2, section 2.8.2) or stained intracellularly (Chapter 2, section 2.8.3) with pre-titrated anchor markers and aliquots of fluorochrome conjugated monoclonal antibody dilutions. For detection of IFNγ and CD107a, PBMCs were stimulated with SEB (Chapter 2, section 2.6.2).

Anchor markers were gated and antibodies under titration were next gated off these populations. A representative example using CD8 QDot 705 as an anchor marker for IFNγ and CD107a antibody titrations is depicted below.



APPENDIX D
Determination of primary fluorecence

To achieve primary fluorescence, the voltage for a given detector was adjusted to a level where the mean fluorescent intensity (MFI) of the fluorochrome specific for that detector, was greater than that in secondary detectors and with minimal spillover fluorescence. The process was repeated with each voltage adjustment in both primary and secondary detectors until primary fluorescence was obtained. Primary fluorescence was determined as the lowest voltage gain in which the MFI value was highest in the primary detector with the least spillover into secondary detectors. An example of a primary fluorescence matrix for FITC (highlighted in red box) is given below.

Experiment Name: Flu Panel 09012014
Specimen Name: Compensation Controls
Tube Name: CD16 FITC Stained Control
Record Date: Jan 10, 2014 9:12:32 AM

Population	CD16 FITC-A Mean	PE-A PE-Texas R... Mean	Mean	PE-Cy5-A PerCP-Cy5-... Mean	Mean	PE-Cy7-A Mean	APC-A Alexa Fluor ... Mean	Mean	APC-Cy7-A Pacific Blue... Mean	Mean	Qdot 605-A Mean	Violet1-A Mean
☒ P2	3,914	921	383	75	27	6	4	3	2	358	89	15

APPENDIX E
List of fluorochrome conjugated antibodies

Laser	Wavelength	Detector	Antigen	Fluorochrome	Clone	Company	Rationale for inclusion in panel
Blue	488	F	CD16	FITC	3G8	Biolegend	Identify/phenotype NK cell subsets
		E	NKp46	PE	9E2	BD Pharmingen	Identify activating receptor
		D	CD45RO	ECD	UCHL1	Beckman Coulter	Phenotype memory T cells
		C	CD27	PE-Cy5	0323	Biolegend	Phenotype NK cell subsets T cell memory
		B	CD4	PE-Cy5.5	RM4-5	Biolegend	Phenotype T cell subsets
		A	CD3	PE-Cy7	UCHT1	Biolegend	Identify T cells/ non NK cell lineage exclusion
Red	640	D	CD62L	APC	DREG-56	BD Pharmingen	Phenotype NK cell subsets/T cell memory
		C					
		B	IFNγ	Alexa fluor 700	B27	BD Pharmingen	Detection of cytokine responses
		A	CD14 CD19 Near infra-red amine LIVE/DEAD discriminator	APC-Cy7 or APC-H7 APC-Cy7 or APC-H7	MϕP9 MϕP9 SJ25C1 SJ25C1	BD Pharmingen	Non NK cell lineage exclusion Non NK cell lineage exclusion Exclusion of dead cells
Violet	405	F	CD107a	Pac Blue	H4A3	Biolegend	Marker of degranulation
		E					
		D					
		C					
		B	CD56	BV 605	NCAM 16.2	Biolegend	Identify/phenotype NK cell subsets
		A	CD8	QDot® 705 or BV 711	3B5 RPA-T8	Biolegend	Phenotype T cell subsets
Ultra Violet	355	B					
		A					

APPENDIX F
Flow cytometer optimization

The quality of signals to detect photon emission by flow cytometers is reliant on laser alignment, optical filters, fluidics and precision of fluorescent measurements. Efficiency of detector sensitivity and reflection properties of optical filters and mirrors is of critical importance for accuracy of polychromatic flow cytometry data.

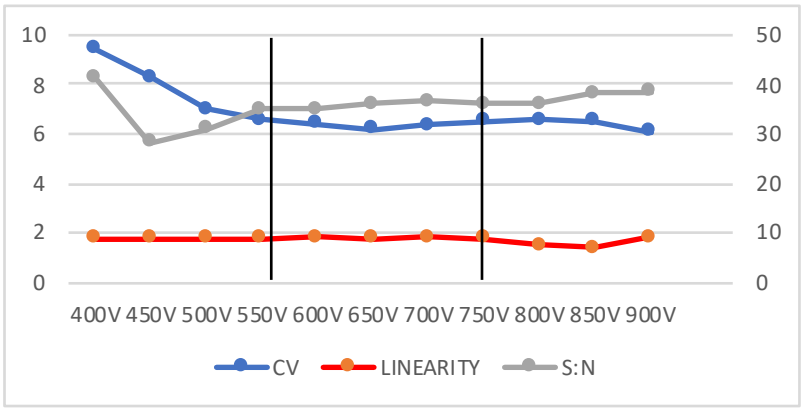
Laser power was checked using a laser power meter before commencement of the study and then reassessed 2 to 3 times year. Dichroic mirrors were checked to ensure that band-pass and long-pass mirrors were in the correct positions for each laser, as per manufacturers specifications and a cascade test as described by Perfetto *et al*., (2006) was performed to determine photoelectron efficiency. Electronic noise (e noise) for each detector was determined to ensure that values fell below 100 so as to reduce interference with true signal.

APPENDIX G
Flow cytometer system calibration

Following system optimization, a voltage range was determined for each photomultiplier tube (PMT). Voltages were set at 350 V and two single peaks (able to be detected over the voltage series) gated on 8 peak rainbow beads (Spherotec). 10,000 beads were acquired and the process repeated over a series of 50 V increments. The MFI of the lower bead peak was defined as M1 and the upper bead as M2. PMT linearity was determined with the following formula: (M1 - M2) / M1.

To determine background, 10,000 unstained compensation beads were collected over the same voltage range. Signal to noise ratio was calculated as: M1 divided by background, for each voltage series.

The co-efficient of variation (CV) for M1 was recorded over the voltage series and the CV, signal to noise ratio (S:N ratio) and PMT linearity were plotted onto a graph. The voltage range was deemed, as the voltage range for which the CV was lowest, with the highest signal to noise ratio and with linearity over a range of voltages. The example below depicts the linear PMT range for the APC channel of the red laser. Black vertical lines indicate the linear range as defined by the range giving the best compromise between low CVs, best signal to noise ratio and PMT linearity.



Voltages obtained from primary fluorescence validation (**Appendix D**) were applied to each PMT to ensure that they fell within the linear range and a tolerance range was determined for MFIs and CVs for each PMT from data collected over 30 daily readings. The target MFIs were calculated as the mean of 30 daily readings and a 10% greater or lesser variance than this value was calculated as the tolerance range. The tolerance range for CVs was considered as a value no greater than the mean of 30 daily readings.

APPENDIX G
Flow cytometer system calibration

Standardisation

To ensure optimal signal synchronization, peak 3 midrange fluorescent beads (Spherotech) were used to check the area scaling factor (ASF) and adjusted, if required, before each experiment to ensure that the height MFI was equivalent to the area MFI for each laser. Laser delay settings were tested to confirm peak signal location relative to the reference laser.

Performance was measured and monitored on a daily basis before each experiment was run, by acquiring 10,000 peak 3 midrange fluorescent beads (Spherotech), to ensure that MFIs and CVs for each PMT were within the tolerance range. If daily readings fell outside of the acceptable range, a troubleshooting procedure was followed, until MFIs and CVs fell within the tolerance range.

Spectral compensation of fluorochrome labelled antibodies

The emission spectrum of a fluorochromes can be sufficiently broad enough to be detected in more than one detector. Compensation is a mathematical process that corrects for this overlap.

Polystyrene BD CompBeads™ were single stained for each fluorochrome by adding a drop of CompBeads to 100µl of phosphate buffered saline (PBS) and the same volume fluorochrome conjugated antibody as test samples. Tubes were incubated in the dark for 10 minutes and then washed by adding 2.5ml PBS followed by centrifugation at 1000 rpm for 10 minutes. The supernatant was discarded and tubes gently blotted on clean paper toweling. Beads were resuspended in 300µl 1% paraformaldehyde and refridgerated at 4^0 C in the dark for no longer than 24 hrs. Unstained BD CompBeads™ resuspended in 300µl 1% paraformaldehyde were used as a negative.

Following acquisition of compensation beads, but before acquisition of test samples, the compensation matrix electronically generated by FlowJo™ software for Mac (version 9.9.4) was examined to ensure correct allocation of negative and positive populations to all parameters. A representative example of a FlowJo “wizard” generated table showing correct allocation of negative and positive populations is shown below.

APPENDIX G
Flow cytometer system calibration

Use	Sample Name	Primary Color	Positive	Negative
▾ •	Compensation Controls_IFNg Alexa Fluor 700 Stained Control.fcs	▾Alexa Fluor 700-A	ow_Size/ow_Alexa Fluor 700-A	▾
▾ •	Compensation Controls_CD62L APC Stained Control.fcs	▾APC-A	ow_Size/ow_APC-A	▾
▾ •	Compensation Controls_Dump APC-Cy7 Stained Control.fcs	▾APC-Cy7-A	ow_Size/ow_APC-Cy7-A	▾
▾ •	Compensation Controls_CD16 FITC Stained Control.fcs	▾FITC-A	ow_Size/ow_FITC-A	▾
▾ •	Compensation Controls_CD107a Pacific Blue Stained Control.fcs	▾Pacific Blue-A	ow_Size/ow_Pacific Blue-A	▾
▾ •	Compensation Controls_NKp46 PE Stained Control.fcs	▾PE-A	ow_Size/ow_PE-A	▾
▾ •	Compensation Controls_CD27 PE-Cy5 Stained Control.fcs	▾PE-Cy5-A	ow_Size/ow_PE-Cy5-A	▾
▾ •	Compensation Controls_CD3 PE-Cy7 Stained Control.fcs	▾PE-Cy7-A	ow_Size/ow_PE-Cy7-A	▾
▾ •	Compensation Controls_CD45RO EC PE-Texas Red Stained Control.fcs	▾PE-Texas Red-A	ow_Size/ow_PE-Texas Red-A	▾
▾ •	Compensation Controls_CD4 PE Cy5_5 PerCP-Cy5-5 Stained Control.fcs	▾PerCP-Cy5-5-A	ow_Size/ow_PerCP-Cy5-5-A	▾
▾ •	Compensation Controls_CD56 Br V 605 Qdot 605 Stained Control.fcs	▾Qdot 605-A	ow_Size/ow_Qdot 605-A	▾
▾ •	Compensation Controls_CD8 Br V 711 Violet1 Stained Control.fcs	▾Violet1-A	ow_Size/ow_Violet1-A	▾
▾ •	Compensation Controls_Unstained Control.fcs	▾Unstained	▾	ow_Size

Compensation matrices for each experiment were next analysed to ensure that compensation for spectral spillover was not more than 100% for any parameter ie primary fluorescence was maintained. Below is an example of a FlowJo generated compensation matrix.

APPENDIX H
Anti-influenza virus A human IgM ELISA

Background

The anti-influenza virus A human *in vitro* ELISA kit (Abcam, United Kingdom, cat no ab108747) qualitatively measures IgM antibodies against influenza A in human plasma and serum.
The ELISA kit uses a 96-well plate that has been pre-coated with influenza A antigens to bind cognate antibodies. Controls or test samples are added to the wells and the plate incubated. Following a wash step, horseradish peroxidase (HRP) labelled anti-human IgM conjugate is added, which binds to the immobilized influenza virus-A specific antibodies. Following a further incubation and wash step a substrate solution (TMB) is added to each well which is catalysed by the bound HRP to produce a blue colour which changes to yellow on addition of an acidic stop solution. The intensity (optical density) of the yellow colouration is directly proportional to the amount of influenza virus A IgM captured on the plate.

Optical density determination

Plates were read at 450 nm using 620 nm as a reference wavelength using a Techkon plate reader (Techkon, Germany). The mean optical density (OD) of the substrate blanks (background blank) was subtracted from the mean of each sample reading and compared to the mean cut-off control value.

Data analysis

Calculations

The following criteria must be met for the IgM assay to be considered valid:

- Substrate blank: Absorbance value < 0.100
- Negative control: Absorbance value < 0.200 and < cut-off
- Cut-off control: Absorbance value 0.150 - 1.300
- Positive control: Absorbance value > cut-off
-

Interpretation of results

Samples are considered to give a positive signal if the absorbance value is greater than 10% over the cut-off value.

Samples with an absorbance value of less than 10% above or below the cut-off control value should be considered inconclusive and be repeated. If the second test result is again less than 10% above or below the cut-off control value the sample must be considered negative.
Samples are considered negative if the absorbance value is lower than 10% below the cut-off value.

APPENDIX H
Anti-influenza virus A human IgM ELISA

Results in standard units

$$\text{Standard units} = \frac{\text{Mean patient absorbance value} \times 10}{\text{Cut-off}}$$

Cut-off:	10 Standard units
Grey zone:	9 - 11 Standard units
Negative:	< 9 Standard units
Positive:	> 11 Standard units